Proceedings of the Fifteenth Annual Pacific Climate (PACLIM) Workshop

The Wrigley Institute for Environmental Studies (WIES)
Two Harbors, Santa Catalina Island, California
April 27-30, 1998

Edited by
Raymond Wilson and Lauren Buffaloe

Technical Report 64
of the
Interagency Ecological Program for the
Sacramento-San Joaquin Estuary

April 1999

PACLIM

Climate Variability of the Eastern North Pacific and Western North America

Table of Contents

Sponsors

The Fifteenth Annual Pacific Climate (PACLIM) Workshop is sponsored by:

The Wrigley Institute for Environmental Sciences .... Anthony Michaels
The US Geological Survey, Geological Division .... Elliot Spiker
The American Geophysical Union .... A.F. Spilhaus, Jr.
The State of California Department of Water Resources .... Randall Brown

Publication of this proceedings was sponsored by:

**The Interagency Ecological Program
for the
Sacramento–San Joaquin Estuary**

A cooperative program of the following member agencies:

California Department of Water Resources
State Water Resources Control Board
US Bureau of Reclamation
US Geological Survey
California Department of Fish and Game
US Fish and Wildlife Service
US Army Corps of Engineers
US Environmental Protection Agency

National Marine Fisheries Service

These proceedings were published by the Interagency Ecological Program for the Sacramento–San Joaquin Estuary (IEP) in a cooperative effort with the US Department of the Interior, Geological Survey, Menlo Park, California. Information generated by the PACLIM Workshop provides the Interagency Program with a climatological perspective that cannot be obtained from its own studies. Views and conclusions contained in this publication do not necessarily reflect the opinions of the IEP or its member agencies.

Authors

Susanne Clement
Kent State University
Department of Geology
Kent, OH 44242
(P) 330 672 7987
(F) 330 678 7949

Rachael Craig
Kent State University
Department of Geology
Kent, OH 44242
(P) 330 672 7987
(F) 330 678 7949

John A. Dracup
University of California, Los Angeles
Department of Civil and Environmental Engineering
5731/5732 Boelter Hall
Los Angeles, CA 90095–1593
(P) 310 206 8612

Hugo G. Hidalgo
University of California, Los Angeles
Department of Civil and Environmental Engineering
5731/5732 Boelter Hall
Los Angeles, CA 90095–1593
(P) 310 206 8612

Masao Kanamitsu
Climate Prediction Center
NCEP/NWS/NOAA
4700 Silver Hill Road, Stop 9910
Washington, D.C. 20233–9910

Thor Karlstrom
4811 SW Brace Point Drive
Seattle, WA 98136
(P) 206 935 7087

Steven W. Leavitt
University of Arizona
Laboratory of Tree Ring Research
Tucson, AZ 85721
(P) 520 621 6468
(F) 520 621 8229

Austin Long
University of Arizona
Department of Geosciences
Tucson, AZ 85721
(P) 520 621 8888

Glen Mac Donald
University of California, Los Angeles
Departments of Geography and Biology
40 Bunche Hall
Los Angeles, CA 90095–1524
(P) 310 825 2568

Kingtse Mo
Climate Prediction Center
NCEP/NWS/NOAA
4700 Silver Hill Road, Stop 9910
Washington, D.C. 20233–9910
(P) 301 763 8000 ext. 7540
wd52km@sgi44.wwb.noaa.gov

Thomas Piechota
University of California, Los Angeles
Department of Civil and Environmental Engineering
5731/5732 Boelter Hall
Los Angeles, CA 90095–1593
(P) 310 206 8612

Maurice Roos
California Department of Water Resources
3310 El Camino Avenue, Room 200
P.O. Box 219000
Sacramento, CA 95821–9000
(P) 916 574 2625

Marina Timofeyeva
Kent State University
Department of Geology
Kent, OH 44242
(P) 330 672 7987
(F) 330 678 7949
mtimofey@geology.kent.edu

Xueliang Wang
Climate Prediction Center
NCEP/NWS/NOAA
4700 Silver Hill Road, Stop 9910
Washington, D.C. 20233–9910

William E. Wright
University of Arizona
Laboratory of Tree Ring Research
Tucson, AZ 85721
(P) 520 621 2518
(F) 520 621 8229

Acknowledgments

The PACLIM workshops are produced by an array of enthusiastic volunteers. For the 1998 meeting, thanks go to the following people and institutions.

The Wrigley Institute for Environmental Studies: Special thanks to the Wrigley Institute for Environmental Studies and Tony Michaels for co-sponsoring and hosting the 1998 PACLIM workshop on Santa Catalina. The logistics of getting us all onto (and back off) the island were ably handled by Maureen Oudin and Gina Long, who arranged for ferry trips, luggage trucks, vans and water taxis, and made us mainlanders feel welcome in this beautiful place.

US Geological Survey: Mike Dettinger chaired the meeting and organized the agenda; Mary Ann Rouse provided administrative assistance; and Lucenia Thomas coordinated travel arrangements.

Scripps Institution of Oceanography: Larry Riddle operated the PACLIM web site and obtained the foam board and easels (lent by George Hemingway of California Coop Fisheries) for the poster session. Nicki Pyles assembled the abstracts.

Long Beach City College: Special thanks to Janice Tomson for a superb job of planning, organizing, and supervising the nuts-and-bolts operation of the meeting—getting us there, getting us fed, watered, and roomed, and thinking of all the thousands of things that need thinking about. Thanks also to Long Beach City College students: Melissa Andrews, Erin Boyd, Jill Brooks, Jacquie Cote, and Dusty Hardy. Jill and Erin helped with check in, registration, set ups and all other projects. Dusty Hardy assumed the responsibility of driving the van; Melissa sold T-shirts and helped with registration; and, most especially, Jacquie Cote helped hold the workshop together by keeping us all organized.

Thanks also to the Conservation Corps representative Dustin Platter who helped with check-in, registration, set ups, and late night food and entertainment. Finally, our profound gratitude to Lowell Stott (University of Southern California) for beverages.

Sponsorship and funding for the workshops come from a wide variety of sources. In addition to the agencies and programs responsible (see Sponsors, page 1), we also thank all those who helped in the funding process, including Tony Michaels, Harry Lins, Dick Poore, Eliot Spiker, Fred Spilhaus, Paul Weiss, Lowell Stott, and Randy Brown.

For the scientific agenda of the workshop, we thank Mike Dettinger, with logistic support from Larry Riddle. The meeting chairs and moderators are also gratefully acknowledged: Janice Tomson, Dan Cayan, Mike Dettinger, Curt Ebbesmeyer, Malcolm Hughes, Caroline Isaacs, and Ray Wilson. Finally, we thank all our speakers and poster presenters (see Appendix A: Agenda, page 137) for their contributions and enthusiasm.

For the production and printing of the proceedings, thanks go once again to Randy Brown and the California Department of Water Resources Interagency Ecological Program for the Sacramento–San Joaquin Estuary. The production of this volume was performed by my co-editor, Lauren Buffaloe, whom I thank for her patience with diverse format types, her expertise with technical editing, graphics, tables, and highly skilled "pagemaking." Special thanks to Lauren for her initiative and efficiency in accepting this challenge in late January and pulling it all together in time to make the 1999 meeting. Special thanks also to Nancy Ullrey, Lauren's able predecessor, who handled the initial production details, before moving on to a new position. Invaluable precedents for the 1997 and 1998 volumes were established by the previous editors of the PACLIM Proceedings: Dave Peterson (1984–1988), with the able assistance of Lucenia Thomas; Julio Betancourt and Ana MacKay (1989–1990); Kelly Redmond and Vera Tharp (1991–1993); and Caroline Isaacs and Vera Tharp (1994–1996).

Ray Wilson
US Geological Survey
Menlo Park, California

Statement of Purpose

In 1984, a workshop was held on "Climatic Variability of the Eastern North Pacific and Western North America." From it has emerged an annual series of workshops held at the Wrigley Institute for Environmental Studies at Two Harbors, Santa Catalina Island, California. These annual meetings, which involve 80–100 participants, have come to be known as the Pacific Climate (PACLIM) Workshops, reflecting broad interests in the climatologies associated with the Pacific Ocean and western Americas in both the northern and southern hemispheres. Participants have included atmospheric scientists, hydrologists, glaciologists, oceanographers, limnologists, and both marine and terrestrial biologists. A major goal of PACLIM is to provide a forum for exploring the insights and perspectives of each of these many disciplines and for understanding the critical linkages between them.

PACLIM arose from growing concern about climate variability and its societal and ecological impacts. Storm frequency, snowpack, droughts and floods, agricultural production, water supply, glacial advances, stream chemistry, sea surface temperature, salmon catch, lake ecosystems, and wildlife habitat are among the many aspects of climate and climatic impacts addressed by PACLIM Workshops. Workshops also address broad concerns about the impact of possible climate change over the next century. From observed changes in the historical records, the conclusion is evident that climate change would have large societal impacts through effects on global ecology, hydrology, geology, and oceanography.

Our ability to predict climate, climate variability, and climate change critically depends on an understanding of global processes. Human impacts are primarily terrestrial in nature, but the major forcing processes are atmospheric and oceanic in origin and transferred through geologic and biologic systems. Our understanding of the global climate system and its relationship to ecosystems in the Eastern Pacific area arises from regional study of its components in the Pacific Ocean and western Americas, where ocean-atmosphere coupling is strongly expressed. Empirical evidence suggests that large-scale climatic fluctuations force large-scale ecosystem response in the California current and in a very different system, the North Pacific central gyre. With such diverse meterologic phenomena as the El Niño–Southern Oscillation and shifts in the Aleutian Low and North Pacific High, the eastern Pacific has tremendous global influences and particularly strong effects on North America. In the western US, where rainfall is primarily a cool-season phenomenon, year-to-year changes in the activity and tracking of North Pacific winter storms have substantial influence on the hydrological balance. This region is rich in climatic records, both instrumental and proxy. Recent research efforts are beginning to focus on better paleoclimatic reconstructions that will put present-day climatic variability in context and allow better anticipation of future variations and changes.

The PACLIM Workshops address the problem of defining regional coupling of multifold elements, as organized by global phenomena. Because climate expresses itself throughout the natural system, our activity has been, from the beginning, multidisciplinary in scope. The specialized knowledge from different disciplines has brought together climatic records and process measurements to synthesize and understanding of the complete system. Our interdsciplinary group uses diverse time series, measured both directly and through proxy indicators, to study past climatic conditions and current processes in this region. Characterizing and linking the geosphere, biosphere, and hydrosphere in this region provides a scientific analogue and, hence, a basis for understanding similar linkages in other regions and for anticipating the response to future climate variations. Our emphasis in PACLIM is to study the interrelationships among diverse data. To understand these interactive phenomena, we incorporate studies that consider a broad range of topics both physical and biological, time scales from months to millennia, and space scales from single sites to the entire globe.

Introduction

Raymond Wilson
US Geological Survey

The Fifteenth Annual PACLIM Workshop was held at the Wrigley Institute of Environmental Studies campus at Two Harbors on Catalina Island, California. An island is a highly appropriate place for a conference concerned with interactions between the atmosphere and ocean and their effects on terrestrial processes. Attended by about 84 registered participants (see Appendix C: Attendees, page 147), the workshop included 38 talks and 16 poster presentations. The talks consisted of a one-day theme session, "1997–1998—El Niño of the Century?", with eleven featured talks (see Appendix A: Agenda, page 137). Throughout the remainder of the meeting were 27 talks on a variety of climate-related topics. Poster presenters gave a short one- to two-minute introduction to their posters, which were displayed during the entire meeting (see Appendix B: Poster Presentations, page 145). On Tuesday evening, Marty Hoerling provided some interesting speculations about the next radical shift in global climate, "What to Expect from an Extreme La Nina—The Opposite of the Effect from an Extreme El Niño?"

All presenters were invited to expand their abstracts into a manuscript for inclusion in the Proceedings volume, and nearly all presentations are included in manuscript or abstract form. In this Proceedings volume, nine papers are presented full-length, and two as extended abstracts. The abstracts submitted are printed in this volume, beginning on page 111.

What Makes PACLIM Special?

The Statement of Purpose briefly summarizes the history of the PACLIM workshops and ably summarizes our corporate goals: to understand the interaction of atmospheric and oceanic processes, their connection with terrestrial processes through geologic and biologic systems, the temporal and spatial climatic variations they produce, and the impact of these variations on society and the ecology on regional (eastern Pacific and Americas) and global scales. Over the past decade and a half, the PACLIM workshops have brought together a large "extended family" from a very broad range of disciplines--meteorology, hydrology, oceanography, glaciologists, paleontologists, limnologists, geomorphologists, and biologists, both marine and terrestrial. Particularly valuable, in my opinion, has been the mix of people representing the complete spectrum from "pure" academic research to the front lines of resource management.

The PACLIM workshops are useful both to climate specialists and to newcomers: The specialists exchange data and news of the latest developments within their fields (for example, Quaternary palynology, tree-ring studies, or ocean-continent teleconnections), just as in a technical session at the American Geophysical Union or American Meteorological Society, only at PACLIM they have an audience that includes specialists in many other fields. For the newcomer, however, the smaller, informal PACLIM Workshop presents an opportunity to not only hear lectures by the leading authorities, but to sit down and talk with them over dinner and to present their own ideas from a newcomer's perspective.

The biggest difference I see between PACLIM and the larger meetings of national organizations, however, is in the tone of the interchanges after the talks. PACLIM discussions usually take place in a spirit of cooperation and mutual exploration, rather than in competition for turf or priority. Younger investigators, and those wandering in from other fields, are encouraged to speak up and share ideas and perspectives. The field of climate studies, even when focused on the eastern Pacific and western Americas, is complex and covers vast scales in time and space, so that there is plenty of room for everyone to participate in its exploration.

El Niño 1998, a Prophecy Come to Pass

The first I heard of the 1997–1998 El Niño was as rumors at the 1997 PACLIM conference—the first held at Two Harbors. Sea surface temperatures were already rising, wind regimes shifting, and various other harbingers had already been noted around the dinner table by various meeting participants. By early summer of 1997, the PACLIM rumors had become formal predictions of a new El Niño in the Pacific. By late summer, it had come to pass, a formidable El Niño, stronger even than 1982–1983, with global consequences: drought and fires in Indonesia, floods in Peru (including mudslides covering part of the ancient "lines" across the Nazca Plain), disastrous ice storms in New England and the Maritimes, and floods and mudslides in northern California.

These events were described in a number of interesting presentations at PACLIM 1998. For the second year in a row, Maurice "Maury" Roos had an exciting flood story to tell (see page 85). Ray Garnett described the El Niño's impact on the world grain yields. Several authors described the impact of the sea-surface temperature changes on marine fisheries and other marine biologic communities. Gary Sharp presented a fascinating multi-media experience celebrating the complex dance between the ocean, atmosphere, biosphere, and human activities.

For balance, a number of other authors described their work on tree-ring, pollen, and other long-term records of climatic variations on scales of decades to millennia, reminding all of us that the history of Holocene climatic variations contain excursions—wet and dry, warm and cold—that provide a sobering context for our present troubles.

Along with the climatological anomalies of the past couple of years, have come some social and political perturbations. For a period of over a year, the national media had an insatiable interest in El Niño and its consequences. They became fascinated with the whole subject—teleconnections, sea-surface temperatures, sea-level variations, and all. What does all this mean to those of us involved with PACLIM? We have a lot more of the public's attention now—however we decide to use it. Years of work that has seemed arcane and obscure is now in great demand. We live in "interesting times," with some of the sense of the old Taoist lament, but also a sense of new opportunities. I'm sure we will have much to tell each other at the 1999 PACLIM Workshop.

Estimates of Glacial Climate and Runoff for the Bonneville Basin

Marina Timofeyeva, Susanne Clement, and Rachael Craig
Kent State University, Department of Geology
Kent, Ohio 44242

Abstract

We estimate climatic conditions in the basin of Lake Bonneville at the time of the last glacial (glacial) using a local climate model. When comparing modern temperature solutions (spatial average) to those for the glacial, we find that glacial climate was cooler on average by 3.2 °C. During the glacial winter (November through April), the temperature is as much as 6.3 °C cooler and averages 4.4 °C cooler, while the glacial summer (May through September) is only 1.5° C cooler when compared with modern conditions and July is actually 0.3 °C warmer than modern. The glacial age seasonal distribution of precipitation is more variable than today. Wet season precipitation (November through April) is estimated to be 2.3 times higher on average for the glacial, while dry season precipitation (May through October) is estimated to be 1.8 times higher. Precipitation is greater at the glacial in all months and the larger increase in winter leads to much greater snowpack. Rainfall is less in winter as a result of the cooler temperatures; more precipitation falls as snow. This implies fewer rain-on-snow events, less ripening of snowpack, and delays in snowmelt compared to modern. Using a modified version of a previously-developed runoff model, driven by the output of the climate model, we find that runoff during the glacial was 3.1 times higher during the warm season (May through October) but was unchanged during the cold season (November through April), which is expected due to precipitation remaining trapped as snowpack for a longer time. The runoff peak occurs at the same time (May), but reaches that peak much more abruptly at glacial compared to modern. These model solutions compare favorably with paleoclimatic and paleohydrologic evidence from the Bonneville Basin at this time, which suggests the following: (1) increased abundance of subalpine conifers and shrubs; (2) extensive valley glaciers in the Wasatch; (3) an increase of runoff of two to three times; (4) large prograding deltas at the mouths of the major rivers; and (5) the existence of a high stand of Lake Bonneville.

Introduction

Geologic records suggest the presence of a spacious Lake Bonneville in the basin of the present Great Salt Lake during the Late Pleistocene (Benson and Thompson 1987). At about 15 ka, lake level reached 1552 m above sea level (O'Connor 1993), about 300 m higher than the present lake surface. General Circulation Model (GCM) analysis using boundary conditions representing this period indicate that the strong glacial age anticyclone and 3–km thick Laurentide ice sheet may have created atmospheric circulation within this area that was dramatically different than the present pattern (COMAP members 1988). Antevs (1948) suggested that such a shift in atmospheric circulation was responsible for the growth and high stand of Lake Bonneville during the Late Quaternary. Hostetler and Giorgi (1992) and Hostetler and others (1994) have demonstrated that positive feedback occurs once a large lake forms due to downwind precipitation; however, no direct link between atmospheric circulation and lake initiation has been demonstrated to date. Here we examine the question whether this altered circulation pattern is capable of creating the recorded paleolake.

We use a Local Climate Model (LCM) (Stamm and Gettelman 1995) to estimate the climatic conditions that prevailed in the basin of Lake Bonneville (Figure 1) at the time of the last glacial (glacial) and compared these to a control (modern) solution. The LCM results are applied as input to Snow and Surface Hydrology Models (Orndorff 1994), which yield hydrologic characteristics for the same area. The hydrologic solutions are used as input to a model (Singer 1985), which computes the resulting lake volume, surface area, and depth. The solution domain covers an area about 6° latitude and 5.5° longitude with spatial resolution of 5 x 5 km (see Figure 1).

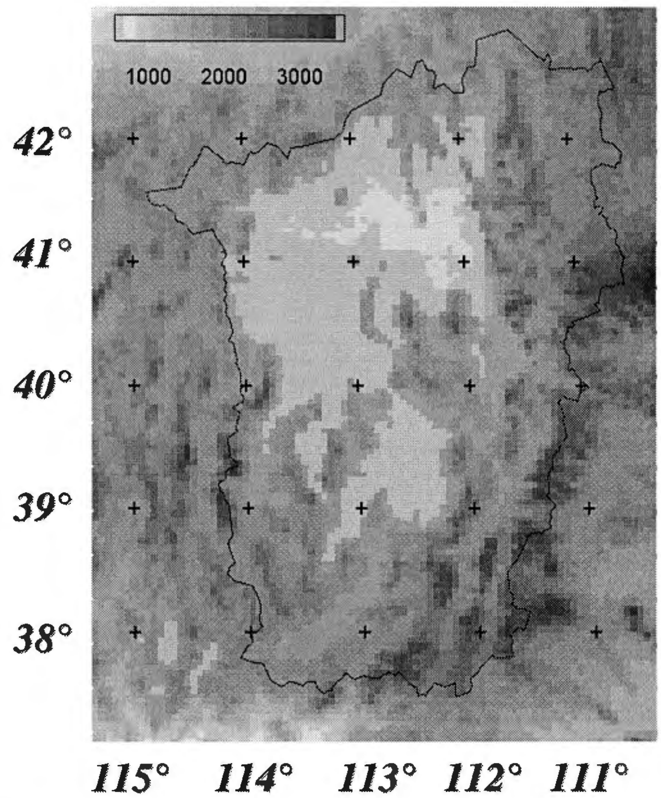

Figure 1 Digital elevation matrix for the solution domain. The drainage basin boundary of Bonneville Lake is indicated by the black solid line. Elevations (m) are scaled to the image legend. Tick marks indicate 1° intervals of latitude and longitude.

Modeling Procedure

We model mean monthly maximum daily temperature (TMAX, °C) and the natural logarithm of total monthly precipitation (PREC, mm) using the LCM, which performs statistical downscaling from global climate features to local climate characteristics and is calibrated with instrumental climate records. The LCM is solved for modern (control) and for the glacial by specifying appropriate boundary conditions from a GCM. The boundary conditions are the following: a digital elevation model (DEM), sea level, CO_2 concentration in the atmosphere, solar insolation, wind fields, sea surface temperature, and geopotential height. In this study, the forcing domain DEM represents 10 km x 10 km terrain elevations generated from 5' latitude and longitude topographic data provided by NGDC (National Geophysical Data Center 1987). Both the forcing domain and solution domain DEMs are assumed to be unchanged between glacial and control solutions of the LCM. These domains and other model details are explained by Stamm and Gettelman (1995). Sea level is specified as a change about the modern value (0 m for control run). For the glacial run, we use a sea level change of -121 m as suggested by Fairbanks (1989). The level of CO_2 in the atmosphere for the control run is assumed to be 300‰ for the modern run and 194‰ for the glacial run (Barnola and others 1987). Solar insolation is computed as a function of latitude (Berger 1978). The LCM uses the Geophysical Fluid Dynamic Laboratory GCM control and 18 ka results for wind fields, sea surface temperature, and geopotential height (Manabe and Broccoli 1985).

Since windfields and sea surface temperatures (SSTs) are the key boundary conditions for our model, we first evaluated the effect of using two different sources of these data during calibration of the model: (1) observational windfields derived from the National Meteorological Center (NMC) octagonal-gridded analysis and SST derived from the combined Advanced Very High Resolution Radiometer and Comprehensive Ocean Atmosphere Data Set; and (2) GFDL GCM solutions of both windfields and SST. Monte Carlo solutions of climate for each of these control run boundary conditions were compared to instrumental records at four climate stations, considering both means and variances. We find that the calibration using GFDL windfields yields solutions that closely match those using NMC observed climate. For each of the windfield and SST sources, both means and variances calculated from the climate model are both accurate and precise estimators of the instrumental record.

It is reassuring to find that the GCM can yield results as good as obtained using the observed values since only GCM estimates are available for the glacial. The solutions we have made for the glacial use the GFDL results as boundary conditions (Manabe and Broccoli 1985) for our model. These analyses are a refinement of earlier work (Timofeyeva and Craig 1997, 1998) in two regards: (1) we have used a more complete method of estimating the parameters of the frequency distribution of monthly precipitation; and (2) we have used a modified water balance calculation in the hydrology model.

As the distribution of PREC is highly skewed, we transform from the natural logarithm into metric units using methodology based on log-normal distribution properties (Aitchison and Brown 1957). We use the standard error of prediction (Draper and Smith 1981) of the canonical correlation to estimate the standard deviation of PREC in the transformation procedure (Timofeyeva and Craig 1997, 1998).

TMAX and PREC provide climate input to the Snow and Surface Hydrology models (Orndorff 1994). The Snow Model quantifies the proportion of precipitation in liquid and solid phases, snow and ice accumulation and ablation, and snow and ice melt. The snowfall fraction is computed by integrating the (cell-dependent) joint probability distribution function of TMAX and PREC. Snowmelt is computed from a degree day factor (Martinec 1975). The Surface Hydrology Model uses the LCM and Snow model results to compute evapotranspiration, the fraction of total available water contributing to soil moisture, changes in storage, overland flow and actual runoff. Both of these models are based on conservation of mass. Hydrology parameters are specified for the modern situation and assumed to be unchanged for the last glacial solutions.

The Lake Model (Singer 1985) uses change in temperature from the modern conditions to compute lake evaporation for the glacial period and determines the balance of this with annual runoff and streamflow into the lake for that same time to compute lake volume, surface area, and depth.

Results

We summarize results for a series of variables that have been computed for two scenarios: modern (control run) and glacial. Results are presented in several forms: (1) images showing the spatial distribution of the variable; (2) barplots comparing the variables for the two scenarios; and (3) plots showing the ratios in variables for the two scenarios. Only a few representative graphics are presented here to illustrate the major findings. Images are shown only for the month of April, as that describes the status of the water system at the end of the (modern) snow year.

TMAX (Figure 2) shows a clear relation to topography (compare to Figure 1) as is typical of this area and generally is less throughout the study area in the glacial scenario compared to the control. The decrease is greater in the mountains than in the lower elevations and this differential holds in all months. The difference in the annual spatial average of TMAX is -3.2 °C and the greatest change (-6 °C) occurs in the winter months. The change in summer is very small (-1.5 °C) and in July there is a very slight increase (Figure 3). The spatial distribution of PREC also reflects the strong orographic control typical of the western US with most precipitation falling on the mountain crest. No strong seasonal distribution of PREC is indicated but PREC nearly doubles in the glacial scenario compared to the control (Figure 4). The change in PREC mostly reflects a large increase in snowfall which increases by a factor of 2 (July) to 3.5 (March). Rainfall actually decreases in winter (the decreased temperatures lead to more snowfall at the expense of rainfall), increases by a factor of two in July, and shows a clear seasonal cycle in the change.

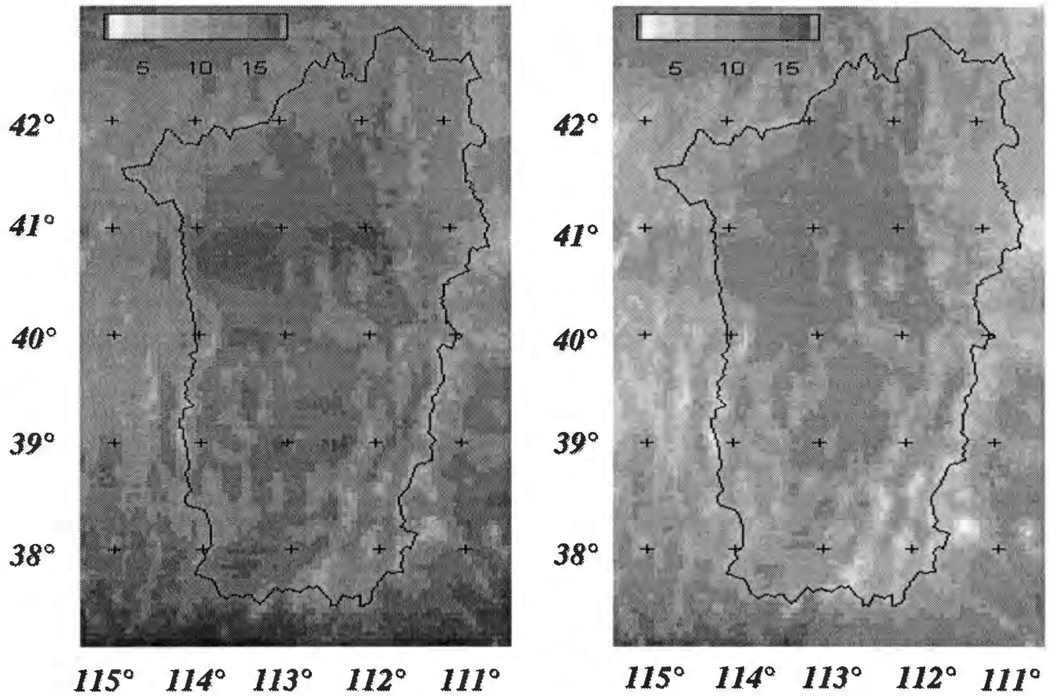

Figure 2 Spatial distribution of April TMAX (°C) for the control run (left) and for the glacial (right) scenarios. Image legends are scaled identically to simplify comparison.

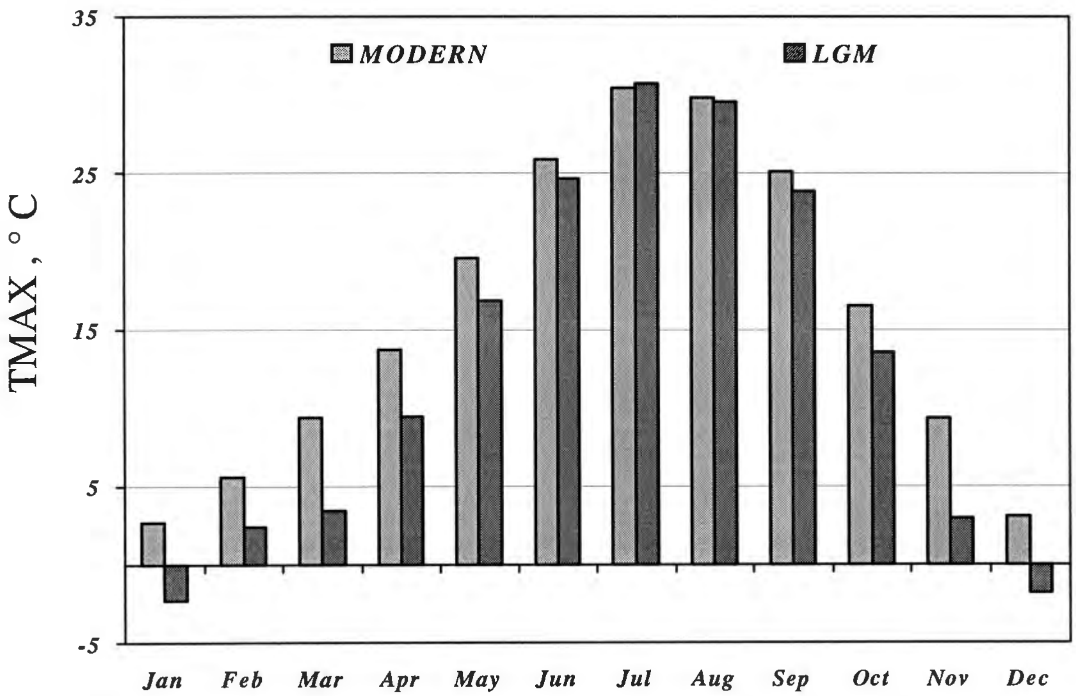

Figure 3 Seasonal patterns of spatial means of TMAX (°C) for the control run and for the glacial.

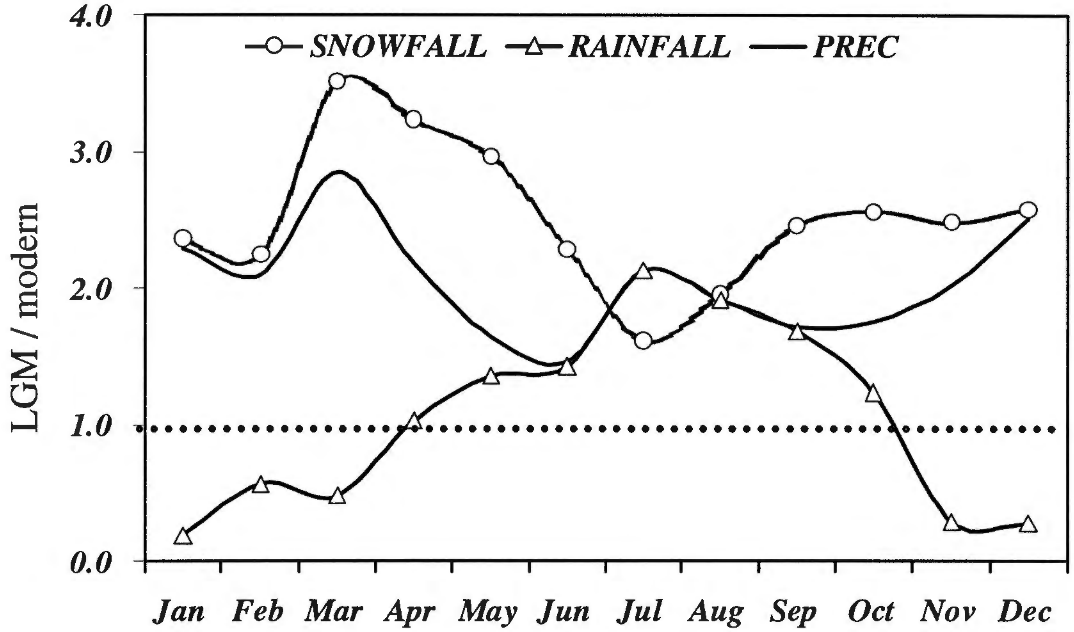

Figure 4 Seasonal patterns of ratios of glacial to control: total precipitation, snowfall, and rainfall

The increased snowfall together with lower temperatures leads to large increases in snowpack (not shown) and snowmelt (Figure 5). Glacial snowmelt exceeds control snowmelt over the year by a factor of two (Figure 6). Much of this snowmelt goes to increased runoff (although ET, not shown, also increases) so that glacial runoff is increased by the same ratio. The surface area of the lake computed to be in equilibrium with the climate and hydrology of the glacial scenario is 25,000 km^2.

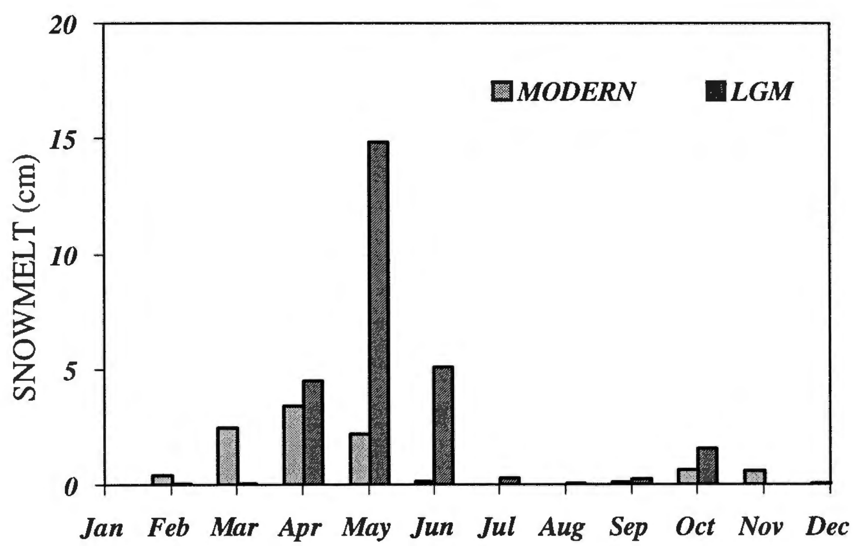

Figure 5 Seasonal patterns of spatial means of snowmelt (cm) for the control run and for the glacial

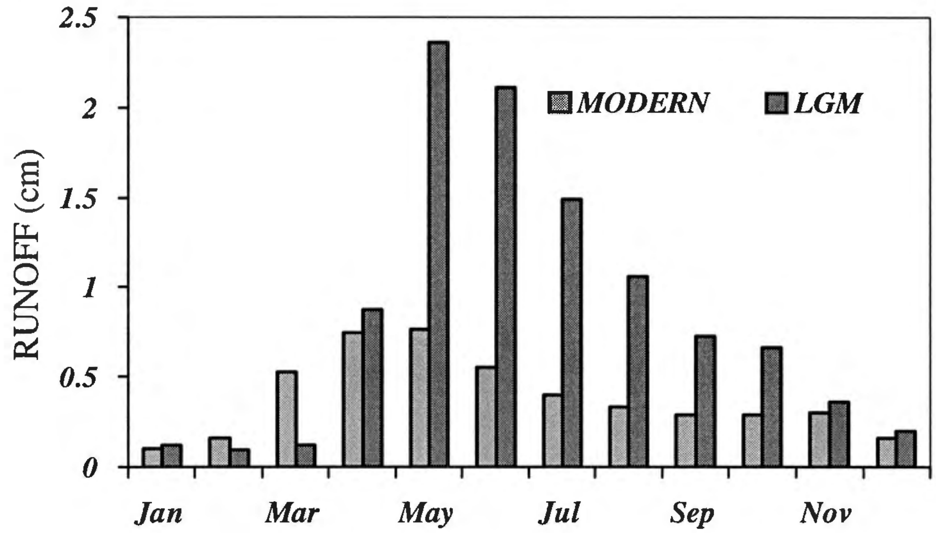

Figure 6 Seasonal patterns of spatial means of runoff (cm) for the control run and for the glacial

Summary

We summarize some of the important results for the two scenarios in Table 1. Here we emphasize the climatic variables that most affect the stability of the hydrologic system of Lake Bonneville. The decrease in temperature and increase in available moisture is in keeping with paleoclimatic evidence from this time period. All of these changes point toward a significant positive modification of the hydrologic regime of Lake Bonneville.

Table 1 Summary of paleoclimatic inferences for the Bonneville basin from the two scenarios

Variable	*Change*	*Modern*	*Glacial*
TMAX	−3.2 °C	15.1 °C	−6 °C November, max cooling
Rainfall	+1.1 x	0.97 cm	Decreased November through March
Snowfall	+3.0 x	0.83 cm	Greater in all months
Peak snowmelt	+3.8 x	April (4 cm)	May (15 cm)
Runoff	+2.7 x	0.32 cm (peak April through May)	0.85 cm (peak May through June)

The comparison of our results with paleoclimate reconstructions based on the field evidences is shown in Table 2. Most of the paleoclimate reconstructions were made for individual geologic sites where the data for paleoclimate interpretations were collected (Figure 7). Our results are annual means for the whole area of monthly grid-wise solutions and so direct comparison may be misleading.

Table 2 Comparison of the modeling results with paleoclimate reconstructions

Source	*Temperature*	*Precipitation*
Thompson and others 1997	-6 °C	x 2.5 to 3.0
Mehringer 1985	Cooler	Moister
Lemons and others 1996	-13 °C	+ 33%
Our results	-3.2 °C	x 2.0

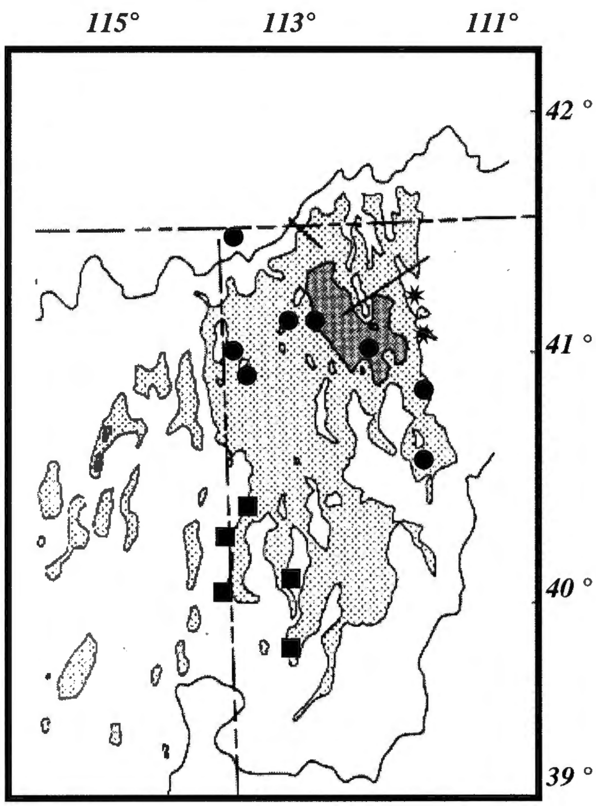

Figure 7 Localities of geologic sites where paleoclimate was estimated. Sources: ■ Thompson (1997); ● Mehringer (1985); ✳ Lemons (1996). The map area was compiled after Oviatt and Miller (1997).

Thompson and others (1997) reported an increased abundance of subalpine conifers and shrubs in the area of Lake Bonneville. From that they infer a climate substantially cooler and wetter than that of today. Our results suggest that at least the area above 2,500 m would have been cool enough (more than 10 °C in the warmest month and less than -3 °C in the coolest month) and wet enough (at least 3 mm precipitation in each month) to support subalpine vegetation (Hidor and Oliver 1993).

We compute increased snowpack in the glacial scenario compared to the modern and that snowpack is most extensive in the Wasatch mountains. Numerous authors (Benson and Thompson 1987; Antevs 1952) have noted the same phenomenon based on the field geologic evidence.

We compute that total runoff in the Lake Bonneville drainage basin was greater, by a factor of two, in the glacial scenario. This result compares favorably with results for other areas in the western US (Smith and Street–Perrott 1983), although we do not know of direct estimates of runoff for the Wasatch. The large deltas that formed at the mouths of rivers discharging into Lake Bonneville during the Late Quaternary (Morrison 1965) would seem to support the notion that discharge of those rivers, most of which drain from the Wasatch Mountains, was considerably higher than today.

Our computed glacial lake surface area (25,000 km^2) corresponds to the Stansbury stand of the Lake Bonneville. Oviatt and Miller (1997), and Currey (1990) indicate that Lake Bonneville reached this size at the Stansbury level during the Late Quaternary.

We have shown that variables (boundary conditions for the LCM) derived from a GCM that is itself driven with global boundary conditions representing conditions during the time that Lake Bonneville was large can yield a local climate and hydrology consistent with the presence of a larger lake. Such a connection between global processes (continental glaciation, reorientation of windfields, and lowered sea level and sea surface temperatures) and the local response of this major hydrologic feature has been suggested in the literature (Antevs 1948; Benson and Thompson 1987), but the complete connection has not been previously demonstrated.

References

Antevs EA. 1952. Cenozoic climates of the Great Basin. *Geologische Rundschau* 40:94–108.

Antevs E. 1948. Climatic changes and pre-white man. In: The Great Basin, With Emphasis on Glacial and Postglacial Times. Bulletin of the University of Utah 38:20. p. 168–191.

Aitchison J and JAC Brown. 1957. The Lognormal Distribution. New York: Cambridge University Press. 176 p.

Barnola JM, D Raynaud, YS Korotkevitch, and C Lorius. 1987. Vostok ice core provides 160,000-year record of atmospheric CO_2. *Nature* 329:408–14.

Benson L and RS Thompson. 1987. The physical record of lakes in the Great Basin. In: North America and Adjacent Oceans During The Last Deglaciation. p 241–260.

Ruddiman WF and HE Wright, Jr., editors. Geological Society of America. The Geology of North America, Volume K-3.

Berger AL. 1978. Long-term variations of daily insolation and Quaternary climate change. *Journal of Atmospheric Science* 35:2362–7.

COHMAP members. 1988. Climatic changes of the last 18,000 years: observations and model simulations. *Science* 241:1043–52.

Currey DR. 1990. Quaternary palaeolakes in the evolution of semidesert basins, with special emphasis on Lake Bonneville and the Great Basin, USA. *Palaeogeography, Palaeoclimatology, Palaeoecology* 76:189–214.

Draper NR and H Smith. 1981. Applied Regression Analysis. John Wiley and Sons, Inc. 709 p.

Fairbanks RG. 1989. A 17,000–year glacio-eustatic sea level record; influence of glacial melting rates on the Younger Dryas event and deep-ocean circulation. *Nature* 342:637–42.

Hidor JJ and JE Oliver. 1993. Climatology: An Atmospheric Science. Macmillan, Inc. p 253–71.

Hostetler SW and F Giorgi. 1992. Use of a regional atmospheric model to simulate lake-atmospheric feedbacks associated with Pleistocene Lakes Lahontan and Bonneville. *Climate Dynamics* 7:39–44.

Hostetler SW, F Giorgi, GT Bates, and PJ Bartlein. 1994. Lake-atmosphere feedbacks associated with paleolakes Bonneville and Lahontan. *Science* 263:265–7.

Lemons DR, MR Milligan, and MA Chan. 1996. Paleoclimatic implications of late Pleistocene sediment yield rates for the Bonneville Basin, Northern Utah. *Paleogeography, Paleoclimatology, Paleoecology* 123(1–4):147–59.

Manabe S and AJ Broccoli. 1985. The influence of continental ice sheets on the climate of an ice age. *Journal of Geophysical Research* 90(C2):2167–90.

Martinec J. 1975. Snowmelt-runoff model for the stream flow forecast. *Nordic Hydrology* 6:145–54.

Mehringer PJ, Jr. 1985. Late-Quaternary pollen records from the interior Pacific Northwest and Northern Great Basin of the United States. In: Pollen Records of the Late Quaternary North American Sediments. American Association of Stratigraphic Palynoligists. p 167–89.

Morrison RB. 1965. Quaternary geology of the Great Basin. In: Wright HE, Jr. and DG Frey, editors. The Quaternary of the United States. A review volume for the VII congress of the International Association for Quaternary Research. Princeton University Press. p 265–86.

National Geophysical Data Center. 1987. Bathymetry/Topographic Data. Data Announcement 88–MGG–002.

O'Connor JE. 1993. Hydrology, Hydraulics, and Geomorphology of the Bonneville Flood. Special Paper #274. The Geological Society of America, Inc. p 5–7, 9–12.

Orndorff RL. 1994. Development of a Surface Hydrological Model and its Application to Modern and Last Glacial Conditions within the Great Basin [dissertation]. Kent (OH): Kent State University. 178 p.

Oviatt CG and DM Miller. 1997. New exploration along the northern shores of Lake Bonneville. *Brigham Young University Geology Studies* 42(Part II):345–71.

Singer M. 1985. Computer Simulation of the Growth and Dessication of Pluvial Lakes in the Southwestern United States [MSc thesis]. Kent (OH): Kent State University. 436 p.

Smith GI and FA Street-Perrott. 1983. Pluvial lakes of the Western United States. In: Proter SC, editor. Late-Quaternary Environments of the United States. Minnesota: University of Minnesota Press. p 190–212.

Stamm JF and A Gettelman. 1995. Simulation of the effect of doubled atmospheric CO_2 on the climate of northern and central California. *Climatic Change* 30:295–325.

Thompson RS, CG Oviatt, AP Roberts, and KH Anderson. 1997. Long-term climatic changes and Great Basin aquatic history. In: Great Basin Aquatic System History (GBASH) Program Abstract Field Guide.

Timofeyeva M and R Craig. 1997. Monte Carlo simulation of streamflow of the Salt River, Arizona. In: CM Isaacs and VL Tharp, editors. Proceedings of the 13th Annual Pacific Climate (PACLIM) Workshop, Technical Report 53 of the Interagency Ecological Program for the Sacramento–San Joaquin Estuary; 1996 Apr 14–17; Asilomar, CA. Sacramento (CA): Interagency Ecological Program for the Sacramento–San Joaquin Estuary. p 93–104.

Timofeyeva M and R Craig. 1998. Using A Monte Carlo technique for modeling the natural variability of streamflow in the headwater of the Sierra Nevada, USA. In: Kovar K, U Tappeiner, NE Peters, and RC Craig, editors. Hydrology, Water Resources and Ecology in Headwaters. International Association of Hydrological Sciences Publication 248. p 59–65.

The 1572–1593 Severe Sustained Drought in the Colorado River Basin: A Reexamination

Hugo G. Hidalgo[1], John A. Dracup[1], Glen Mac Donald[2], and Thomas Piechota[1]
[1]Department of Civil and Environmental Engineering, 5731/5732 Boelter Hall
University of California, Los Angeles
Los Angeles, California 90095-1593
[2]Departments of Geography and Biology, 40 Bunche Hall
University of California, Los Angeles
Los Angeles, California 90095-1524

Introduction

More water is exported from the Colorado River Basin than from any other river basin in the United States. The Colorado River supplies water to more than 25 million people living in seven states: Denver, Salt Lake City, Las Vegas, Phoenix, and Los Angeles. It supplies the extensive holdings of the federal government, as well as dozens of American Indian tribes and the Republic of Mexico. In addition, it generates electricity to supply the annual needs of three million people and irrigates three and one-half million acres of farmland. In fact, about 80% of Colorado River water is used by agriculture (Water Education Foundation 1998).

Rising in the Rocky Mountains northwest of Denver, the Colorado River drops more than 10,000 feet in elevation, into a 246,000 square mile area in the arid Southwest comprising the Upper and Lower Colorado River basins, traveling in all some 1,440 miles before reaching its natural outlet in the Gulf of California. The recorded annual average flow of the Colorado River and its tributaries is approximately 15 million acre-feet per year (Water Education Foundation 1998). This water is fully apportioned; not surprisingly, most years the river never reaches its outlet in the Gulf of California.

In fact, in recent years, the Lower Colorado River basin has been consuming close to or beyond its normal apportionment of 7.5 million acre-feet (maf) (Water Education Foundation 1998), increasing its vulnerability to the occurrence of a severe, sustained drought (SSD). Of even greater concern is the possibility that the Upper Colorado River basin, which supplies most of the water to the system, is vulnerable to a SSD.

Such a drought, one of exceptionally long duration and large magnitude, has been found to have occurred in the Upper Colorado River basin (UCRB). This drought was identified through reconstructions of streamflow at Lee's Ferry, the dividing point between the upper and lower basins, and was based on tree ring records (as proxy indicators) from the runoff producing mountainous areas of the Upper Basin

(Stockton and Jacoby 1976). This drought as reconstructed occurred in the late 1500s and lasted approximately 20 years, during which time the mean annual flow is estimated to have dropped to 10.95 maf, a drop of approximately 20% when compared to the long term reconstructed mean of the 13.5 maf estimated by Stockton and Jacoby in 1976. These figures are yet more disturbing if we consider that the Colorado River Compact, signed in 1922, originally overestimated the annual average flow, basing its water allocations on the availability of 16.4 maf per year (MacDonnell and others 1995).

Michaelson and others (1990) also reconstructed the Lee's Ferry record from tree rings. Their results, when compared to those of the Stockton and Jacoby (1976) reconstruction, are different in drought history, but as in Stockton and Jacoby (1976), results from Michaelson and others (1990) also show evidence of a SSD in the late 16^{th} century. The reconstruction by Michaelson and others (1990) starts very close to the beginning year of the drought; this starting date may not give chronologies with sufficient sample depth (number of cores) for the period of the drought. The present study, therefore, uses the original Stockton and Jacoby reconstructed records, a decision reinforced by the statistical justification of Tarboton (1994, 1995).

Over 75 years ago, the Colorado River Compact was signed and its waters divided among the states according to a series of documents known as the "Law of the River." For the southwestern US, the Law of the River reflects the inherent complexity of managing a diverse source of economic and social interests whose source is the Colorado River (Figure 1). For this reason, making changes in the Law of the River is very difficult and attempts to make changes have been a source of political and legal conflicts among the states for many years. These conflicts have resulted in the Colorado River being one of the most heavily regulated and manipulated rivers in the world (Kenney 1995).

Since the signing of the Colorado River Compact, several researchers have regarded the drought identified in the late 1500s (based on the 1976 Stockton and Jacoby study) to be sufficiently accurate to justify a change in the Law of the River (Tarboton 1995). Other researchers have proposed options for water allocation in the event of a SSD (Henderson and Lord 1995; Sangoyomi and Harding 1995; Lord and others 1995; Booker 1995).

Any changes in the Law of the River should be considered only after new research studies justify such changes. These studies should be designed to address specifically the identification and characteristics of severe sustained droughts in the Upper Colorado River basin.

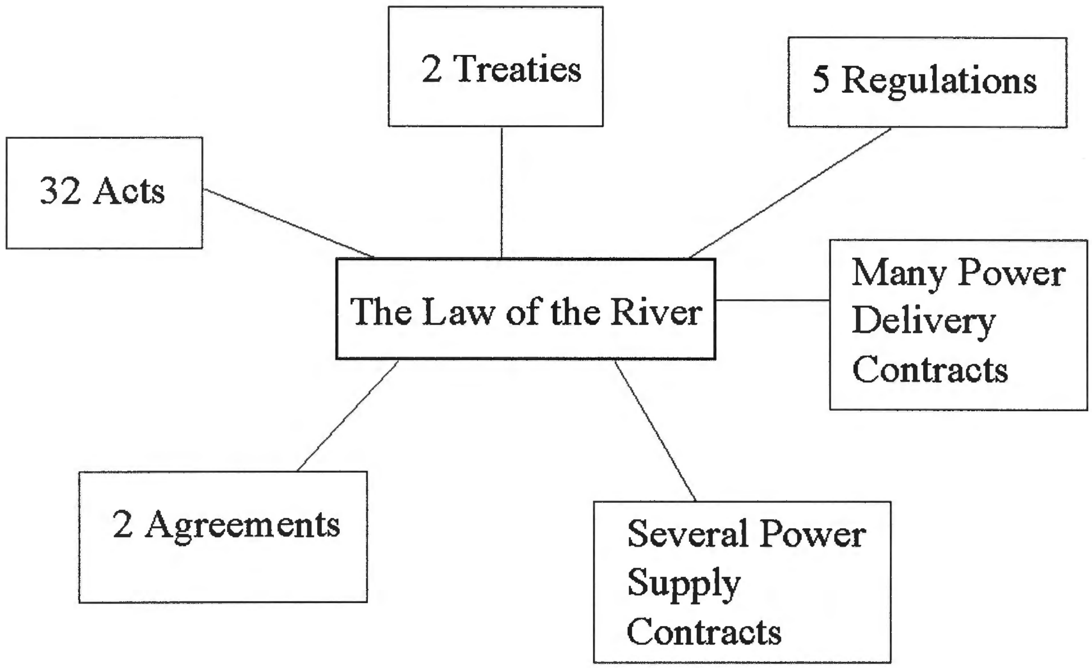

Figure 1 Principle components of "The Law of the River"

Accordingly, we hope to use new data and analytic techniques to refine the tree ring record of the SSD in the late 1500s.

Research Approach

This paper is the preliminary step of a study intended to improve the accuracy of previous streamflow reconstructions based on tree ring analysis in the Upper Colorado River Basin. The study will focus on identifying streamflow characteristics during the 20– to 30–year period in the late 1500s, identified as a SSD through the Stockton and Jacoby record (1976).

To improve the accuracy of natural flow reconstruction in the Colorado River, we will investigate the possibility of updating the Stockton and Jacoby (1976) data by incorporating 30 years of additional climatic and hydrological data as well as recent tree ring chronologies that are available. In addition, new tree ring sites may be sampled and new data processing and reconstruction techniques included.

New Data Available and New Sampling

The flow data set that has been generally used for previous reconstructions of streamflow in the Upper Colorado River basin is the Lee's Ferry record, measured at the legal dividing point between the Upper and the Lower Colorado River basins, immediately downstream of Glen Canyon Dam.

Unimpaired flow data for Lee's Ferry record (LFR) is available from 1896 to 1963. However, from 1896 to 1913, the LFR was extrapolated from other basins surrounding the area, making it less reliable. From 1914 to 1921, the LFR was generated from the Colorado River's three main tributaries: the Green, the Upper Colorado, and the San Juan rivers; the data are assumed to be accurate enough for hydrological studies. Starting in June 1921, reference stakes and staff gages were used to reference the flow to the actual gaging site, which began recording directly in 1923 (Stockton and Jacoby 1976).

Glen Canyon Dam was completed in 1963, seriously impairing the natural flow of the river and discouraging Stockton and Jacoby from continuing their record keeping. We obtained, therefore, a natural (unimpaired) flow record for Lee's Ferry from the US Bureau of Reclamation (Bureau) (1994) covering the years 1905 to 1990. The gaged record for the years following 1963 was adjusted by the Bureau to account for upstream consumption and other losses, especially from diversions and evaporation from Lake Powell (Figure 2).

Preliminary statistical analyses on the Bureau record show significant differences in the autocorrelation structure, variance, and flood frequency in the Colorado River flow after 1970 (Figure 3). Part of the differences in flow characteristics may be attributed to a systematic error in the estimation of the flow adjustment due to consumption upstream of Lee's Ferry. It is apparent, however, that another part of these differences has the characteristics of a real climate shift that occurred around the year 1976, a shift identified by other researchers who examined more than 40 geophysical variables affecting the climate of the Pacific (Ebbesmeyer and others 1991; Francis 1994; Graham 1994; Miller 1994). Further analyses of the Bureau's record may provide more insights about the validity of our interpretation.

If the post–1963 data can extend the calibration period by 27 years, we will be able to use recent tree ring chronologies to calibrate the reconstruction model and thus capture a more accurate picture of the climatic variability in the UCRB.

The tree ring chronologies for calibrating our new reconstruction model were obtained from the NOAA Paleoclimate Data Bank (1997). The data set includes 18 of the 30 sites used in 1976 by Stockton and Jacoby in the original reconstruction at Lee's Ferry. See Table 1 for characteristics of these chronologies and Figure 4 for the location of tree ring sites.

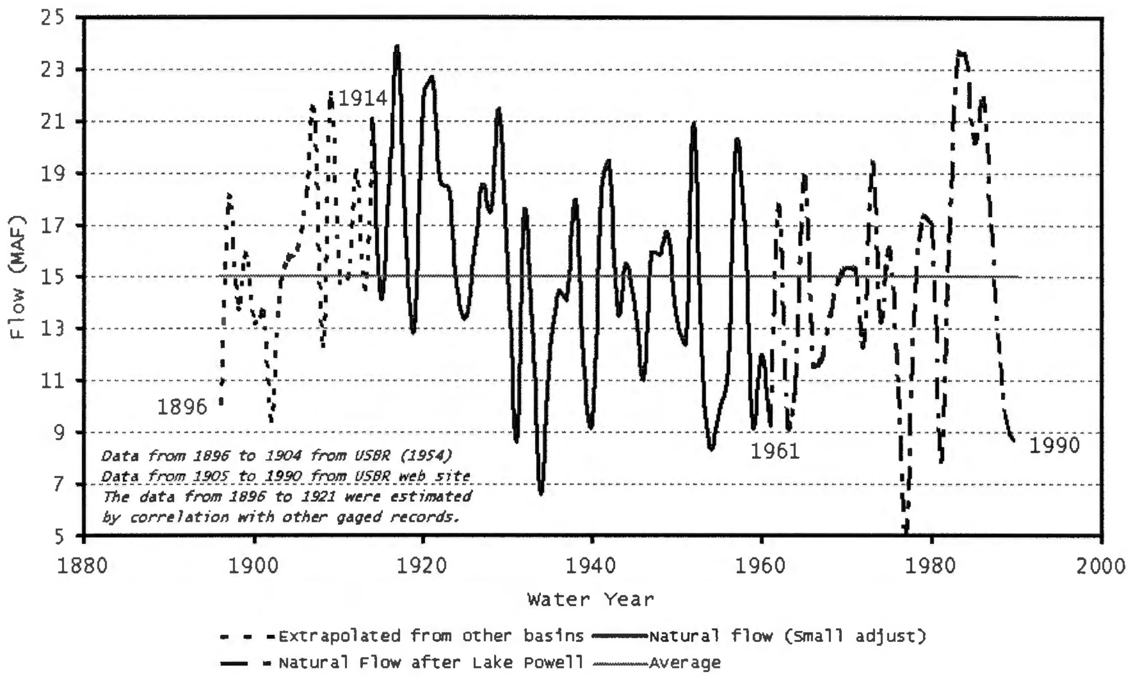

Figure 2 Annual natural flow at Lee's Ferry (Arizona) in million acre feet (maf)

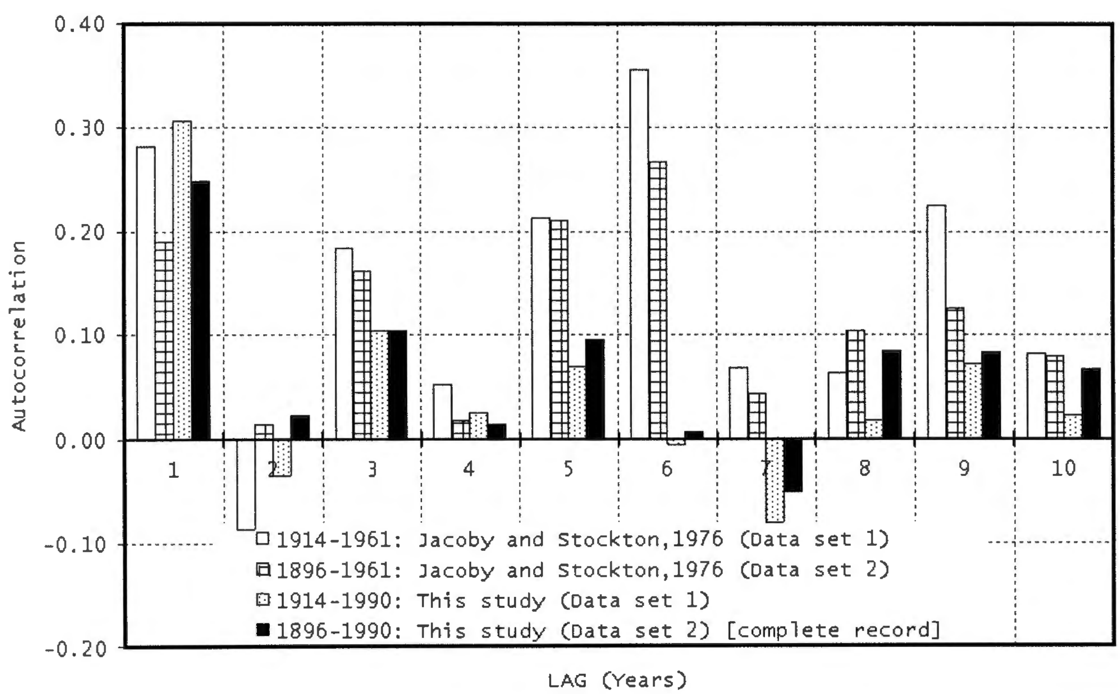

Figure 3A Comparative correlograms, Lee's Ferry Station (Arizona)

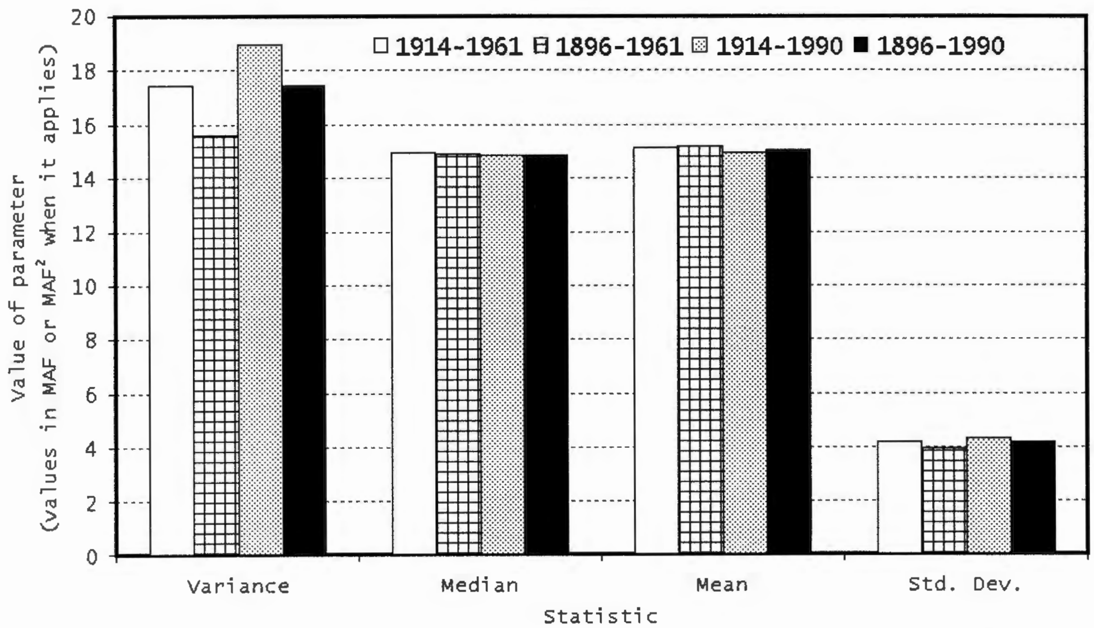

Figure 3B Comparative basic statistical parameters for Lee's Ferry Station (Arizona)

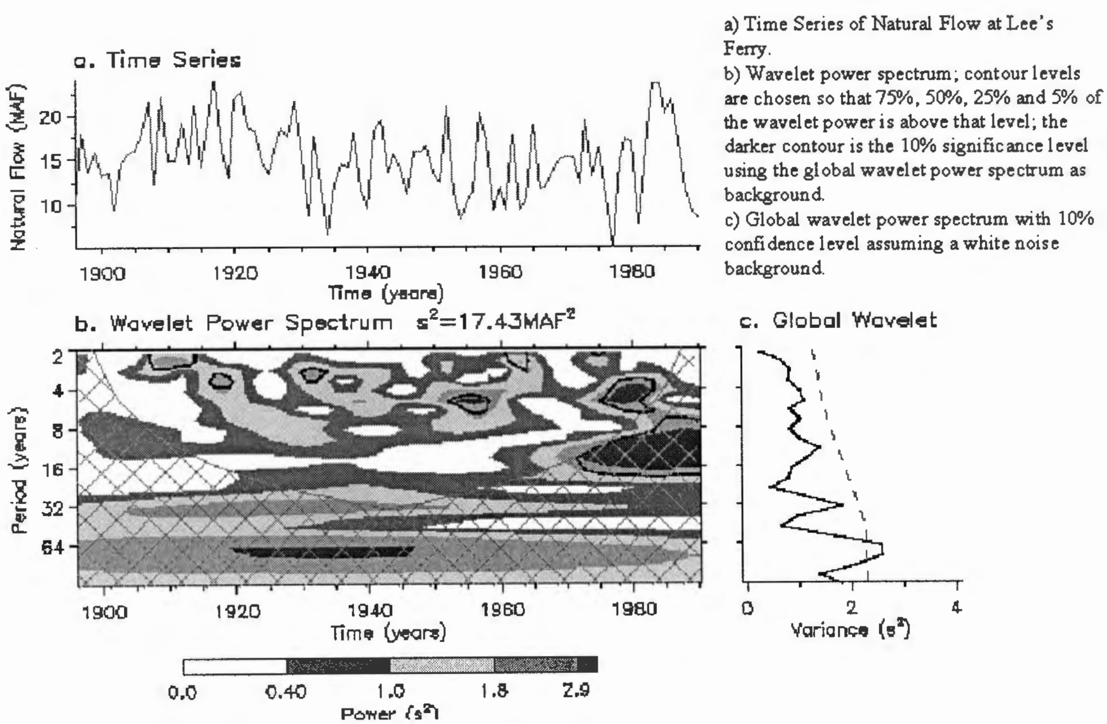

Figure 3C Wavelet power spectrum scaled by the time series variance (s^2) for Lee's Ferry Station (Arizona), computed using the Interactive Wavelet Plot Interface (Torrence 1998)

Table 1 Characteristics of 87 standardized tree ring chronologies in the Upper Colorado River Basin. * Indicates stations in the original Jacoby and Stockton (1976) reconstruction.

#	ID #	NAME	ST	LAT	LON	ELEV	InlY	EndY	SPID	RESEARCHER	mean	var.	Auto correl	MSE	1573-1592	chron. depth
1	ITC599	ITALIAN CANYON	NM	36.73	-105.47	2894	837	1987	PIFL	SWETNAM T.W.	999.73	442.05	0.05	0.53	38	44
2	ISLSTD	ISLAND LAKE STANDARD	CO	40.03	-105.58	3200	1169	1989	PIFL	WOODHOUSE C.	995.03	152.19	0.43	0.13	37	40
3	MAM519	MAMMOTH CREEK	UT	37.65	-112.67	2590	0	1989	PILO	GRAYBILL D.A.	1031.52	369.04	0.14	0.42	31	37
4	GOL519	MT GOLIATH	CO	39.63	-105.58	3535	525	1983	PIAR	GRAYBILL D.A.	982.80	192.42	0.61	0.14	26	27
5	HER519	HERMIT LAKE	CO	38.10	-105.63	3660	1048	1983	PIAR	GRAYBILL D.A.	977.89	217.55	0.68	0.15	25	35
6	WIN519	WINDY RIDGE	CO	39.32	-106.08	3570	1050	1985	PIAR	GRAYBILL D.A.	995.02	178.25	0.62	0.13	25	28
7	WHR519	WILD HORSE RIDGE	UT	39.42	-111.07	2805	286	1985	PILO	GRAYBILL D.A.	982.14	275.27	0.30	0.29	23	23
8	SFP519	SAN FRANCISCO PEAKS	AZ	35.50	-111.67	3535	548	1983	PIAR	GRAYBILL D.A.	966.60	190.55	0.72	0.12	20	28
9	SHEIND	Sheep Mountain INDEX	WY	41.13	-106.05	2375	1412	1990	PSME	EARLE C.J.	988.73	369.13	0.26	0.40	20	40
10	151000	BETATAKIN CANYON	AZ	36.68	-110.53	2042	1263	1972	PSME	SCHULMAN E.	996.00	441.76	0.35	0.47	19	37
11	112549 *	EAGLE	CO	39.65	-106.87	1951	1107	1964	PSME	STOKES M.A.	991.76	351.61	0.63	0.27	19	21
12	433099	TSEGI POINT ROAD	AZ	36.68	-110.53	2196	1490	1972	PIED	DEAN J.S.	1022.10	560.45	0.19	0.73	16	20
13	NIL599	NIWOT RIDGE	CO	40.05	-105.55	3169	1330	1987	PIFL	GRAYBILL D.A.	946.66	171.95	0.73	0.11	16	35
14	640106	SCHULMAN OLD TREE N 1, MESA VERDE	CO	37.20	-108.50	2103	1400	1963	PSME	SCHULMAN E.	1030.20	449.31	0.32	0.47	14	14
15	123000	KANE SPRING	UT	37.53	-109.90	1966	1445	1971	PIED	DEAN J.S.	1014.14	356.69	0.36	0.37	14	20
16	461103	NAVAJO NATIONAL MONUMENT	AZ	36.67	-110.50	2012	1304	1962	PSME	DEAN J.S.	999.89	448.14	0.30	0.49	13	34
17	RCL599	RAINBOW CURVE	CO	40.40	-105.67	3352	1070	1987	PIFL	GRAYBILL D.A.	1021.89	194.37	0.65	0.13	13	21
18	246620	HARD ROCK	AZ	36.20	-110.28	1920	1380	1967	PIED	STOKES M.A.	985.46	413.91	0.41	0.44	12	24
19	123549 *	NINE MILE CANYON (HIGH), UTAH	UT	39.78	-110.30	1920	1194	1964	PSME	STOKES M.A.	990.92	409.71	0.41	0.39	12	14
20	141000	WHITE CANYON	UT	37.62	-110.02	1859	1347	1972	PSME	DEAN J.S.	1015.95	408.31	0.45	0.37	12	20
21	183000	SHONTO PLATEAU	AZ	36.83	-110.73	2134	1365	1971	PIED	DEAN J.S.	1010.55	565.04	0.14	0.77	11	23
22	473629	DOLORES	CO	37.58	-108.55	2195	1270	1978	PIED	HARLAN T.P.	995.18	288.05	0.23	0.32	10	21
23	283000	FORT WINGATE	NM	35.43	-108.53	2268	1478	1972	PIED	ROBINSON W.J.	999.47	441.56	0.33	0.49	10	26
24	130649	WATER CANYON, BRYCE CYN NATL PARK	UT	37.67	-112.10	2098	1336	1964	PIPO	STOKES M.A.	1012.37	259.96	0.51	0.22	10	18
25	091000	CANYON DE CHELLY	AZ	36.10	-109.38	1828	1376	1972	PSME	DEAN J.S.	994.07	294.65	0.55	0.25	9	15
26	75854W	SPRUCE CANYON DB0417	CO	37.18	-108.48	2115	1373	1978	PSME	CLEVELAND M.K.	976.97	321.86	0.42	0.30	9	16
27	133099 *	NAVAJO MOUNTAIN	UT	37.02	-110.85	2286	1469	1971	PIED	DEAN J.S.	1003.53	435.02	0.21	0.53	9	20
28	552590	GROS VENTRE + UHL HILL	WY	43.70	-110.52	2179	1400	1971	PIFL	FERGUSON C.W.	970.49	264.29	0.44	0.24	9	24
29	MB4IND	Medicine Bows 4 INDEX	WY	41.40	-106.28	3290	1421	1990	PCEN	EARLE C.J.	1000.26	194.69	0.55	0.15	9	41
30	423000	MILK RANCH POINT	UT	37.62	-109.73	2286	1276	1970	PIED	DEAN J.S.	1016.49	452.33	0.23	0.53	8	20
31	120549	SALIDA	CO	38.48	-105.93	2195	1328	1964	PSME	STOKES M.A.	933.38	343.46	0.18	0.42	7	10
32	113629 *	EAGLE EAST (JOB 105 REWORKED)	CO	39.67	-106.72	2164	1314	1964	PIED	STOKES M.A.	988.31	291.35	0.34	0.30	7	22
33	273000	TURKEY SPRINGS	NM	35.40	-108.52	2377	1411	1972	PIED	DEAN J.S.	998.71	333.40	0.29	0.35	7	20
34	277550 *	UNITA MOUNTAIN A	UT	40.78	-110.00	3353	1433	1971	PCEN	HARSHA J.B.	990.98	140.39	0.56	0.10	7	20
35	951000	DEAD JUNIPER WASH	AZ	36.17	-110.50	1920	1310	1972	JUSP	DEAN J.S.	973.62	800.15	0.34	0.96	6	6
36	096510	MT. EVANS	CO	39.63	-105.58	3535	977	1968	PIAR	LAMARCHE V.C.	995.94	207.50	0.69	0.13	6	10
37	JCO649	JEFFERSON COUNTY	CO	39.68	-105.20	1965	1550	1987	PIPO	GRAYBILL D.A.	984.40	326.36	0.50	0.28	6	24
38	285620 *	LA SAL MOUNTAINS-SITE A	UT	38.50	-109.25	2323	1489	1972	PIED	HARSHA J.B.	979.27	329.16	0.36	0.34	6	18
39	318599	UHL HILL	WY	43.80	-110.47	2225	1400	1971	PIFL	FERGUSON C.W.	951.88	293.11	0.49	0.26	6	13
40	EDO549	ELDORADO CANYON	CO	39.93	-105.28	1981	1550	1987	PSME	GRAYBILL D.A.	781.36	293.17	0.43	0.32	5	16
41	171000	ECHO AMPHITHEATER	NM	36.35	-106.52	2042	1362	1972	PSME	DEAN J.S.	1002.70	432.04	0.32	0.45	5	22
42	ELR649	ELEPHANT ROCK	NM	36.70	-105.43	2743	1391	1987	PIPO	SWETNAM T.W.	1014.11	439.19	0.33	0.46	5	35
43	283590 *	WIND RIVER MOUNTAINS-SITE D	WY	43.08	-110.07	2500	1492	1972	PIFL	HARSHA J.B.	996.52	259.95	0.56	0.19	5	20
44	158540	DEFIANCE WEST (DEFIANCE/NAZLINI)	AZ	35.87	-109.43	2134	1474	1965	PSME	STOKES M.A.	1019.21	448.49	0.38	0.44	4	18
45	WCP549	WALNUT CANYON	AZ	35.17	-111.52	2057	1420	1987	PIPO	GRAYBILL D.A.	977.76	403.21	0.54	0.40	4	21
46	091519	JICARITA PEAK	NM	36.05	-105.53	3719	1436	1968	PIAR	LAMARCHE V.C.	944.38	367.32	0.89	0.17	4	13
47	FEN649	FENTON LAKE	NM	35.88	-106.67	2560	1532	1986	PIPO	SWETNAM T.W.	1003.49	360.51	0.36	0.37	4	23
48	RIO649	RIO PUEBLO	NM	36.15	-105.60	2469	1555	1986	PIPO	SWETNAM T.W.	1008.43	361.61	0.27	0.38	4	29
49	HIDDEN	Hidden Peak Wasatch Mtn.	UT	40.57	-111.63	3150	1511	1983	PCEN	BRIFFRA K.	978.12	151.67	0.58	0.11	4	24
50	316597	GROS VENTRE, WYOMING	WY	43.63	-110.50	2179	1462	1971	PIFL	FERGUSON C.W.	989.73	279.88	0.36	0.26	4	12
51	113000	DINNEBITO WASH	AZ	36.17	-110.50	1920	1470	1971	PIED	DEAN J.S.	990.11	483.47	0.43	0.52	3	22
52	101099	TSEH-YA-KIN CANYON	AZ	36.22	-109.35	1951	1500	1971	PSME	DEAN J.S.	980.56	336.80	0.54	0.29	3	20
53	159640	DEFIANCE EAST (FT. DEFIANCE)	AZ	35.83	-109.12	2316	1554	1965	PIPO	STOKES M.A.	1006.16	508.78	0.33	0.56	3	16
54	061099 *	BOBCAT CANYON	CO	37.17	-108.52	2042	1390	1971	PSME	DEAN J.S.	969.54	429.23	0.27	0.46	3	18
55	115549 *	CHICAGO CREEK	CO	39.68	-105.63	2835	1441	1964	PSME	STOKES M.A.	993.30	385.58	0.29	0.39	3	8
56	426549	WAGON WHEEL GAP	CO	37.80	-106.83	2743	1452	1940	PSME	SCHULMAN E.	1001.64	618.24	0.47	0.61	3	5
57	012000	DITCH CANYON	NM	37.00	-107.82	2073	1555	1971	PIPO		1012.12	395.92	0.50	0.36	3	24
58	161000	SATAN PASS	NM	35.60	-108.13	2286	1381	1972	PSME	DEAN J.S.	1047.13	597.18	0.39	0.58	3	24
59	292099	EL MORRO	NM	35.03	-108.35	2225	1536	1972	PIPO	DEAN J.S.	1017.49	552.67	0.45	0.56	3	22
60	280620 *	UINTA MTNS, SITE D, UTAH	UT	40.62	-109.95	2289	1423	1971	PIED	HARSHA J.B.	999.25	316.36	0.45	0.30	3	8
61	503649	PEDRO MTNS A + ALCOVA A + SEMINOE	WY	42.35	-106.85	2185	1536	1964	PIPO	STOKES M.A.	996.03	256.64	0.39	0.24	3	42
62	108549	LARAMIE, SITE A (WOODS CREEK)	WY	41.10	-106.08	2591	1444	1964	PSME	STOKES M.A.	988.02	438.74	0.38	0.46	3	16
63	617629	PARIA PLATEAU	AZ	36.83	-112.05	1860	1481	1975	PIED	HARLAN T.P.	991.02	403.42	0.27	0.47	2	24
64	KBE639	KAIBAB PLATEAU	AZ	36.63	-112.10	2100	1482	1976	PIED	STOKES M.A.	968.81	322.78	0.19	0.38	2	26
65	SNOWBO	Snow Bowl San.Fr. Peak	AZ	35.43	-110.20	3150	1453	1983	PCEN	BRIFFA K.	1005.32	173.27	0.63	0.12	2	23
66	472540	DOLORES	CO	37.58	-108.55	2286	1457	1978	PSME	HARLAN T.P.	973.08	342.14	0.53	0.29	2	22
67	533000	OWL CANYON	CO	40.80	-105.18	1859	1560	1964	PIED	FRITTS H.C.	985.30	318.17	0.44	0.31	2	20
68	117549 *	BLACK CANYON OF THE GUNNISON RIVER	CO	38.57	-107.70	2426	1478	1964	PSME	STOKES M.A.	949.14	345.91	0.51	0.30	2	7
69	TIO559	TIMBERLINE PASS	CO	40.37	-105.67	3505	1510	1987	PCEN	GRAYBILL D.A.	980.01	180.19	0.57	0.13	2	23
70	092519	RED DOME	NM	36.55	-105.38	3688	1535	1968	PIAR	LAMARCHE V.C.	953.43	255.47	0.86	0.12	2	14
71	642649	LOS ALAMOS	NM	35.87	-106.30	2164	1513	1969	PIPO	O'BRIEN D.	1012.67	409.98	0.39	0.40	2	9
72	105599	PEDRO MTNS, SITE B (PRAIRIE)	WY	42.35	-106.85	2225	1508	1964	PIFL	STOKES M.A.	1004.47	308.13	0.40	0.27	2	7
73	051549	ELBOW CAMPGROUND, JACKSON	WY	43.22	-110.78	1981	1490	1965	PSME	FERGUSON C.W.	972.73	337.45	0.59	0.27	2	32
74	MEDICI	Medicine Bow Peak	WY	41.30	-107.70	3150	1401	1983	PCEN	BRIFFA K.	994.25	176.24	0.49	0.14	2	28
75	182649	WALNUT CANYON NATIONAL MONUMENT	AZ	35.18	-111.52	2073	1447	1966	PIPO	STOKES M.A.	974.93	409.37	0.38	0.46	1	26
76	110549 *	NEW NORTH PARK	CO	40.92	-106.33	2469	1354	1964	PSME	STOKES M.A.	1000.69	366.42	0.57	0.29	1	21
77	116549 *	UPPER GUNNISON	CO	38.68	-106.87	2530	1322	1964	PSME	STOKES M.A.	956.48	341.11	0.29	0.36	1	7
78	MIO559	MILNER PASS	CO	40.42	-105.80	3413	1570	1987	PCEN	GRAYBILL D.A.	978.16	192.26	0.68	0.12	1	24
79	MOP640	MONARCH LAKE	CO	40.10	-105.73	2621	1430	1987	PIPO	GRAYBILL D.A.	1017.67	210.81	0.64	0.13	1	24
80	NWR000	NIWOT RIDGE	CO	40.07	-105.58	3700	1539	1979	PCEN	HANSEN-BRISTOW K.	987.69	232.02	0.68	0.14	1	25
81	07154W	PUEBLITA CANYON DB0418 TOTAL RING	NM	36.68	-107.32	2073	1570	1978	PSME	CLEAVELAND M.K.	974.19	428.15	0.28	0.44	1	9
82	75654W	CRYSTAL DB0415 TOTAL RING	NM	35.97	-108.80	2755	1540	1978	PSME	CLEAVELAND M.K.	983.18	321.72	0.41	0.29	1	12
83	CAT649	CAT MESA	NM	35.78	-106.62	2515	1572	1986	PIPO	SWETNAM T.W.	1029.07	346.96	0.32	0.34	1	21
84	132000	NAVAJO MOUNTAIN	UT	37.03	-110.85	2377	1565	1971	PIPO	DEAN J.S.	1005.92	430.47	0.43	0.45	1	21
85	151211	NINE MILE CANYON, UTAH	UT	39.78	-110.30	1920	1201	1949	PSME	SCHULMAN E.	1018.27	416.38	0.27	0.43	1	1
86	ELECTR	Electric Lake	UT	39.58	-111.33	2970	1542	1983	PCEN	BRIFFA K.	1031.04	233.06	0.57	0.15	1	24
87	104640	ALCOVA RESERVOIR, SITE A	WY	42.52	-106.73	1859	1544	1964	PIPO	STOKES M.A.	991.54	336.24	0.45	0.31	1	20

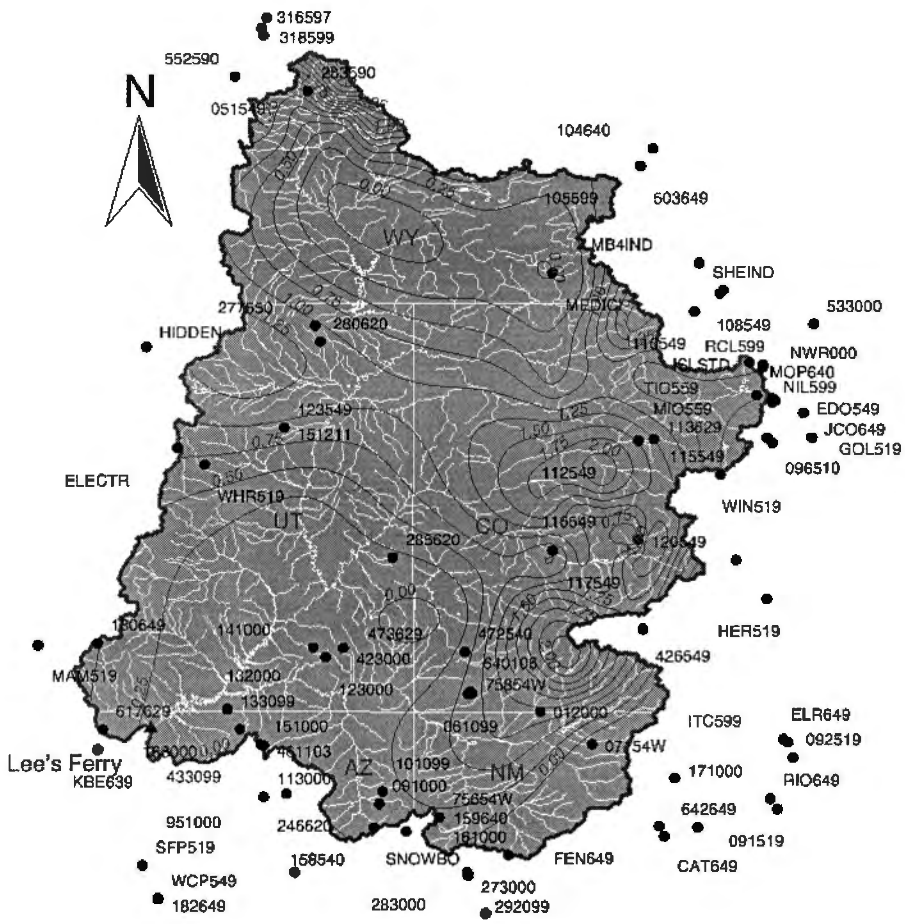

Figure 4 Upper Colorado River basin showing tree ring sites and yield contours (ft/yr)

The reconstruction by Stockton and Jacoby included some chronologies for the late 1500s with a small sample depth. An adequate sample depth is defined as one that will guarantee a small chronology error and can be measured using the signal-to-noise ratio (Cook and Kairiuskstis 1990; Fritts 1991). Fritts (1991) also discusses the sensitivity of the chronology error in relation to this sample depth, which is the number of cores that form a chronology. Figure 5 summarizes the sensitivity of this relationship. Any study that focuses on the flow characteristics in the UCRB during the late 1500s should include an adequate sample depth for all the chronologies used in reconstructing flow during those latter decades.

In addition, new tree ring data should be sampled in those sites where a good climatic signal is expected and where recent chronologies are not available. These areas correspond to high yield areas in northeastern Utah and southeastern Wyoming, which produce most of the water for the Green River subbasin and contribute 35% to the total flow at Lee's Ferry, as well as the San Juan River subbasin located in the Four Corners area, which contributes approximately 16% of the total flow at Lee's Ferry (Stockton and Jacoby 1976) (see Figure 4).

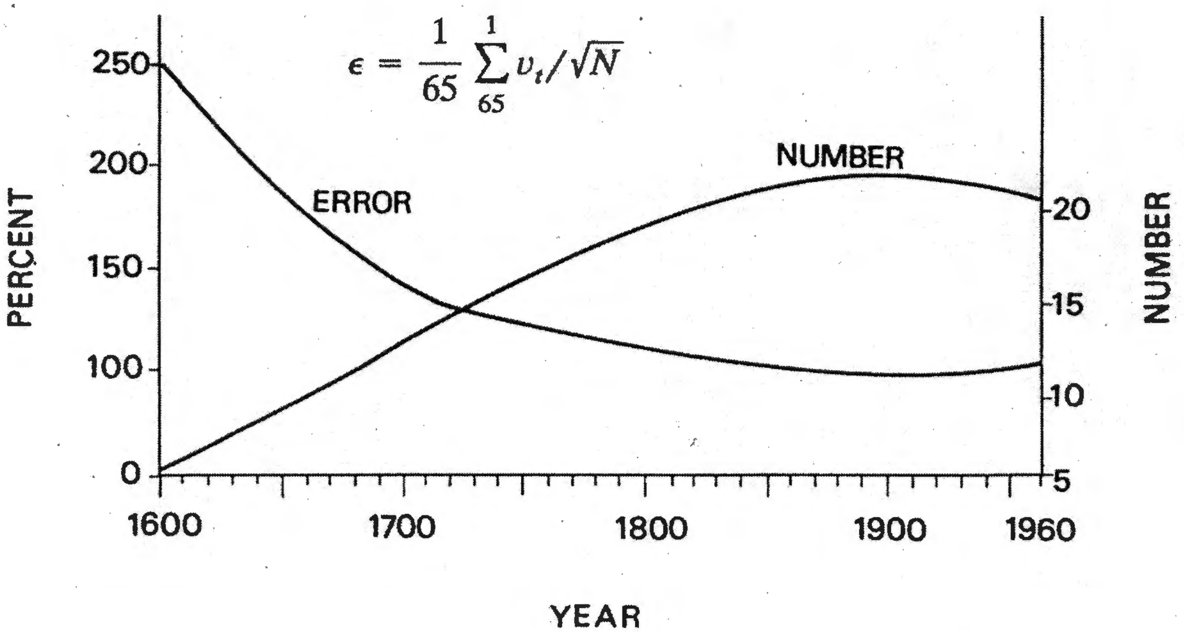

Figure 5 Average number of cores and the estimated average error of 65 standardized chronologies plotted as a function of the year in which the rings were formed. Where ϵ: chronology error, v_t: variance in common up to year t, and N: number of cores that composes a chronology. From Fritts (1991).

New Data Processing and Reconstruction Techniques

Since the original Stockton and Jacoby (1976) study was done, reconstruction procedures have greatly improved. New procedures for detrending raw measurements are available for correcting ring width series in trees with special growth characteristics (Cook and Peters 1981; Cook and Peters 1997). Adjustments and filters to stabilize the variance and reduce the influence of non-climatic information are now part of dendrochronology studies (Meko and others 1993).

Dendrohydrological reconstructions have traditionally been done using measurements of tree ring widths. However, the density of late wood has also been shown to be sensitive to climatic variations (Schweingruber 1996). Wood density is measured using X-rays and can provide an additional record of droughts. New ring samples should be collected at a number of sites in the basin in order produce a reconstruction of the Upper Colorado River flow using tree ring density records.

Principal Components Analysis (PCA), the technique that has been used most extensively for reconstructing past climatic variability, regresses the components derived from tree ring chronologies onto the climatic variable (in other words, streamflow). This technique has always allowed several procedural choices that may result in very different reconstructions (Figure 6). But today, researchers are more aware of the need for proper validation procedures and for statistics that allow selection of the model with the least predicting error and the fewest number of variables, ensuring the necessary connection with the physical processes modeled.

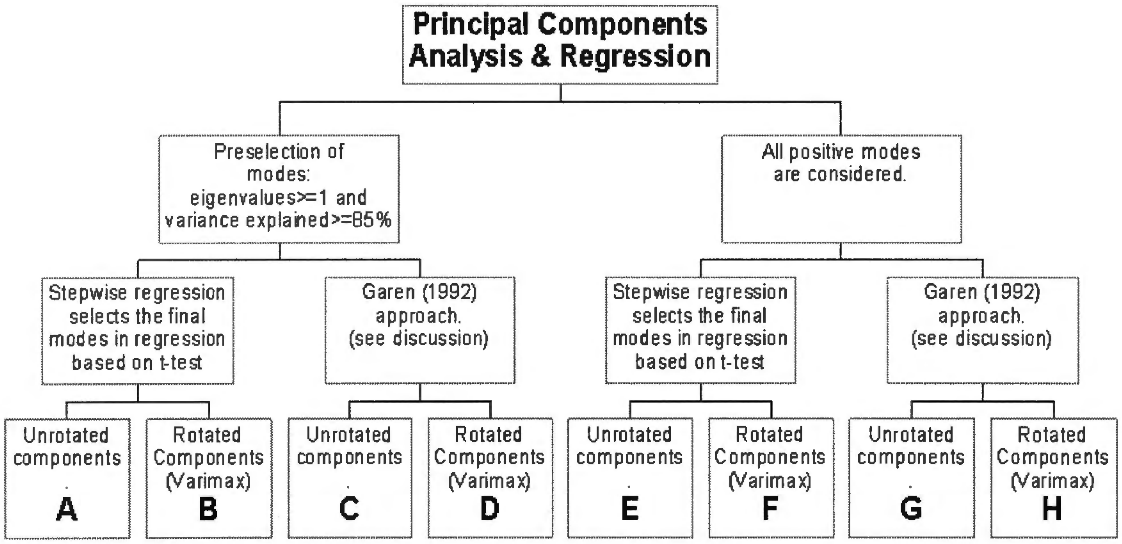

Figure 6 Possible different models obtained by changing options in reconstructions regressing principal components of tree rings onto the climatic variable

The coefficient of determination (R^2) and the standard error of the mean ($S_{\bar{x}}$) may not be sufficient conditions to optimize the selection of the model that most accurately predicts climatic variability. Independent testing or cross validation may be a better way to identify the model that best represents the physical processes (Jackson and Chan 1980; Wu 1986; Das Peddada and Patwardhan 1992; Garren 1992), and this involves using the minimum number of variables (a parsimonious model) that reduces the influence of unrelated noise.

Because of the relatively high autocorrelation in tree ring chronologies, even after detrending, and to account for the biological carryover effects from year to year, it is common practice to include lagged chronologies in the reconstruction model. Including too many variables, however, may result in "overfitting" the model, making it able to predict even the smallest variations in the observed data, but with a low predictive skill for unobserved cases (Jackson and Chan 1980). Cross validation can be a way to overcome this "overfitting" problem and to improve the accuracy of the model. Meko (1997) proposes using cross validation techniques to calibrate the model, but suggests using individual trees instead of site chronologies.

An alternative solution to lagging the series is to "prewhiten" them, using low order autoregressive (AR) models that amplify the contemporaneous signal (Meko and others 1993), but not all chronologies are simple enough to serve as AR models.

Finally, Young (1994) gives procedures for measuring the skill from streamflow reconstructions using tree rings. Errors in streamflow drought statistics reconstructed from tree ring data have been studied by Brockway and Bradley (1995), who propose methods to measure these errors.

Conclusions

The validity of the drought in the Colorado River Basin in the late 1500s has to be confirmed by a specific paleoclimatic study designed to investigate this period. This study should include all the new streamflow and tree ring data and should employ techniques not available in previous reconstructions. A new study should also include any confirming proxy data from fields outside dendrochronology, such as archaeology, paleontology, sedimentology, and paleolimnology.

Significant improvements in the reconstructions of the UCRB can be obtained from new data and techniques presently available to the researchers. These improvements can be summarized as the possibility of using new climatic and tree ring data, the availability of new procedures for detrending tree ring width measurements, the use of wood density records as an alternative to ring width measurements, and the use of analytical procedures for "prewhitening" and stabilizing variance from tree ring chronologies. Additionally, reconstruction techniques can be refined by proper validation procedures designed to select the model with the best predictive skill. Recent techniques allow us to measure this predictive skill, the accuracy of both the resulting flow estimation, and the drought parameters derived from the reconstructed flow.

Acknowledgments

The research leading to this report was supported by the University of California Water Resources Center, as part of the Water Resources Center Project UCAL-WRC-W-889. We thank Judy King and Miriam Reed for editing this paper.

References

Booker JF. 1995. Hydrologic and economic impacts of drought under alternative policy responses. *Water Resources Bulletin* 31(5):889–906.

Brockway CG and AA Bradley. 1995. Errors in streamflow drought statistics reconstructed from tree ring data. *Water Resources Research* 31(9):2279–93.

(USBR) US Bureau of Reclamation. United States Department of the Interior. 1994 [cited 21 September 1998]. Biological Assessment [Project]. In: United States Bureau of Reclamation Homepage [on-line]. Available from World Wide Web: http://www.usbr.gov/main/index.html.

Cook E and Kairiukstis. 1990. Methods of Dendrochronology: Applications in the Environmental Science. The Netherlands: Kluwer Academic Publishers. 582 p.

Cook ER and K Peters. 1981. The smoothing spline: a new approach to standardizing forest interior tree-ring width series for dendrochronology studies. *Tree-ring Bulletin* 41:45–53.

Cook ER and K Peters. 1997. Calculating unbiased tree-ring indices for the study of climatic and environmental change. *Holocene* 7:361–70.

Das Peddada S and G Patwardhan. 1992. Jacknife variance estimators in linear models. *Biometrika* 79(3):654–7.

Ebbesmeyer CC, DR Cayan, DR McClain, FH Nichols, DH Peterson, and KT Redmond. 1991. 1976 step in Pacific climate: forty environmental changes between 1968–1975 and 1977–1984. In: Betancourt JL and VL Tharp, editors. Proceedings of the 7th Annual Pacific Climate (PACLIM) Workshop, Interagency Ecological Study Program Technical Report 26; 1990 Apr; Asilomar, CA. Sacramento (CA): Interagency Ecological Study Program. p 115–126.

Francis RC and SR Hare. 1994. Decadal-scale regime shifts in the large marine ecosystems of the north-east pacific: a case for historical science. *Fisheries Oceanography* 3(4):279–91.

Fritts HC. 1991. Reconstructing Large-scale Climatic Patterns from Tree-Ring Data: A Diagnostic Analysis. Tucson (AZ): The University of Arizona Press. 286 p.

Garen DC. 1992. Improved techniques in regression-based streamflow volume forecasting. *Journal of Water Resources Planning and Management* 118(6):654–70.

Graham NE. 1994. Decadal-scale climate variability in the tropical and North Pacific during the 1970s and 1980s: observations and model results. *Climate Dynamics* 10:135–62.

Henderson JL and WB Lord. 1995. A gaming evaluation of Colorado River drought management institutional options. *Water Resources Bulletin* 31(5):907–24.

Jackson DN and DW Chan. 1980. Maximum-likelihood estimation in common factor analysis: a cautionary note. *Psychological Bulletin* 88(2):502–8.

Kenney DS. 1995. Institutional options for the Colorado River. *Water Resources Bulletin* 31(5):837–50.

Lord WB, JF Booker, DM Getches, BL Harding, DS Kenney, and RA Young. 1995. Managing the Colorado River in a severe sustained drought: an evaluation of institutional options. *Water Resources Bulletin* 31(5):939–44.

MacDonnell LJ, DH Getches and WC Hugenberg, Jr. 1995. The law of the Colorado River: coping with severe sustained drought. *Water Resources Bulletin* 31(5):825–36.

Meko D, ER Cook, DW Stahle, CW Stockton, and MK Hughes. 1993. Spatial patterns of tree-growth anomalies in the United States and southeastern Canada. *Journal of Climate* 6:1773–86.

Meko D. 1997. Dendroclimatic reconstruction with time varying predictor subsets of tree indices. *Journal of Climate* 10:687–96.

Michaelsen J, HA Loaiciga, L Haston, and S Garver. 1990. Estimating Drought Probabilities in California Using Tree-Rings. Completion report to California Department of Water Resources. California: University of California, Santa Barbara, Department of Geography.

Miller AJ, DR Canyan, TP Barnett, NE Graham, and JM Oberhuber. 1994. The 1976–1977 climate shift of the Pacific Ocean. *Oceanography* 7:21–6.

(NOAA) National Oceanographic and Atmospheric Administration. United States Department of Commerce. 1997 [cited 3 January 1998]. International Tree Ring Data Bank. NOAA Paleoclimatology Program at the National Geophysics Data Center. Boulder Colorado. In: WDC Paleoclimatology Program Homepage [on-line]. Available from World Wide Web: http://www.ngdc.noaa.gov/paleo/treering.html.

Sangoyomi TB and BL Harding. 1995. Mitigating impacts of a severe sustained drought on Colorado River water resources. *Water Resources Bulletin* 31(5):925–38.

Schweingruber FH. 1996. Tree rings and Environment. Paul Haupt, Berne. 609 p.

Stockton CW and GC Jacoby, Jr. 1976. Long-term Surface-Water Supply and Streamflow Trends in the Upper Colorado River Basin Based on Tree-Ring Analysis. Lake Powell Research Project Bulletin Nr. 18. California: Institute of Geophysics and Planetary Physics, University of California Los Angeles, California. 70 p.

Tarboton DG. 1994. The source hydrology of severe and sustained drought in the southwestern United States. *Journal of Hydrology* 161:31–9.

Tarboton DG. 1995. Hydrologic scenarios for severe sustained drought in the southwestern United States. *Water Resources Bulletin* 31(5):803–13.

Torrence C and GP Compo. 1998. A practical guide to wavelet analysis. *Bulletin of the American Meteorological Society* 79(1):61–78.

Water Education Foundation. 1998. Layperson's Guide to the Colorado River. Sacramento (CA): Water Education Foundation. 28 p.

Wigley TML, KR Briffa, and PD Jones. 1984. On the average value of correlated time series with applications in dendrochronology and hydrometeorology. *Journal of Climate and Applied Meteorology* 23:201–13.

Wu CFJ. 1986. Jacknife, bootstrap and other resampling methods in regression analysis. *The Annals of Statistics* 14(4):1261–95.

Young KC. 1994. Reconstructing streamflow time series in central Arizona using monthly precipitation and tree-ring records. *Journal of Climate* 7:361–74.

No El Niño, But Variable Precessional Insolation, Antiphase Interhemispheric Climate Trends, and Globally Synchronous Secondary Cycles

Thor Karlstrom
US Geological Survey, retired
4811 SW Brace Point Drive
Seattle, WA 98136

Abstract

Additional time series, analyzed since the publication of my last paper (Karlstrom 1997), continue to support the Solar Insolation/Tidal Resonance Climate Model by recording latitudinal variability for longer-term climate trends, but globally-synchronous, shorter-term trends.

Introduction

Evaluation of marine and terrestrial climate records (Karlstrom 1955, 1956, 1961) suggested support for the Milankovitch Climate Model. The probable distinction between the 20,000–year precessional insolation controls of lower latitudes and the 40,000–year obliquity insolation controls, operating synchronously in both polar regions, was emphasized. In addition, the highest resolution records then available suggested a harmonic series of smaller cycles (those with wavelengths of several thousands and fewer years). However, because of numerous geographic gaps (mainly in the Southern Hemisphere) and extant dating uncertainties, better geographic coverage and many more well-dated records were required to empirically validate and refine these conclusions.

Subsequent Work

Since then, hundreds of dated climate time series have been published in the international literature. Based largely on marine chronostratigraphy, most geologists by the 1970s had accepted the Milankovitch Climate Model and, along with this, the concept of inter hemispheric synchrony modulated solely by the obliquity-dominated, 60°N–65°N latitude solar insolation (Hays and others 1976; Martinson and others 1987). Also by the 1970s, most researchers were correlating their terrestrial records with the “standard” marine record (Figure 1) on the assumption of global synchrony. Some, however, also produced high-resolution glacial chronologies that correlate surprisingly well with dated sea level records (Richmond 1976; Terasmae and Dreimanis 1976) and with the precessionally-dominated, 45°N latitude insolation curve of the Milankovitch Model (Figure 2).

Since the early 1960s, I have analyzed scores of high-resolution proxy climate records dated by history, tree rings, varves, archaeology, radiocarbon, Th/U, and K/A (Karlstrom 1966, 1975, 1976, 1988, 1995, 1996, 1997, 1998; Hevly and Karlstrom 1974; Euler and others 1979). These records collectively support elements of both latitudinal variability (Figure 3) and high-frequency global synchrony (Figures 7, 12, 14, and 17).

Additional Supporting Records

This paper presents additional supporting records analyzed since my last paper (Figures 4–12, 15, 16, and 20), along with examples of previously published records to clarify cyclical context and regional correlations (Figures 1–3, 13, 14, 7–19, and 21–23).

Long-term Climate Trends and Interhemispheric Correlations

Figures 4 through 9 provide examples of Northern Hemisphere climate records whose primary trends most closely parallel those of local insolation that varies latitudinally because of changing precessional components.

By contrast, Figures 11 and 12 exemplify Southern Hemisphere records that most closely parallel local precessional insolation curves which trend 180 degrees out of phase with their Northern Hemisphere counterparts. Temporal displacement of summer solar insolation peaks and troughs across the equator is approximately 10,000 years, or sufficiently large so that correlative antiphasing climatic trends should be distinguishable by using more accurate, current dating procedures.

Northwest Paleoclimatic Records: the Cook Inlet Glacial Chronology and Correlates

Figures 13 through 17 provide pollen and organic-content records from Alaska and the Yukon Territory, Canada. These records essentially confirm the cyclical elements first inferred from glacial and bog chronostratigraphy in the Cook Inlet region of Alaska and as fortified by corroborative evidence from other parts of the Northern Hemisphere (see Figure 18).

Tree Ring Records, Higher Frequency Cycles, and Regional Patterns

Figures 19 and 20 show tree ring records that represent the most accurately dated proxy climate time series, however, they also vary appreciably in the amount of climatic information they contain (<50% to >90%). Numerous Southwest records from New Mexico to California define by half-cycle smoothing a robust 139–year Event Cycle (see Figure 19). This Event Cycle is one-half of the Subphase Cycle (278 years), as defined by tidal bog chronostratigraphy (see Figure 13), tree rings (see Figure 20), historical record (see Figure 21), marine record (see Figure 22), as well as by statistical analyses of basal-contact (Point Boundary) dates (see Figures 13 and 19).

The widespread occurrence of the Event Cycle suggests that it probably reflects the regional dynamics of Southwest atmospheric circulation patterns. Thus, similar analyses of tree ring records in other regions may provide similar or differing patterns that may enhance understanding of overall circulation or differing biologic responses.

To test this possibility, I have extended analyses to the longest of the tree ring records defined by numerical indices in Schulman (1956). Localities of these records range from Canada to the Southwest and from western to midwestern states. The resulting half-cycle patterns vary appreciably, but more than half show strong tendencies to phase with subharmonic elements of the Solar Insolation/Tidal Resonance Climate Model (see Figure 20).

Whereas two records taken east of the southern Rocky Mountains phase strongly with the 139–year Event Cycle (or similar to the pattern defined west of the Southern Rocky Mountains), several of the records from more northern localities oscillate in phase with its half cycle of 69.5 years, the Subevent Cycle.

By timing and duration, the Subevent Cycle is the same as the 70–year cycle recorded in global temperatures (Schlesinger and Ramankutty 1994) and as extended back into the mid-Holocene by correlation with the dated beach sequence of northern Lake Michigan (Delcourt and others 1996). The northerly distribution of this pattern suggests that it relates to jet stream displacements and resulting dynamics of southward penetrating Arctic and Polar air masses.

Tidal/Sunspot/Climate Correlation

Finally, Figure 23 provides the strongest empirical evidence to date for an interrelated tidal and solar modulator of terrestrial climate. Solar process is apparently related to both tidal process and climate by common phasing with the 3/1 (46.33 year) resonance of the Event Cycle and its double, the Gleissberg Cycle (92.67 years).

Summary

Additional time series presented in this paper continue to support the Solar Insolation/Tidal Resonance Climate Model and suggest explanations for both climate variability and climate synchrony of cycles ranging in wavelengths from tens of thousands of years to decades. According to the model, there has been a natural cyclical trend toward increasing temperatures since the 1850s (see Figure 23). Such a natural trend has not been considered by meteorological programmers who have assumed instead that the instrumentally recorded temperature rise since the industrial revolution results solely from man's own progressive CO_2 contamination of the atmosphere. Thus, it is not clear how much of the recent "global warming" is man's doing or the product of natural climatic process. Unless this question is quantitatively resolved, simple projections of current short-term CO_2

trends into the future remain uncertain. Because of variability in recurrences (two to seven years), it is also unclear how the El Niño seasonal (winter) phenomenon relates to the long-term climatic trends discussed above (see also Karlstrom 1996).

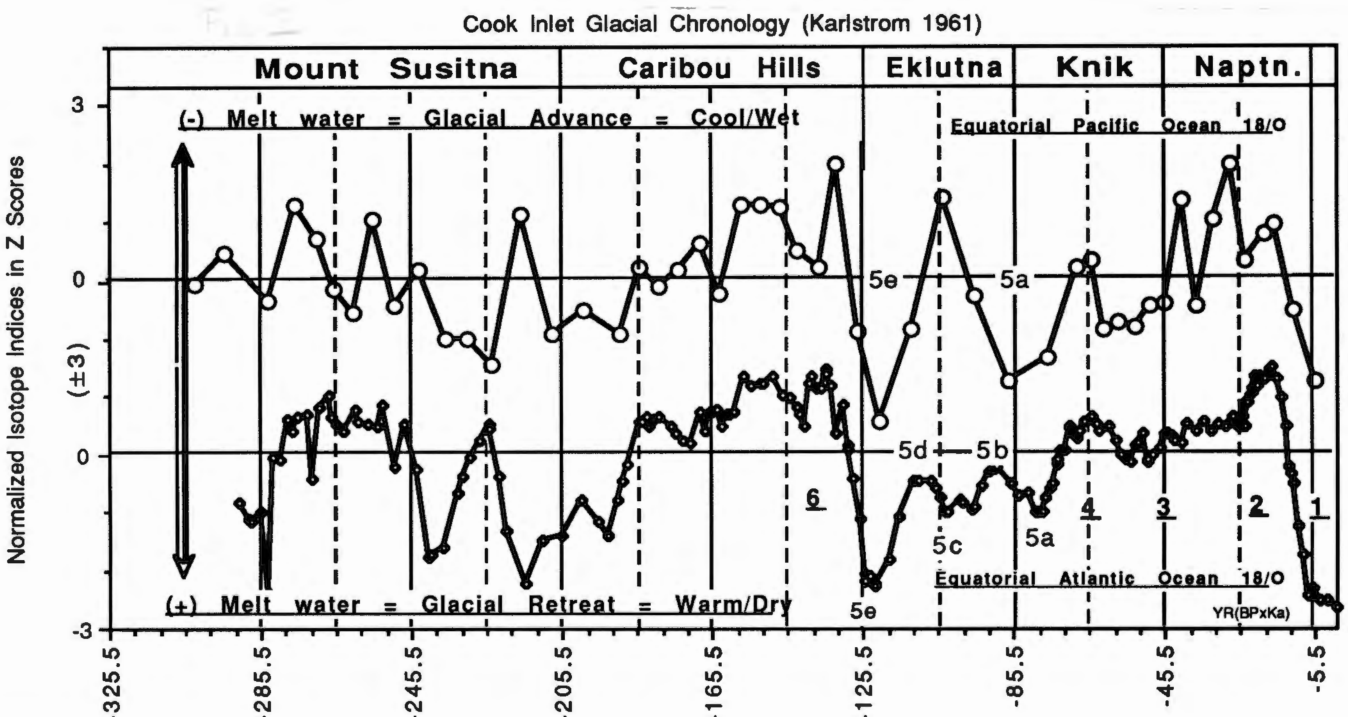

Figure 1 Two "standard" marine ice age chronologies on time scale of the obliquity insolation cycle (40,000-year) and its 2/1 (20,000-year) resonance assuming a response lag of about 4,500 years (Karlstrom 1961). Isotope indices of an equatorial Pacific Ocean core from Chuey and others (1987); the equatorial Atlantic record from Martinson and others (1987). Both chronologies are fine-tuned to the Milankovitch 60°N lat climatic model assuming corresponding response lags. The two records differ mainly in (1) out-of-phase relations about 225,000 years BP and (2) relative glacial amplitudes of the last 125,000 years. These differences suggest either heterogenieties in the global record or remaining difficulties with dating procedures and sample mixing. Note the tendency for near in-phase oscillations with the obliquity 2/1 (about 20,000 year) resonance. Most Quarternary researchers continue to correlate terrestrial paleoclimatic records with Martinson and others isotope record on the assumption that it provides a global climatic signal. Scores of terrestrial records in this and previous papers appear to contradict this assumption and to support the solar insolation/tidal resonance model, which requires opposing longer-term climatic trends in the two hemispheres, but globally synchronous secondary climatic oscillations. From Figure 28 in Karlstrom (1995).

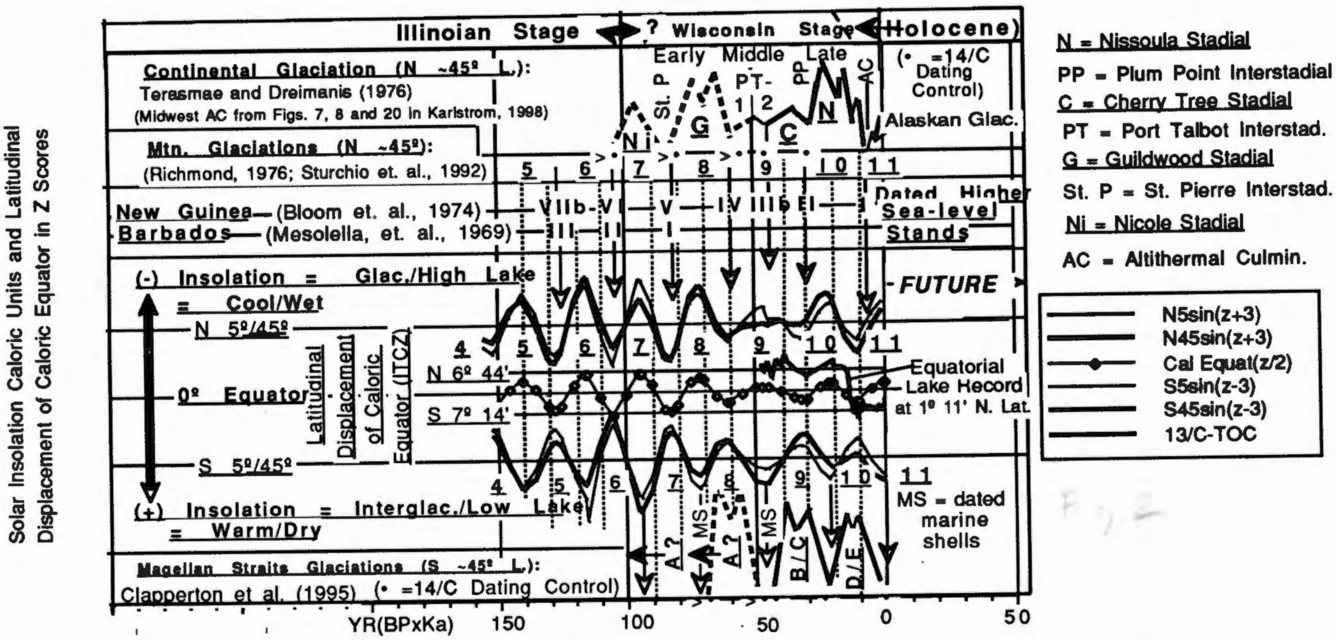

Figure 2 Correlation of highest resolution Northern and Southern Hemisphere glacial records with marine chronostratigraphy (glaceoeustatic sea levels), with antiphasing hemispheric precessional trends and with displacement of caloric equator and its associated intertropical convergence zone. Richmond (1976) and Terasmae and Dreimanis (1976) see a remarkable coincidence between their glacial chronostratigraphies and those of the dated sea level records. This supports the concept of glaceoeustasy, but not necessarily that of interhemispheric climatic synchrony. This is so because the much greater volume of glacial ice in the Northern Hemisphere can mask opposing melt-water trends in the interconnected oceans of the Southern Hemisphere (Karlstrom 1966). Because of remaining dating uncertainties, Clapperton and others (1995) do not attempt specific correlation of their Southern Hemisphere glacial events with those of the Northern Hemisphere. However, their B/C and D/E glacial complexes, as broadly dated between 45,000 and 25,000 years, and the present, most closely align with the local Southern Hemisphere precessional trends, which, as shown above, are displaced 10,000 years from their Northern Hemispheric precessional counterparts and their correlative continental-glacial and global glaceoeustatic events. Insolation curves after Milankovitch (1941); his calculations are essentially confirmed by von Woerkom (1953), Verneker (1972) and Berger (1981). Alternate north-south displacement of the caloric equator and reversing insolation gradients may serve to force or facilitate modulation of changing summer circulation patterns in the two hemispheres. In this regard, note the parallelism of the equatorial lake-level record with calculated oscillations of the caloric equator. Also note the apparent absence in the lower Southern Hemisphere of the classic Northern Hemisphere's "Little Ice Age" (Alaskan glaciation) due to antiphasing precessional trends across the equator (also see Figure 13 in Karlstrom 1998).

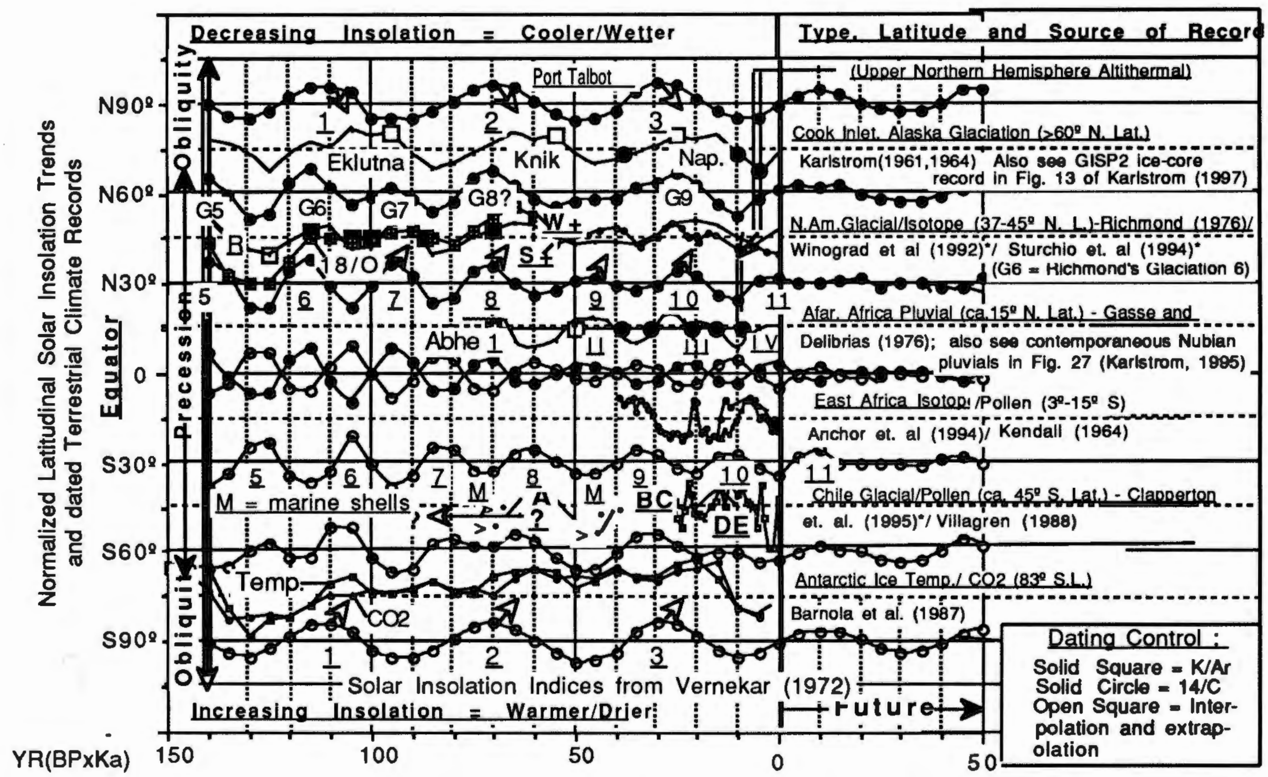

Figure 3 Latitudinal control of terrestrial climate records. These dated records seemingly parallel more closely the local latitudinal insolation trends than the dated records at other latitudes. If these climate records are representative of their respective latitudinal belts, the conventional concept of interhemispheric climatic synchrony dominated by high latitude Northern Hemisphere insolation must be reassessed as a basis for Ice Age correlations and global paleoclimatic reconstructions (Karlstrom 1961). Other records discussed in Karlstrom (1997) (Figures 8, 9, 10, 11, 12, 14, 15, 16, and 24) substantially strengthen the case for latitudinal insolation controls and for the opposite phasing of longer-term climatic trends across the equator. Modified from Figure 29 in Karlstrom (1995) and Figure 24 in Karlstrom (1997).

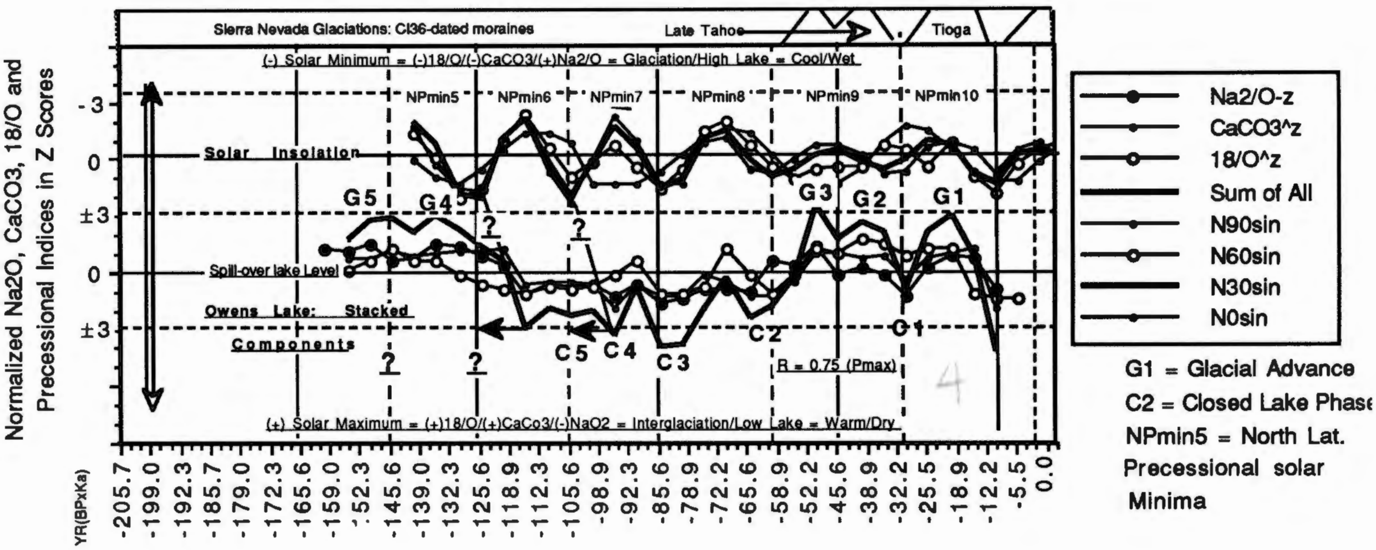

Figure 4 Owens Lake stable isotope record on time scale of the 6,672-year cycle, and correlation with local precessional insolation. Owens Lake indices, climatic interpretation and designation of closed lake (C1) and glacial (G1) events from Bischoff and others (1997); C1–36 dated morains from Phillips and others (1996); summer solar insolation indices from Vernekar (1972). Bischoff and others (1997) note the divergence of the oldest part of their lake record from the Devil's Hole isotope record (Winograd and others 1992) and suggest that this may result either from the use of different proxies or from dating errors in the early part of their own record. Adjustments to match the Devil's Hole record (see Figure 3) essentially provide a one-to-one match of lower lake-level phases with precessional maxima as shown above.

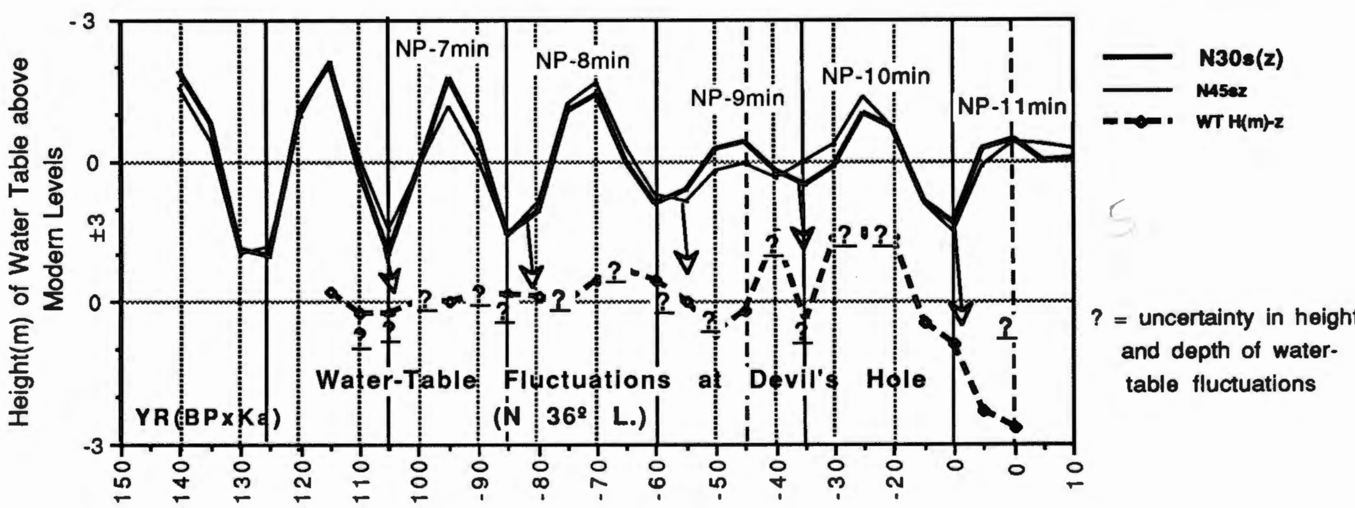

Figure 5 Water table fluctuations in Brown's Room, Devil's Hole, NV (lat 36°30'N) and correlation with local precessional trends. T/U series-dated indices from Figure 5 of Szabo and others (1995). The record extends the higher resolution record of Winograd and others (1992) from 50,000 year BP to the present by evidently completing the one-to-one correlation with local precessional trends, in this case, of higher water tables with precessional minima 9 and 10. The results are consistent with those of Sturchio and others (1994) (see Figure 3).

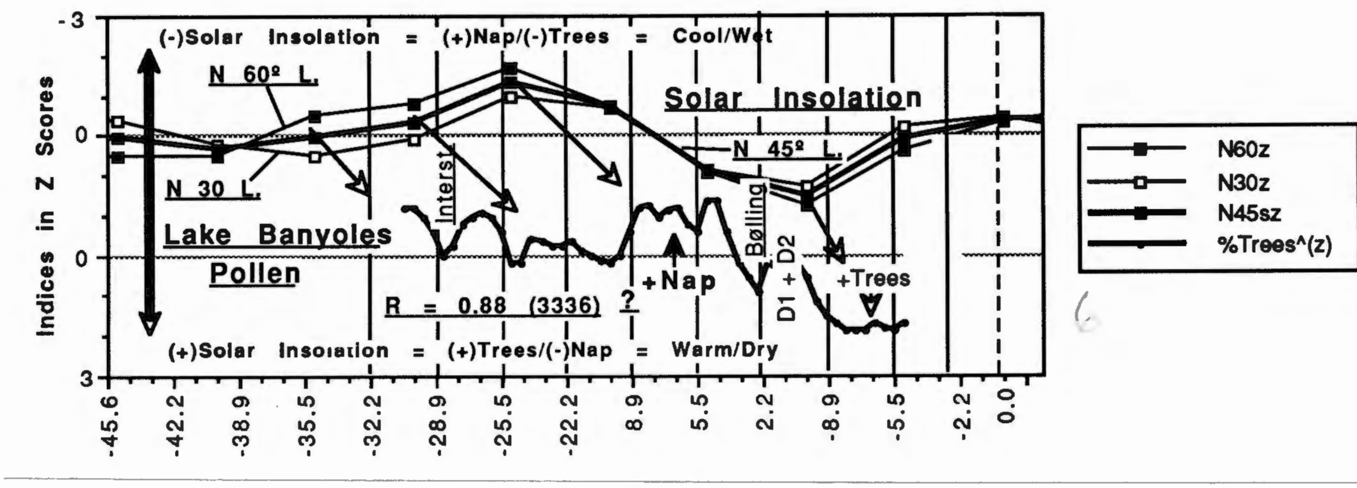

Figure 6 Radiocarbon and T/U series-dated pollen record from Banyoles Lake, Spain (lat 42°N) on time scale of the 3,336–year substage cycle. Pollen indices replotted at 500-year intervals from Figure 4 in Perez–Obiol and Julia (1994). The authors recognize the Bølling and an unnamed interstadial about 28,000 BP, but not the other secondary trends towards warming which appear to also phase strongly with the 3,336–year substage cycle. The primary trends of the record, consistent with its latitudinal location, most strongly parallel (with a requisite lag) that of middle northern latitude solar insolation (see Figure 3).

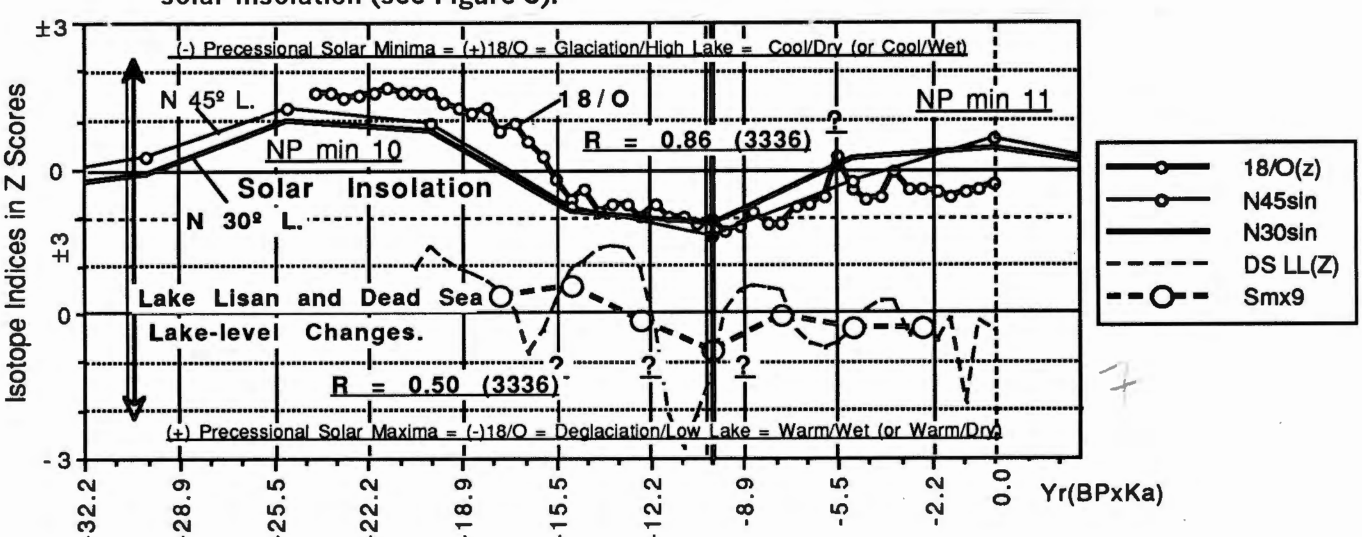

Figure 7 Speleothem stable isotope record of Soreq Cave, Israel (lat 32°N) on time scale of the 3,336–year substage cycle with correlations to local lake-level changes and precessional insolation. 18/O indices from Bar–Matthews and others (1997); lake-level indices of the Dead Sea and its precursor Lisan Lake after Begin and others (1985) and Frumkin and others (1991); and solar insolation indices from Vernekar (1972). Note: (1) the apparent, quick response of the isotopic composition of meteoric water to the local precessional insolation controls and (2) the strong tendency of the isotope record, but not the lower resolution lake record, to phase with the substage cycle. Based on several years of readings of annual rainfall and isotopic composition, Bar–Matthews and others (1997) assume that the apparent negative correlation applies to the past as well. They, thus, interpret their record to indicate cold and dry conditions during the last major glaciation (and associated higher lake levels) vs. warmer and wetter with associated lower lakes during the Holocene.

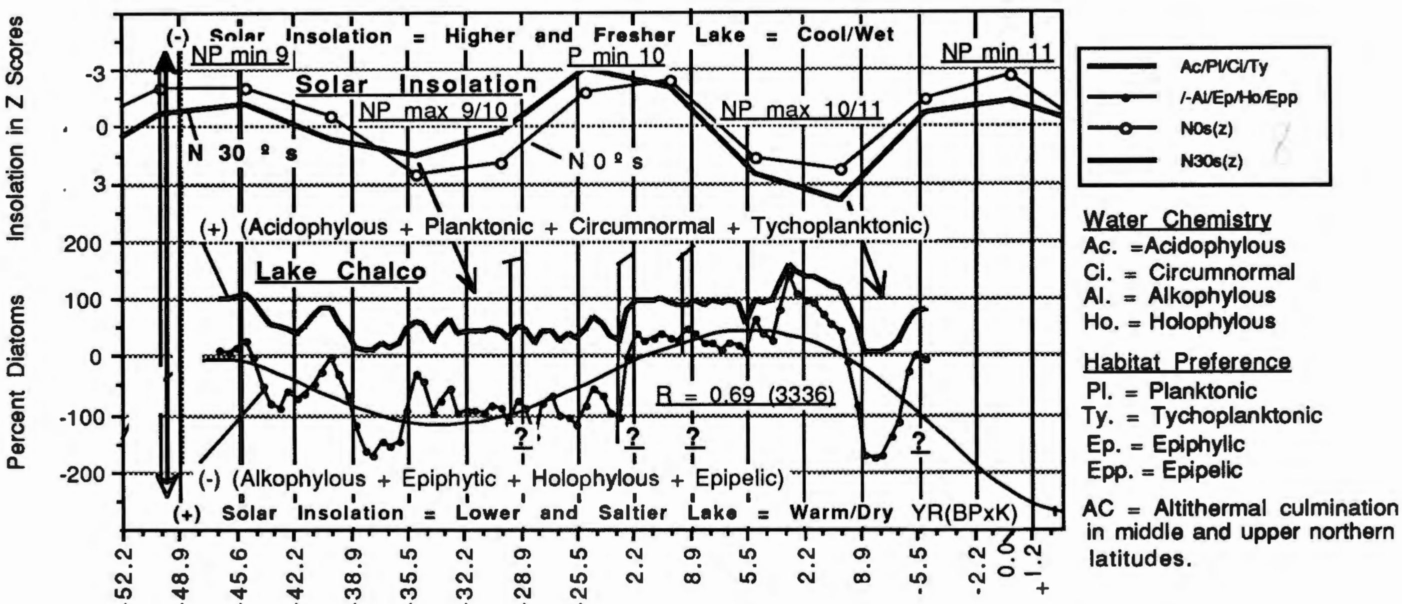

Figure 8 Lacustral diatom record near Mexico City (lat 19°N) and local precessional trends on the time scale of the 3,336–year substage cycle and its 3/1 (1,112–year) stadial resonance. Diatom water chemistry and habitat preference indices from Caballero and Guerrero (1998) replotted at 500–year intervals; precessional indices from Verneker (1972). Deeper and fresher water indicators are summed in upper curve; shallower and saltier indicators are summed and inverted in the lower curve to satisfy the indicated paleoclimatic equation and correlation with the local precessional insolation trends. Primary trends by 5th-order polynomial. Note: (1) the striking parallelism of the stacked lake record's primary trends (with an appropriate cause-and-effect lag) to the local precessional insolation trends and with inferred lower lakes coinciding with insolation maxima and (2) the tendency of the secondary oscillations to phase with the substage cycle. Though this tendency of the record as dated is weak, the correlation can be greatly improved by minor fine-tuning that is within dating uncertainties resulting from sigma errors and the assumption of uniform depositional rates between dated horizons.

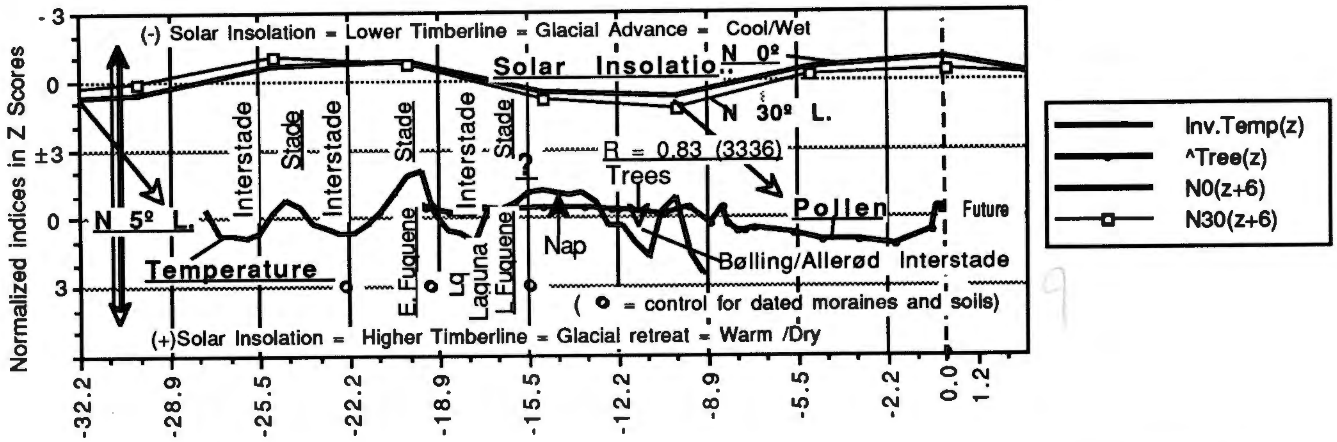

Figure 9 Pollen, inferred temperature, and dated glacial records from La Laguna, Columbia (lat 5°N) on time scale of the 3,336–year substage cycle. Dated indices from Helmens and others (1996). Pollen from their Figure 2 replotted at 10-cm intervals, assuming uniform depositional rates between dated horizons. Their inferred temperature curve from Figure 5 as replotted at 500-year intervals. Note the lagged parallelism with the local precessional trends and the strong tendency of the temperature record to phase with the substage cycle. The evidence for the Bølling–Allerød warmer interval and for their La Laguna interstade is indicated but not the equally pronounced warmer intervals (also labelled above as interstades) that associate with other turning points of the substage cycle. The about 15,500–year BP interstade, though not clearly recorded in the pollen record, is more directly defined by doted buried soils in morphostratigraphic sections.

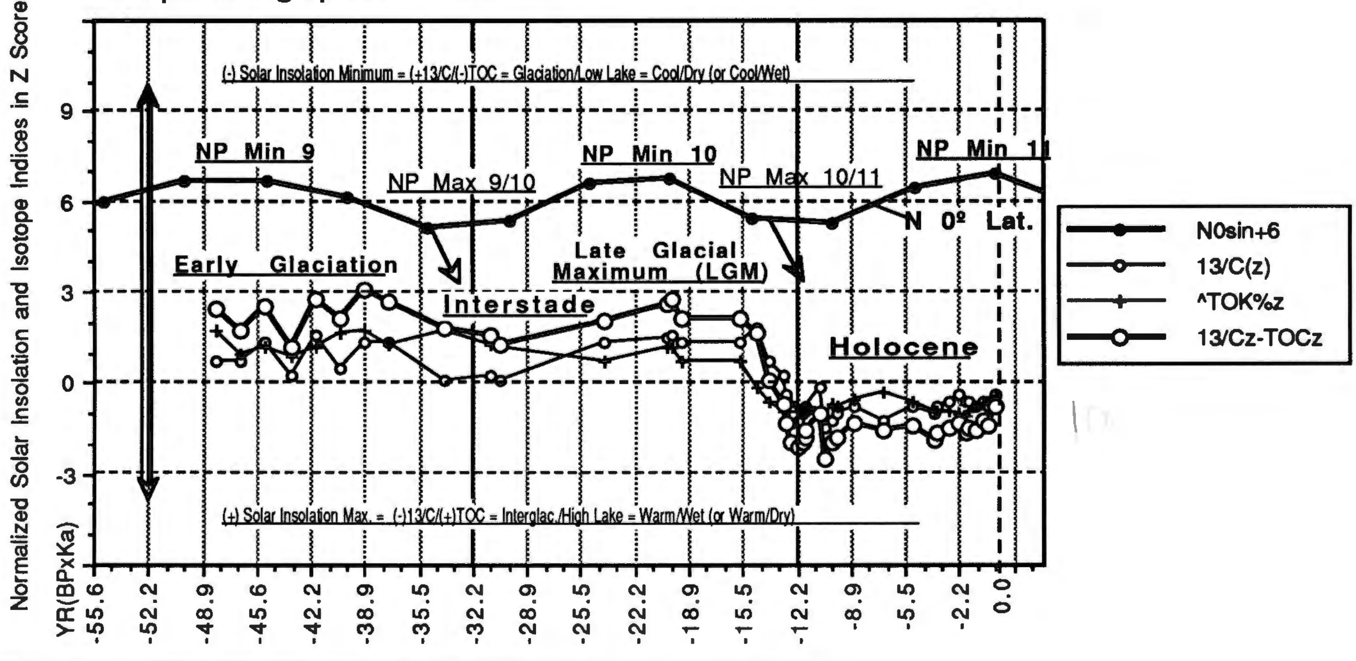

Figure 10 Correlation of equatorial lake record (lat 1°11'N) with precessional solar insolation positioned on time scale of the 3,336–year substage cycle. Note the strikingly appropriate lagged parallelism with the local precessional insolation trends and the correlation of glaciations with precessional minima. As shown in Figure 2, the same parallelism exists between this record and the oscillations of the caloric equator as calculated by Milankovitch (1941), suggesting that such caloric displacements modulated equatorial climate (Karlstrom 1998).

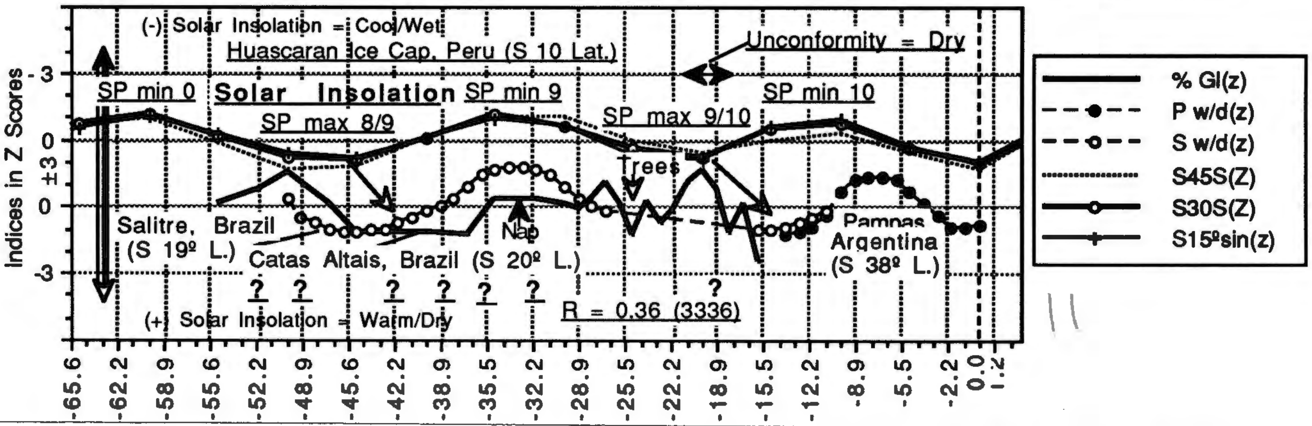

Figure 11 South American pollen records and local precessional solar insolation on time scale of the 3,336–year substage cycle. Catas Altais pollen indices from Berling and Lichte (1997) replotted at 1,000–year intervals from their Figure 3B. Schemata of nearby Salitre record as defined by Ledru and others (1996); that of the Pampas record in Argentina as interpreted by Prieto (1996). Prieto suggests that the wetter pampas conditions between 10,500 and 5,000 years BP reflects decreased continentality resulting from higher sea levels or from a poleward shift of the Atlantic convergence zone. Behling and Lichte interpret the Catas Altais pollen as indicating drier as well as colder conditions between 40,000 and 27,000 years BP on the premise that the general absence of trees at these upper elevations must reflect drier conditions during the last major glaciation as this is defined by the Northern Hemisphere ice sheets and by the standard marine record (see Figure 1). They also note their differences with colleagues who interpret other regional pollen records to indicate wetter as well as cooler intervals in the same time frame. As shown above, those intervals that have been defined as wet as well as cold provide patterns that most closely parallels the summer solar insolation trends, which are 180° out-of-phase with their North American counterparts (see Figures 2 and 3). Most recently Ledru and others (1998) reevaluate South American pollen lake records and conclude that because of dessication and inconformities in all seven records between 18,000 and 20,000 years BP there is no stratigraphic evidence of the last major glaciation as defined and dated in the Northern Hemisphere.

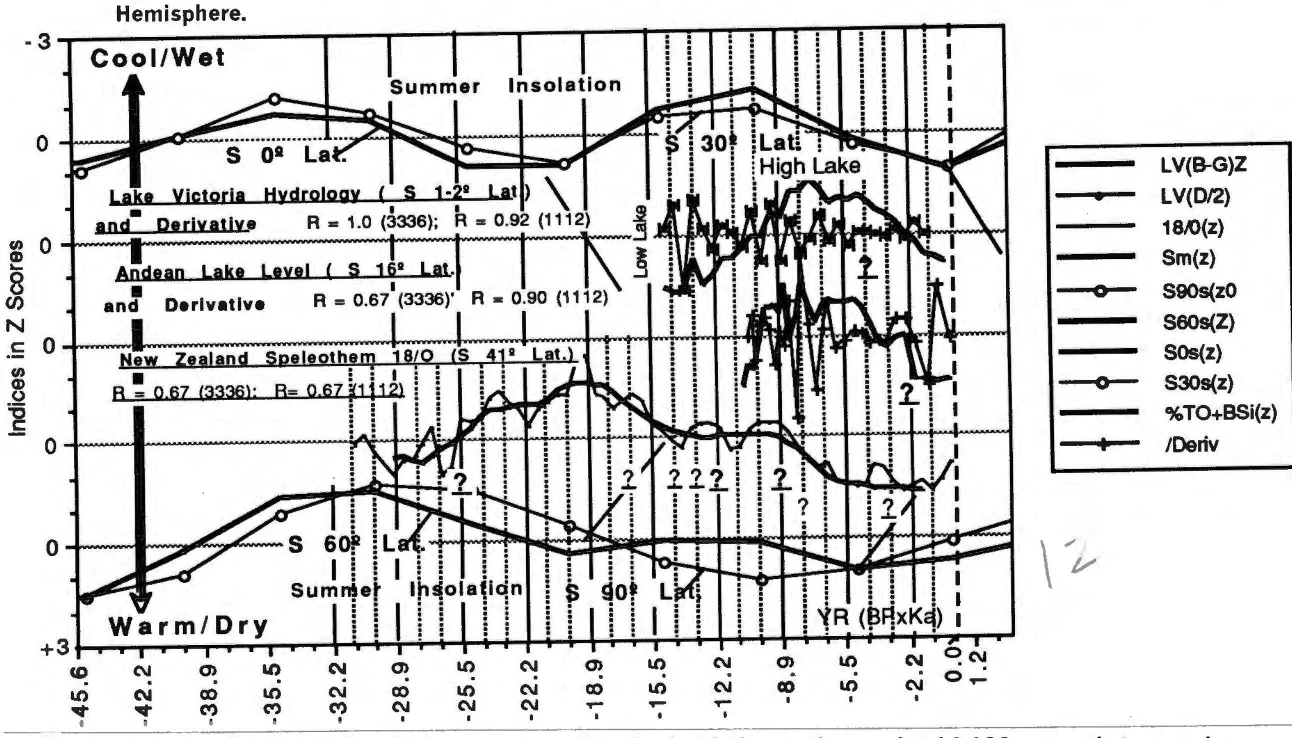

Figure 12 Correlation of Southern Hemisphere records with solar insolation on time scale of 3,336–year substage cycle and its 3/1 (1,112–year) stadial cycle. Lake Victoria pollen indices and hydrologic interpretation from Kendall (1969) (also see Figure 11 in Karlstrom 1995). Andean lake record in percent biologic production from Abbott and others (1997). Th/U-dated, New Zealand stable isotope record from Hellstrom and others (1998). Note: (1) parallelism with local precessional insolation and progressive shifting toward obliquity trends with increasingly higher latitudes and (2) the weak-to-strong tendencies of these records to phase with turning points of the substage and stadial cycles or synchronous counterparts north of the equator.

Cook Inlet, Alaska Glacial Time-stratigraphic Classification (Karlstrom 1961)

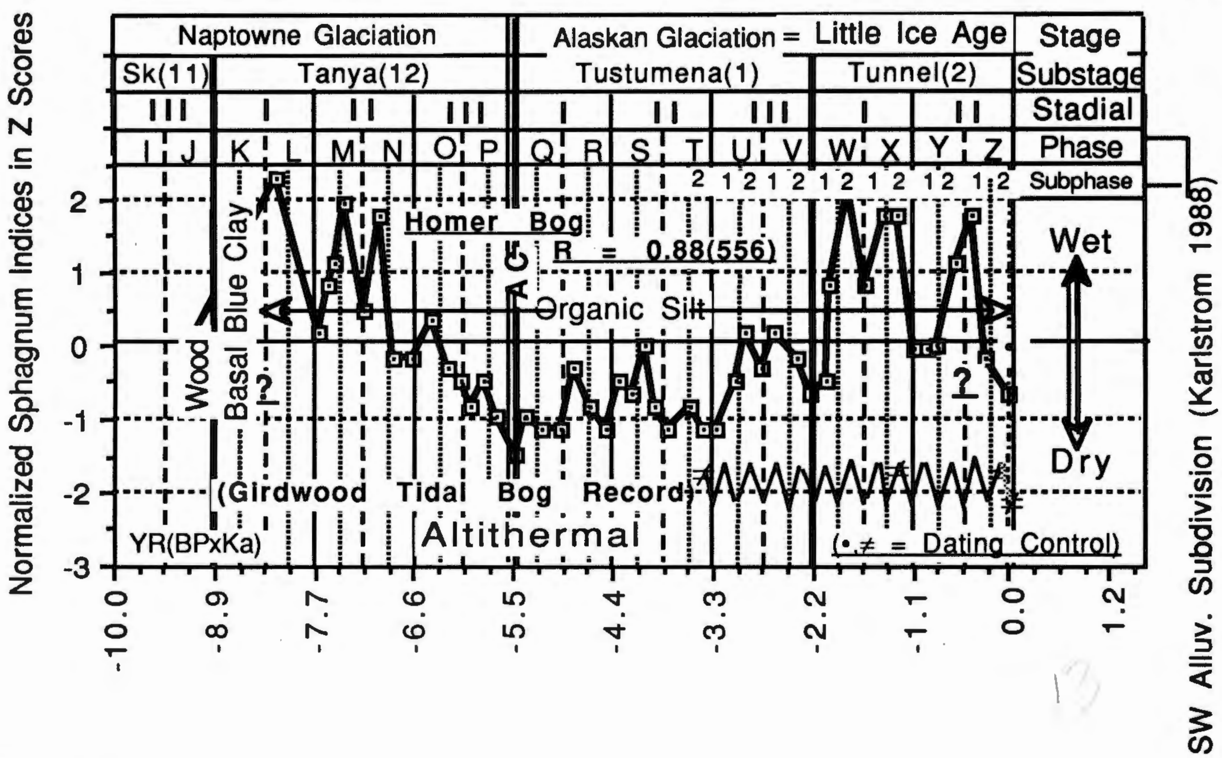

Figure 13 Bioclimatic record of Homer Bog, Cook Inlet, Alaska, on time scale of the 1,112-year stadial cycle and its 2/1 (556-year) phase resonance and 4/1 (278-year) subphase resonance. Pollen indices from Heuser (1965) time calibrated by basal date listed in Karlstrom (1964). The higher frequency in Girdwood Bog record is schematically plotted as interpreted climatically in Karlstrom (1961). Because of lesser sensitivity and wider sampling intervals, Homer Bog shows the strongest tendency to oscillate in phase with the 556-year phase cycle and positions the driest postglacial interval contemporaneous with that of the Southwest altithermal (AC) and in the late Atlantic of northern Europe (see Figure 18). Figure modified from Figure 18 in Karlstrom (1995). Note the strong correlation between the inferred dry troughs of this pollen record and the subdivision boundaries of the Cook Inlet glacial chronology estimated to mark the approximate timing of retreat culminations between glacial advances.

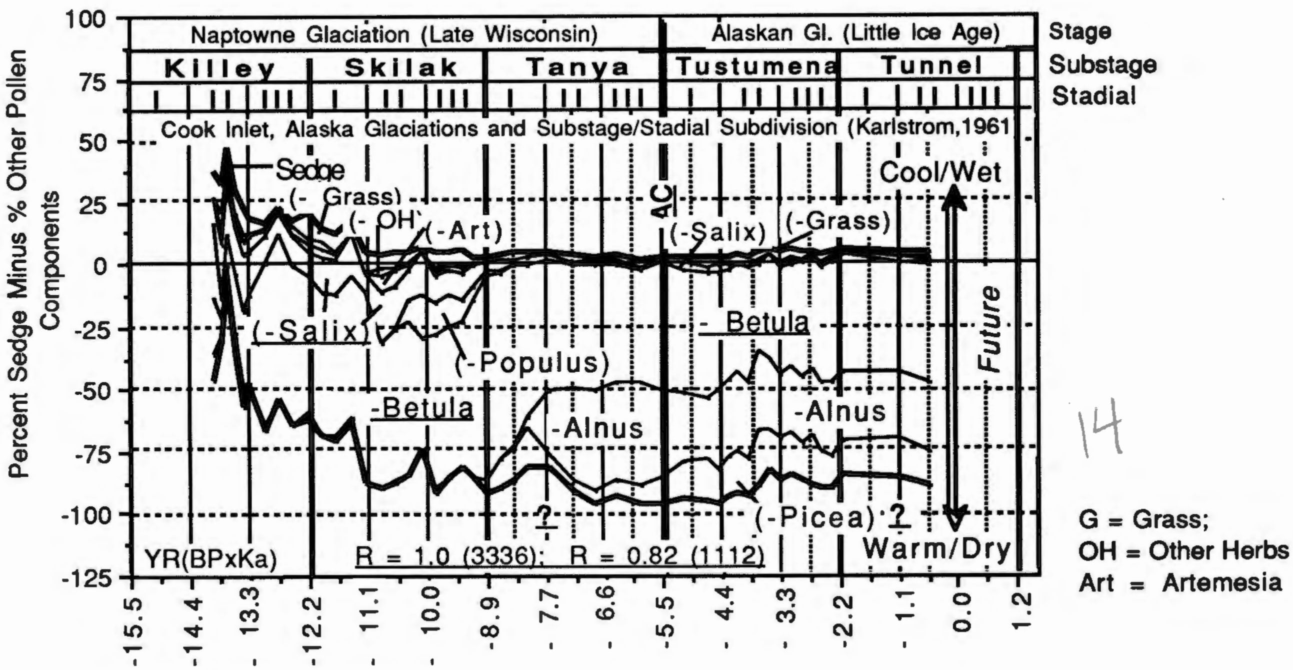

14

Figure 14 Bioclimatic record of Sithylemankat Lake, northern Alaska, (lat 66°N) on time scale of the 1,112–year stadial cycle and its 2/1 (556–year) phase resonance. Radiocarbon-dated indices from Anderson and others (1990). This high latitude record seemingly replicates middle latitudes Northern Hemisphere records in placing the warmest and driest postglacial interval between 5,000 and 6,000 years BP. This result, however, does not agree with what appears to be a developing palynological consensus that the warmest postglacial interval in Alaska is marked by the populus maximum about 10,000 years BP. The lake record also suggests a strong tendency to phase with both the stadial and substage cycles derived from moraine and bog stratigraphy in the more southerly Cook Inlet region of Alaska.

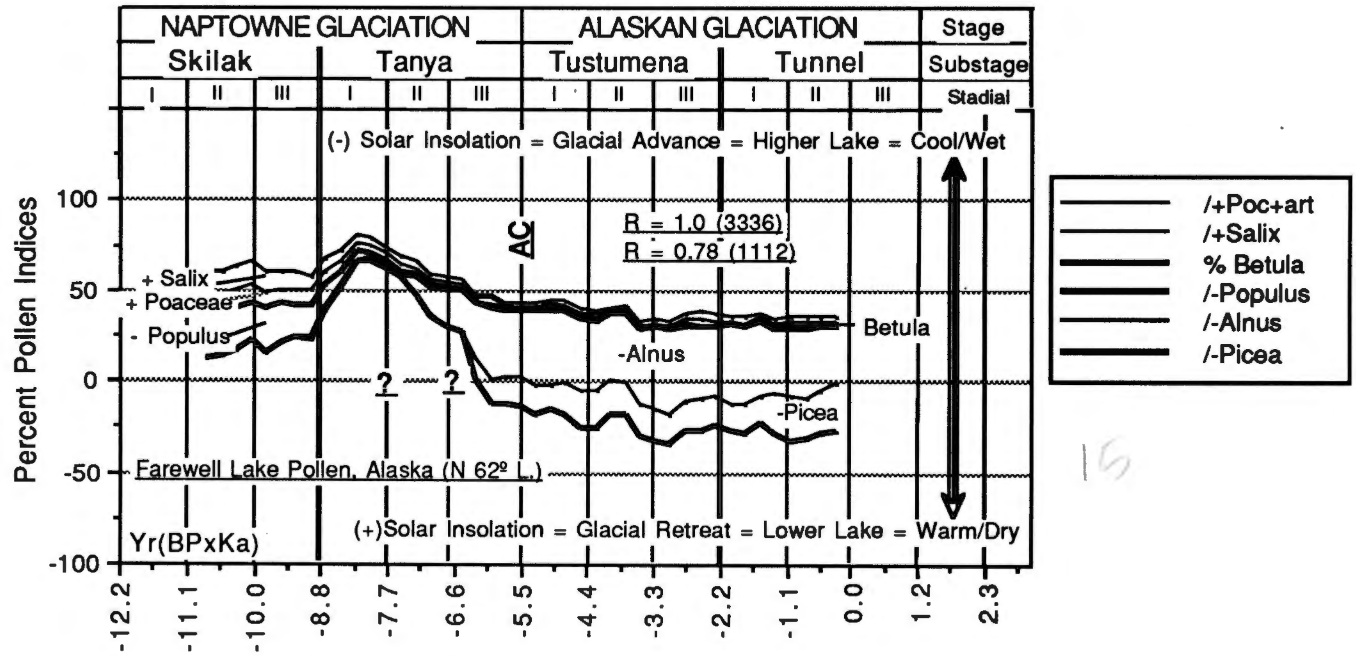

Figure 15 Bioclimatic record of Farewell Lake, Alaska, (lat 62°N) on time scale of the 1,112–year stadial cycle. Three-point smoothed pollen indices from Hu and others (1996) replotted at 250–year intervals. The record is reconstructed by the same procedures used in interpreting the other pollen records showing the transition from tundra to forests during the glacial-postglacial transition to warming (see Figures 14 and 18). Based on the correlation between glacier size and proximity to precipitation sources (Karlstrom 1961), I continue to assume that postglacial retreat was also facilitated by diminishing precipitation (less snowfall above rising snow lines), thus, the paleoclimatic equation shown on this and previous figures. Hu and others, however, conclude from associated chemical components that the *Betula* shrub tundra with *Populus* at the beginning of the record was colder and drier than the later forest-tundra types which reflect warmer and wetter conditions. They also note that this interpretation is not corroborated by concentrations of carbonate interpreted by other researchers to reflect reversed lake-level and climatic relations. Also note: (1) that their inferred early postglacial warm period occurs during a series of recessional glacial advances of Skilak and Tanya age in the nearby Cook Inlet region; (2) that their pollen record as reconstructed above suggests the warmest and driest postglacial interval about 3500 years BP rather than earlier, as suggested by many western North American records (for examples, Figures 14 and 18); (3) that this discrepancy may result from lack of separate graphs for white and black spruce, whose temporal distribution is interpreted by Hu and others as suggesting cooler and wetter climate after 6000 years BP; and (4) the fairly strong tendency for the secondary warming trends to phase with the stadial cycle as defined in the Cook Inlet glacial chronology (Karlstrom 1961, 1964).

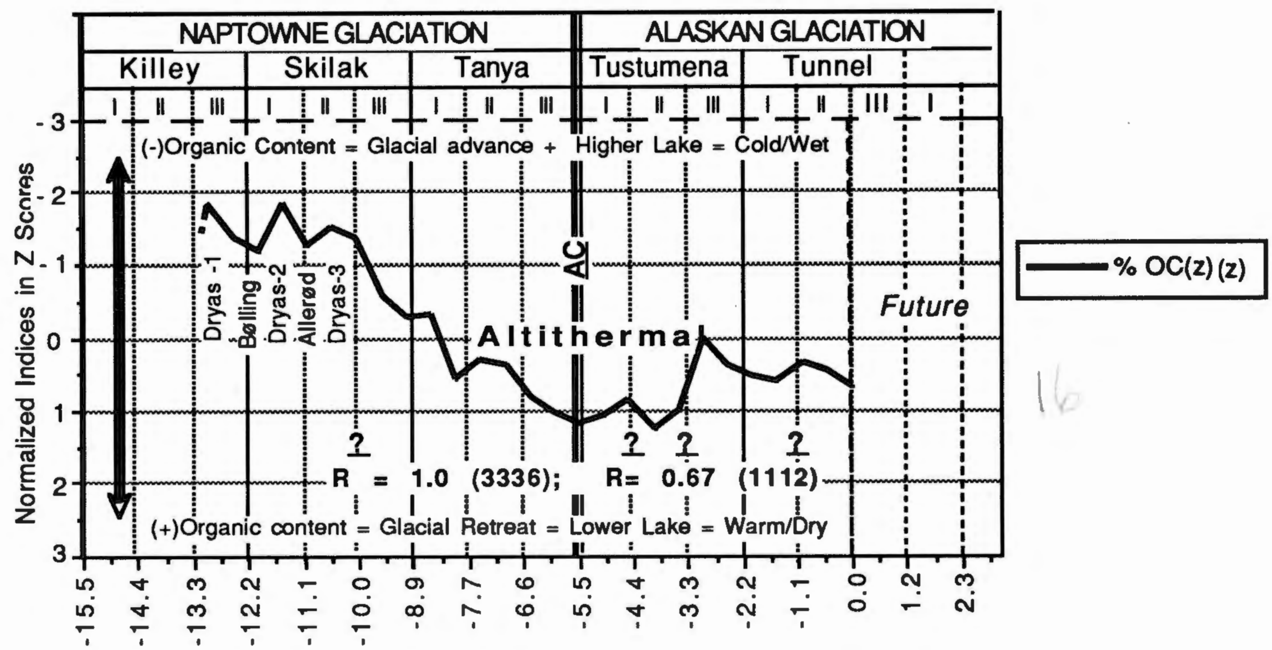

Figure 16 Bioclimatic record of Pleasant Island, southeastern Alaska, (lat 58°N) on time scales of the 1,112-year stadial cycle. Organic carbon indices from Figure 14 in Hanson and Engstrom (1996) replotted at 500-year intervals. Interpreted in the sense of lesser organic production during colder and deeper lake phases and greater production during shallower and warmer phases provides a strikingly parallel record to that of the glacial history constructed for the nearby Cook Inlet region to the north from moraine, bog, and lake chronostratigraphy (Karlstrom 1961, 1964). Note: (1) the strong phasing with the substage cycle, but the much weaker phasing with the stadial cycle, probably due to differing regional climates, response functions, or levels of smoothing; (2) general parallelism with the higher resolution Homer Bog record on Cook Inlet (Figure 13); and (3) confirmation of the youngest Dryas correlation suggested by Hansen and Engstrom and also of correlatives to the Allerød, older Dryas, Bølling, and part of the oldest Dryas, as these are defined and radiocarbon dated in type areas and other localities in Europe and as marked by turning points of the cyclical classification of nearby Cook Inlet (see above and Figure 18).

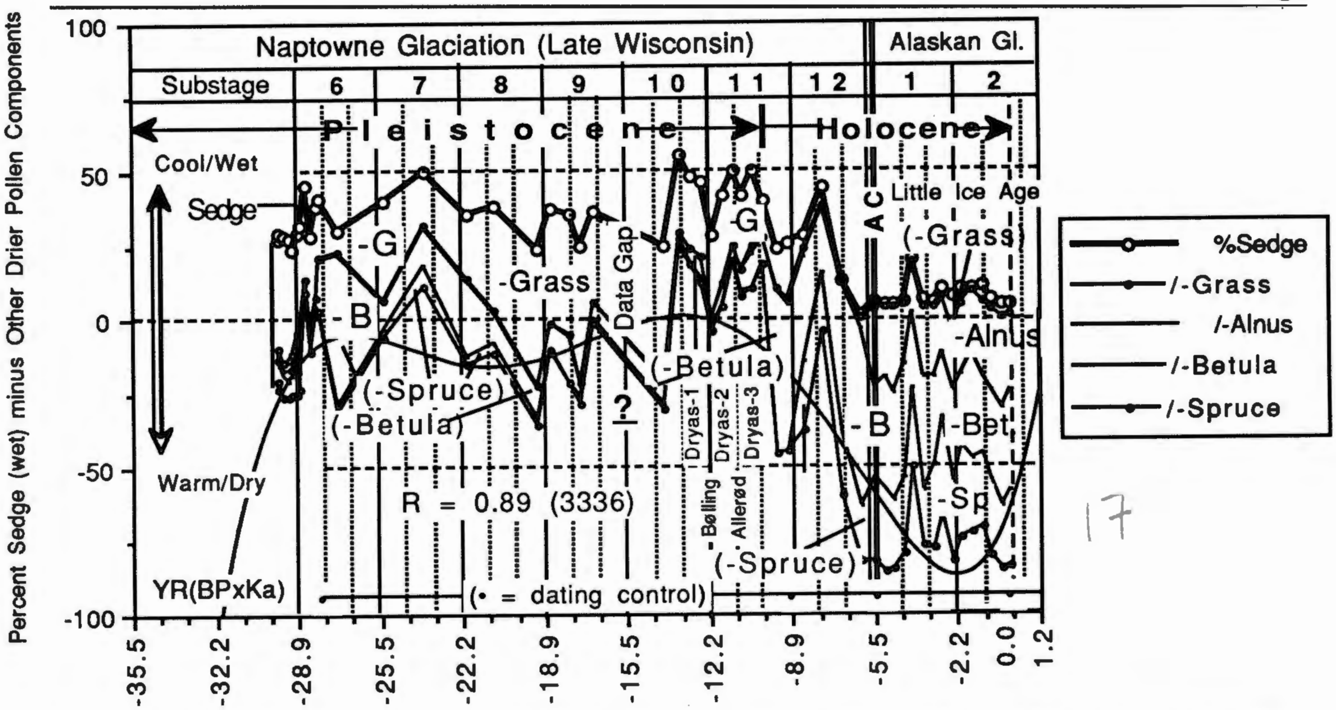

Figure 17 Bioclimatic record of Antifreeze Pond, Yukon Territory, Canada, on time scale of the 3,336–year substage cycle and its 3/1 (1,112–year) stadial resonance. Pollen indices from Rampon (1970). Alaska glacial classification and cyclical subdivision from Karlstrom (1961). Trend analysis suggests a strong response to the substage cycle and where the sampling interval is sufficiently close, to the stadial cycle as well. Figure modified from Figure 24 in Karlstrom (1995). Note the well-defined oscillations in phase with the classic Dryas sequence of northern Europe.

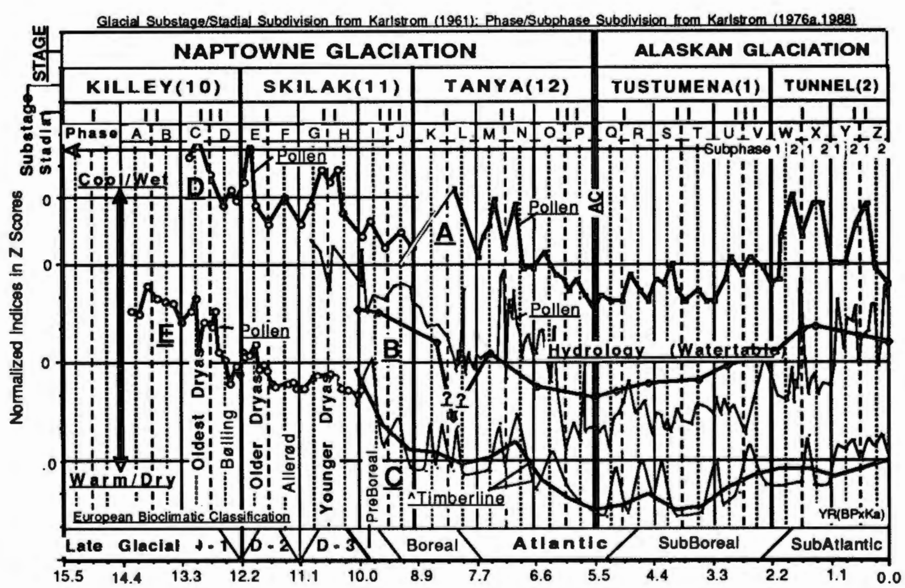

Figure 18 Cook Inlet bioclimate and collated European high-resolution records on time scale of the 1,112–year stadial cycle and its 2/1 (556–year) and 4/1 (278–year) resonances. A: Cook Inlet Homer Bog. B: Agarode Bog/hydrology of Sweden (Nilsson 1964a, 1964b). C: Alps timberline fluctuations (Beug 1982). D: Danish Bølling Bog (Karlstrom 1961). E: Swiss Wachseldorn Bog (oeschger and others 1980) that, though sampled at shorter time intervals, replicates with some fidelity the classic late glacial/Dryas sequence of Denmark in D. Data from Figures 2 and 3 in Karlstrom (1996). Note that Nilsson's hydrologic reconstruction of the Agarode Bog record favors the interpretation that the late Atlantic was the driest and warmest interval in postglacial time or consistent with other European and North American records (Karlstrom 1956).

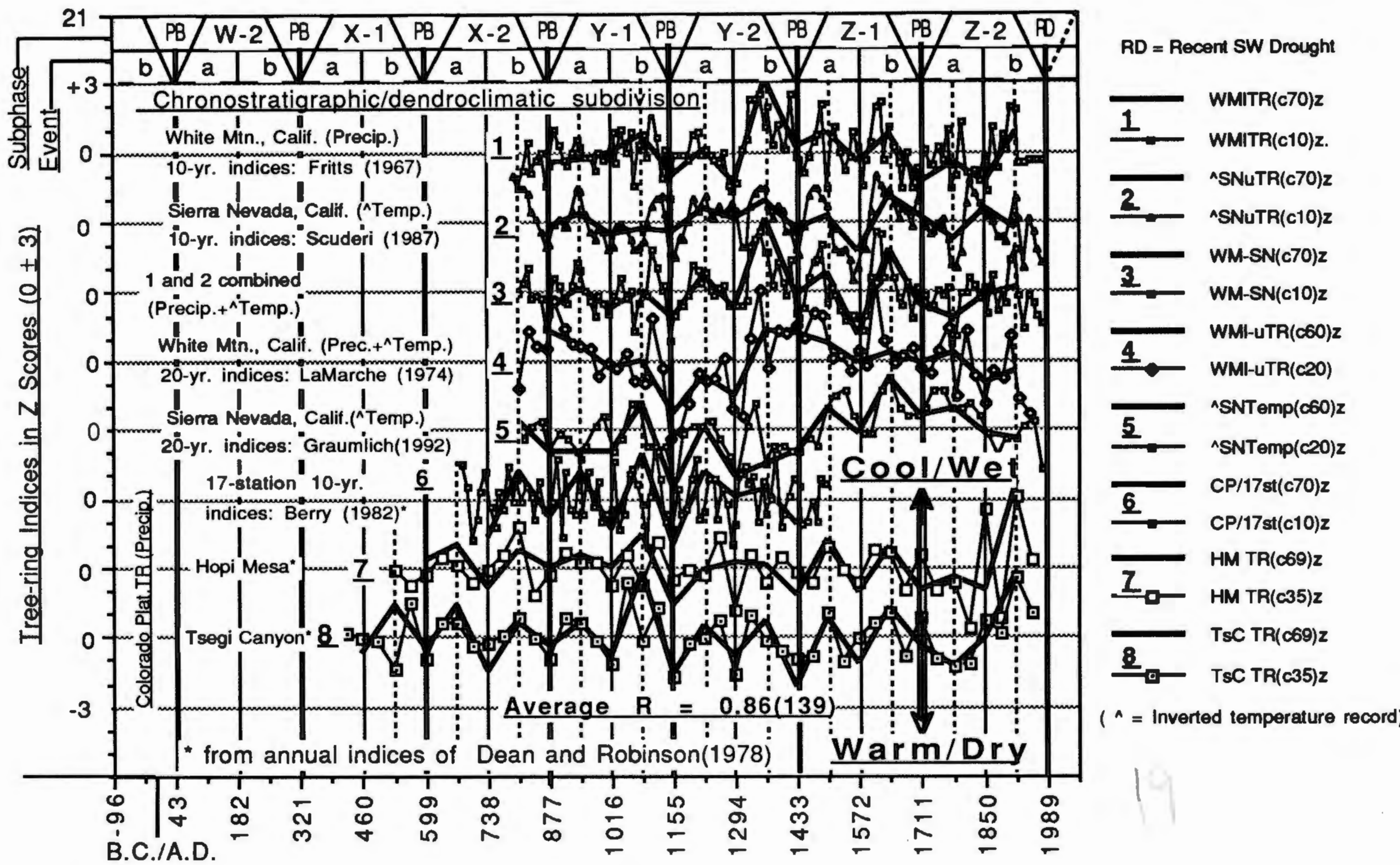

Figure 19 Summary evidence for a dendroclimatic cycle in phase with the 139–year event cycle. Half-cycle smoothing positioned on cycle turning points. Trend correlations, temperature, and precipitation range from 0.75 to >0.90 or within the upper range of tree ring and climate calibrations. This suggests that the cycle is real, regionally robust, and related to changing atmospheric dynamics and circulation patters. Similar half-cycle analyses of other records may define differing regional patterns and responses, advancing understanding of climatic and biologic process. Modified from Figure 10 in Karlstrom (1995). PB = Point Boundary (clustering of Southwest alluvial basal-contact dates) from Karlstrom (1976a, 1998).

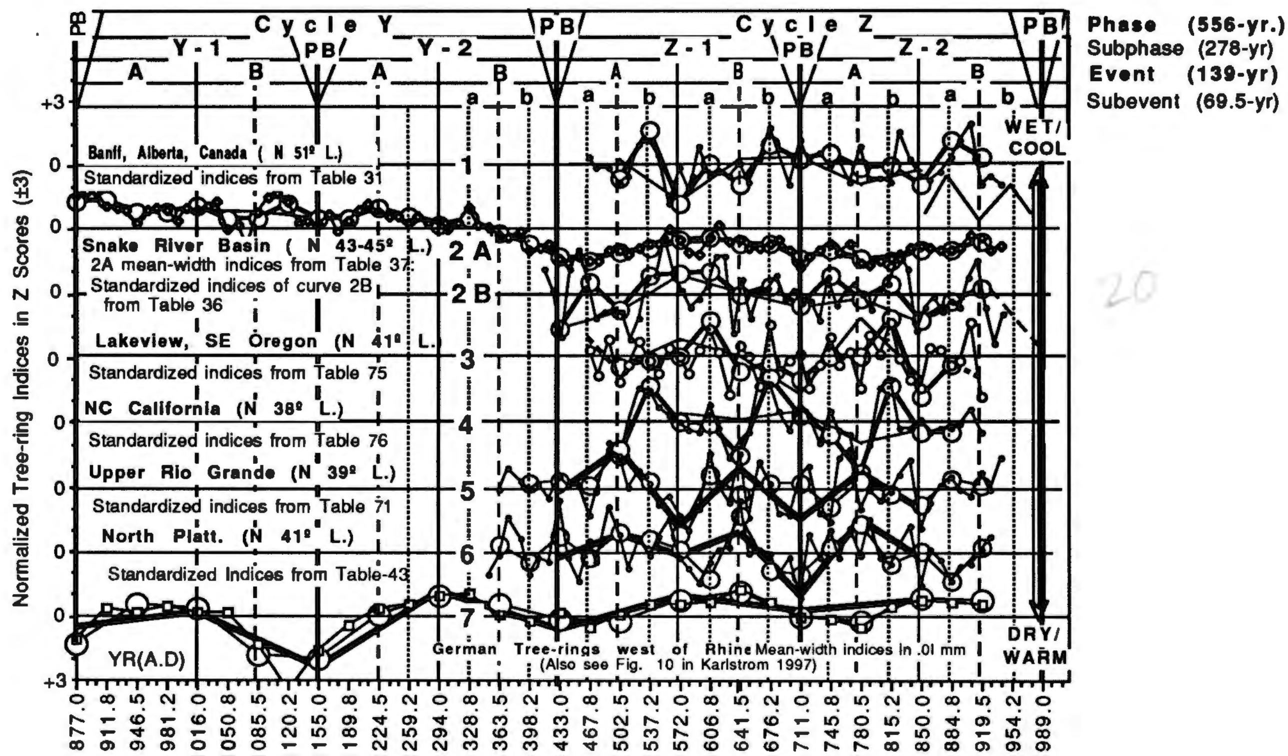

Figure 20 North American and German tree ring records on time scale of the 2/1 (34.75–year) resonance of the 69.5–year subevent cycle. Half-cycle smoothing positioned on turning points of the inferred tidal resonances. North American tree ring indices from the indicated tables in Schulman (1956); German indices from Appendix 16 in Ladurie (1972). Note that these records phase strongly with different elements of the tidal resonance modal suggesting differing regional air-mass dynamics: the higher latitude western North American records with the 69.5–year subevent cycle; the mid-latitude records east of the Rocky Mountains with the 139–year event cycle; and the German record with the still-longer 278–year subphase cycle. The tree ring evidence for the higher latitude subevent cycle is apparently reflected in Delcourt and others' (1996) northern Lake Michigan strandline evidence for a 70–year temperature cycle extending back to mid-Holocene time. Note parallelisms between the two mean tree ring width records (curves 2A and 7).

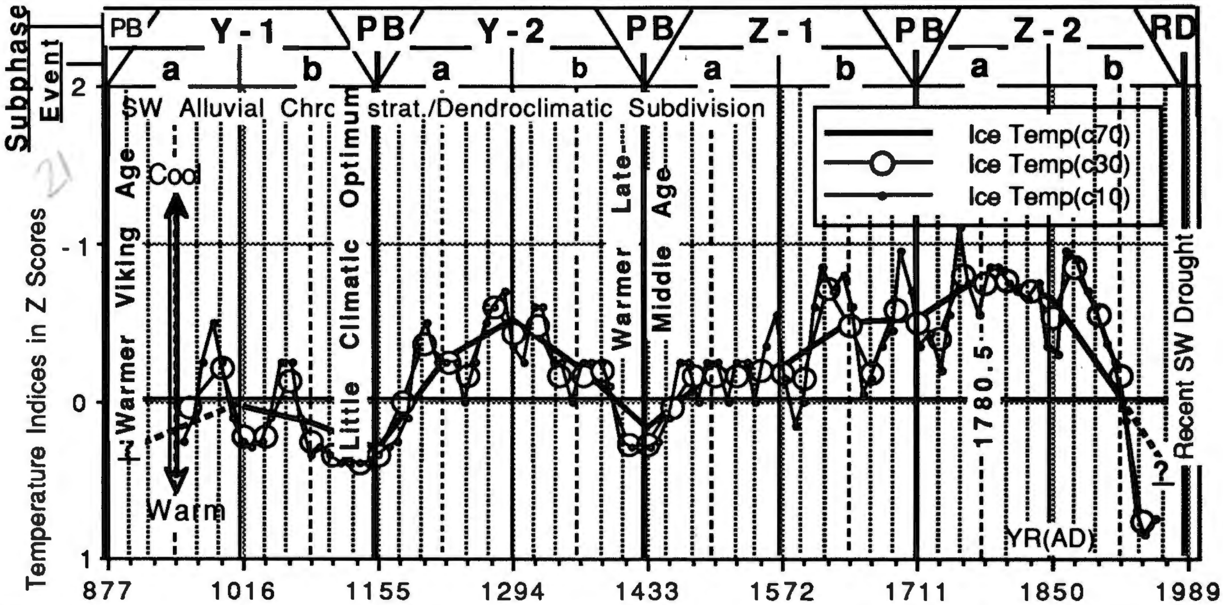

Figure 21 Iceland temperature record on time scale of the 139–year event cycle and its 2/1 (69.5–year) and 6/1 (23.166–year) resonances. Ten-year temperature indices from Bergthorson (1969). Half-cycle smoothing as before. Note the strong tendency to oscillate in phase with the 278–year subphase cycle and the lesser tendencies with the 139–year event cycle and its resonances. The medieval warm period, placed between about AD 900 and 1300 by Lamb (1977) is dated later by other researchers. For correlation of the post-AD 1700 part of the Iceland temperature record with sunspots see Friis–Christiansen and Lassen (1991) and Figure 12 in Karlstrom (1995). This figure also includes a tree ring-dated isotope record and a marine record (Figure 22) that also seem to phase with the sunspot record.

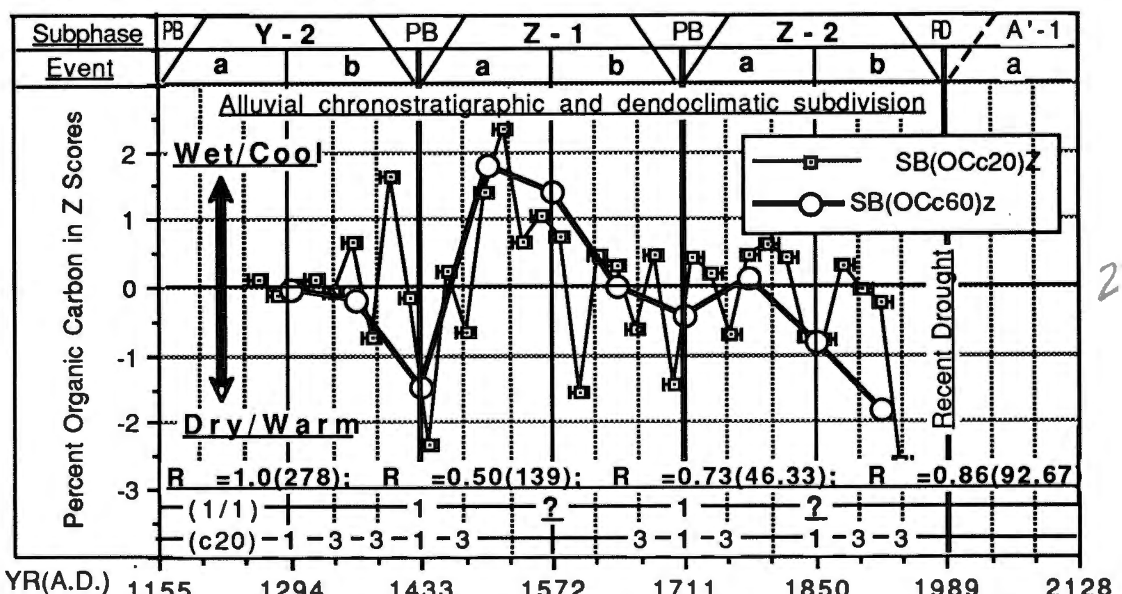

Figure 22 Varve-dated marine record of the Santa Barbara Basin, California, on the time scale of the 139–year event cycle and its 3/1 (46.33–year) resonance. Indices from Pandolfi and others (1980) replotted at 20–year intervals. Original indices collated with a Japanese tree ring record that reflects cycles of 273 20 years (U) and 271 11 years (D/H). The Santa Barbara core record demonstrates a similar length marine cycle that is in phase with the 278–year subphase cycle. These correlations suggest that a greater amount of organic carbon was supplied during major Southwest wet (depositional) intervals than during major dry intervals. The record also shows a strong tendency to phase with the about 46–year resonance and a stronger tendency with its double (93–year) Gleissberg cycle. Analysis by half-cycle smoothing positioned on turning points of the 139–year event cycle. From Figure 15 in Karlstrom (1995).

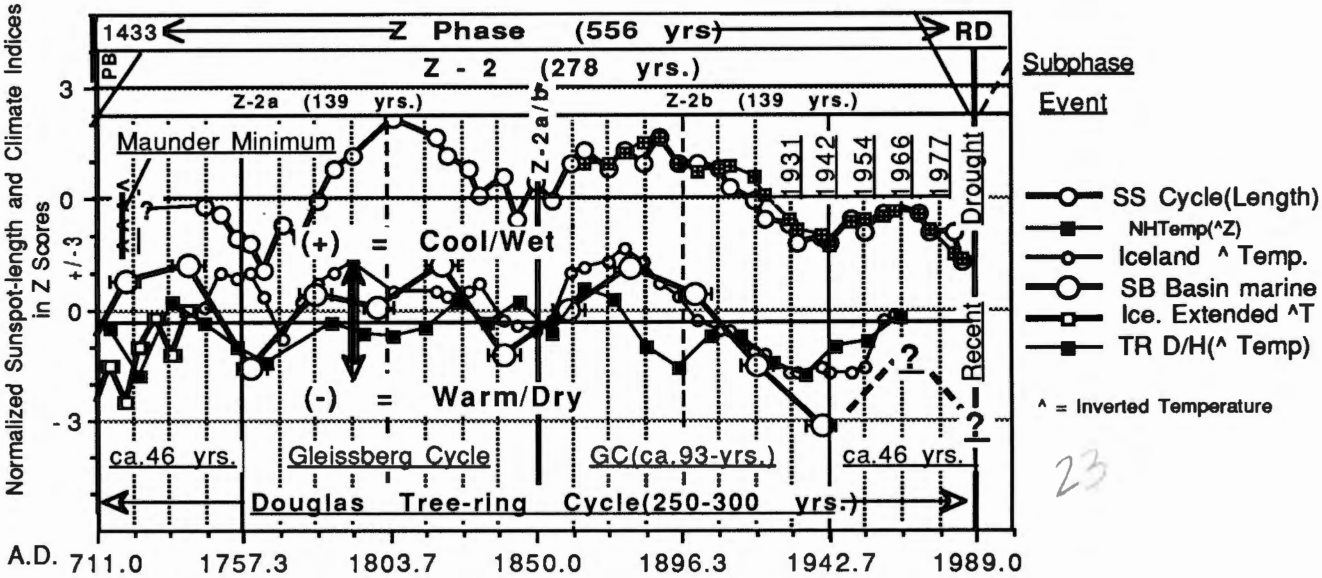

Figure 23 Sunspot and climate records on time scale of the 139–year event cycle and its 3/1 (46.3–year) and 12/1 (11.5–year) resonances. Sunspot, hemispheric temperature, and Iceland indices to 1745 from Friis–Christiansen and Lassen (1991); extension of Iceland temperature record by indices from Bergthorsen (1969); Santa Barbara marine indices from Pandolfi and others (1980) and tree ring-dated isotope indices from Epstein and Yapp (1976). Sunspots and collated climatic records appear to be directly related to the tidal resonance model through in-phase relations with the 46–year resonance and its double Gleissberg sunspot cycle. Weaker tendency for sunspot lengths and higher resolution climate records to oscillate in phase with the 11.5–year resonance. These correlations constitute the strongest empirical evidence to date for tidal and solar modulation of climate.

References

Abbott MB, GO Seltzer, KR Kelts, and J Southon. 1997. Holocene paleohydrology of the tropical Andes from lake records. *Quat Research* 47:70–80

Ancour A, C Hillaire-Marchel, and R Bonnefille. 1994. Late Quaternary biomass changes from ^{13}C measurements in a highland peat bog from equatorial Africa (Burundi). *Quat Research* 41:225–33.

Barnola JM, D Raymond, YS Korotkevich, and C Lorius. 1987. Vostock ice core provides 160,000–year record of atmospheric CO_2. *Nature* 329:4–10

Bartlein PJ, ME Edwards, SL Shafer, and ED Barker, Jr. 1995. Calibration of radiocarbon ages and the interpretation of paleoenvironmental records. *Quat Research* 44:417–24.

Bar-Matthews M, A Ayalon, and A Kaufman. 1997. Late Quaternary paleoclimate in the eastern Mediterranean Region from stable isotope analysis of speleothems at Soreq Cave, Israel. *Quat Research* 47:144–68.

Begin ZB, W Broecker, B Buchbinder, Y Druckman, A Kaufman, M Margaritz, and D Neev. 1985. Dead Sea and Lake Lisan levels in the last 30,000 years: a preliminary report. *Israel Geological Survey Report* 29:1–18.

Behling, Herman, Lichte, and Martin. 1997. Evidence of dry and cold climatic conditions at glacial times in tropical Southeastern Brazil. *Quat Research* 46:348–58.

Bergthorsen P. 1969. An estimate of drift ice and temperature in Iceland in 1,000 years. *Jour Jokull* 19:94–101.

Berry MS. 1982. Time/Space and Transition in Anasazi Prehistory. Salt Lake City (UT): University of Utah Press. 147 p.

Bischoff J, I Kirsten, M Menking, JP Fitts, and JA Fitzpatrick. 1997. Climatic oscillations 10,000–155,000 yr BP at Owens Lake, California reflected in glacial rock flour abundance and lake salinity in core OL–92. *Quat Research* 46

Bloom AL and others. 1974. Quaternary sea level fluctuations on a tectonic coast: new $^{230}Th/^{234}U$ dates from the Huon Peninsula, New Guinea. *Quat Research* 4:185–205.

Bueg H. 1982. Vegetation history and climatic changes in central and southern Europe. In: Anthony Harding, editor. Climatic Change in Late Prehistory. Edinburgh: Edinburg University Press. p 85–102.

Caballero M and B Guerrero. 1998. Lake levels since about 40,000 years ago at Lake Chalco, near Mexico City. *Quat Research* 50:59–79.

Chuey JM, DK Rea, and NG Pisias. 1987. Late Pleistocene paleoclimatology of the central Equatorial Pacific: a quantitative record of eolian and carbonate deposition. *Quat Research* 38:323–33.

Clapperton CM, DE Sudgen, DS Kaufman, and RD McCulloch. 1995. The last glaciation in Central Magellan Strait, southernmost Chile. *Quat Research* 44:133–48.

Dean JS and WJ Robinson. 1978. Expanded tree-ring chronologies for the southwest United States. Chronology Series III, Laboratory of Tree-Ring Research. Tucson (AZ): University of Arizona. 58 p.

Delcourt PA, WH Petty, and HR Delcourt. 1996. Late-Holocene formation of Lake Michigan beach ridges correlated with a 70–year oscillation in global climate. *Quat Research* 45:321–31.

Epstein S and CI Yapp. 1976. Climatic implications of the D/H ratio of hydrogen in C/H groups in tree cellulose. *Earth Planet Sci Letters* 30:252–66.

Euler RC, GJ Gumerman, TNV Karlstrom, JS Dean, and RH Hevly. 1979. The Colorado Plateaus: cultural dynamics and paleoenvironment. *Science* 205:1089–1101.

Friis-Christensen E and K Lassen. 1991. Length of solar cycle: an indicator of solar activity closely associated with climate. *Science* 254:698–700.

Fritts HC. 1967. Tree-ring analysis (dendroclimatology). In: Fairbridge R, editor. The Encyclopedia of Atmospheric Sciences and Astrogeology. New York (NY): Reinhold. p 1008–26.

Frumkin AM, I Magaritz, I Carmi and I Zak. 1991. The Holocene climatic record of the salt caves of Mount Sedom, Israel. *Holocene* I:191–200.

Hansen B, CS and DR Engstrom. 1996. Vegetation history of Pleasant Island, southeastern Alaska, since 13,000 yr BP. *Quat Research* 48:161–70.

Heusser CJ. 1965. A Pleistocene phytogeographic sketch of the Pacific Northwest and Alaska. In: Wright HE and BG Frey, editors. The Quaternary of the United States. Princeton (NJ): Princeton University Press. p 469–83.

Gasse F and G Delibrious. 1976. *Les Lacs de L'afar Centrol (Ethiopie et F. T. A. I.).* In: Shoji H, editor. Paleoclimatology of Lake Biwa and the Japanese Pleistocene. p 529–75.

Graumlisch LJ. 1992. A 1,000–year record of climatic variability in the Sierra Nevada, California [handout]. Am. Quat. Assoc. 12th Biennial Meeting; 24–26 Aug; Davis, California.

Hays JD, J Imbrie, and NJ Shackleton. 1976. Variations in the earth's orbit: pacemaker of the ice ages. *Science* 94:1121–32.

Hellstrom J, M McCulloch, and J Stone. 1998. A detailed 31,000–year record of climate and vegetation change from the isotope geochemistry of two New Zealand speleothems. *Quat Research* 50:167–78.

Helmens K, P Kahry, NW Rutter, K Van Der Borg, and AFM DeJong. 1996. Warming at 18,000 yr BP in the tropical Andes. *Quat Research* 45:289–99.

Heusser CJ. 1965. A Pleistocene phytogeographic sketch of the Pacific Northwest and Alaska. In: Wright HE and BG Frey, editors. The Quaternary of the United States. Princeton (NJ): Princeton University Press. p 469–83.

Hevly RH and TNV Karlstrom. 1974. Southwest paleoclimate and continental correlations. In: Karlstrom TNV, G Swann, and RL Eastwood, editors. Geology of Northern Arizona and Notes on Archaeology and Paleoclimate. Geological Society of America Field Guide 1. Rocky Mountain Meeting; Flagstaff, Arizona. p 257–295.

Hu FS, LB Brubaker, and PM Anderson. 1996. Boreal ecosystem development in the northwestern Alaska Range since 11,000 yr BP. *Quat Research* 45:188–201.

Karlstrom TNV. 1955. Late Pleistocene and recent glacial chronology of southcentral Alaska. *Geol Soc of America Bull* 66:1581–2.

Karlstrom TNV. 1956. The problem of the cochrane in Late Pleistocene chronology. *US Geol Survey Bull* 1021J:303–33.

Karlstrom TNV. 1961. The glacial history of Alaska: its bearing on paleoclimatic theory. *Annals New York Academy of Science* 95:290–340.

Karlstrom TNV. 1964. Quaternary geology of the Kenai Lowland and glacial history of the Cook Inlet Region, Alaska. US Geological Survey Professional Paper. 69 p.

Karlstrom TNV. 1966. Quaternary glacial record of the North Pacific Region and worldwide climatic change. In: Blumenstock DJ, editor. Pleistocene and Post-pleistocene Climatic Variations in the Pacific Area. Honolulu (HI): Bishop Museum Press. p 153–82.

Karlstrom TNV. 1975. Cenozoic time-stratigraphy of Colorado Plateaus, continental correlations and some paleoclimatic implications [handout]. Symposium on Quaternary Stratigraphy; 1975 May; York University, Toronto, Canada.

Karlstrom TNV. 1976a. Stratigraphy and paleoclimate of the Black Mesa Basin. *US Geological Survey Circular* 778:18–22.

Karlstrom TNV. 1976b. Quaternary and upper Tertiary time-stratigraphy of the Colorado Plateaus, continental correlations and some paleoclimatic implications. In: Mahany WC, editor. Quaternary Stratigraphy of North America. Stroudsburg (PA): Bowden, Hutchinson and Ross Inc. p 275-282.

Karlstrom TNV. 1988. Alluvial chronology and hydrologic change of Black Mesa and nearby Regions. In: Gumerman GJ, editor. The Anasazi in a Changing Environment. School of American Research Advance Seminar Book. London, United Kingdom: Cambridge University Press. p 45–91.

Karlstrom TNV. 1995. A 139–year dendroclimatic cycle, cultural/environmental history, sunspots and longer-term cycles. In: Isaacs CM and VI Tharp, editors. Proceedings of the 11th Annual Pacific Climate (PACLIM) Workshop, Technical Report 40 of the Interagency Ecological Program for the Sacramento–San Joaquin Estuary; 1994 Apr 19–22; Asilomar, CA. Sacramento (CA): Interagency Ecological Program for the Sacramento–San Joaquin Estuary. p 137–59.

Karlstrom TNV. 1996. The QBO, El Niño, and Tidal Resonance Model. In: Isaacs CM and VI Tharp, editors. Proceedings of the 12th Annual Pacific Climate (PACLIM) Workshop, Technical Report 46 of the Interagency Ecological Program for the Sacramento–San Joaquin Estuary; 1995 May 2–5; Asilomar, CA. Sacramento (CA): Interagency Ecological Program for the Sacramento–San Joaquin Estuary. p 241–53.

Karlstrom TNV. 1997. Addendum 1: paleoclimate and the solar insolation–tidal resonance climate model. In: Isaacs CM and VI Tharp, editors. Proceedings of the 13th Annual Pacific Climate (PACLIM) Workshop, Technical Report 53 of the Interagency Ecological Program for the Sacramento–San Joaquin Estuary; 1996 Apr 14–17; Asilomar, CA. Sacramento (CA): Interagency Ecological Program for the Sacramento–San Joaquin Estuary. p 201–24.

Karlstrom TNV. 1998. Addendum II: paleoclimate and the Solar Insolation/Tidal Resonance Model. In: Wilson RC and VL Tharp, editors. Interagency Ecological Program Technical Report 57. Proceedings of the 14th Annual Pacific Climate (PACLIM) Workshop; 1997 April 6–9; (place of conference). Sacramento (CA): California Department of Water Resources. p 65–93.

Karlstrom TNV, GJ Gumerman, and RC Euler. 1976. Paleoenvironmental and cultural correlates in the Black Mesa Region. In: Gumerman GJ and EC Euler, editors. Papers on the Archaeology of Black Mesa, Arizona. Carbondale: Southern Illinois University Press. p 149-161.

Kendall RL. 1969. An ecological history of the Lake Victoria Basin. *Ecological Monographs* 39:121–76.

Ladure EL. 1971. Times for Feast and Times of Famine: A History of Climate Since the Year 1000. New York (NY): Doubleday.

Lamb HH. 1977. Climate: Present, Past and Future 2, Climate History and the Future. London, United Kingdom: Methuen.

Ledru MP. 1993. Late Quaternary environment and climatic changes in Central Brazil. *Quat Research* 39:90–8.

Ledru MP, J Bertaux, A Sifeddine, and K Sequio. 1998. Absence of last glacial maximum records in lowland tropical forests. *Quat Research* 49:233–7.

Martinson DG, NG Pisias, JD Hays, J Imbrie, TC Moore Jr., and NJ Shackleton. 1987. Age dating and the orbital theory of the ice ages: development of a high-resolution 0 to 300,000–year chronostratigraphy. *Quat Research* 27:1–29.

Mesolella KJ. 1969. The astronomical theory of climatic change, Barbados data. *Jour Geology* 2:250–74.

Menking KM, JL Biskof, JA Fitzpatrick, JW Burdette and RO Rye. 1997. Climatic/hydrologic oscillations since 155,000 years B.P. at Owens Lake, California, reflected in abundance and stable isotope composition of sediment carbonate. *Quat Research* 48:58–68.

Milankovitch M. 1941. Canon of Insolation and the Ice-age Problem. Translated from German by Israel Program for Scientific Translation, Jerusalem. Available from: US Department of Commerce, Springfield, Virginia.

Nilsson T. 1964a. *Standardpollen diagramme und ^{14}C daterungen aus dem Agarods Mosse im Mittieren Schonen*. Lund Universitets Arskrift N. F. Avd 2, Bd 59, Nr. 7: 1-52. Lund: Hakan Ohssons Boktryceri.

Nilsson T. 1964b. *Enwicklungsgeschichtliche studien im Agarods Mosse, Schonen*. Lunds Universitets Arskrift N.N. Avd 2. Bd 59, Nr 8:1-34. Lund: Hakan Ohlssons Boktryckeri.

(NASC). 1983. North American Stratigraphic Code.

Oeschger H, M Welten, U Eicher, M Moll, T Riesen, U Siegenthaler, and S Wegmüller. 1980. ^{14}C and other parameters during the Younger Dryas cold phase. *Radiocarbon* 22:299–310.

Pandolfi LJ, EK Kalil, PR Doose, LH Levine, and LM Libby. 1980. Climate periods in trees and a sea sediment core. *Radiocarbon* 22:740–5.

Perez-Obiol R and J Ramon. 1994. Climatic change on the Iberian Peninsula recorded in a 30,000–year pollen record from Lake Banyoles. *Quat Research* 41:91–8.

Phillips FM, MG Zreda, LV Benson, MA Plummer, D Elmore, and P Sharma. 1996. Chronology for fluctuations in Late Pleistocene Sierra Nevada glaciers and lakes. *Science* 2174:749–51.

Prieto AR. 1996. Late Quaternary vegetational and climatic changes in the Pampa grassland of Argentina. *Quat Research* 45:73–88.

Rampton V. 1970. Late Quaternary vegetation and climatic history of the Snag-Klutlan Area, southwestern Yukon Territory, Canada. *Geol Soc America Bull* 81.

Richmond GM. 1976. Pleistocene stratigraphy and chronology in the mountains of western Wyoming. In: Many WC, editor. Quaternary Stratigraphy of North America. Stroudsburg (PA): Douden, Hutchinson and Ross Inc. p 353–79.

Schulman E. 1956. Dendroclimatic Changes in Semiarid America. Laboratory of Tree-ring Research, University of Arizona. Tucson (AZ): University of Arizona Press.

Schlesinger ME and Ramankutty N. 1994. An oscillation in the global climate system of period 65–70 years. *Nature* 367:723–6.

Sturchio NC, KL Pierce, MT Murrell, and ML Sorey. 1994. Uranium-series ages of travertine and timing of the last glaciation in the northern Yellowstone Area, Wyoming–Montana. *Quat Research* 42:265–77.

Szabo BL, PT Kolesar, AC Riggs, IJ Winograd, and KR Ludwig. 1994. Paleoclimatic inferences from a 120,000–year calcite record of water-table fluctuations in Browns Room of Devils Hole, Nevada. *Quat Research* 41:59–69.

Terasmae J and A Dreimanis. 1976. Quaternary stratigraphy of southern Ontario. In: Mahany WC, editor. Quaternary Stratigraphy of North America. Stroudsburg (PA): Douden, Hutchinson and Ross Inc. p 51–63.

Vernekar AD. 1972. Long period global variations of incoming solar radiation. *Meteorological Monographs* 12:19 p + 170 unnumbered pages.

Villagren C. 1988. Late Quaternary vegetation of southern Isla Grande de Chloe, Chile. *Quat Research* 29:294–306.

von Woerkom AJJ. 1953. Astronomical Theory. In: Shapley H, editor. Climatic Change. Cambridge (MA): Harvard University Press. p 147–57.

Winograd IJ, TB Coplen, JM Landwehr, AC Riggs, KB Ludwig, BJ Szabo, PT Kolegar, and KM Revesz. 1992. Continuous 500,000–year climate record from vein calcite in Devils Hole, Nevada. *Science* 258:255–60.

Evidence for ENSO in Tree-Ring $\delta^{13}C$ along a 500-km E-W Transect in Southern Arizona and New Mexico

Steven W. Leavitt[1], William E. Wright[1], and Austin Long[2]
[1]Laboratory of Tree Ring Research and [2]Department of Geosciences
The University of Arizona
Tucson, Arizona 85721

Abstract

Ponderosa pine tree rings were sampled at ten sites in nine mountain ranges extending from the Santa Catalina Mountains in southern Arizona to the Guadalupe Mountains in southern New Mexico. We developed stable-carbon isotope ($\delta^{13}C$) chronologies at eight sites for 1985–1995 by pooling rings from multiple trees at each site, subdividing rings into pre- and post-summer, monsoon-onset segments, and analyzing the cellulose component. The $\delta^{13}C$ values are considered a useful proxy of the seasonal moisture stress experienced by the trees. Two chronologies developed at separate sites in the Chiricahua Mountains, Arizona, showed good coherence despite being separated by about 13 km and 800 m of elevation. This evidences effective reproducibility of the method, with the differences between the two chronologies perhaps a consequence of the microclimatic and hydrological disparities between sites. For the full network of chronologies, the $\delta^{13}C$ seasonal pattern shows remarkable coherence across the full length of the transect, with the farthest east Sacramento Mountains chronology tending to be more frequently dissimilar with respect to those farther west. The strongest correlations (positive) were between $\delta^{13}C$ of the earliest formed portion of the rings and Southern Oscillation Index, consistent with reduced moisture stress early in the growing seasons of El Niño years and higher moisture stress in La Niña years.

Introduction

Tree rings of ponderosa pine (*Pinus ponderosa*) in the southwestern US frequently exhibit a "false latewood" band within each annual growth ring, indicating an interruption of ring development associated with the fore-summer drought conditions of May and June. The onset of precipitation from the southwest US monsoon commonly results in reinitiation of growth and completion of the growth ring. Consequently, there appears to be two tree rings in one growing season, when in fact there is a single ring containing an interior false-latewood band. This band serves as a time marker, the end of which approximates the onset of monsoon rainfall that occurs on average in the first week in July.

Previous stable-carbon isotope studies of tree rings have revealed strong relationships with moisture conditions to which the trees are exposed (Dupouey and others 1993; Leavitt 1993; Leavitt and Long 1989a; Livingston and Spittlehouse 1993). Under conditions of moisture stress, stomatal closure restricts entry of CO_2 into the leaves, and photosynthesis takes place with a limited reservoir of CO_2 resulting in a relatively high proportion of ^{13}C isotopes (to ^{12}C isotopes). Under average or high water availability conditions, ^{13}C atoms are more efficiently excluded by enzymatic isotope fractionation and plant $^{13}C/^{12}C$ ratios are lower.

This research exploits the false latewood time marker and tree ring $\delta^{13}C$ analysis to infer seasonal moisture conditions. Fundamental findings reveal isotopic variability (1) among trees at a site, (2) between sites in close proximity, and (3) among all sites. Finally, comparison of isotopic results with Southern Oscillation Index (SOI) exposes spatial and timing relationships between ENSO (El Niño–Southern Oscillation) and tree ring $\delta^{13}C$.

Methods

From 1995 to 1997, *Pinus ponderosa* trees were sampled in southern Arizona and New Mexico at ten mountain sites, nine of which were in a limited elevation range of 2,100 to 2,500 m, with the tenth situated at 1,700 m (Figure 1). Preliminary test cores were taken to help ensure that resident trees had a high occurrence of "false" rings over the past 15 years, and that rings were sufficiently wide to provide enough material for carbon as well as oxygen (and possibly hydrogen) isotopic analysis. Typically, eight to ten trees were then sampled with increment cores 12 mm in diameter from four orthogonal sides of each tree to ensure representative samples (Leavitt and Long 1984).

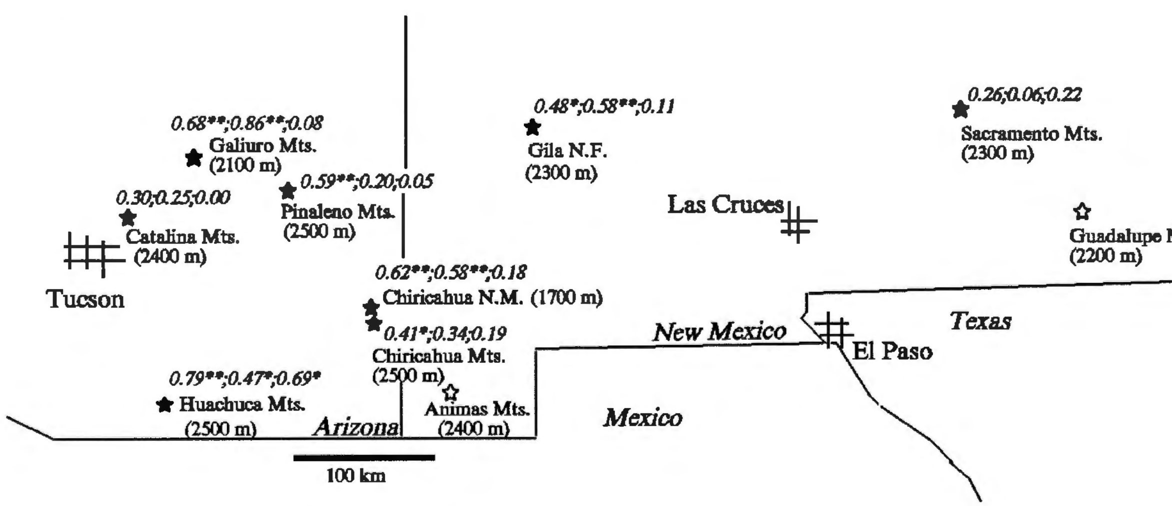

Figure 1 Location map for ponderosa pine sites used in this study. Elevations are given in parenthesis. The three italicized numbers above eight of the sites are the r^2 values of correlations between $\delta^{13}C$ of the pre-2 portion of the ring and December, January, and February SOI, respectively. (* = *P*<.05; ** = *P*<.01).

Core samples from all trees were sanded, dated, and carefully inspected for ring size and false ring presence. Absence of sufficient false rings and problems in dating prevented completion of analysis of samples from the Animas Mountains and Guadalupe Mountains, respectively. A subset of four to six trees (two trees at the Catalina Mountains site) with best ring characteristics was selected for subsequent processing and isotopic analysis. Pre- and post-false latewood ring widths were measured. Prior to the destructive processing for isotopic analysis, images of each of the rings back to 1980 were taken and archived.

Tree rings were subdivided into pre-1, pre-2, and post-false latewood bands. The false latewood band itself was contained in the pre-2 subdivision, but never in the post-false subdivision. Samples were ground, extracted first with toluene and ethanol and then ethanol alone, and delignified to holocellulose in an acidified sodium-chlorite solution (Leavitt and Danzer 1993). Holocellulose was combusted to CO_2 in the presence of excess oxygen in a recirculating microcombustion system. The CO_2 was measured with a mass spectrometer and results were expressed as $\delta^{13}C$ in ‰ (= $[^{13}C/^{12}C_{sample} \div {}^{13}C/^{12}C_{PDB\ standard} - 1] \times 1000$) with respect to the international PDB standard (Craig 1957; Coplen 1996). Repeated combustion and analysis of two different holocellulose lab standards during the period of isotopic measurement gave standard deviations of 0.16‰ ($n = 32$) and 0.17‰ ($n = 24$).

Results and Discussion

The $\delta^{13}C$ variability among ponderosa pine trees at a site is typically 1‰ to 3‰, effectively the same range reported among various pine species in the western US (Leavitt and Long 1989b). Figure 2 illustrates this isotopic variability among the 5 trees at the Huachuca Mountains site for 1993–1995. Seasonal isotopic patterns are very similar within each year, but absolute values among trees are different, although the order of $\delta^{13}C$ enrichment among trees tends to be about the same from year to year.

The two sites in the Chiricahua Mountains are separated by 13 km and differ in elevation by about 800 m. Isotopic chronologies from the two sites (Figure 3) show similar secular trends of isotopic values over ten years, with high absolute $\delta^{13}C$ at both sites in 1989, 1990, 1994, and 1995, and low values in 1987 and 1992. This secular trend conforms to the pattern originally seen in ponderosa pine from the Catalina Mountains described by Leavitt and others (1998). Within years, the seasonal patterns of the sites are usually very similar; the biggest exception being 1989 when the low elevation site (Chiricahua, New Mexico), $\delta^{13}C$ continuously rises during the growing season and the high elevation site $\delta^{13}C$ declines. The 1989 year was a strong drought year in the Southwest. The canyon-bottom locality of the low elevation site may have been particularly susceptible to the conditions of sustained lack of rainfall (for example, low water retention capacity of alluvium), while the high elevation site received more moisture or the trees were better able to exploit available moisture. Despite such individual year differences, a significant correlation ($r^2 = 0.41$, $n = 30$, $P < .01$) exists between the isotopic chronologies.

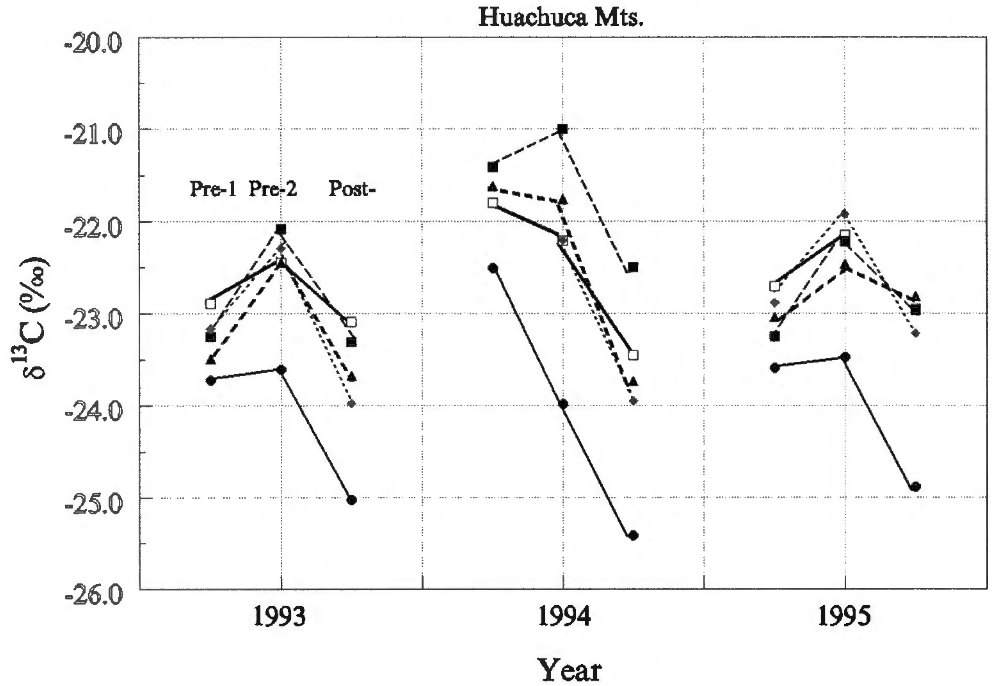

Figure 2 The pre-1, pre-2, and post-false latewood band $\delta^{13}C$ of the five trees at the Huachuca Mountains site

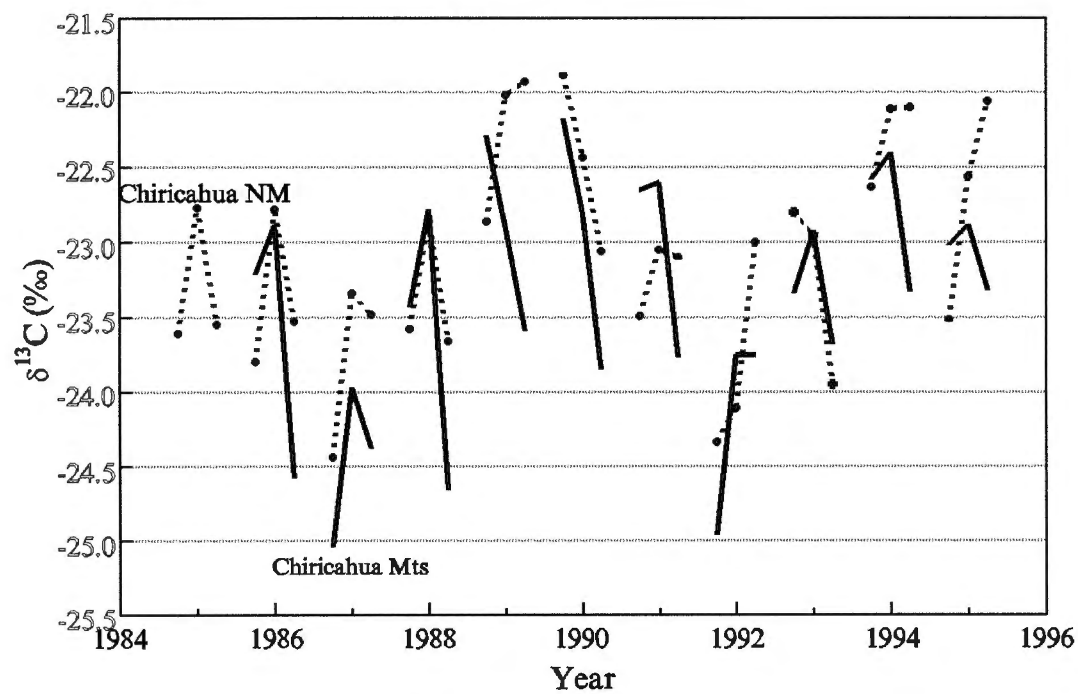

Figure 3 The average pre-1, pre-2, and post-false latewood band $\delta^{13}C$ for the low elevation (1,700 m) Chiricahua, New Mexico, and the high elevation Chiricahua Mountains sites

The interannual $\delta^{13}C$ patterns for all eight sites are represented with spline curves in Figure 4 fitted to unweighted isotopic means of each year. Most show the largest maximum in the 1989 (or 1990) drought year, with a minimum in 1991 or 1992. The two sites farthest east in the Gila and Sacramento mountains, however, show their greatest $\delta^{13}C$ maximum in 1994. This suggests the length of the east-west transect is sufficiently long that isotope analysis can reveal regional differences in moisture conditions and that 1994 was notably drier than 1989 toward the east.

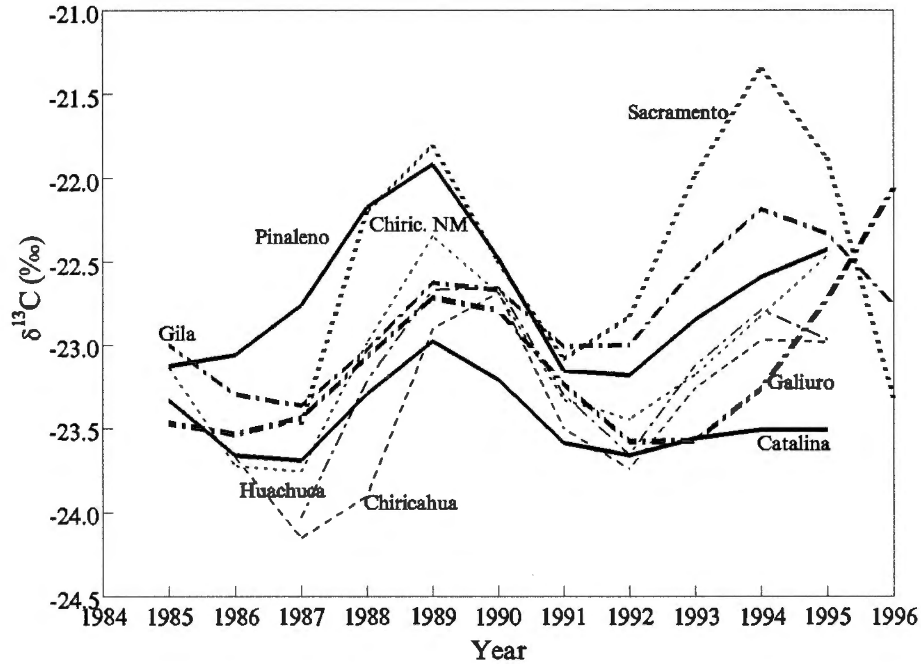

Figure 4 Spline curves fit to the unweighted average $\delta^{13}C$ values of each of the eight ponderosa pine sites

These regional effects are further illustrated in Figure 1 where results of correlation (r^2) between $\delta^{13}C$ of the pre-2 portion of the ring are correlated against SOI for December, January, and February before the beginning of the growing season. $\delta^{13}C$ and SOI in the farthest east and farthest west site on the transect show no correlation, whereas the central sites show some significant correlations. For $\delta^{13}C$ of the pre-1 ring segment, the reverse is actually true with the strongest correlations at the eastern and western edges of the transect (not shown). For all sites, the $\delta^{13}C$ of the post-false ring portion show little relationship with SOI of any month (not shown).

Conclusions

Despite 1‰ to 3‰ variability among trees at a site, the seasonal $\delta^{13}C$ patterns among ponderosa pine trees tend to be very coherent. This implies site-scale environmental forcing of isotopic composition. Likewise, despite the long distances between sites in the transect, the interannual secular pattern of $\delta^{13}C$ is also quite coherent. This implies regional-scale environmental forcing of ponderosa $\delta^{13}C$. There are similarities between these secular patterns and meteorological drought and SOI conditions. The strong correlations of pre-1 and pre-2 $\delta^{13}C$, with winter SOI for some sites, are consistent with ENSO's strong relationship with southwestern winter and spring precipitation.

Differences in the seasonal $\delta^{13}C$ patterns among sites may reflect different moisture histories, perhaps influenced by local hydrology. A more careful site-by-site analysis of the $\delta^{13}C$ chronologies with local climatological records is continuing to better understand differences among sites.

Acknowledgments

We thank K. Kuehn, T. Stier, B. McCaleb, and N. Ricketts for valuable field and laboratory assistance and mass spectrometer operation. This research was supported by NSF Grant #ATM-9421041.

References

Coplen TB. 1996. New guidelines for reporting stable hydrogen, carbon and oxygen isotope-ratio data. *Geochimica et Cosmochimica Acta* 602:3359–60.

Craig H. 1957. Isotopic standards for carbon and oxygen and correction factors for mass spectrometric analysis of carbon dioxide. *Geochimica et Cosmochimica Acta* 12:133–49.

Dupouey JL, S Leavitt, E Choisnel, and S Jourdain. 1993. Modeling carbon isotope fractionation in tree rings based on effective evapotranspiration and soil water status. *Plant, Cell and Environ* 16:939–47.

Leavitt SW. 1993. Seasonal $^{13}C/^{12}C$ changes in tree rings: species and site coherence, and a possible drought influence. *Canadian Journal of Forest Research* 23:210–18.

Leavitt SW and SR Danzer. 1993. Method for batch processing small wood samples to holocellulose for stable-carbon isotope analysis. *Anal Chem* 65:87–9.

Leavitt SW and A Long. 1989a. Drought indicated in carbon–13/carbon–12 ratios of southwestern tree rings. *Water Resources Bulletin* 25:341–7.

Leavitt SW and A Long. 1989b. Intertree variability of $\delta^{13}C$ in tree rings. In: Rundel PW, JR Ehleringer, and KA Nagy, editors. Stable Isotopes in Ecological Research. New York (NY): Springer-Verlag. p 95–104.

Leavitt SW, and A Long. 1984. Sampling strategy for stable carbon isotope analysis of tree rings in pine. *Nature* 301:145–7.

Leavitt SW, WE Wright and A Long. 1998. ENSO signal in $\delta^{13}C$ of pre- and post-false latewood of ponderosa pine tree rings in Southeastern Arizona. In: Wilson R and VL Tharp, editors. Proceedings of the 14th Annual Pacific Climate (PACLIM) Workshop, Technical Report 57 of the Interagency Ecological Program for the Sacramento-San Joaquin Estuary; 1997 Apr 6–9. Santa Catalina Island, CA. Sacramento (CA): Interagency Ecological Program for the Sacramento–San Joaquin Estuary. p 37–44.

Livingston NJ and DL Spittlehouse. 1993. Carbon isotope fractionation in tree rings in relation to the growing season water balance. In: Ehleringer JR, AE Hall, and GD Farquhar, editors. Stable Isotopes and Plant Carbon-Water Relations. San Diego (CA): Academic Press. p 141–53.

Decadal Variability in the Strength of ENSO Teleconnections with Precipitation in the Western United States

Gregory J. McCabe
US Geological Survey, Denver Federal Center, MS 412
Denver, Colorado 80225

Michael D. Dettinger
US Geological Survey, Climate Research Division
Scripps Institution of Oceanography, Department 224
University of California, San Diego
La Jolla, California 92093-0224

Abstract

Changing patterns of correlations between the historical average June-through-November Southern Oscillation Index (SOI) and October-through-March precipitation totals for 84 climate divisions in the western United States (US) indicate a large amount of variability in SOI-precipitation relations on decadal time scales. Correlations of western US precipitation with SOI and other indices of tropical El Niño–Southern Oscillation (ENSO) processes were much weaker from 1920 to 1950 than during recent decades. This variability in teleconnections is associated with the character of tropical air-sea interactions as indexed by the number of out-of-phase, SOI-tropical, sea surface temperature episodes, and with decadal variability in the North Pacific Ocean as indexed by the Pacific Decadal Oscillation (PDO). ENSO teleconnections with precipitation in the western US are strong when SOI and NINO3 sea surface temperatures are out of phase and PDO is negative. ENSO teleconnections are weak when SOI and NINO3 are in phase and PDO is positive. Decadal modes of tropical and North Pacific Ocean climate variability are important indicators of periods when ENSO indices, like SOI, can be used as reliable predictors of winter precipitation in the US.

Introduction

Over the past three decades, research has identified global teleconnections between El Niño–Southern Oscillation (ENSO) and surface climate in several parts of the world (Horel and Wallace 1981; Namias and Cayan 1984; Trenberth 1976; 1984; Yarnal and Diaz 1986; Redmond and Koch 1991). Redmond and Koch (1991) identified significant correlations between the average June-through-November Southern Oscillation Index (SOI) and winter precipitation in the western United States (US) for the period 1934–1995. The analysis indicates positive correlations between SOI and winter precipitation in the northwestern US and negative correlations between SOI and winter precipitation in the southwestern US.

Research also has indicated that SOI teleconnections may not be consistent through time (Trenberth and Shea 1987; Elliott and Angell 1988; Trenberth and Hoar 1996; Trenberth 1997). There has been speculation that the variability in SOI-precipitation relations may be due to data problems in the SOI (Ropelewski and Jones 1987; Elliott and Angell 1988; Trenberth 1997), or that the SOI may not be the best index of ENSO (Elliott and Angell 1988). Other research has indicated that the SOI is reliable and that changes in the ocean-atmosphere system in the North Pacific Ocean may be the driving force of the variability in SOI-precipitation relations (Ropelewski and Jones 1987; Elliott and Angell 1988). The objectives of this study are to (1) examine variability in the strength of the relations between SOI and winter precipitation in the western US, (2) determine whether variability in these relations is isolated to the SOI or whether other indices of ENSO exhibit similar variability, and (3) examine long-term tropical and extratropical conditions that may be related with the major variations in SOI-precipitation relations.

Correlations Between SOI and Winter Precipitation

Correlations between SOI and winter precipitation for the 84 climate divisions in the western US have varied through time (Figure 1). In general, winter precipitation in the northwestern US is positively correlated with SOI and winter precipitation in the southwestern US is negatively correlated with SOI. For 1901–1930, winter precipitation for many of the climate divisions in the northwestern US was significantly (at a 95% confidence level) correlated with SOI. Winter precipitation at only a few climate divisions in the southwestern US was significantly correlated with SOI during this period. The number of significant correlations between SOI and winter precipitation in the western US decreased dramatically for the periods 1911–1940 and 1921–1950. During 1921–1950, the only significant correlations between SOI and winter precipitation were in the southwestern US. During 1931–1960, a few significant correlations occurred in the northwestern US and several occurred in the southwestern US. During 1941–1970, 1951–1980, and 1961–1990, a relatively large number of significant correlations between SOI and winter precipitation occurred. The series of maps indicate a large amount of variability in the number and location of significant correlations between SOI and winter precipitation in the western US, especially during 1911–1940 and 1921–1950.

Significant correlations between winter precipitation in the western US and SOI have been more numerous during recent years than during 1920–1950 (Figure 2a). The change in precipitation correlations have paralleled the character of tropical air-sea interactions as indexed by the number of episodes in which strongly negative SOIs coincided with warm NINO3 SSTs (out-of-phase, SOI-NINO3 events) and vice versa (Figure 2b). The variability in SOI-precipitation correlations is not directly related to changes in the mean or variability of SOI (Figures 2c and 2d).

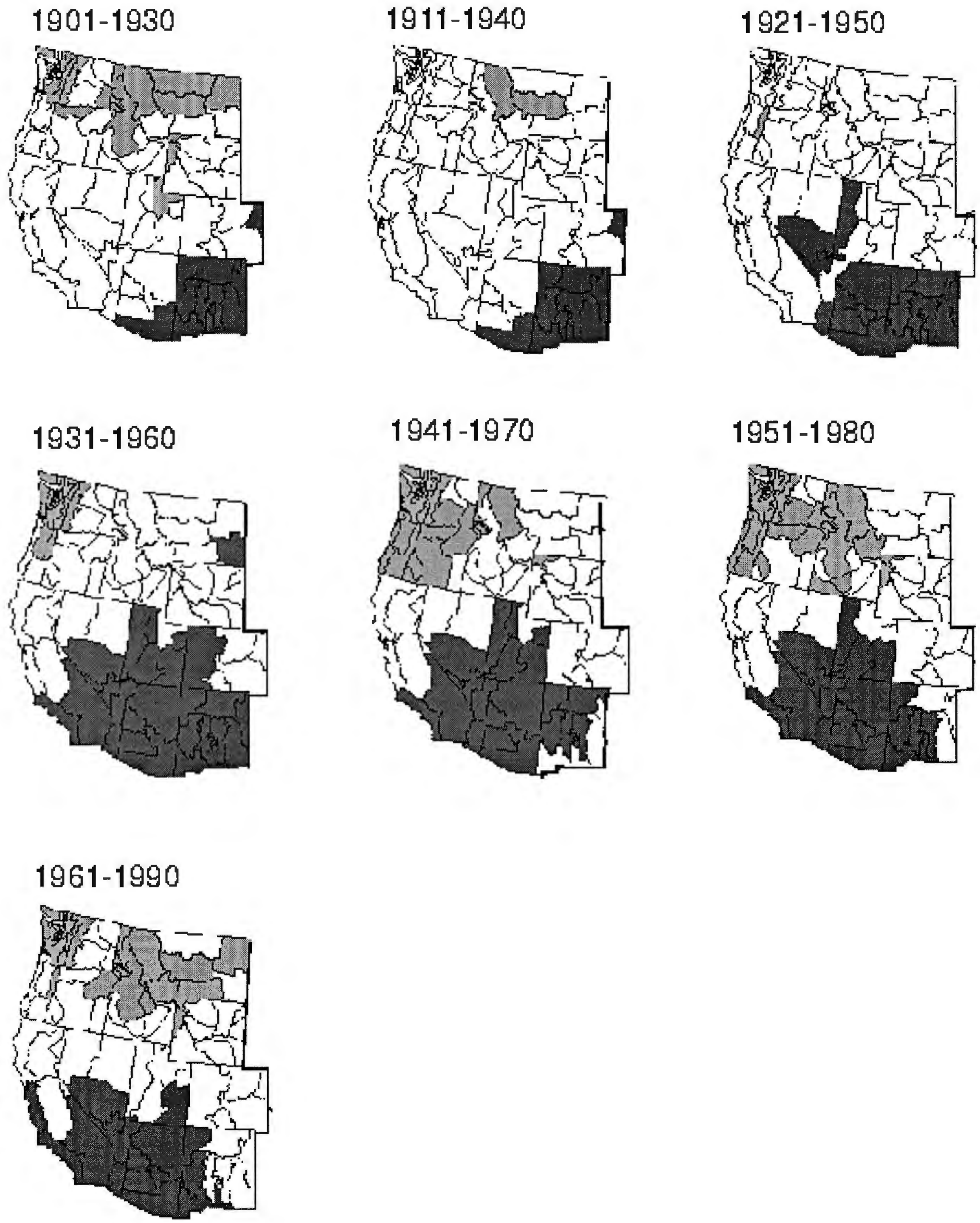

Figure 1 Positive (light gray) and negative (dark gray) correlations (significant at a 95% confidence level) between the average June-through-November SOI and October-through-March climate division precipitation in the western US for a series of 30–year periods

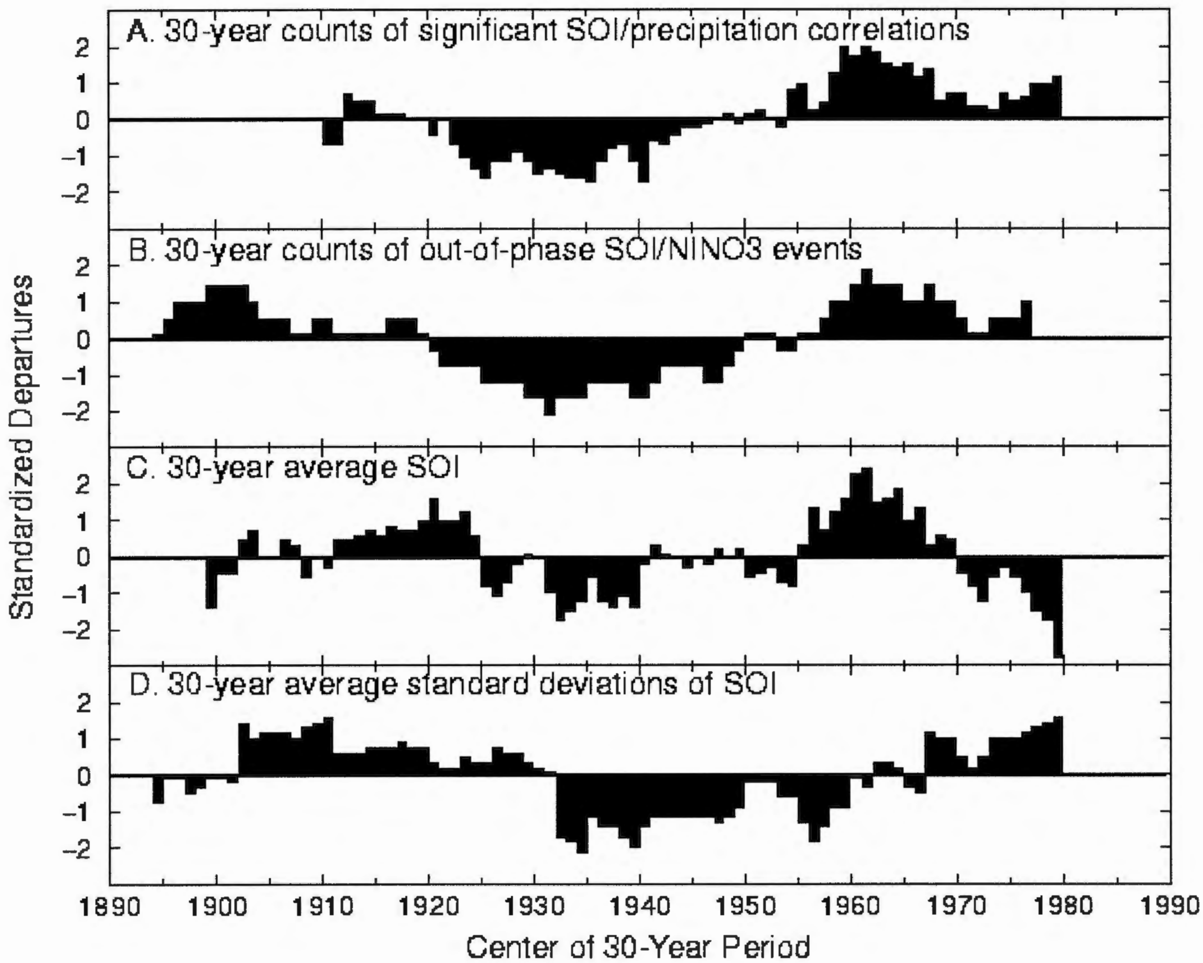

Figure 2 **(A) Standardized 30–year moving counts of significant correlations between the average June-through-November SOI and October-through-March climate division precipitation in the western US, (B) standardized 30–year moving counts of years when the extremes of the average June-through-November SOI are out of phase with the extremes of the average June-through-November NINO3 sea surface temperatures, (C) standardized 30–year moving average June-through-November SOI, and (D) 30–year moving standard deviations of June-through-November SOI**

Correlations Between Sea Level Pressures and SOI

The weak relations between SOI and extratropical climate from 1920–1950 are illustrated by correlations between SOI and winter sea level pressures for the Northern Hemisphere (Figure 3). The small correlations for 1920–1950 indicate proportionately weaker forcing of North American winter weather by the tropical ENSO processes represented by SOI.

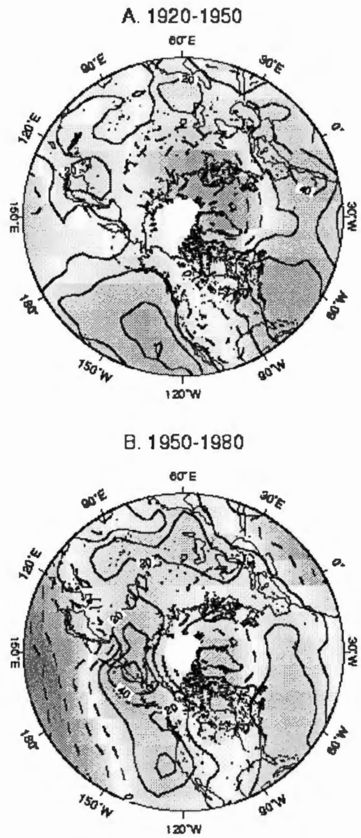

Figure 3 Correlations between September-through-November SOI and January sea level pressures (taken from five-month moving averaged data) for the Northern Hemisphere for (A) 1920–1950 and (B) 1950–1980. The solid lines indicate positive correlations and the dashed lines indicate negative correlations. The first solid line is the zero correlation isoline and the contour interval is 0.20.

Correlations Between Sea-Surface Temperatures and SOI

Some of the disconnection between tropical air-sea measures of ENSO processes and tropical-extratropical teleconnections presented in previous figures can be evaluated by correlations of SOI and Arizona precipitation with global sea surface temperatures (SSTs). Correlations of SOI with SSTs during 1921–1950 were weak and did not resemble the tropical patterns associated with ENSO observed in more recent decades (Figures 4a and 4b). Similarly, correlations between Arizona winter precipitation (for climate division 5 in Arizona) and SSTs during 1921–1950 also were weak and also did not indicate the tropical ENSO patterns observed more recently (Figures 4c and 4d). The lack of teleconnections of tropical SSTs with precipitation in the western US suggest a failure of more than just the reliability of a specific ENSO index like SOI, and instead indicates that tropical processes and their teleconnections with western US precipitation were globally weakened and disconnected for a period of several decades.

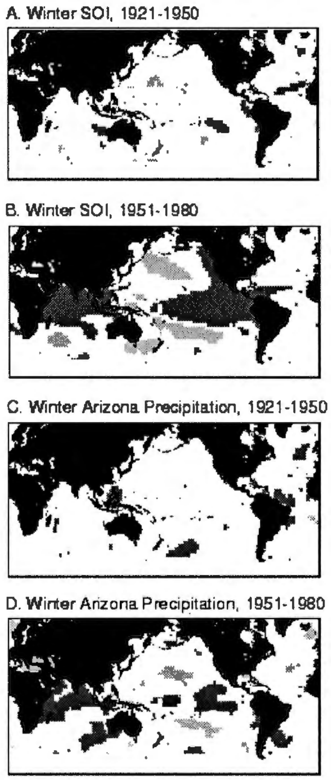

Figure 4 Correlations between winter SST anomalies (Parker and others 1995) and the negative of the December-through-February SOI (–1*SOI, the sign of SOI was reversed for ease of comparison with Arizona precipitation) for (A) 1921–1950 and (B) 1951–1980, and between SST anomalies and January-through-March precipitation for Arizona climate division 5 (ARIZONA PPT) for (C) 1926–1950 and (D) 1951–1970

Decadal Variability in North Pacific Ocean Climate

Variability in the strength of SOI-precipitation relations also appears to be related to decadal-scale variations in the North Pacific Ocean climate. The Pacific Decadal Oscillation (PDO) is an index of the dominant form of decadal variability of SSTs in the North Pacific Ocean (Mantua and others 1997), and is calculated as the leading principal component of monthly SSTs in the Pacific basin poleward of 20 degrees north latitude. When PDO is negative, the SSTs in the central North Pacific Ocean are warmer than average. When PDO is positive, the SSTs in the central North Pacific Ocean are cooler than average. A 30–year moving average of the June-through-November PDO index exhibits variability that closely mirrors the strength of SOI-precipitation relations, as depicted by 30–year counts of significant correlations (Figure 5). Thirty-year moving averages of the PDO were higher than average from 1920 to the late 1940s, and lower than average from the late 1940s to the late 1970s. The 30–year moving averages of the June-through-November PDO and 30–year counts of significant SOI-precipitation correlations is highly anticorrelated ($r = -0.88$).

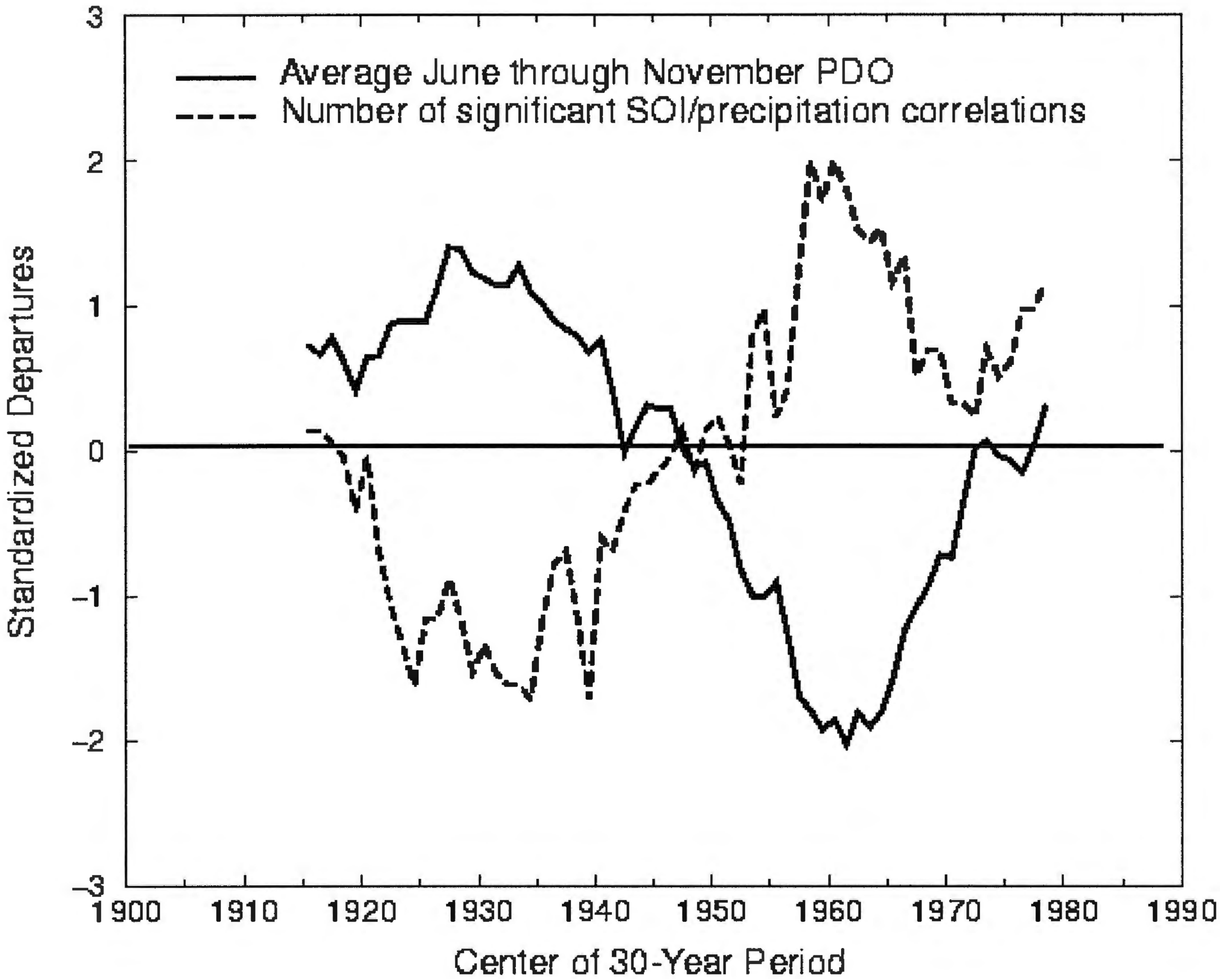

Figure 5 Thirty-year moving average of June-through-November PDO indices and 30–year counts of significant correlations between average June-through-November SOI and October-through-March precipitation in the western US. The data are plotted for the year of the SOI-precipitation correlations.

The variability in SOI-precipitation relations also is observed for other indices of the condition of the tropical Pacific Ocean. Correlations between winter precipitation in the western US and NINO3 SSTs and Darwin SLP parallel the variability for SOI-precipitation correlations (Figure 6). The variations of NINO3 and Darwin SLP teleconnections, however, do not appear to be as sensitive to PDO as are SOI teleconnections. Most likely, the shape and extent of the Southern Oscillation SLP pattern changes when PDO changes sign and this change is reflected in variations of the tropical teleconnections to precipitation in the western US.

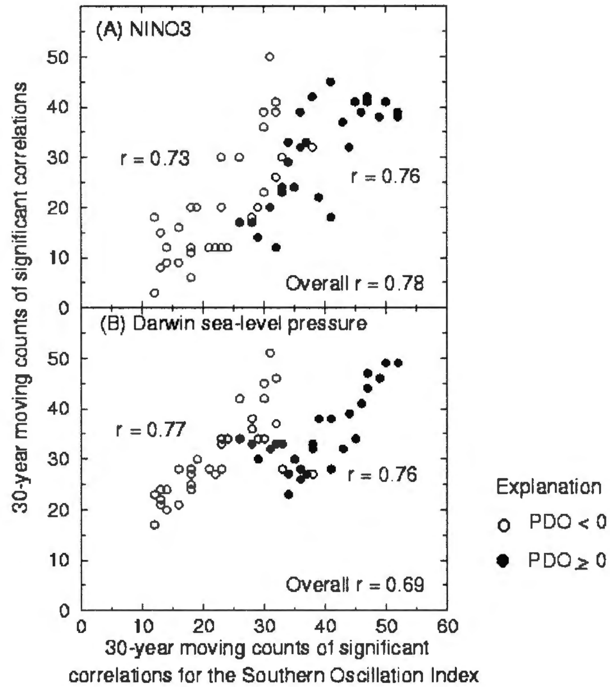

Figure 6 Comparison of 30–year moving counts of significant correlations between the average June-through-November SOI and October-through-March climate precipitation and 30–year moving counts of significant correlations between (A) average June-through-November NINO3 sea surface temperatures and October-through-March climate division precipitation, and (B) average June-through-November Darwin sea level pressures and October-through-March climate division precipitation. Counts during 30–year periods with positive and negative values of the PDO are indicated by filled and open circles, respectively

Summary

Correlations between SOI and winter precipitation in the western US for overlapping 30–year periods varied in strength and pattern during the 20th century. These variations appear to relate to how closely the oceanic and atmospheric components of ENSO interact from decade to decade to form the out-of-phase SOI and NINO3 relations (negative SOIs coinciding with warm NINO3 SSTs and vice versa) that have been observed in recent decades. The variations also appear to be associated with large-scale variability of the North Pacific Ocean climate system as indexed by the PDO. ENSO teleconnections with precipitation in the western US are strong when SOI and NINO3 are out of phase and PDO is negative. ENSO teleconnections with precipitation in the western US are weak when SOI and NINO3 are in phase and PDO is positive.

An understanding of the state and nature of decadal variations of tropical and North Pacific Ocean climate systems is necessary for interpretation of teleconnections between the tropical Pacific Ocean and the climate of the US (Latif and Barnett 1996). The results of this study indicate that teleconnections change on decadal time scales so that analysis of longer climate series need not always improve the depiction or statistical significance of a particular hydroclimatic teleconnection. Analysis of short time series, however, may lead to overconfident estimates of teleconnection strength. In particular, hydroclimatic responses to ENSO during the several decades before about 1950 were different and weaker than responses since then. If such a change in teleconnections were to reoccur (for example, Hodge 1997) the skill of long-range forecasting of climatic conditions in the western US might be adversely affected and many existing ENSO-based management strategies could be threatened. Knowledge of the states of the decadal modes of tropical and North Pacific Ocean climate variability, however, may enable the discrimination between periods when ENSO indices, like SOI, can be used as reliable predictors of winter precipitation in the US and periods when SOI would be an unreliable predictor.

References

Elliott WP and JK Angell. 1988. Evidence for changes in southern oscillation relationships during the last 100 years. *Journal of Climate* 1:729–37.

Hodge S. 1997. Glacier mass balances suggest recent changes in Pacific hemisphere teleconnections. *EOS, Transactions of the American Geophysical Union* 78:F101.

Horel JD and JM Wallace. 1981. Planetary scale atmospheric phenomena associated with the Southern Oscillation. *Monthly Weather Review* 109:813–29.

Latif M and TP Barnett. 1996. Decadal climate variability over the North Pacific and North America: dynamics and predictability. *Journal of Climate* 9:2407–23.

Mantua NJ, SR Hare, Y Zhang, JM Wallace, and RC Francis. 1997. A Pacific interdecadal climate oscillation with impacts on salmon production. *Bulletin of the American Meteorological Society* 78:1069–79.

Namias J and DR Cayan. 1984. El Niño: implications for forecasting. *Oceanus* 27:41–7.

Parker DE, CK Folland, A Bevan, MN Ward, M Jackson, and K Maskell. 1995. Marine surface data for analysis of climatic fluctuations on interannual to century time scales. Natural Climate Variability on Decade to Century Time Scales. Climate Research Committee, National Research Council. National Academy Press. p 241–50.

Redmond KT and RW Koch. 1991. Surface climate and streamflow variability in the western United States and their relationship to large scale circulation indices. *Water Resources Research* 27:2381–99.

Ropelewski CF and PD Jones. 1987. An extension of the Tahiti–Darwin southern oscillation index. *Monthly Weather Review* 115:2161–5.

Trenberth KE. 1976. Spatial and temporal variations in the southern oscillation. *Quarterly Journal of the Royal Meteorological Society* 102:639–53.

Trenberth KE. 1984. Signal versus noise in the southern oscillation. *Monthly Weather Review* 112:326–32.

Trenberth KE and TJ Hoar. 1996. The 1990–1995 El Niño–Southern Oscillation event: longest on record. *Geophysical Research Letters* 23:57–60.

Trenberth KE. 1997. The definition of El Niño. *Bulletin of the American Meteorological Society* 78:2771–77.

Trenberth KE and DJ Shea. 1987. On the evolution of the southern oscillation. *Monthly Weather Review* 115:3078–96.

Yarnal B and HF Diaz. 1986. Relationship between extremes of the southern oscillation and the winter climate of the Anglo-American Pacific coast. *Journal of Climate* 6:197–219.

Climate Prediction for Winter 1997–1998

Kingtse Mo, Xueliang Wang, and Masao Kanamitsu
NCEP/NWS/NOAA
Climate Prediction Center
Washington, D.C. 20233–9910

Abstract

The ensemble regional forecasts over the United States (US) were made in October 1997 for winter 1997–1998. Ensemble global forecasts were performed with surface temperature anomalies (SSTA) in the tropical Pacific taken from the NCEP-coupled, atmospheric ocean model, ensemble forecast. The global forecasts were then downscaled using the NCEP regional spectral model (RSM), nested in the global model outputs to enhance the precipitation forecasts.

The global forecasts for the winter mean have high skill over the Northern Hemisphere. The model is able to capture the wave train extending from the area of convection to the Pacific North America. Precipitation anomalies due to the influence of SSTA show wet conditions in California and Florida and dry conditions over the Ohio Valley. Rainbelt also extends from the Gulf of Mexico to the central US. The forecasted ensemble anomaly pattern for the T62 model is similar to that observed, but the low resolution model is not able to capture the magnitudes of rainfall and it misses rainfall at high elevations over California.

The NCEP RSM is embedded in the T62 global model outputs to enhance the precipitation prediction over the US. Both 50 km resolution RSM ensemble over the US and 30 km resolution RSM over the western region were performed. The 50 km resolution RSM improves the rainfall amounts in California, but it is still not able to resolve orographic-related features. The 30 km resolution RSM provides a better forecast of precipitation at high elevations and centers along the coast of California. This experiment indicates that it is feasible to make regional forecasts one to two months in advance for water resources management.

Introduction

The objective of this paper is to demonstrate that it is feasible to make regional climate forecasts one month in advance for water resources planning. We report a downscaling experiment made during October 1997. With SSTA in the central Pacific provided by the NCEP-coupled, atmosphere-ocean coupled model, global ensemble forecasts for winter 1997–1998 were made using one version of the NCEP AGCM. These forecasted large-scale atmospheric anomalies are then downscaled via a regional mode (RSM) (Juang and others 1997). The purpose of this experiment is to assess the possibility of predicting precipitation and other variables in specific locations for hydrological applications.

Experimental Design

All AGCM integrations were performed using a version of the NCEP/MRF model. Two sets of ensemble seasonal forecasts with forecasted SSTA were produced for winter 1997–1998 from 16 to 20 October 1997. The only difference between the two sets is the model resolution. One set has T62 horizontal resolution with 28 levels in the vertical and the other set has T40 horizontal resolution with 18 levels in the vertical. The SSTA in the tropical Pacific (lat 15°S to 15°N, long 120°E to 70°W) were taken from the coupled atmosphere–ocean model ensemble forecast and climatology was used elsewhere. We refer to them as the T62 SSTA and T40 SSTA forecasts, respectively. The initial conditions were taken from the NCEP analyses.

We then made ensemble regional forecasts by nesting the RSM in the T62 SSTA outputs. The downscaling forecasts were made using both 50 km resolution over the United States (US) and 30 km resolution over the western US. We focused over the western US because precipitation in that region is influenced by tropical convection (Mo and Higgins 1998). The vertical resolution is 28 levels consistent with the T62 AGCM. Each ensemble consists of five integrations. We refer to these runs as RSM 50 and RSM 30 forecasts.

For verification, the circulation fields were obtained from the NCEP/NCAR CDAS/reanalysis (Kalnay and others 1996). The anomalies were departures from the climatology from 1958 through 1959. Precipitation over the US was taken from 1° x 1° precipitation data set from the NCDC.

AGCM Results

During winter 1997–1998, the forecasted tropical SSTA produced by the NCEP coupled model were very realistic. The model captures the SSTA greater than 4 °C extending from the eastern Pacific to the central Pacific. In addition to SSTA in the central Pacific, there are positive anomalies greater than 1 °C in the Indian Ocean and in the southern Atlantic. Negative anomalies are located in the North Pacific with positive anomalies along the west coast of North America and the east coast of China. These anomalies are not recognized by the model.

The differences between T62 and T40 SSTA ensemble means of 500 hPa height anomalies are not large, so we show the ensemble seasonal mean 500 hPa height anomalies averaged over five T62 SSTA and T40 SSTA runs together. The observed winter climatology from 1958 through 1959 was taken out from both forecasts and analysis to form anomalies (Figure 1). There is no correction of the model systematic errors. Overall, the model is able to capture the wave train extending from the convective area of North America with negative anomalies in the North Pacific close to the west coast of North America and in Florida and positive anomalies over Canada. The anomaly correlation over the NH (lat 30°N to 90°N) is 0.64 and over the Pacific North American region (lat 30°N to 90°N, long 180°W to 40°W) is

0.81. The forecasted anomalies are stronger than those observed. The standing waves are more realistic than the total anomalies. That implies that the model has zonal mean biases. When the model is forced by global observed SSTA, the forecast over the Eastern Hemisphere improves (not shown).

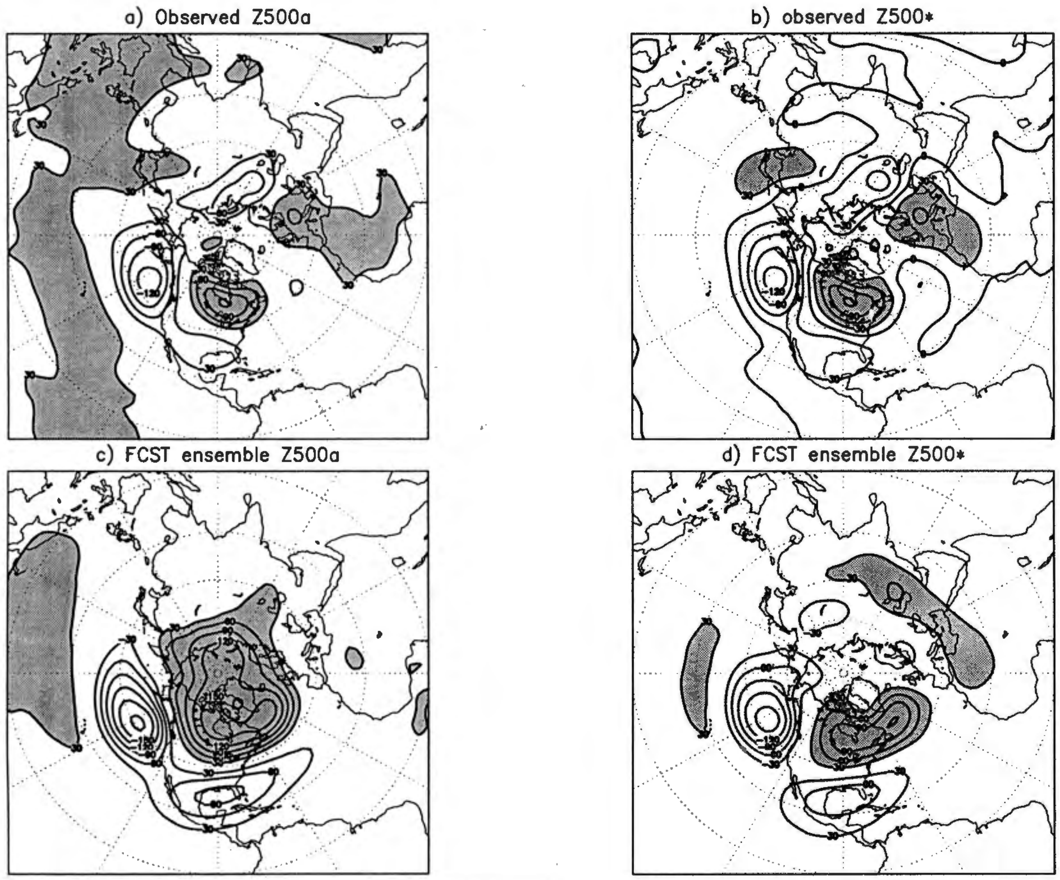

Figure 1 Observed ensemble mean 500 hPa height anomaly for December 1997 through February 1998. Contour interval is 30 m. Areas where values are greater than 30 m are shaded, (b) same as (a), but for anomalies with zonal means removed, (c) same as (a), but for ensemble forecasts with T62 SSTA and T40 SSTA combined, (d) same as (c), but with zonal means removed.

The observed large-scale precipitation and anomaly over the US show a typical signal during warm El Niño–Southern Oscillation (ENSO) events. There are positive rainfall anomalies in California and negative anomalies over the Pacific Northwest. Such dipole rainfall pattern has been documented by Mo and Higgins (1998) and Cayan and Redmond (1994). It also shows positive anomalies over Florida and Texas and negative anomalies extending from Tennessee to Ohio. In comparison with station reports, the one-degree resolution precipitation analysis is not able to capture details and regional features of precipitation. It misses a rain belt over high elevations and many rainfall centers along the California coast.

Regional Model Precipitation Forecasts

With the uncertainty of precipitation analysis in mind, we discuss the precipitation forecast. The RSM50 ensemble mean precipitation forecast (Figure 2) captures the maximum located at northern California and another center over southern California. It shows precipitation over 150 mm per month in the southeast, which is about 50 mm per month less than the observations. While the RSM 50 forecasts are able to capture the rainfall pattern, the model is still not able to capture the rainbelt over the mountains.

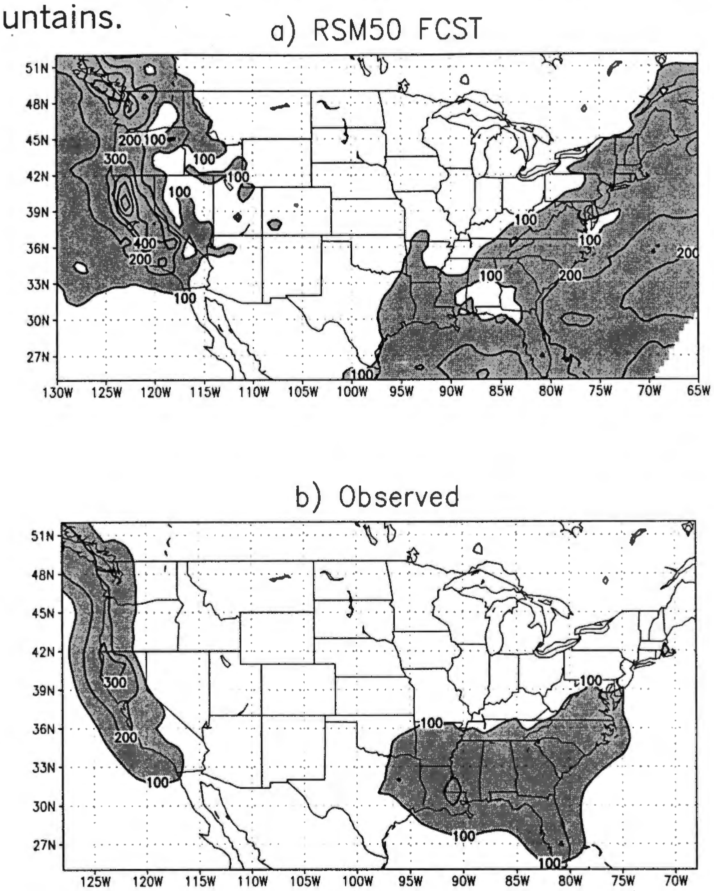

Figure 2 (a) Ensemble seasonal mean RSM50 precipitation forecast for December 1997 through February 1998. Contour interval is 100 mm/mo. Area where values are greater than 100 mm/mo are shaded. (b) same as (a), but for observations.

Figure 3 shows the ensemble mean precipitation for RSM30. Precipitation over the western region has more detailed structure. There is a rainbelt over the high mountains and there are many rainfall maxima along the coast. The rainfall amounts also increase. The problems are that the rainfall centers are located inland instead of along the coast and the model tends to generate spurious maximum centers of rainfall. Considering these forecasts were made in October 1997, results are encouraging. More work needs to be done, but our results suggests that it is possible to make regional ensemble forecasts a few months in advance for hydrological applications during strong ENSO winters.

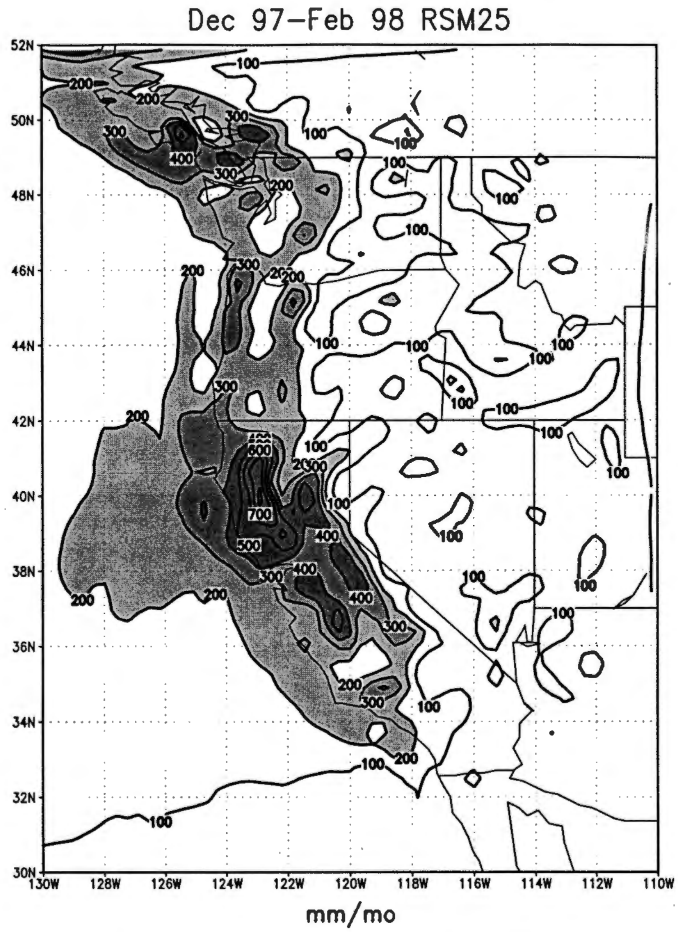

Figure 3 Ensemble seasonal mean RSM30 precipitation forecast for December 1997 through February 1998. Contour interval is 100 mm/mo. Area where values are greater than 100 mm/mo are shaded.

References

Cayan D and KT Redmond. 1994. ENSO influences on atmospheric circulation and precipitation in the western United States. Proceedings of the 10th Annual Pacific Climate (PACLIM) Workshop, Technical Report of the Interagency Ecological Studies Program for the Sacramento–San Joaquin Estuary; 1993 Apr 4–7; Santa Catalina Island, CA. Sacramento (CA): Interagency Ecological Studies Program for the Sacramento–San Joaquin Estuary. p 5–26.

Juang HM, SY Hong, and M Kanamitsu. 1997. The NCEP regional spectral model: an update. *Bull Amer Meteor Soc* 78:2125–43.

Kalney E and others. 1996. The NCEP/NCAR 40–year reanalysis project. *Bull Amer Meteor Soc* 77:437–72.

Mo KC and RW Higgins. 1998. Tropical influences on California precipitation. *Journal of Climate* 11:412–30.

How Does 1998 Compare with 1997 and 1983 on Floods and Water Supply?

Maurice Roos, Chief Hydrologist
California Department of Water Resources
3310 El Camino Avenue, Room 200
P.O. Box 219000
Sacramento, California 95821-9000

Introduction and Summary

Water year 1997–1998 was the fourth wet year in a row for northern California (Location Map). This was unusual because a series of wet years of this duration has probably happened only twice before in this century (Figure 1). The previous series occurred during 1940–1943 and perhaps during 1904–1907. (There is some doubt about whether water year 1905 was "wet enough" to be labeled a wet year). Flood patterns in 1998 were strikingly similar to 1983, although timing was different. Flood patterns in 1998 were much different from that of the great New Year's flood of 1997.

The coastal watersheds and smaller basins generated the floods in 1998. New flood peaks were observed on the Pajaro River near Watsonville, at Farmington and Los Banos reservoirs and on Merced area creeks. The upper Sacramento Valley was also wet; flooding there was comparable with the larger floods of record, despite effective flood control operations at Shasta Reservoir. Flood runoff from major Sierra rivers was not unusually large; peak three-day rates were near median. Figure 2 shows peak three-day flood runoff rates for the American River near Sacramento.

After a slow start in December, winter 1998 turned wet. Both January and February were extremely wet and February precipitation was nearly three times above normal. However, the February storms were relatively cool and helped build up a large snowpack in the mountains. Some of the largest snowpack percentages were on the ridge separating the Sacramento and Trinity river basins. With the exception of 1995, 1998 had the heaviest snowpack since 1983, another strong El Niño year. The Sacramento River system can easily handle snowmelt floods because of its large rain flood channel capacity. But San Joaquin River system floodways are only about one-tenth as large, taxing the reservoirs and channels in large snowmelt years. Snowmelt in 1998 was delayed about two weeks, which helped to control high San Joaquin River system runoff. The water supply forecasts were useful for coordinating releases and operating the reservoirs to minimize snowmelt flood damage.

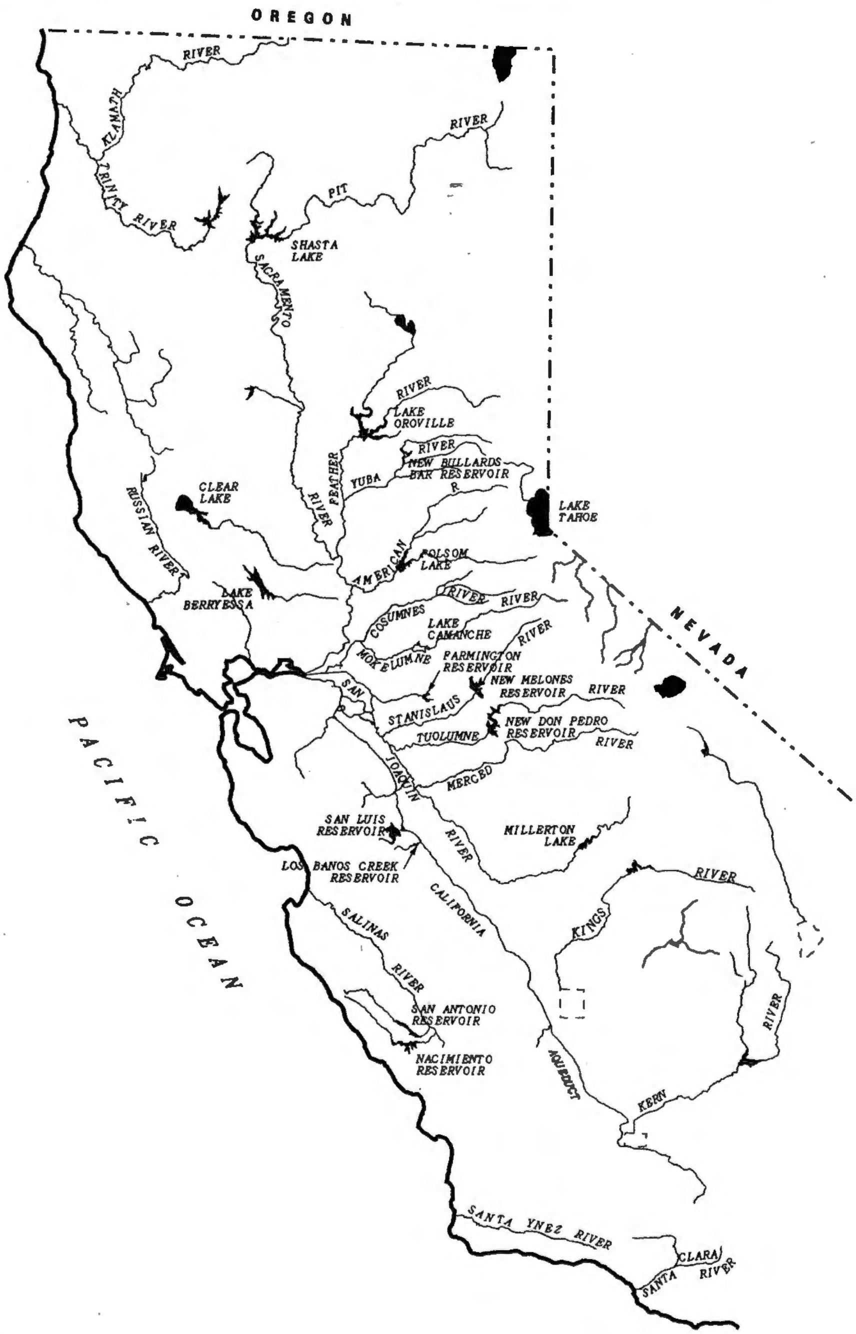

Location Map

May 1998 was cool and wet, more typical of March weather. A surprise storm in the upper Sacramento Valley near the end of May produced moderate flood flows in the Sacramento River and the latest inundation of the Sutter and Yolo bypasses observed.

Runoff in water year 1998 in the Central Valley rivers was less than in 1983 (the last strong El Niño year) or 1995. However, water year 1998 runoff was about 25% more than in 1997. Total runoff for the eight major rivers of the Sacramento–San Joaquin River system will be about 42 million acre-feet, about 175% of average and the sixth wettest of record.

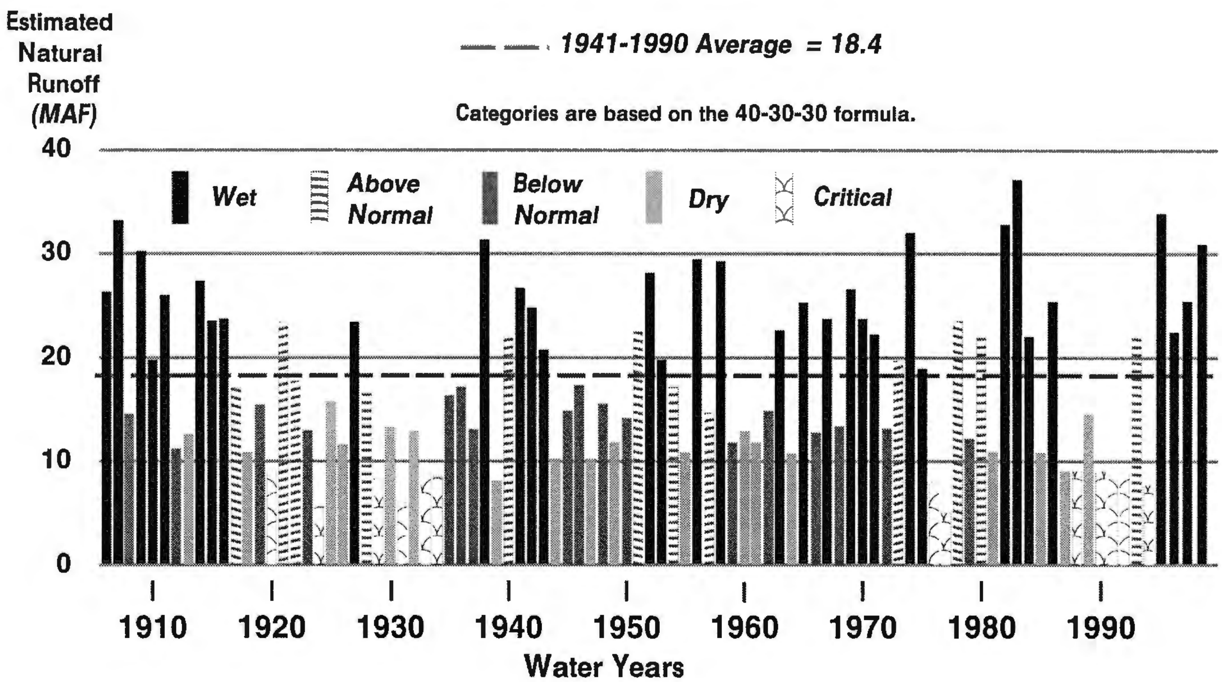

Figure 1 Sacramento River unimpaired runoff since 1906

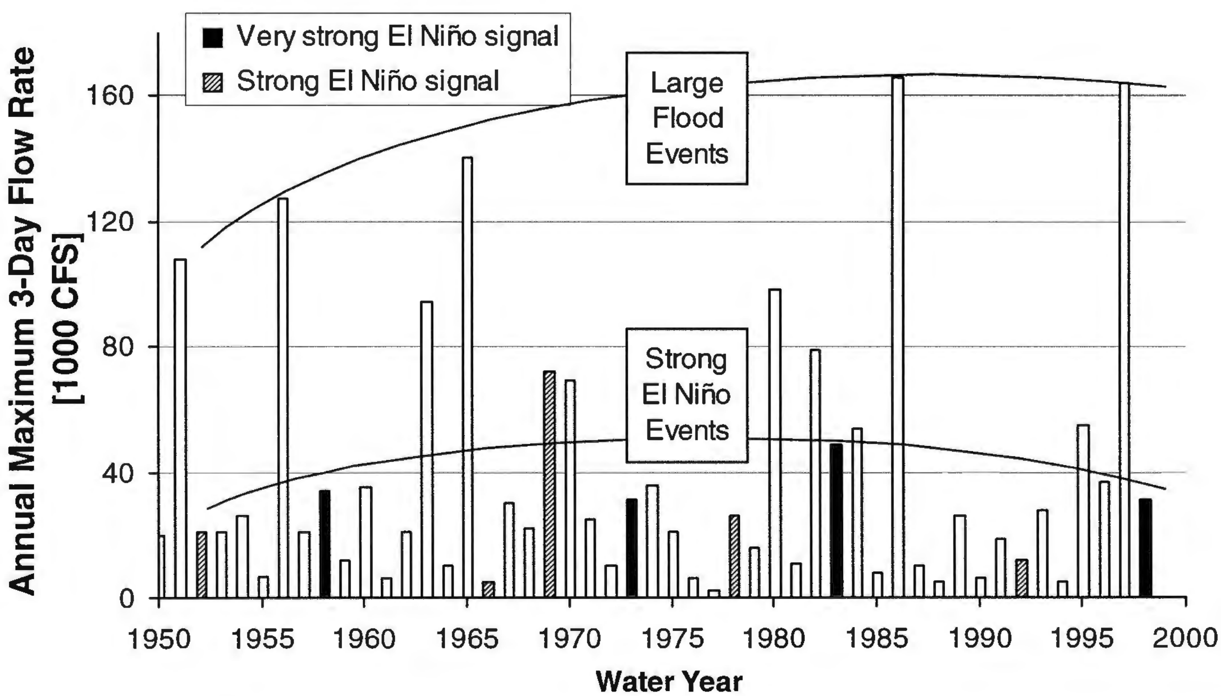

Note: American River Runoff is the unimpaired flow at Fair Oaks.

Figure 2 American River annual peak three-day runoff since 1950

Water Supply

In the northern Sierra, an estimated 82 inches of precipitation had fallen by late September, about 165% of average for the season. This represents the fourth wettest year of record, begun in 1922. Figure 3 shows monthly precipitation for 1998 (through June), 1997, and the strong El Niño years of 1983 and 1973. Figure 4 presents the same information in accumulated seasonal amounts.

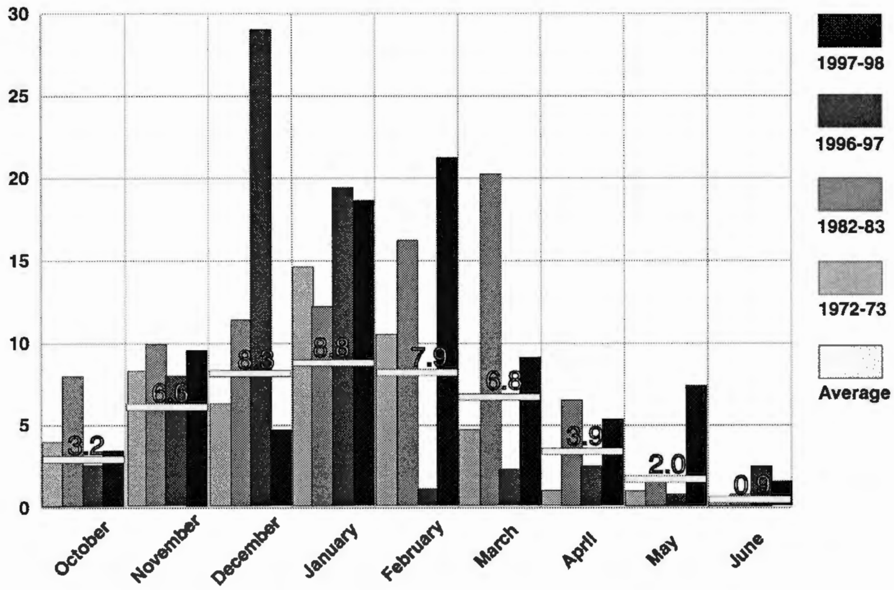

Figure 3 North Sierra precipitation, in inches

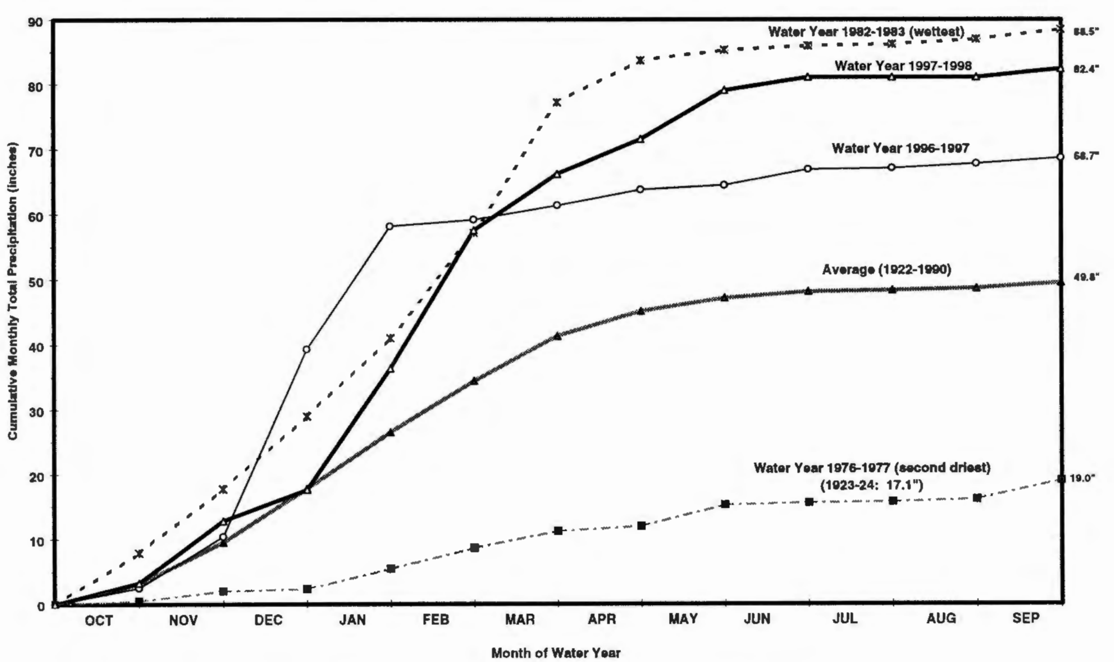

Figure 4 Northern Sierra precipitation accumulation, 8-station Index, 30 Sep 1998

Water year 1997–1998 was wet, but contrasted with water year 1996–1997. A couple of concentrated storms caused some extreme flooding in 1997. Frequent storms with moderate snow levels occurred in 1998. One of the century's stronger El Niño events strengthened the southern jet stream track to push storm after Pacific storm into California, especially the coastal region. (Figure 5 shows the distribution of seasonal precipitation.) As a result, once the large snowpack melted, the total rainfall and runoff were greater in 1998 than in 1997. The crossover in statewide volume of runoff occurred soon after 1 June. In 1997, most of the runoff was practically over by 1 June because of an early and below-average snowmelt. In 1998, the bulk of snowmelt runoff, especially from the southern Sierra, came after 1 June, eventually boosting runoff to much more than in 1997 with its dry spring.

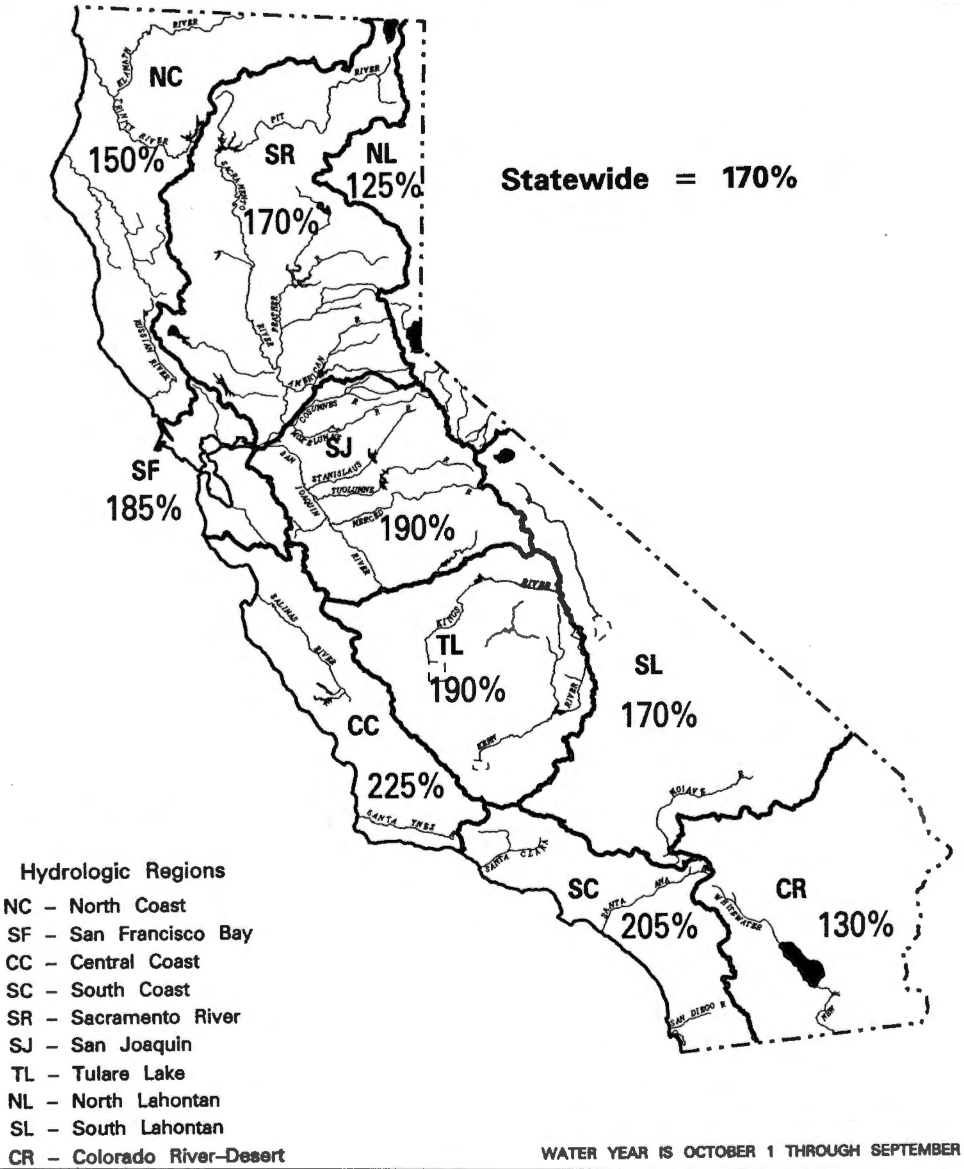

Figure 5 Seasonal precipitation in percent of average to date, 1 Oct 1997 through 31 Aug 1998

I expect statewide runoff in water year 1998, ending on 30 September, to be 175% of average, compared to 145% in 1997 and 220% in 1983. Both major water projects, the Central Valley Project and the State Water Project, made full water deliveries to their customers in 1998.

Floods

Most major Central Valley foothill reservoirs operated in the flood control mode during February and March. Excess waters were released in a controlled manner into the Sacramento and San Joaquin river systems. All Sacramento system fixed weirs flowed during most of February and 16 of 48 gates in the Sacramento Weir near Sacramento were opened in early February. The San Joaquin River near Vernalis almost reached its 29–foot flood stage in mid-February, then fluctuated about a foot lower to the 28–foot level as reservoir operations controlled much of the storm runoff.

Most of the winter storms were rapidly moving systems with short breaks in between. No special problems were posed to the floodway systems. The one exception was a powerful storm on 2 and 3 February, which stalled just off the northern California coast and dumped heavy amounts of rain on the coastal range and the upper end of the Sacramento Valley. Upper Sacramento River flood stages, almost entirely generated below Shasta Dam, reached levels comparable to the big floods of the past. (Figure 6 shows the stage comparisons in the upper, middle, and lower Sacramento Valley.) The storm was similar to the big storm and upper Sacramento flood of 1 March 1983. The Central Valley west-side streams gushed large volumes of water, overtaxing the limited drainage capacity of the Colusa basin. This also occurred later at Clear Lake, which rose to 11.5 feet on 24 February, slightly over the 1986 peak stage of record in February 1986 (11.3 feet) and nearly as high as in March 1983. Historical county records from the Rumsey gage show that Clear Lake stages were 13.4 feet in February 1909 and nearly 13.7 feet in January 1890. But the outlet was different in those days. Some channel cleanup work by Lake County (as much as allowed by an old judicial decree), reduced the stage in 1998 by perhaps 0.5 feet from what it could have been.

In the Sacramento–San Joaquin Delta, high tides at Rio Vista exceeded ten feet on several days during the first two weeks of February. There were problems, but no delta islands were flooded, thanks in part to strenuous flood fight work.

On 3 February, the Russian River at Guerneville crested 6.5 feet above flood stage, about ten feet lower than the peak levels observed in February 1986 and January 1995.

The Napa River at Napa crested nearly two feet above flood stage, also well below record levels. Heavy rain on the central coast produced a new peak of record on the Pajaro River at Chittenden, over two feet above flood stage during the first week of February. (The previous record was in 1958.) The coastal mountains of southern

California experienced heavy rain, which generated large flows in Santa Barbara, Ventura, Orange, and San Diego counties. Reported Cuyama River inflow to Twitchell Reservoir near Santa Maria was also a new record.

Peak inflows to major Central Valley reservoirs during winter 1998 were quite modest, due primarily to colder storms with relatively low snow levels. The surprise occurred at two lower elevation reservoirs seldom heard about: Farmington Reservoir east of Stockton and Los Banos Reservoir west of Los Banos. A strong local storm filled the 52,000 acre-feet Farmington Reservoir on 8 February with a small amount of water going over the spillway. Outlet structure releases into Littlejohn Creek were curtailed to account for the extra water coming over the spillway in order to remain within safe channel flow levels downstream. The reservoir peaked on 9 February to about 53,000 acre-feet. Ten days later, on 19 February, the reservoir was about 80% full and reasonably ready for a new storm. The other surprise occurred at Los Banos, a 34,600 acre-feet reservoir with 14,000 acre-feet of flood reservation space to protect the California Aqueduct and provide some local recreation. That reservoir filled to about 90% of capacity on 3 February and there were fears that another predicted strong storm two days later could fill the dam with only partially controlled flow over the spillway. Preparations were made to handle the uncontrolled flow downstream, including intercepting a portion of the peak flows into the California Aqueduct and an emergency dike to protect the City of Los Banos. Fortunately, the second storm turned out to be much smaller; the reservoir did not fill and inflow was fully controlled.

Storm patterns during winter 1998 produced significant creek flows below the foothill reservoirs. Two periods of heavy thunderstorms, one in mid-January and one in late March, produced flooding in Merced from local creeks. Bear Creek, just east of Merced, peaked at record levels near midnight on 15 January. On 24 March, heavy thunderstorms produced another sharp rise, which exceeded the January peak.

Snowpack

The cold winter storms of 1998 produced significant snow accumulations in the high mountain watersheds. From about 75% of average on 1 January, snowpack water content increased to 115% of average statewide on 1 February and to 185% on 1 March, but then leveled off during March. Relatively dry conditions during the first half of March slowed the rate of snow accumulation with some melting at mid-March at lower elevations and a boost from storms during the last ten days. By 1 April, statewide snowpack was 160% of average, compared to only 75% in 1997. By comparison, water year 1983 was 220% of average and water year 1995 was 180% of average on 1 April. In 1993, California also had about as much statewide snowpack as in 1998 (150%). However, snowpack in the north coast region was only 115% in 1993 compared to 180% in 1998.

By May, the snowpack comparisons looked different. Cool storms during the first half of April delayed melting for about two weeks. The statewide snowpack on 1 May, slightly less than on 1 April, was now 190% of average for the date. This was less than the 210% reported in 1995, but quite a bit more than in 1993. It was still much less than in 1983, which was 290% on 1 May.

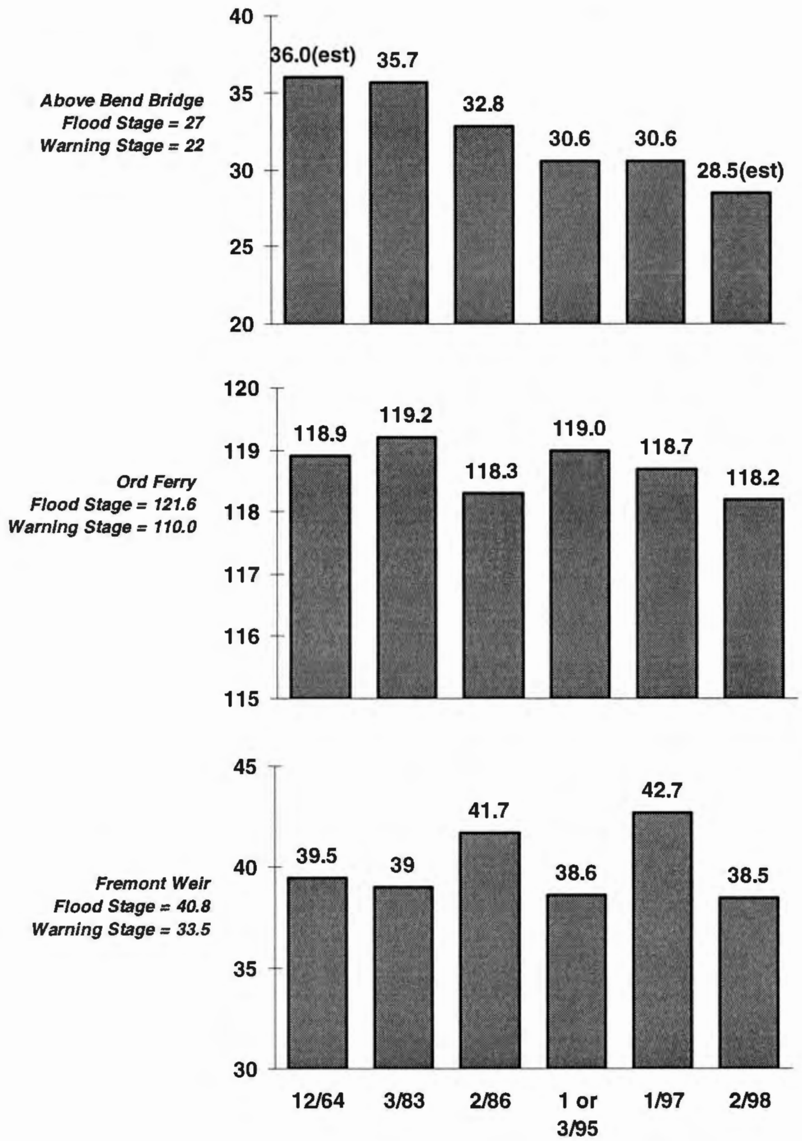

Figure 6 Peak flood stages, in feet, for the upper, middle and lower Sacramento River

Figure 7 shows the chronology of mountain snow water content for the 1997–1998 season and previous years. Table 1 compares statewide snowpack water content during the heavier snowfall years of the past several decades.

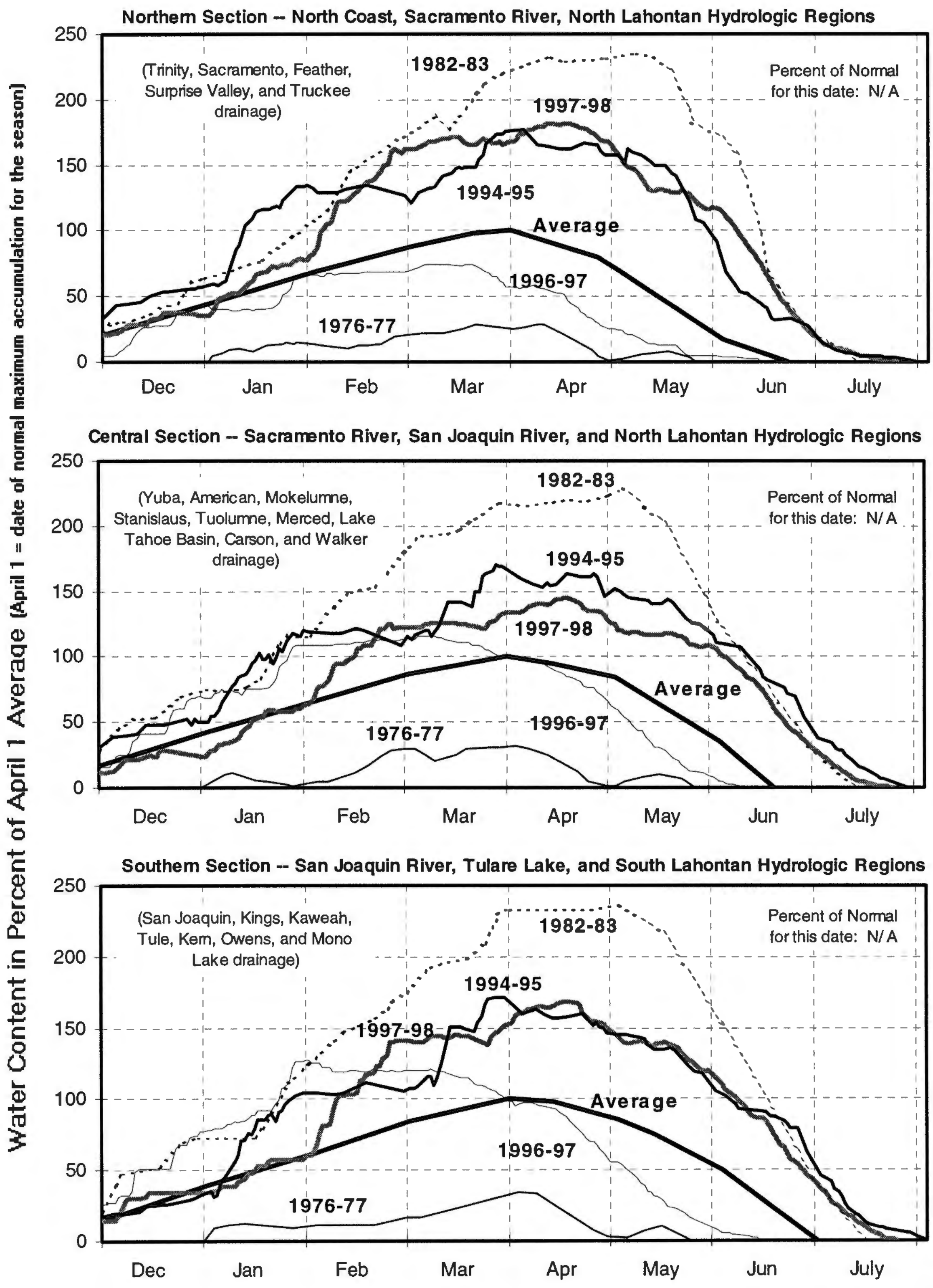

Figure 7 Telemetered California snow water content for the 1997–1998 season

Table 1 Numerical comparison of statewide snowpack water content during heavy snowfall years of the past three decades

	Snowpack Water Content	*Percent of Average for Date*
Year	*1 April*	*1 May*
1998	160	190
1997	75	55
1995	175	210
1993	150	150
1983	220	290
1978	150	190
1969	210	225
1967	130	225

Cool storms in May would further delay snowmelt, while adding to high elevation snowpack. Eventually the southern Sierra peak melt occurred about mid-June, two weeks later than usual, and continued steadily into the first part of July. The delay was a blessing because it allowed the San Joaquin and Tulare Lake foothill reservoirs to control a huge snowmelt runoff without a great deal of flooding on the Central Valley floor. There was some flooding of low ground, including about 40,000 acres of Tulare Lake bed, but much less than was possible.

Based on past El Niño experience, the upper Colorado River basin was also expected to be wet. Instead, conditions there were normal. The preliminary estimate of the unregulated April-through-July inflow to Lake Powell was 8.6 million acre-feet, 110% of average. Water storage on the Colorado River in lakes Powell and Mead was excellent: 94% of capacity on 1 September. There will be some excess water released as extra flow in fall 1998 to provide necessary flood control space for next season.

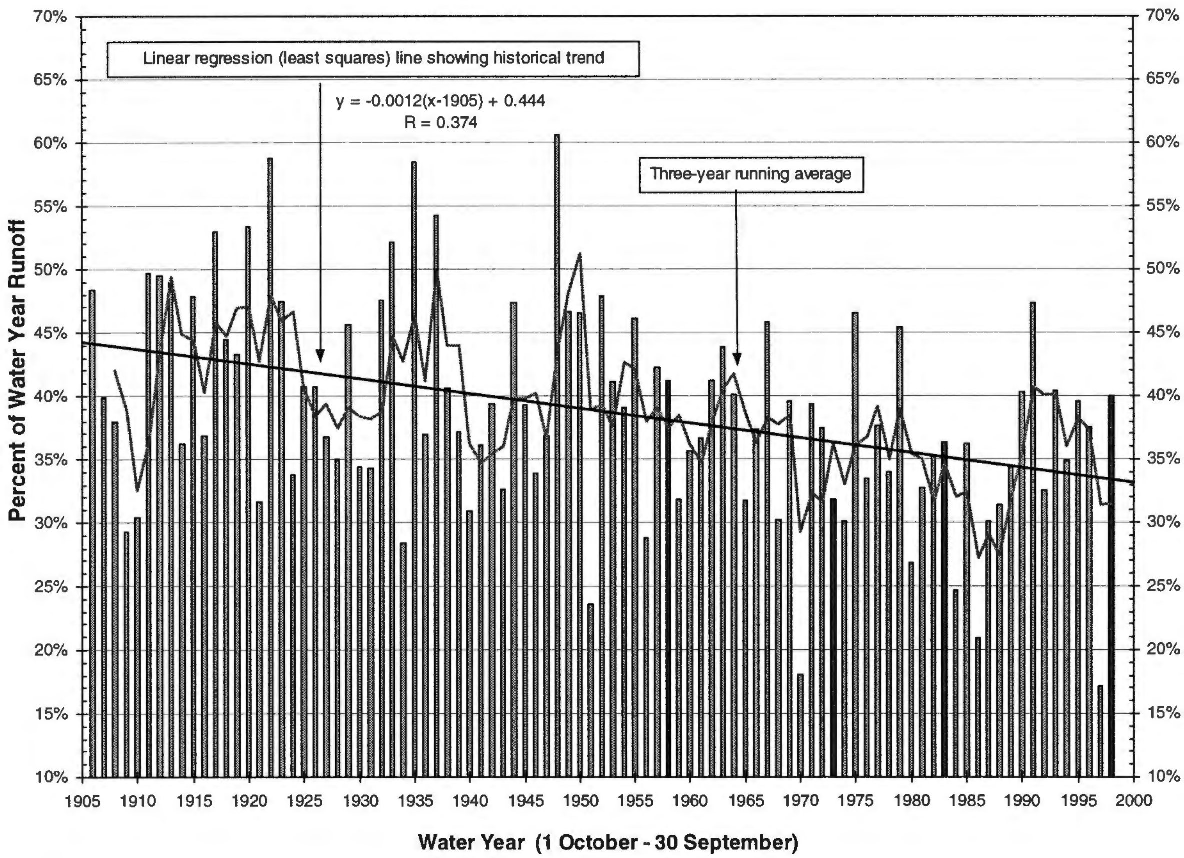

Figure 8 Sacramento River runoff, April-through-July runoff in percent of water year runoff

About ten years ago I reported that there was an apparent trend for a decreasing fraction of water year runoff to occur during the April-through-July snowmelt period. Some have investigated this effect further. One would think a year of big snowpack would increase the percentage, and it does to some extent (Figure 8), but not to the extent observed in previous decades. The trend is still there.

ENSO Teleconnections: Eastern Pacific Sea Surface Temperature Correlations with $\delta^{18}O$ in Southeastern Arizona Precipitation and Tree Cellulose

William E. Wright[1], Steven W. Leavitt[1], and Austin Long[2]
[1]Laboratory of Tree-Ring Research and [2]Department of Geosciences
The University of Arizona
Tucson, Arizona 85721

Abstract

Many researchers have identified the eastern Pacific and Gulf of California as the dominant maritime summer moisture source for southeastern Arizona. Despite this understanding, strong direct El Niño–Southern Oscillation (ENSO) teleconnections with precipitation and temperature in the region have not been identified. Our research identifies clear ENSO teleconnection between precipitation in southeastern Arizona and eastern Pacific sea surface temperatures manifested in the year-to-year variance of the precipitation stable isotopic ratios.

Stable isotopes in Tucson, Arizona, precipitation ($\delta^{18}O$ and δD) have been analyzed per event from 1981 to present, a unique time series in the western United States. High correlations are noted between weighted $\delta^{18}O$ summer season values with eastern Pacific sea surface temperatures (SSTs). Cellulose $\delta^{18}O$ values derived for the same period from ponderosa pine trees in the Santa Catalina Mountains near Tucson also reveal high correlation with local precipitation $\delta^{18}O$ and eastern Pacific SSTs.

Introduction

Precipitation Stable Isotopes

The stable isotopic ratios of hydrogen ($^{2}H/^{1}H$) and oxygen ($^{18}O/^{16}O$) in precipitation are determined by the ratios in the original source water and a number of physical effects that modify (fractionate) the ratios at various points between initial evaporation and final precipitation. The most important of these effects are related to the temperature of the original liquid source, the temperature and relative humidity of the atmosphere above the original source, the preferential loss of the heavier isotopes during intermediate rainouts, and the relative humidity of the atmosphere through which the final precipitation falls. Observations by Dansgaard (1964), Gat (1980), and Ingraham and Craig (1993) describe specific examples of fractionations caused by these factors.

The long-term relationship between the isotopic ratios of hydrogen and oxygen in each precipitation event from a given area over time is described by a linear function called a meteoric water line (MWL). The slope and intercept of the global MWL have been determined to be $\delta D = 8\delta^{18}O + 10$ (Craig 1961), where

$$\delta \equiv \left(\frac{Heavy/Light_{Sample}}{Heavy/Light_{Standard}} - 1\right) \times 1000$$

and *Heavy/Light* is $^2H/^1H$ for δD and $^{18}O/^{16}O$ for $\delta^{18}O$. Departures of regional MWLs from the global MW88L are caused by differences in the magnitude of the effects of physical processes acting on water molecules differing by one neutron ($^2H/^1H$) versus two neutrons ($^{18}O/^{16}O$), these being the mass differences between the hydrogen and oxygen isotopes of interest.

Tucson Summer Precipitation, El Niño Teleconnections, and Precipitation Stable Isotopes

Summer precipitation in the Tucson area is tied to the formation of a thermal low pressure center over the desert regions combined with large-scale position and circulation changes associated with the Azores (Bermuda) high pressure center (Adams and Comrie 1997). The terms Mexican Monsoon (Douglas and others 1993), North American Monsoon (Adams and Comrie 1997), and North American Monsoon System (Higgins and others 1997) are applied to this phenomenon because a significant shift in mean wind direction and pressure occurs between winter and the development of the summer precipitation pattern. The timing of the summer precipitation onset is very consistent (Higgins and others 1997), but questions remain about the location of the dominant summer moisture source region (see Adams and Comrie 1997 for discussion).

Most previous research considering US Southwest summertime precipitation has not found strong connections relating El Niño–Southern Oscillation to precipitation patterns (Andrade and Sellers 1988), though some relationships have been identified (Carleton and others 1989; Harrington and others 1992; Hereford and Webb 1992). Our research, however, has found evidence for a strong El Niño teleconnection in correlations between changes in the isotopic ratios of hydrogen and oxygen in summer precipitation in the northern Sonoran Desert, specifically Tucson, Arizona, and changes in sea surface temperatures in the eastern Pacific Ocean. This finding supports other work identifying a moisture source dominantly in the eastern Pacific Ocean and Gulf of California (Reitan 1957; Rasmussen 1967; Hales 1972; Reyes and Cadet 1988; Douglas 1995). A mechanistic explanation is provided below.

Precipitation Stable Isotopes in Trees

The hydrogen and oxygen fixed in various chemical constituents of plant tissues is derived ultimately from local environmental water entering through the roots (DeNiro and Epstein 1979). The number of precipitation events contributing to the local moisture source for a plant depends on the rooting depth, soil depth, root access to groundwater, and the characteristics of the local precipitation regime. Trees tend to use deeper sources of water than grasses, forbs, and shrubs. Consequently, they often use water with isotopic ratios reflecting a long-term precipitation isotopic mean. However, trees in appropriate settings within semi-arid environments should have access to only short-term water inputs (White and others 1985). Logically, the chemical constituents of the wood (xylem) in these settings should also reflect water input from a short time.

But this will only be true if there are no other significant isotopic fractionation factors to alter the isotopic ratios. Evaporation, for instance, can cause large changes in these ratios during photosynthesis. Leaf pores called stomata must open during photosynthesis to allow carbon dioxide to enter the leaf. A necessary trade off to access atmospheric carbon dioxide is the loss of water through these stomata. Periods of low humidity can result in leaf water which is enriched in the heavier water molecules as more of the lighter molecules evaporate. It also follows that periods of high humidity may result in leaf water which sees little or no isotopic change. For this reason, the stable isotopes in the leaf water may reflect the isotopic ratios in the source water, the local relative humidity, or a mixture of both.

Leaf water is used to manufacture photosynthates, the building blocks of plant tissues, and in this way the plant incorporates an isotopic signal. The photosynthates are either stored for later use or used immediately to manufacture various products. These products have different chemical stabilities over time depending on their composition. Cellulose, the principal structural material in most plants, is particularly stable and accounts for about half of the plant's total mass. These qualities make cellulose the material of choice for many stable isotopic studies involving plants.

Additional fractionation occurs in the biochemical processes which lead to cellulose synthesis. A discrimination of 27‰ against the heavier oxygen isotopes is seen in the end product of the cellulose synthesis pathway. However, this fractionation appears to be constant and may be viewed as a consistent offset from the leaf water values (Ehleringer and Dawson 1992). Additional research suggests that some degree of reequilibration with environmental water may occur at the point of cellulose deposition (DeNiro and Cooper 1991; Terwilliger and DeNiro 1995), but the overall evidence is currently ambiguous.

Southern Arizona Trees and the Monsoon

Trees growing on Sky Islands in parts of the Southwest US desert are subjected to a consistent growing season climate fluctuation. A two- to three-month hyperarid period occurs between a winter frontal storm-dominated precipitation peak and a summer convective storm-dominated precipitation peak. This period, often called the "foresummer drought," is brought to an end in July by the arrival of the monsoonal precipitation mentioned above. The occurrence of this drought and the timing of the precipitation onset (see above) display tremendous consistency; the transition occurring almost invariably within a two week period centered on 4 July.

This arid period occurs during the growing season of many tree species, driving important physiological responses. Certain tree species physiologically respond to this arid period by partially ceasing growth, then renewing vigorous growth when the summer rains appear. In an annual growth band this appears as a reduction in cell size with increased lignification followed by an increase in cell size and a reduction in lignification (Figure 1). This feature is called a false latewood band, or false ring. The time constancy of formation for this feature can provide an intra-annual link between wood produced and time of the year for tree rings of any age. Division of the rings just after the false ring should allow wood produced with winter precipitation to be separated from wood produced with summer precipitation.

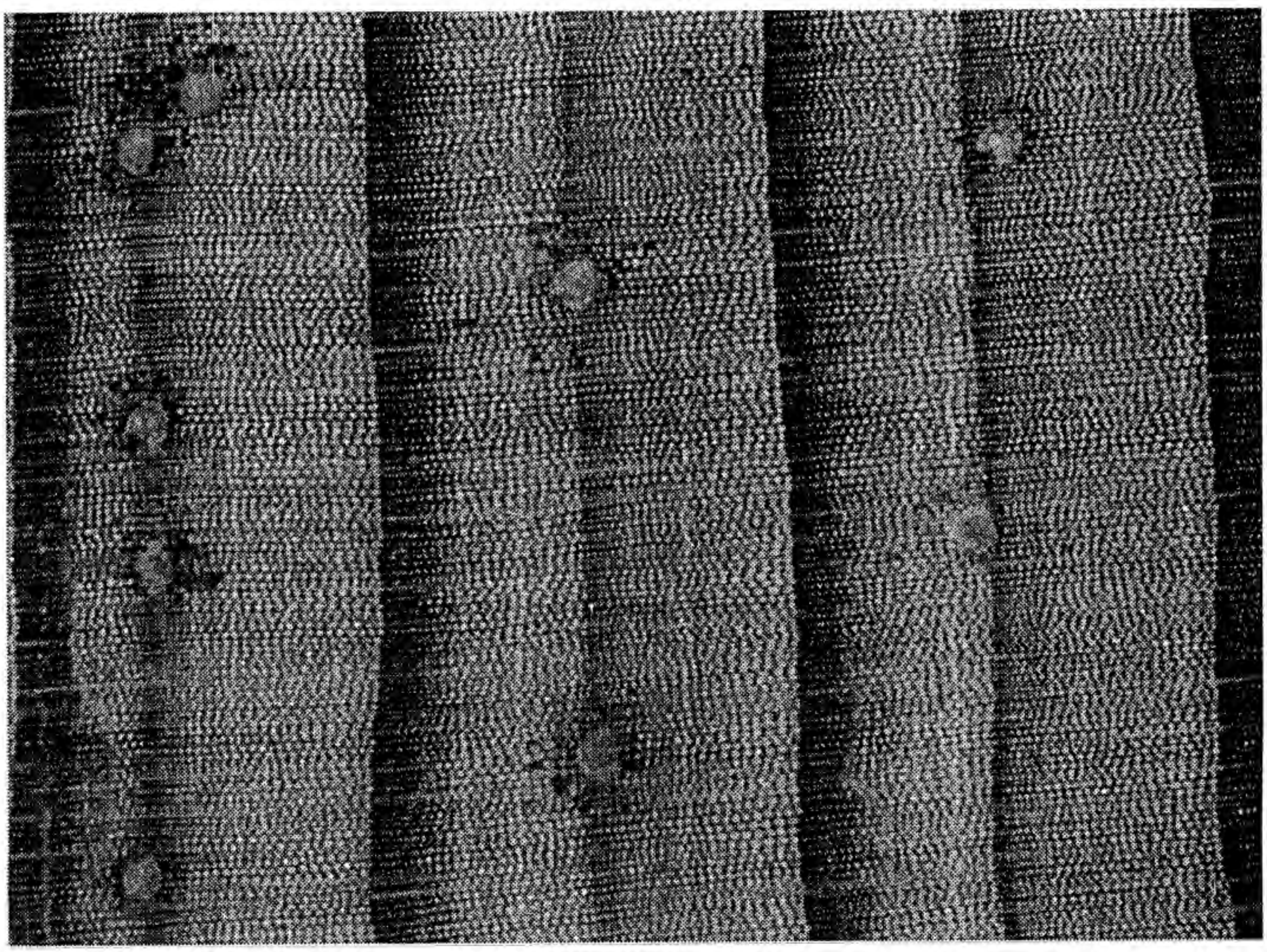

Figure 1 Ponderosa pine tree rings showing false latewood bands

Methods

Tucson Precipitation Isotopes

One author (AL) has collected precipitation at his home since 1981. An eighteen-year Tucson precipitation isotopic data set now exists consisting of stable isotopic determinations for each precipitation event. Both hydrogen and oxygen isotopic ratios have been determined for each sample.

The isotopic determinations were performed using a zinc reduction technique for hydrogen and a CO_2 equilibration technique for oxygen. Work was done on either a VGMicromass602C or a Finnagan Delta-S mass spectrometer. An internal lab water standard was used to calibrate the mass spectrometers.

Santa Catalina Mountains: Cellulose and Precipitation Isotopes

Ponderosa pine trees growing at 2,300 m in the Santa Catalina Mountains immediately north of Tucson were identified by increment coring as having consistent false latewood band production. Cores 12 mm in diameter were taken orthogonally from four directions on the trees. The tree rings were separated into three segments: one after the false latewood band and two of equal divisions from the portion before the false latewood band. All non-cellulosic components were extracted from the whole wood using a soxhlet-type extraction and sodium chlorite delignification, similar to Leavitt and Danzer (1993).

Cellulose from the four directions was combined, dried, and pyrolyzed using a variation of the nickel pyrolysis technique reported by Edwards and others (1994). The resulting carbon monoxide and carbon dioxide mix was converted to carbon dioxide by spark discharge (Thompson and Gray 1977).

It was necessary to begin a long-term analysis of precipitation isotopic values from near the trees in order to legitimize a comparison between the stable isotopic ratios in tree cellulose from 2,300 m in elevation and the long precipitation isotopic data set in Tucson at 800 m. Precipitation has now been collected for three years using a bulk collection system similar to that described by Claussen and Halm (1994). Most samples represent one- to two-week periods and, as such, may be individual events or composites of multiple events. The collector placement near the Palisades Ranger Station at 2,450 m in the Santa Catalina Mountains allows the use of a daily record (unofficial) of precipitation amount. This site is about 0.5 mi north and 150 m higher in elevation than the tree sampling site. Stable isotopic ratios for the Palisades Ranger Station precipitation were determined in the same manner as for Tucson precipitation.

Results and Discussion

Tucson Precipitation Isotopes

The 18 years of Tucson precipitation isotopic values were gathered into a single spreadsheet, after which quality control checks were performed and additional samples were run to fill in gaps or to test questionable values. Pertinent meteoric water lines were then determined (Figure 2). The annual isotopic ratios in precipitation separate readily into two periods based on the slopes of the meteoric water lines: winter (November through April) and summer (May through October). The seasonal differences in slope are a product of the larger summer $\delta^{18}O$ fractionation during rain throughfall when temperatures are high and relative humidity is low. This difference is particularly noticeable for smaller rain events.

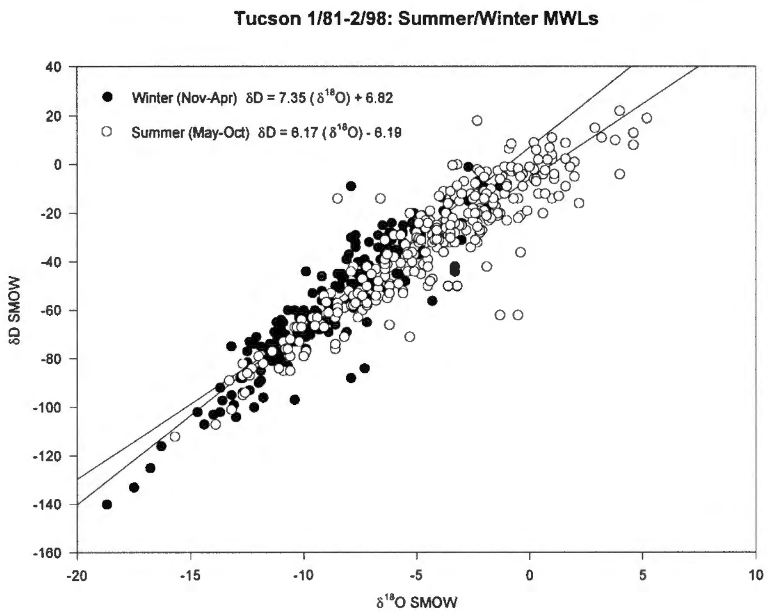

Figure 2 Tucson seasonalized meteoric water lines

A "seasonally" weighted isotopic time series was produced as follows: (1) the ratio of the amount of precipitation received during the event to the total amount for the period of interest was calculated; (2) the isotopic composition of each individual event was multiplied by its respective ratio; and (3) the numbers from the second step were totaled for the period of interest (Figure 3). Isotopic time series were also developed for various combinations of months, each combination being weighted independently. These data sets were then regressed against monthly, bimonthly, and trimonthly means of sea surface temperature (SST) time series: Niño 1+2; Niño 3; and Niño 4. The highest correlations ($r = -0.79$) found for all the data sets was between the Tucson August-through-September mean isotopic values ($\delta^{18}O$) and various lags of three-month means of SSTs (Figure 4). The lags of highest correlation decreased from west to east as follows: Niño 4, 15 months; Niño 3, 14 months; and Niño 1+2, 11 months (Figure 5). The relation between these SSTs and the SSTs in the moisture source region is uncertain, but the reduction in the time lags with increasing proximity of ocean area to the Americas suggests a much shorter lag would be found for regression with SSTs from the marine source region, an area receiving the northward deflection of equatorial surface waters. This data set has not yet been derived.

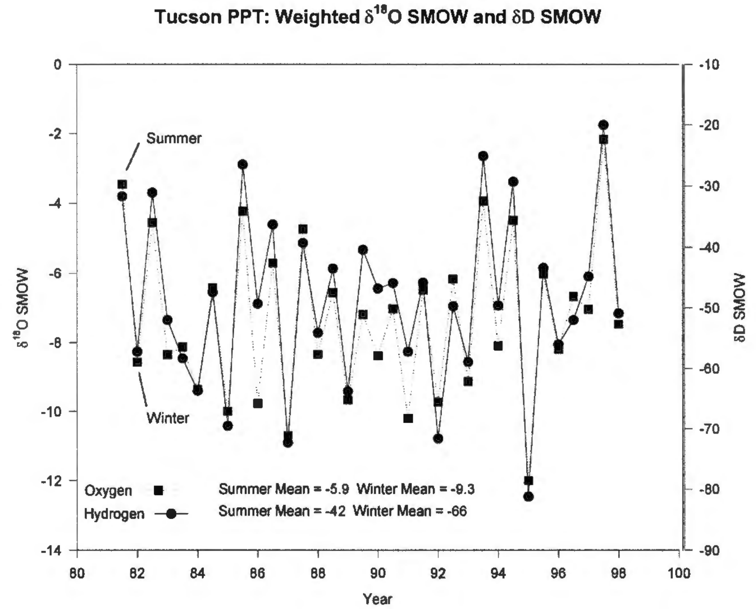

Figure 3 Weighted seasonalized stable isotopes in Tucson precipitation. Note the large seasonal differences in most years.

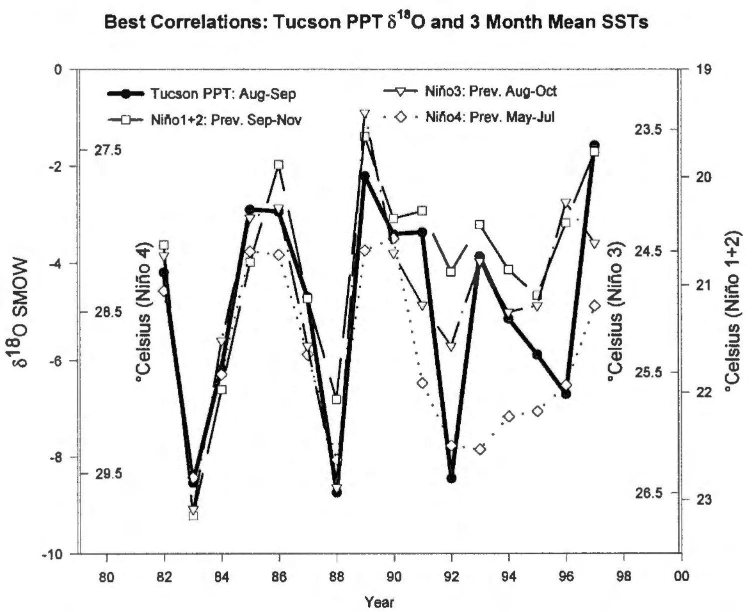

Figure 4 August-through-September weighted mean $\delta^{18}O$ in Tucson precipitation plotted against three-month sea surface temperature means at the lags showing the highest correlations

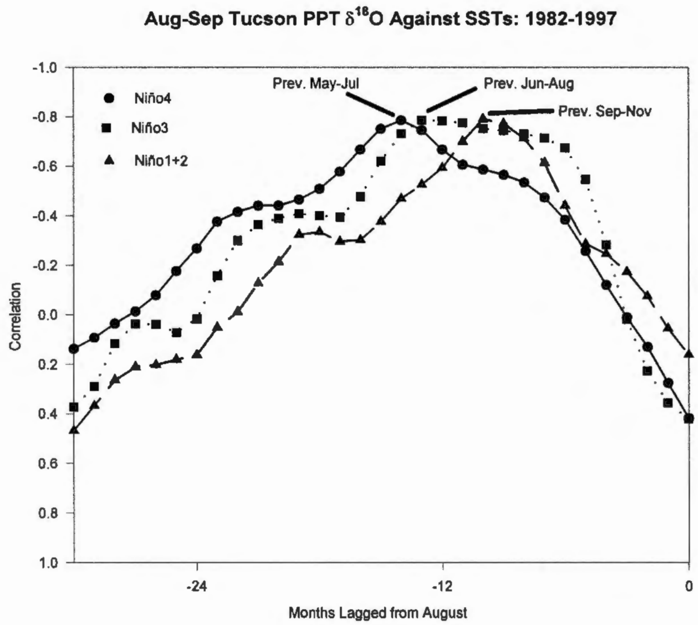

Figure 5 Running lagged correlations between three-month means of Niño 1+2, 3, 4 SST data sets and August-through-September weighted mean $\delta^{18}O$ from Tucson precipitation as 1982–1997 time series. The lag equals zero at zero on the x axis.

These high correlations may be explained using the following reasoning. Consistency in the timing of Tucson summer precipitation onset and moisture source region mean that the isotopic ratios in the precipitation in the summer season are largely controlled by the temperature of the marine source water and associated atmosphere, rainout during airmass transport, and changes in the local atmospheric humidity. The degree of rainout probably does not vary tremendously because the storm track is largely unvarying and the local humidity tends to remain high once the monsoonal precipitation has begun, so the dominant factor affecting the stable isotopic ratios in the precipitation should be temperatures in the source region. If the sea surface temperatures in the source region dominate the variation in the ratios, then the year-to-year variation in the mean weighted stable isotopic ratios of the precipitation can be expected to correlate with the sea surface temperatures. The source region should be influenced by El Niño-related shifts in sea surface temperatures along the equatorial Pacific because the west-to-east movement of the surface water recurves along the Mexican coast after reaching the Americas. A lag on the order of months is suggested by our research.

Santa Catalina Mountains Precipitation Isotopes

Seasonally weighted means have been determined for this data for comparison with the Tucson data set (Figure 6). The relative seasonal changes are similar and most likely reflect elevational temperature differences. Less seasonal difference is seen between the meteoric water line slopes for the high elevation site than was noted for the Tucson data set (Figure 7). This may be attributed to lower mountain temperatures and generally higher local humidity, reducing the fractionating effects of physical processes in the summer, and evaporation from the snow surface in winter. These differences from the situation in Tucson act in opposite directions making the MWL slopes more similar. For these reasons, the summer isotopic ratios in the mountain precipitation should more closely reflect the marine source moisture isotopic values than do the summer isotopic values for Tucson precipitation, while the winter isotopic values in the mountains should be less similar to the marine source moisture values than the Tucson values.

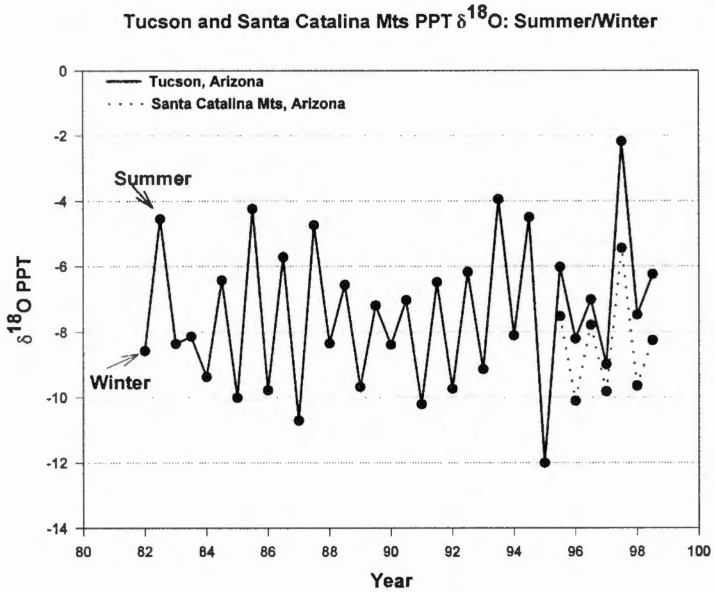

Figure 6 Weighted, seasonalized $\delta^{18}O$ in Tucson and Santa Catalina Mountains precipitation. The similarity between the two records helps support the use of cellulose $\delta^{18}O$ from the mountains as a long-term proxy for isotopic activity in Tucson precipitation.

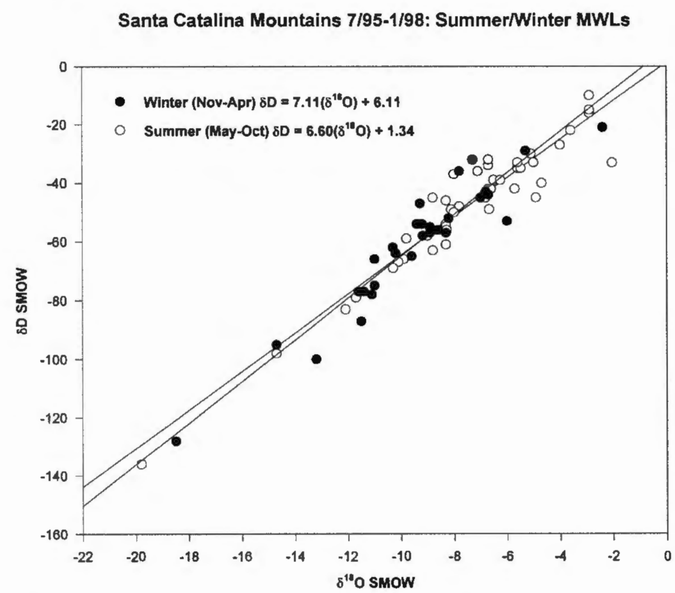

Figure 7 Santa Catalina Mountains seasonalized meteroic water line (compare with Figure 1)

Oxygen Isotopes from Santa Catalina Mountains Cellulose

Stable isotopic ratios of oxygen from the summer wood cellulose, a time of high humidity, reflect the mean-weighted isotopic ratios of the local (Tucson) precipitation during the period of growth (Figure 8). The correlation ($r = 0.90$) is similar to the correlations between the Tucson precipitation isotopes and the Pacific SSTs. Because a connection has already been demonstrated between the local mean-weighted stable isotopic ratios and eastern Pacific sea surface temperatures, it is not surprising that a high correlation is also found between cellulose produced during the summer and the same SST lags (Figure 9). Therefore, the possibility exists for a long-term reconstruction of Pacific SSTs using tree cellulose.

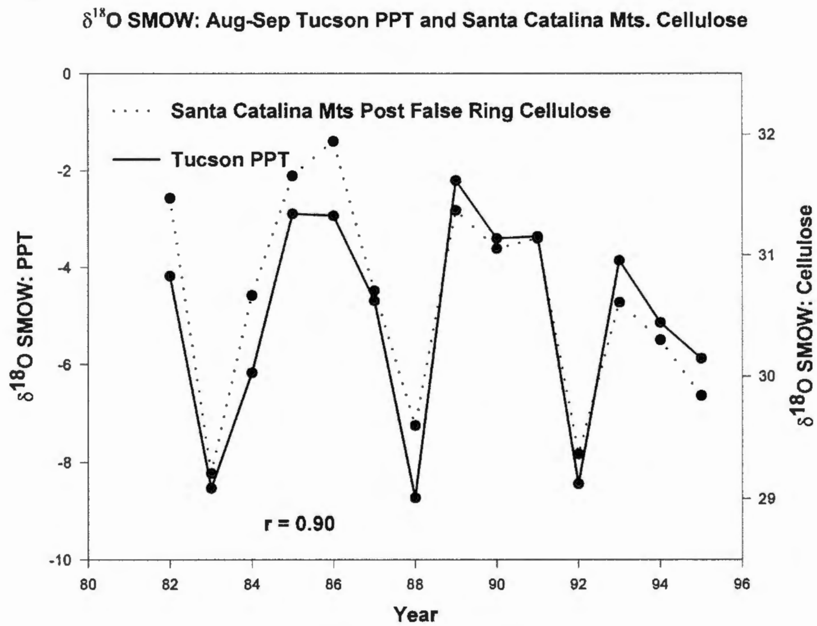

Figure 8 August-through-September weighted mean $\delta^{18}O$ in Tucson precipitation and $\delta^{18}O$ values from Santa Catalina Mountains cellulose after the false latewood band (summer wood)

The long-term stability of the spatio-temporal relationship identified between the SST data sets was explored using the entire SST time series to assess the potential for long-term SST reconstruction (Figure 10). A five-year running correlation between the Niño 1+2 and Niño 3 SST data sets at the previously identified time lags reveals a generally high correlation between the two regions. A single year in the 1960s and two years in the early 1990s account for departures from the high correlations. A simple running difference, Niño 3 minus Niño 1+2, reveals a fairly stable mean and variance in the data set. If this fifty-year level of stability is representative of the pre-instrumental SST stability (a questionable assumption), then a reconstruction of Pacific SSTs from tree cellulose would be largely successful. However, the periods when spatio-temporal relationships between the SST regions depart from the long-term mean must be further explored in attempts to identify those departures using other non-instrumental data.

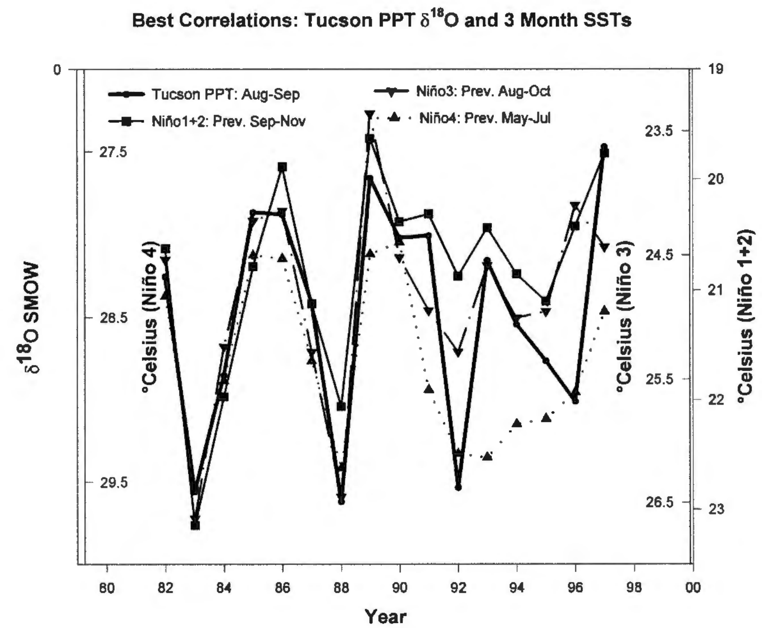

Figure 9 $\delta^{18}O$ values from Santa Catalina Mountains cellulose after the false latewood band plotted against three-month sea surface temperature means at the lags showing the highest correlations with August-through-September weighted mean $\delta^{18}O$ in Tucson precipitation

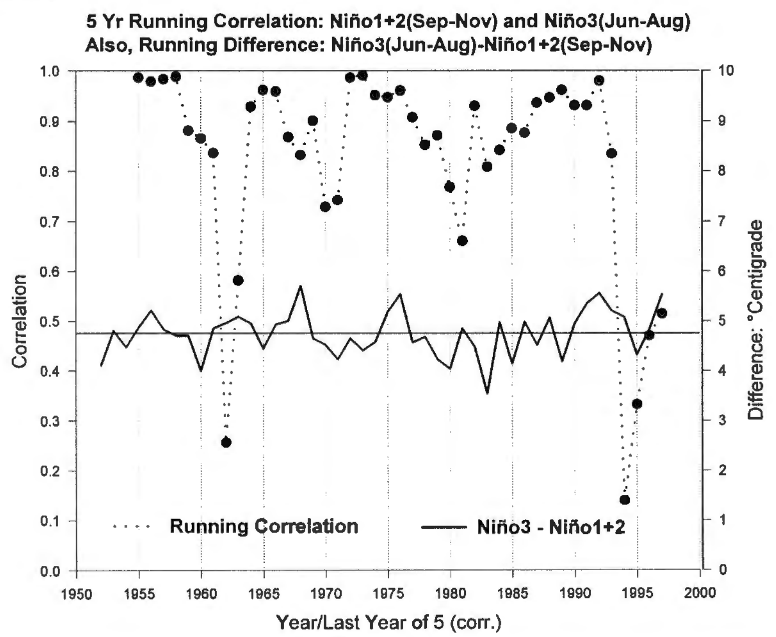

Figure 10 Comparison of Niño 1+2 and Niño 3 SST at the lags showing the highest correlation with the August-through-September weighted mean $\delta^{18}O$ in Tucson precipitation. The upper plot is a five-year running correlation plotted on the last year of the five. The lower plot shows the yearly temperature differences between the three-month means at the given lags.

Acknowledgments

We thank K. Kuehn, B. McCaleb, N. Ricketts, S. Schorr, and T. Stier for their efforts in the field, the laboratory, and on the mass spectrometers. This Research was sponsored by NSF Grant #ATM–9421041.

References

Adams DK and AC Comrie. 1997. The North American monsoon. *Bulletin of the American Meteorological Society* 78(10):2197–2213.

Andrade ER and WD Sellers. 1988. El Niño and its effects on precipitation in Arizona and western New Mexico. *Journal of Climatology* 8:403–10.

Carleton AM, PJ Weser, and DA Carpenter. 1989. Pacific sea surface temperature associations with Southwestern United States summer rainfall and atmospheric circulation. In: Betancourt JL and AM MacKay, editors. Proceedings of the 6th Annual Pacific Climate (PACLIM) Workshop, Technical Report 23 of the Interagency Ecological Studies Program for the Sacramento–San Joaquin Estuary; 1989 Mar 5–8; Asilomar, CA. Sacramento (CA): Interagency Ecological Studies Program for the Sacramento–San Joaquin Estuary. p 55–60.

Claassen HC and DR Halm. 1994. Performance characteristics of a bulk precipitation collector with respect to measurement of water isotopes oxygen–18 and deuterium (94–4008). US Geological Survey.

Craig H. 1961. Isotopic variation in meteoric waters. *Science* 133:1702–3.

Dansgaard W. 1964. Stable isotopes in precipitation. *Tellus* 16:436–68.

DeNiro MJ and S Epstein. 1979. Relationship between the oxygen isotope ratios of terrestrial plant cellulose, carbon dioxide, and water. *Science* 204:51–3.

DeNiro MJ and LW Cooper. 1991. Post-photosynthetic modification of oxygen isotope ratios of carbohydrates in the potato: implications for paleoclimatic reconstruction based upon isotopic analysis of wood cellulose. *Geochimica et Cosmochimica Acta* 53:2573–80.

Douglas MW, RA Maddox, K Howard, and S Reyes. 1993. The Mexican monsoon. *Journal of Climate* 6:1665–77.

Douglas MW. 1995. The summertime low-level jet over the Gulf of California. *Monthly Weather Review* 123:2334–47.

Edwards TWD, WM Buhay, RJ Elgood, and HB Jiang. 1994. An improved nickel-tube pyrolysis method for oxygen isotope analysis of organic matter and water. *Chemical Geology* 114:179–83.

Ehleringer JR and TE Dawson. 1992. Water uptake by plants: perspectives from stable isotope composition. *Plant, Cell and Environment* 15:1073–82.

Gat JR. 1980. The isotopes of hydrogen and oxygen in precipitation. In: Fritz P and JC Fontes, editors. Handbook of Environmental Isotope Geochemistry. Elsevier. p 21–47.

Hales JE. 1972. Surges of maritime air northward over the Gulf of California. *Monthly Weather Review* 100:298.

Harrington JA, Jr., R Cerveny, and R Balling, Jr. 1992. Impact of the southern oscillation on the North American southwest monsoon. *Physical Geography* 13:318–30.

Hereford R and RH Webb. 1992. Historic variation of warm-season rainfall, southern Colorado plateau, southwestern USA. *Climatic Change* 22:239–56.

Higgins RW, Y Yao, and XL Wang. 1997. Influence of the North American monsoon system on the US summer precipitation regime. *Journal of Climate* 10(10):2600–22.

Ingraham NL and RG Craig. 1993. Constraining estimates of evapotranspiration with hydrogen isotopes in a seasonal orographic model. In: Swart PK, KC Lohmann, J McKenzie, and S Savin, editors. Climate Change in Continental Isotope Records (vol. Geophysical Monograph Nr. 78). American Geophysical Union. p 47–53.

Leavitt SW and SR Danzer. 1993. Method for batch processing small wood samples to holocellulose for stable-carbon isotope analysis. *Analytical Chemistry* 65:87–9.

Rasmusson EM. 1967. Atmospheric water vapor transport and the water balance of North America: part 1, characteristics of the water vapor flux field. *Monthly Weather Review* 95:403–27.

Reitan CH. 1957. The Role of Precipitable Water Vapor in Arizona's Summer Rains (No. 2). Institute of Atmospheric Physics. The University of Arizona.

Reyes S and DL Cadet. 1988. The southwest branch of the North American monsoon during summer 1979. *Monthly Weather Review* 116:1175–87.

Terwilliger VJ and MJ DeNiro. 1995. Hydrogen isotope fractionation in wood-producing avocado seedlings: biological constraints to paleoclimatic interpretations of δD values in tree ring cellulose nitrate. *Geochimica et Cosmochimica Acta* 59(24):5199–207.

Thompson P and J Gray. 1977. Determination of $^{18}O/^{16}O$ in compounds containing C,H, and O. *International Journal of Applied Radiation and Isotopes* 28:411–15.

White JWC, ER Cook, JR Lawrence, and WS Broecker. 1985. The D/H ratios of sap in trees: implications for water sources and tree ring D/H ratios. *Geochimica et Cosmochimica Acta* 58:851–62.

Abstracts

Oral Presentations

An Overview of Western Climate Since PACLIM 1997

Kelly Redmond
Regional Climatologist
Western Regional Climate Center
Desert Research Institute
Reno, Nevada 89506–0220

The winter of 1997–1998 was remarkable in two senses. For the first time ever, a confident and credible long-term climate forecast—based on both historical observations and physical numerical simulations—was issued well in advance and, more importantly, taken seriously by a considerable fraction of the population. The widespread attention, and the sense of anticipation, and in some cases apprehension, associated with this geophysical prediction, were part of a situation unprecedented in this country's history. Public interest remained high throughout the event which was in some sense a "watershed" event for climatology. The general perception of success will likely have significant ramifications for climate studies across a broad spectrum of topics extending beyond ENSO, as well as for future use of seasonal climate predictions.

Secondly, the weather itself made for yet another memorable winter. Prior to the cool season, a summer with a much delayed monsoon was followed by an active autumn tropical storm season, including six major hurricanes, and the two strongest on record. Split flow affected a number of autumn and early winter storms approaching the West Coast. After halting starts, an enhanced subtropical jet was firmly in place by early December. Exceptionally mild conditions persisted nearly the entire winter in the northern tier, with about the anticipated low number of cold outbreaks and expected temperature minima; the same region was generally dry. To the south, unusual snowstorms occurred. Powerful storms lashed California repeatedly during February, converting steadily rising numbers of El Niño skeptics. Parts of the interior Southwest overcame their winter-long precipitation deficit in February and March. In Hawaii, strong drought conditions developed and persisted, leading to the driest month ever in rainy Hilo. Wet conditions were found in parts of the coastal Pacific Northwest, a feature possibly characteristic of very strong El Niños, and also in southwest coastal Alaska. In its temperature, precipitation, snowpack, and circulation patterns, this winter strongly resembled the canonical or "classical" El Niño pattern. Its most surprising feature so far (early April 1998) is the lack of major surprises—yet.

How Does 1998 Compare with 1997 and 1983 on Floods and Water Supply?

Maurice Roos
Chief Hydrologist
California Department of Water Resources
P. O. Box 219000
Sacramento, CA 95821-9000

Water year 1997–1998 was the fourth wet year in a row for northern California, unusual because this long series of wet years has happened only twice before this century. The previous wet runs were 1940–1943 and perhaps 1904–1907 (with some doubt about whether 1905 was wet enough to be labeled wet). Flood patterns in 1998 were strikingly similar to 1983, although timing was different. Flood patterns were much different from that of the great New Year's flood of 1997. This time it was the coastal watersheds and smaller basins

which generated the floods. Another wet area was the upper Sacramento Valley where flooding was comparable with the larger floods of record in spite of very effective flood control operations at Shasta Reservoir. Flood runoff from major Sierra rivers was not unusually large with peak three-day rates near median.

Both January and February were extremely wet with February precipitation nearly triple normal. However, the February storms were relatively cool and helped build up a very large snowpack in the mountains, especially in the Trinity Alps, the southern Cascades, and the Sierra Nevada. Some of the largest snowpack percentages were on the ridge separating the Sacramento and Trinity river basins. It was the heaviest snowpack since 1983, also a strong El Niño year. The handling of snowmelt floods is not a problem for the Sacramento River system with its large rain flood capacity. But San Joaquin River system floodways are only about one-tenth as large, which means the reservoirs and channels are strongly taxed in large snowmelt years. The water supply forecasts are a valuable tool for coordinating releases and operating the reservoirs to minimize snowmelt flood damage.

The Evolution and Impacts of the 1997–1998 El Niño Event

Tom Murphree[1], Frank Schwing[2], and Huug Van Den[3]

[1]Naval Postgraduate School
Department of Meteorology
Monterey, California 93943

[2]SWFSC/NMFS/NOAA
Pacific Fisheries Environmental Laboratory
Pacific Grove, California 93950

[3]NCEP/NMC/NOAA
Climate Prediction Center
Washington, D.C. 20233

We have examined a variety of oceanic and atmospheric anomalies in the Pacific and North America before and during the 1997–1998 El Niño event. Our purpose was to identify the major processes which produced those anomalies, especially the mechanisms which governed the event's evolution and its impacts on the North Pacific and North America.

The impacts on North America were very pronounced from November 1997 through February 1998. During much of this period, double wave trains were apparent, extending from both the anomalous heating and the anomalous cooling regions in the tropical Pacific into the North Pacific and North America. These wave trains reinforced each other over the northeast Pacific and much of western North America, leading to especially low sea level pressure and high precipitation there. The predicted temperature and precipitation anomalies for North America from the Climate Prediction Center were, overall, quite accurate, especially for temperature. These predictions were heavily based on the anomalies observed during previous El Niño events, especially previous strong events, such as the one in 1982–1983. This suggests that the anomalies observed during November 1997 through February 1998 were, to a very large extent, the impacts of the ongoing El Niño event. Our analyses of the forecasts' skill and of the dynamics of the observed anomalies strongly support this conclusion. In the southwestern and Great Plains portions of the US, there were some differences between the observed and predicted precipitation anomalies, apparently due to the wave train out of the tropical central and eastern Pacific being farther east than expected.

The November 1997 through February 1998 period of strong impacts on North America was preceded by a period of several seasons in which anomalies in the extratropical North Pacific region may have impacted the development of the El Niño event in the tropical Pacific. During April through June 1997, positive sea surface temperature anomalies in the northeast Pacific appear to have contributed to the development of anomalously low sea level pressure in the northeast Pacific. This led to very weak southwestward trade winds out of the North Pacific

High, which probably made a strong contribution to the very rapid growth and extreme intensity of the El Niño event during this time. During July through September 1997, anomalous atmospheric wave trains emanating from areas of unusual convective heating in east Asia helped keep the northeast Pacific High unusually weak, thereby helping to sustain the weak southwestward trade winds.

Forecasting the Atmospheric Response to the 1997–1998 ENSO

Kingtse C. Mo, M. Kanamitsu and X. L. Wang
NCEP/NWS/NOAA
Climate Prediction Center
Washington, D.C. 20233–9910

The ensemble forecasts have been performed for the 1997–1998 winter with tropical sea surface temperature (SST) anomalies taken from the CPC coupled model forecasts made in October 1997. Several ensembles were made to test the sensitivity of responses to the model resolution and initial conditions. Each ensemble has five members with different initial conditions. There are total 15 forecasts and each forecast starts from mid-October 1997 to 15 March 1998. The ensemble mean shows a wavetrain from the tropical convective area to the Pacific–North American (PNA) region with high skill. The anomaly correlation over the PNA region is above 0.75. Over the United States, the model shows wet conditions in California, Texas, Oklahoma, and Florida and dry conditions over the Ohio Valley similar to the observed precipitation anomaly pattern. While both T62 and T40 models capture the standing wave response, the magnitudes of precipitation anomalies over the United States depend on the model resolution. The surface temperature anomalies indicate warm conditions over the northern United States and cold conditions to the south, but the magnitudes of anomalies are weaker than observed. While the model is able to capture the rainfall pattern over the United States, it fails to forecast the timing of California floods.

To improve rainfall forecast over the western region, we nested the NCEP regional spectral model (RSM) into T62 model outputs. The RSM has 50 km resolution and it is able to resolve orographic-related features. Results will be given during the presentation.

Measuring the Strength of ENSO Events: How Does 1997–1998 Rank?

Klaus Wolter
University of Colorado, Boulder
NOAA-CIRES Climate Diagnostics Center
Boulder, Colorado 80309–0449

The current El Niño event has been hailed as the "El Niño of the century," in effect surpassing the previous title holder: 1982–1983. Is this claim premature? How should we determine the strength of El Niño events? This talk addresses these issues by comparing the temporal evolution of a variety of ENSO measures for both events. The Multivariate ENSO Index (MEI) is prominently discussed, since it integrates the significant features of all observed surface fields in the tropical Pacific basin. Aside from the more obvious sea-level pressure and sea surface temperature data, the MEI monitors the zonal and meridional surface wind fields, near-surface air temperature, and total cloudiness. The contributions of each of these fields to the overall evolution of the 1997–1998 and 1982–1983 events are compared against each other and against the evolutions of other events since 1950. Conventional ENSO indices like the Southern Oscillation Index and various Niño-region sea surface temperature anomalies are considered as well.

Although unprecedented in its growth and early size since at least 1950, the current event has recently ceded its "front runner" position back to 1982–1983 (using data through the end of February 1998). The final outcome of this "horse race" may not be decided until after PACLIM 98.

Toward Regional Downscaling of 1997–1998 El Niño GCM Predictions

Andrew W. Robertson
University of California, Los Angeles
Department of Atmospheric Sciences
Los Angeles, California 90095

General circulation models (GCMs) provide a basis for predicting the large-scale circulation changes in the North Pacific–North American (NPNA) sector, associated with El Niño. At best, however, they do not have sufficient spatial resolution to accurately represent precipitation on regional scales. A natural method of "downscaling" GCM predictions is to use empirical relationships between large-scale atmospheric circulation patterns and regional daily temperatures and precipitation.

We firstly derive observed downscaling relationships between the atmosphere's preferred low-frequency circulation patterns—"weather regimes"—over the NPNA sector, and distributions of local daily temperature and precipitation in eight subregions of the western US. The leading observed regime is a "PNA-like" pattern, which is found to be more prevalent during El Niño winters. Over the central Sierra Nevada of California, for example, this regime is associated with an increased probability of precipitation.

These empirical downscaling relationships are then applied to ensembles of prediction experiments made with two different atmospheric GCMs (AGCMs), driven by NCEP-predicted SST anomalies over the tropical Pacific for the period October 1997 through March 1998. An ensemble of 20 AGCM prediction experiments and 20 controls has been made by M. Wehner and G. Balasubramanian using the LLNL–UCLA GCM (http://www-pcmdi.llnl.gov/wehner/clc.html). In addition, nine predictions and nine controls have been made with the higher resolution version of the UCLA AGCM by J. Farrara (http://unilab.atmos.ucla.edu/~vwk206/fcst.html).

To be able to downscale these predictions, we investigate each model's low-frequency variability in terms of its weather regimes. The LLNL–UCLA model's circulation regimes are not found to exhibit realistic spacial patterns and no marked changes were found between the regimes in the control- and prediction-ensembles, nor in their frequency of occurrence. In contrast, the UCLA GCM exhibits a fairly realistic PNA-like pattern and this weather regime is much more frequent in the 1997—1998 forecast ensemble compared to the control. Its predicted increase in frequency of occurrence would imply a downscaled prediction for precipitation frequency in the central Sierra Nevada of the order of +10%.

Biological–Physical Coupling in the Central Equatorial Pacific During the Onset of the 1997–1998 El Niño

Peter G. Strutton[1], Francisco P. Chavez[1], and Michael J. McPhaden[2]
[1]Monterey Bay Aquarium Research Institute
P.O. Box 628
Moss Landing, California 95039
[2]NOAA/PMEL
7600 Sand Point Way NE
Seattle, Washington 98115

The perturbations to phytoplankton biomass associated with the onset of the 1997–1998 El Niño event are described and explained using physical and bio-optical data from moorings in the central equatorial Pacific. The physical progression of El Niño onset is depicted from reversal of the trade winds in the western equatorial Pacific through eastward propagation of equatorially-trapped Kelvin waves and advection of waters from the nutrient-poor western equatorial warm pool. Fluctuations in chlorophyll and quantum yield of fluorescence are rightly coupled to thermocline variations associated with the passage of Kelvin waves. The

magnitude of the variations in chlorophyll implies at 50% reduction in primary productivity during the onset of El Niño.

Regional Transport Covariability in the California and Alaska Currents During the Onset of the 1997–1998 El Niño

P. Ted Strub and Corinne James
Oregon State University
College of Oceanic and Atmospheric Sciences
Corvallis, Oregon 97331-5503

One of the central hypotheses of the US GLOBEC program in the northeast Pacific is that the strengths of the eastern boundary currents in the Subarctic Gyre (the poleward Alaskan Current) and the Subtropical Gyre (the equatorward California Current) covary out of phase on interannual (ENSO) to interdecadal time scales. It is also hypothesized that this covariability is linked to changes in the strength or position of the West Wind Drift current, which flows eastward between the two gyres at approximately 45°N–50°N. The primary evidence for the covariability of the boundary currents comes from coastal tide gauge data, but the link to the West Wind Drift has not been tested. Altimeter data now provide the means of quantifying the covariability of the surface transports in all parts of the two gyres. Approximately five years of TOPEX/POSEIDON (T/P) data are used to show this variability on seasonal and (marginally) interannual time scales. The analysis of transports calculated from T/P and tide gauge data confirm the covariability of the boundary flow in the gyres on seasonal time scales. There is little connection to the West Wind Drift in the central North Pacific. The analysis of the non-seasonal variability is dominated by the 1997–1998 El Niño and shows the development of the coherent anomalous northward transport during the onset of this event between May and November 1997.

El Niño 1997: Simultaneous Extrema in Gulf of Alaska Oceanography and Sockeye Salmon Biology

Skip McKinnell
Ocean Science and Productivity Division
Pacific Biological Station
Nanaimo, British Columbia

The most extreme SSTs recorded in much of the Gulf of Alaska coincided with the most extreme behavior of sockeye salmon in coastal British Columbia waters. The catch per unit effort (CPUE) of sockeye in the Noyes Island (SE Alaska) seine fishery in 1997 was twice the magnitude of the next to last value. In 1997, the highest recorded migration of Fraser River sockeye via the northern route (Johnstone Strait) occurred. The duration of the migration was one of the most protracted in history. Sockeye salmon were observed spawning in many coastal streams and rivers where they had never been seen before, indicating large scale straying of sockeye from their native streams. Sockeye salmon are thought to be the most diligent of the salmon species in seeking out their natal stream. DNA and other stock identification characteristics are being used to identify the source of the straying sockeye.

The Impact of the 1997–1998 El Niño on World Grain Yields

Ray Garnett
Canadian Grain Commission
Winnipeg, Manitoba

The 1997–1998 El Niño event which has often been referred to as the "EL Niño of the Century" has been the most benign event to affect world grain yields since 1960. During this short presentation, the first author will present a brief survey of its effects on world grain yields during 1997.

It appears that the biggest negative impact during the summer of 1997 was on the Chinese corn crop and possibly the Chinese soybean crop as far as major drought impacts are concerned. Some problems were also evident in parts of North Africa which have been linked to El Niño. Elsewhere in the world, crop yields were much higher than many forecasters anticipated in countries such as Australia, India, and South Africa.

El Niño, La Niña, and Flood Frequency in Arizona and Adjacent Regions

Robert H. Webb
US Geological Survey
1675 W. Anklam Road
Tucson, Arizona 85745

The 1997–1998 El Niño conditions in the Pacific Ocean did not cause significant flooding in Arizona and adjacent parts of the lower Colorado River basin despite high winter rainfall. The typical mechanism for large winter floods in Arizona is rainfall on snowpack at elevations above 2,000 m. Most of the precipitation in the high-elevation areas of Arizona in the winter of 1997–1998 was snowfall, and although snow accumulations were high, the cool temperatures of late winter and early spring spread the snowmelt out, preventing significant floods. The lack of a sustained incursion of tropical moisture borne in the subtropical jet is the reason for the difference in hydroclimatic response between the winter of 1992–1993 and 1997–1998. The 1997–1998 response is in accord with the long-term climatological averages of flood frequency at the $P = 0.01$ level (otherwise known as the 100–year flood) doubles or triples during ENSO conditions, whereas flood frequency at the more common $P = 0.50$ to 0.98 level is unchanged. Warm ENSO conditions typically influences the variance and higher-order moments of flood-frequency distributions, leaving the mean unchanged. Despite the lack of floods during the winter of 1997–1998, the probability of flooding in September through October 1998, as a result of incursions of dissipating tropical cyclones, remains high, in accord with long-term history of these severe floods.

Nonstationarity in ENSO and Its Teleconnections: An Exploratory Analysis and a Nonlinear Dynamics Perspective

Upmanu Lall[1], Balaji Rajagopalan[2] and Mark Cane[2]
[1]Utah State University
Utah Water Research Laboratory
Logan, Utah 84322–8200
[2]Columbia University
Lamont-Doherty Earth Observatory
Palisades, New York 10964–8000

The time series of El Niño Southern Oscillation Indices exhibit many "non-stationarities" over the period of record. These include changes in the spectral signature, in the conditional and unconditional probability distributions of different ENSO states, as well as for the basic statistics (mean, variance, and autocorrelation) of the indicator over interdecadal to secular time

scales. The correlations of these indices with streamflow and other regional climate indicators also show significant nonstationarities over the period of record. An interesting observation is that the correlations between the low frequency components of ENSO indicators (for example, a 30–year weighted moving mean and variance of NINO3) and corresponding low frequency components of several US streamflow series are very high, even when the full record correlations between the raw streamflow series and NINO3 are not statistically significant. In some cases, these correlations switch sign over the period of record. There is a suggestion that there is organization in the low frequency dynamics or the nonstationarity of ENSO and its teleconnections. There is some debate as to the source of such non-stationary climate variability. Two paradigms are of interest. The first considers the dynamics to be intrinsically linear and the nonstationarity due to changes in the forcing of the system, for example, by greenhouse gas and other related factors. This scenario may be associated with the apparent recent increase in the frequency and severity of El Niño events and their continental impact. The second considers the apparent nonstationarities to be a manifestation of the internal nonlinear dynamics of the climate system. Under this paradigm, the evolution of the system takes place potentially at multiple time scales leading to regime structure in which different attributes or statistics of the state variables are revealed for protracted periods of time. Such behavior may be identified through the integration of low-order dynamical systems with weakly unstable quasi-periodic nonlinear dynamics. Examples of such models include the Lorenz (1984) model of extratropical circulation and the xxx (What's best here: C-Z or delayed oscillator or other?) model of ENSO. It is unclear that linear correlative analyses and related tools (for example, spectra) are appropriate classifiers of such dynamics and their apparent non-stationarity. Nonparametric time series analysis methods that embody considerations of nonlinearity and nonstationarity in the dynamics are used to show that the return periods of recent ENSO extremes can be significantly smaller than those indicated by stationary, linear, autoregressive models applied to the prior period. Consequently, we argue that the role of internal dynamics and its long-term variability not be discounted when ascribing recent climate trends to external causes.

1997–1998: El Niño of the Past Three Centuries?

Michael E. Mann[1], Raymond S. Bradley[1], and Malcolm K. Hughes[2]

[1]University of Massachusetts
Department of Geosciences
Amherst, Massachusetts

[2]University of Arizona
Laboratory of Tree Ring Research
Tucson, Arizona

Inferences into long-term variability in El Niño and the global ENSO phenomenon over the past three centuries are obtained from mutiproxy-based reconstructions of global surface temperature patterns. The NINO3 index, diagnosed from the reconstructed surface temperature patterns, is used to assess El Niño-related variability back to 1650. The calibration residuals are shown to be unbiased, allowing for a confident assessment of the uncertainties in the reconstructions. Within the limits of these estimated uncertainties, we assess how anomalous recent warm events such as the 1982–1983 and current 1997–1998 events are in the context of the multiple-centuries reconstructed history. We examine the anomalous nature of recent behavior in terms of both the frequency and magnitudes of warm (and cold) events. Possible long-term changes in the extratropical teleconnections of ENSO are also examined by examining the evolution of the relationship between the reconstructed NINO3 and large-scale temperature patterns during past centuries.

What to Expect from an Extreme La Niña—The Opposite of the Effect from an Extreme El Niño?

Martin P. Hoerling
University of Colorado, Boulder
NOAA-CIRES Climate Diagnostics Center
Boulder, Colorado 80309

Double the normal rain inundated California during October 1997 through March 1998, with El Niño awarded the blame. Central and northern California suffered the most, yet these areas are typically spared the brunt of El Niño's impact. Historically, El Niño's effect on the West Coast resembles a dipole, having a strong wet signal south of 40 degrees latitude, and a dry signal in the Pacific Northwest. Even this dry signal has failed to emerge however, with normal snowpack observed in the Cascades as of March 1998.

Can we reconcile this abnormal rainy season with El Niño, and attribute it to the unprecedented state of affairs in the tropics? Observations of such extreme events are too rare to yield a definitive answer, although nature offers some clues. Simulations using models of the atmosphere are very useful in this regard, and the weight of evidence from these is that extreme El Niños do indeed have a unique footprint on West Coast rainfall that is distinguishable from the garden-variety El Niños. What is on the horizon for the next Pacific west coast rainy season? El Niño is declining, and some predictions are for a significant cold event (La Niña) to be in place by fall 1998. Are the climate effects of an extreme La Niña equal and opposite those of El Niño and will recent flooding be replaced by future drought? Results from numerical models will be shown that demonstrate remarkable departures from such an intuitive, linear view point.

Watching Warm Events on Their Global Walkabout

Gary D. Sharp
Center for Climate and Ocean Resources Study
P.O. Box 2223
Monterey, California 93940
http://www.monterey.edu/faculty/SharpGary/world

The idealized ocean has rarely received so much attention as during the recent string of ENSO–Low Southern Oscillation index years, initiating in 1990, and relenting for only 18 months during 1995–1996. The general acceptance of the pattern of changes in the equatorial Walker Circulation, and the upper ocean responses, has helped martial considerable change in the approaches made to monitoring, understanding, and attempting forecasts. The other end of the scale is the lack of appreciation for the longer-term consequences of these ENSO patterns, within the oceans, and across the spectrum of global weather affecters, such as their eventual transfer to and warming the upper ocean of Drake's Passage (that I observed for myself in January 1985), and changes in production pattern D5s as reflected in the decade of measurements associated with antarctic krill research. (Valerie Loeb, Moss Landing Marine Lab, personal communication) The near term heat dynamics of the upper ocean drives a downstream Do-Loop that is being identified within the research community that has been most obvious to those of us that have interests in biological response patterns to upper ocean climatologies, and events.

In 1986, I began by running in reverse the 1982–1983 ENSO imagery from GOES–east and GOES–west satellites, allowing those without access to the hemispheric imagery the opportunity to see where their weather came from. At the same time, I began collating subsurface time-space plots of monthly mean upper ocean thermal structure along the coastlines, across the equatorial ocean and along selected ocean transects. These convinced me that the conventional concepts of what and where ENSO warm and cold events were occurring was faulty, and needed to be better understood. Early COARE studies began focusing on localized heat and upper ocean circulation dynamics (Moum and others 1989; Moum 1998), and recently the addition of LIDAR technology in the study of equatorial thermal fluxes filled the bill for defining the relevance of small scale diel processes, and propagation of heat from point to point, across the upper ocean. Warren White's 1997 PACLIM presentation stimulated me to pull out some of these time series and organize my thoughts and experiences with nighttime ocean dynamics within water column, atmospheric transfers of heat energy to the east, and poleward of these initial processes. I put a number of relevant graphic images into my July 1997 NCAR ENSO Colloquim web site presentation, and I have since brought some of the time series out of retirement, to complete my message about upper ocean dynamics and the patterns of transfer and ecological responses that ensue, along western North and South America, South Africa, and from the Japan Sea south to Indonesia.

There are several givens: (1) pelagic fish populations are directly affected and predictable; (2) following the patterns of energized upper ocean holds the key to forecasts of both weather and ecosystem responses; and (3) the official concepts of the late 1970s and 1980s that El Niño was a phenomenon off northern South America, in which the SST rises by 2 °C are finally falling away, opening the door to global ocean and atmospheric relationships. I have always wondered that this should not have been a starting place, given the existing archived information and understanding what was available (as per Allan and others 1997). If the North American research community had looked far enough upstream, in time space and in the libraries of the various nations they encountered, there might have been a lot more progress made more quickly. In addition, maybe the conclusion that enhanced rainfall also enhances insect disease vectors would not have been so surprising. A time series of disease outbreaks and climate relations has been available for decades or maybe even centuries.

Interaction between ENSO and the North Pacific Oscillation: Implications for Long-range Predictability of Intraseasonal Hydrologic Extremes in the Western US

Alexander Gershunov, Tim Barnett, Dan Cayan and Larry Riddle
Scripps Institution of Oceanography, Climate Research Division
University of California, San Diego

The existence of persistent quasi-decadal variability in the Pacific sector climate has important implications for long-range climate predictability in North America. The spatial manifestations in climate variables around the tropical and north Pacific associated with the North Pacific Oscillation (NPO) and ENSO are rather similar. This suggests that ENSO influence on the US climate can depend on NPO phase. We show that this is indeed the case and discuss implications for ENSO-based long-range hydroclimate predictability. ENSO-based predictability depends on the strength and stability of the El Niño and La Niña signals. We examine the effect of the NPO on ENSO-based predictability of two hydrologic variables in the western US: cold-season heavy precipitation frequency (HPF) and springtime high streamflow frequency (HFF) events. Both HPF and HFF describe interannual variability in daily extremes and are closely related to flooding. Moreover, HPF and HFF are known to be sensitive to ENSO in the western US. Using six decades of daily observations, we compare El Niño and La Niña HPF and HFF signal strength and stability during the high-and low-phase epochs of the NPO. Results suggest that ENSO-based predictability is strongly modulated by NPO phase in a manner consistent with physical considerations.

Interpreting the Observed Patterns of Pacific Ocean Decadal Variations

Art Miller
Scripps Institution of Oceanography, Climate Research Division
La Jolla, California 92093-0224

Basin-scale variations in oceanic physical variables are thought to organize patterns of biological response across the Pacific Ocean over decadal and interannual time scales. Different physical mechanisms can be responsible for the diverse basin-scale patterns of SST, thermocline depth, and horizontal currents, although they are linked in various ways. Using Pacific basinwide ocean model hindcasts of the last 30 years for guidance, we interpret observed basinwide patterns of decadal-scale variations in upper-ocean temperatures. Thermocline changes off the North American coast are linked to westward-intensified thermocline changes driven by the increase in North Pacific wind-stress curl during the 1980s. Surface currents likely respond to the adiabatic forcing of this wind stress curl, forcing and thus following these thermocline changes. Anomalous subduction of cool waters in the central North Pacific is associated with intense diabatic cooling and mixing during the winter of 1983. Although this temperature variation has a decadal time scale, and although it connects the adiabatic changes of the subpolar and the phase-lagged subtropical gyre, it appears to be physically distinct from the westward-intensified thermocline changes. The implications of these results for hypothesized physical mechanisms of Pacific interdecadal variability and possible biological responses will be discussed.

Oceanwide Winter Drift Trajectories in the North Pacific Ocean Computed with the OSCURS Model Show Decadal and El Niño Patterns 1901–1998

W. James Ingraham, Jr.[1] and Curtis C. Ebbesmeyer[2]
[1]Alaska Fisheries Science Center-NMFS-NOAA
7600 Sand Point Way NE
Seattle, Washington 98115-0070
[2]Evans-Hamilton, Incorporated, Western Region
4608 Union Bay Place NE
Seattle, Washington 98103

Sea surface drift trajectories from 201 start points spread across the North Pacific were simulated using the OSCURS (Ocean Surface Current Simulations) model for each winter (1 Dec to 28 Feb) during 1901–1998. To reveal decadal fluctuations in the oceanic current structure, the trajectories were smoothed in time with a five-year running boxcar filter. As the strongly decadal drift from Ocean Weather Station Papa fluctuates between north and south modes, other portions of the subarctic and subtropical gyres also change, but show varying degrees of low frequency fluctuations. Time variability of major circulation features were calculated but not limited to the eastward drift from Papa, the split in flow off Washington, the great garbage patch under the Northeast Pacific Atmospheric High, and the rapidly circulating garbage patch seaward of the Kuroshio. Interannual patterns associated with El Niño years are discussed. Development of OSCURS was motivated by the need in fisheries research for indices that describe variability in ocean surface currents. These synthetic data, derived through empirical modeling and calibration, provide insight that far exceeds their accuracy limitations. OSCURS daily surface current vector fields are computed using empirical functions on a 90 km ocean-wide grid based on monthly mean sea level pressures (1900–1945) and daily sea level pressures (1946–1997); long-term-mean geostrophic currents (0/2,000 db) were added. The model was tuned to reproduce trajectories of satellite-tracked drifters with shallow drogues from the eastern North Pacific.

A Comparison of Ship Winds with NSCAT Scatterometer Measurements in the Western Equatorial Pacific Warm Pool During January–February 1997

Kyozo Ueyoshi
Japan Marine Science and Technology Center, Ocean Research Division
Yokosuka, 273 Japan

A recent study by Bourassa and others (1997) suggests that NSCAT scatterometer sea surface winds agree very well with winds observed from ocean research ships if these measurements simultaneously occur in a narrow spatial and temporal span. In this paper NSCAT Level 2.0 winds are compared with observations from an ocean research ship in the western equatorial Pacific warm pool during January through February 1997. Agreement (or disagreement) appears reasonable considering much larger spatial ranges and time differences allowed (up to 6 hours) between NSCAT measurements and ship observations when a separate study indicates that winds in the open tropical sea become rapidly uncorrelated with themselves within about one hour. Overall bias of ship winds toward higher wind speeds even after taking into account the stratification of air could not be attributed entirely to large spatial and time differences between two kinds of observations. It is suggested that the ship's structure on the air current around the ship has serious effects on the wind measurements aboard the ship.

Decadal Patterns in a Sandy Subtidal Community: Effects of Decreased Oceanic Productivity

Stacy L. Kim, John S. Oliver, and Peter N. Slattery
Moss Landing Marine Laboratories
P.O. Box 450
Moss Landing, California 95039

As the field of ecology matures, we can look at patterns over decadal time scales. Communities in soft-bottom marine habitats (6 to 30 m water depth in Monterey Bay) are divided into two general zones. A shallow zone (<14 m) was primarily occupied by small, mobile crustaceans. The deeper zone (>14 m) was dominated by tubiculous and burrowing polychaete worms. A short-term (1971–1976) study in this area revealed that species abundances and diversities remained constant and the zonation pattern was consistent and controlled by wave action. In 1997, biodiversity had decreased at all stations sampled. The abundances of individuals had also decreased, to one-tenth the densities found in the early 1970s. This decrease is most marked in long-lived species, resulting in relatively high abundances of opportunistic, weedy species. The communities, especially at the deeper sites, have shifted from ones dominated by sedentary predators to ones dominated by mobile scavengers. The remarkable loss of diversity and number of animals are indicators that there has been a major shift in this ecosystem in Monterey Bay. This agrees with information from oceanic studies on the coast of southern California that have observed a marked decrease in the productivity of planktonic communities over the same time frame. It suggests that the shift in the California current system, caused by global changes in climate, is having strong effects both locally and regionally. This is the first example we know of that reveals how a regional decrease in productivity impacts the structure of extant marine communities.

Climatic Inferences from a 1200–year Tree Ring Reconstruction of Sacramento River Flow

David M. Meko, Christopher H. Baisan, and Malcolm K. Hughes
University of Arizona
Laboratory of Tree Ring Research
Tucson, Arizona 85721

Tree ring data and other proxy information indicate that between about AD 900 and AD 1350 the southern Sierra Nevada experienced hydrologic droughts longer and more severe than at any time since. We have recently developed a millennial-length, drought-sensitive, tree ring chronology from western Juniper (*Juniperus occidentalis*) in southern Oregon and combined this with other long chronologies to generate a streamflow reconstruction suitable for estimating long-term hydrologic drought occurrence in the critical water supply area of northern California. The reconstruction can be interpreted as an indicator of cool-season moisture conditions reflecting variations in primarily winter precipitation. The percentage of variance of annual Sacramento River flow accounted for by subperiod reconstruction models exceeds 60% for models applied after AD 900 and 80% after AD 1700. The long-term mean for the entire AD 700–1997 reconstruction is approximately equal to the modern 92–year mean (1906–1997) of 18.0 million acre-feet from gaged data. The reconstruction does, however, contain considerable low-frequency variability, as evidenced by swings in 100–year reconstructed mean flow more than 15% above and 10% below the 1907–1997 gaged mean. Of particular climatic significance, reconstructed flow was high during the period AD 900–1100, when other paleoclimatic data suggest severe drought in the southern Sierra Nevada. This opposition lends support to a theory of a persistent northward-displaced storm track at the time.

Evidence for ENSO in Tree-Ring $\delta^{13}C$ along a 500-km E-W Transect in Southern Arizona and New Mexico

Steven W. Leavitt[1], William E. Wright[1], and Austin Long[2]
[1]Laboratory of Tree Ring Research and [2]Department of Geosciences
The University of Arizona
Tucson, Arizona 85721

Ponderosa pine tree rings were sampled at ten sites in nine mountain ranges extending from the Santa Catalina Mountains in southern Arizona to the Guadalupe Mountains in southern New Mexico. We developed stable-carbon isotope ($\delta^{13}C$) chronologies at eight sites for 1985–1995 by pooling rings from multiple trees at each site, subdividing rings into pre- and post-summer monsoon-onset segments, and analyzing the cellulose component. The $\delta^{13}C$ values are considered a useful proxy of the seasonal moisture stress experienced by the trees. Two chronologies developed at separate sites in the Chiricahua Mountains, Arizona, showed good coherence despite being separated by about 13 km and 800 m of elevation. This evidences effective reproducibility of the method, with the differences between the two chronologies perhaps a consequence of the microclimatic/hydrological disparities between sites. For the full network of chronologies, the $\delta^{13}C$ seasonal pattern shows remarkable coherence across the full length of the transect, with the farthest east Sacramento Mountains chronology tending to be more frequently dissimilar with respect to those farther westward. The strongest correlations (positive) were between $\delta^{13}C$ of the earliest formed portion of the rings and Southern Oscillation Index, consistent with reduced moisture stress early in the growing seasons of El Niño years and higher moisture stress in La Niña years.

ENSO Teleconnections: Sea Surface Temperature Correlations with $\delta^{18}O$ in Southeastern Arizona Precipitation and Tree Cellulose

William E. Wright[1], Steven W. Leavitt[1], and Austin Long[2]
University of Arizona
[1]Laboratory of Tree Ring Research
[2]Department of Geosciences
Tucson, Arizona 85721

Many researchers have identified the eastern Pacific and Gulf of California as the dominant maritime summer moisture source for southeastern Arizona. Despite this understanding, strong direct El Niño–Southern Oscillation (ENSO) teleconnections with precipitation and temperature in the region have not been identified. Our research identifies clear ENSO teleconnection between precipitation in southeastern Arizona and eastern Pacific sea surface temperatures manifested in the year-to-year variance of the precipitation stable isotopic ratios.

Stable isotopes in Tucson, Arizona precipitation ($\delta^{18}O$ and δD) have been analyzed per event from 1981 to present, a unique time series in the western United States. High correlations are noted between weighted $\delta^{18}O$ summer season values with eastern Pacific sea surface temperatures (SSTs). Cellulose $\delta^{18}O$ values derived for the same period from ponderosa pine trees in the Santa Catalina Mountains near Tucson also reveal high correlation with local precipitation $\delta^{18}O$ and eastern Pacific SSTs.

The Late 1500 Severe Sustained Drought in the Colorado River Basin: Is It Real?

John Dracup[1], Hugo Hidalgo[1], Glen Macdonald[2], and Thomas Piechota[1]
University of California, Los Angeles
[1]Department of Civil and Environmental Engineering
[2]Department of Geography
Los Angeles, CA 90095

The Colorado River Basin (CRB) supplies water to nearly 25 million people and to more than one million acres of western farmland. The river's hydroelectrical plants generate about nine billion kilowatt-hour of electricity each year. It also holds six national parks and many recreational parks that provide benefits difficult to quantify. Thus, the CRB represents an important resource of water, especially for the western United States, that justifies any effort aimed to expand the knowledge of the basin characteristics and to optimize its regulation. For this reason, a series of regulations and laws were produced from 1922 to 1963 with the purpose of issuing policies regarding the water allocation in the CRB. The sum of all of these regulations is known as "The Law of the River."

Recently, historical severe and sustained droughts (SSD) in the upper Colorado River basin (UCRB) have been identified based on dendrochronology studies. These studies indicate that a SSD occurred in the basin during the period 1573–1592. Certain individuals or entities consider these findings to be an accurate enough for determining the future availability of surplus water to the lower basin states, and to warrant changing the current "Law of the River." The objective of this study is to verify the existence of a drought in the late 1500 century, and then if its existence can be confirmed, what are the characteristics of this drought (duration, magnitude, and severity)? To accomplish that, it is necessary to review and to improve previous studies in the UCRB, focusing on assessing the accuracy of the duration, magnitude and severity of this drought, by collecting new data and applying new and more precise techniques in the flow reconstruction. In addition we will review other high temporal resolution paleoclimate indicators, to determine the synoptic climatology of this drought. It is unknown at this time whether the results of this research effort will or will not confirm the duration, magnitude and severity of the reconstructed 1573–1592 SSD scenario in the UCRB. However, the potential consequences that may arise from the existence of this scenario to the lower basin states cannot be ignored.

Glacial to Interglacial Contrasts in Organic Matter Production and Preservation on the California Continental Margin

Walter E. Dean[1] and James V. Gardner[2]

[1]US Geological Survey, MS 980 Federal Center, Denver, Colorado 80225

[2]US Geological Survey, 345 Middlefield Road, Menlo Park, California 94225

The production and accumulation of organic matter on the upper continental slope (200–2,700 m) off California and southern Oregon was markedly different during the last glacial interval (about 24–10 ka) than either the Holocene or last interstadial (oxygen-isotope stage 3, about 60–24 ka). In general, organic productivity on the California and Oregon margins was higher during the Holocene and stage 3 than those deposited during the last glacial interval and this contrast is greatest off southern California. This glacial-interglacial pattern in productivity is in contrast to the commonly held view that productivity in the world ocean was higher during the last glacial interval (for example, Sarthtein and others 1998). However, this latter conclusion is based mainly on data from the eastern equatorial Pacific and off northwest Africa. highest productivity on the California margin over the last 60 ky occurred during certain intervals within oxygen-isotope stage 3 when organic-rich laminated sediments accumulated within the present oxygen-minimum zone on the upper continental slope from as far north as the Oregon–California border to as far south as Point Conception. These upper Pleistocene-laminated sediments, interbedded with bioturbulated sediments, contain more abundant, hydrogen-rich (type II), marine algal organic matter than even surface sediments with large amounts of labile, marine organic matter. The stable carbon-isotopic composition of the organic matter does not change with time between bioturbated and laminated sediments, indicating that the greater abundance of type II organic matter in the laminated sediments is not due to a change in source, but rather represents a greater degree of production and preservation of marine organic matter. The laminated, and even some non-laminated, stage 3 sediments contain concentrations of molybdenum that precipitated as sulfides from sulfidic bottom waters. The presence of organic- and molybdenum-rich laminated sediments indicates that the oxygen minimum zone in the northeastern Pacific Ocean was more intense and probably anoxic during the late Pleistocene as a result of increased coastal upwelling that enhanced algal productivity.

Estimates of Glacial Climate and Runoff for the Bonneville Basin

Marina Timofeyeva, Susanne Clement, and Rachael Craig
Kent State University, Department of Geology
Kent, Ohio 44242

We estimate climatic conditions in the basin of Lake Bonneville at the time of the last glacial (glacial) using a local climate model. When comparing modern temperature solutions (spatial average) to those for the glacial, we find that glacial climate was cooler on average by 3.2° C. During the glacial winter (November through April), the temperature is as much as 6.3° C cooler and averages 4.4° C cooler, while the glacial summer (May through September) is only 1.5° C cooler when compared with modern conditions and July is actually 0.3° C warmer than modern. The glacial age seasonal distribution of precipitation is more variable than today. Wet season precipitation (November through April) is estimated to be 2.3 times higher on average for the glacial, while dry season precipitation (May through October) is estimated to be 1.8 times higher. Precipitation is greater at the glacial in all months and the larger increase in winter leads to much greater snowpack. Rainfall is less in winter as a result of the cooler temperatures; more precipitation falls as snow. This implies fewer rain-on-snow events, less ripening of snowpack, and delays in snowmelt compared to modern. Using a modified version of a previously-developed runoff model, driven by the output of the climate model, we find that runoff during the glacial was 3.1 times higher during the warm season (May through October) but was unchanged during the cold season (November through April), which is expected due to precipitation remaining trapped as snowpack for a longer time. The runoff peak occurs at the same time (May), but reaches that peak much more abruptly at glacial compared to modern. These model solutions compare favorably with paleoclimatic and paleohydrologic evidence from the Bonneville Basin at this time, which suggests the following: (1) increased abundance of subalpine conifers and shrubs; (2) extensive valley glaciers in the Wasatch; (3) an increase of runoff of two to three times; (4) large prograding deltas at the mouths of the major rivers; and (5) the existence of a high stand of Lake Bonneville.

A Revised Hypothesis for Evolution and Biogeography of Monterey Pine (*Pinus radiata*) Inferred from Fluctuating Quarternary Climates

Constance I. Millar
US Department of Agriculture Forest Service, PSW Research Station
Albany, California 94706

Monterey pine (*Pinus radiata*) evolved 15–25 million years ago in Latin America and migrated northward to California in the late Tertiary, where it now occurs in three disjunct coastal locations and on two Mexican islands. Evidence from microfossils and oxygen-isotope ratios in sediment cores documents that Quarternary coastal climates have fluctuated with long (glacial and interglacial), medium (interstadial), and short (ENSO-like events) periodicities over the last million years. Historical plant abundances in coastal California habitats reflect these fluctuating climates. Pines, notably Monterey pine, appear to occupy a macrosuccessional role, shifting locations along the coast with increasing representation during transitional climates. That is, during terminations of glacial periods, interstadials, and other cooler intervals, coastal pine increases in abundance, whereas it decreases during other climate phases. Such evidence is used to reject the traditional hypothesis that Monterey pine was broadly distributed along the coast throughout the Pleistocene and that the Hypsitherm triggered contraction into present relictual populations. Instead, it is postulated that the species has a metapopulation strategy and has long existed as a complex of distinct populations that have been subject to repeated events of colonization, coalescence, and local extirpation that follow climate cycles.

ENSO and the Glen Canyon Dam Adaptive Management Program: Eastern North Pacific Forcing of Paria River Floods in 1997

David J. Topping[1], Theodore S. Melis[2], and Roger S. Pulwarty[3]
[1]US Geological Survey, WRD, Lakewood, Colorado
[2]Grand Canyon Monitoring and Research Center, Flagstaff, Arizona
[3]CIRES, Climate Diagnostic Center, Boulder, Colorado

Since completion of Glen Canyon Dam in March 1963, most fine sediment (sand, silt, and clay) crucial to the riparian and aquatic environments of the Colorado River ecosystem in Grand Canyon National Park (GCNP) is derived from the Paria and Little Colorado rivers. These tributaries deliver large quantities of fine sediment to the Colorado River during short-duration, high-magnitude floods. Advance notice of tributary flooding may allow better coordination of the timing of managed high releases from Glean Canyon Dam to improve sediment conservation throughout the Colorado River ecosystem in GCNP. Recent monitoring of sediment input to the Colorado River during Paria River floods in September 1997 suggests that, under normal powerplant releases from Glen Canyon Dam, the residence time of the finest sediment (very fine sand and finer-sized material) in the Colorado River is relatively short. Because effective management of the Colorado River ecosystem in GCNP requires that the dam be operated to retain as much of the tributary-supplied fine sediment in GCNP for as

long as possible, it is desirable to not only know the magnitude of tributary sediment-supplying events (as they occur) but also to have the ability to forecast these events.

To date, we have focused on the Paria River, with emphasis on the development and testing of a physically based model for calculating real-time inputs of fine sediment to the Colorado River (Topping 1997). Our current work focuses on developing moderate and short-term forecasting procedures for predicting extreme flows from this basin. The Paria drains 3,730 km^2 of southern Utah and northern Arizona and is an ephemeral stream dominated by the infrequent, large floods of short duration. From November 1923 through September 1997, the mean 15–minute discharge at its mouth was only 0.77 m^3/s, while the mean annual peak discharge was 88 m^3/s, the bankfull discharge was 90 m^3/s, and the largest flood had a peak discharge of about 320 m^3/s. To illustrate the flashy nature of the river, the bankfull discharge, with a return period of about two years, was equaled or exceeded a total of only 104.5 hours in the 73.9 years of gage record (in other words, only 0.022% of the time). Large Paria River floods can occur during any season, but most occur from mid-July through mid-October, and are generated by rainfall in the uppermost 14% of the drainage basin (Topping 1997) from either local intense thunderstorms or dissipating tropical storms in the eastern North Pacific Ocean.

The two-month period of August and September 1997 was on of the most significant periods of sediment transport in the Paria River this century. During this time, approximately 7.6 x 10^5 m^3 (2.2 million tons) of sand and 9.2 x 10^5 m^3 (2.7 million tons) of silt and clay were delivered to the Colorado River by a series of large floods in the Paria River. Most of this sediment input occurred during four large floods (three of which had peak discharges greater than bankfull), a 116 m^3/s on September 15 and a flood of 93 m^3/s on September 26. These floods resulted from dissipating tropical storms in the eastern North Pacific Ocean. Normally, Pacific tropical storms do not reach as far north as Arizona and Utah. However, these storms may indirectly cause flooding on rivers in the southwestern US when moisture is advected inland from these storms as they move northward offshore of northern Mexico and southern California. Also, when conditions allow, such storms may cause flooding as they recurve inland and dissipate over areas as far north as California, Nevada, Arizona, New Mexico, Utah, and Colorado.

The Paria River has produced bankfull or larger peak discharges 41 times between water years 1924 and 1998. Twenty-five of these 41 peaks (61%, all mid-July through mid-October) are believed to have been caused by combined tropical storm and monsoon precipitation. Of these 25 floods, 15 (36%, four in August, nine in September, and two in October), are documented as having been triggered by dissipating eastern North Pacific Ocean tropical storms (Hansen and Schwarz 1981; Smith 1986). In many cases, precipitation from tropical storms apparently provided wet antecedent conditions for later monsoon-induced floods. Because increased sea surface temperatures to the north allow tropical storms to maintain strength and migrate further north along the Mexican coast, we suspect that during ENSOs (and as we observed from August through September 1997) the following all increase: advection of moisture into Arizona and Utah from tropical storms; the recurvature of tropical storms landward; and the interactions of tropical storms with cutoff lows. Advance forecasts (up to 14 days) of the atmospheric and oceanic conditions that cause extreme Paria River flows may allow better-planned releases from Glen Canyon Dam. Coordination of high releases during or immediately following tributary floods would promote conservation of limited and infrequent sediment inputs to the Colorado River ecosystem, particularly in its most sediment-starved upper reaches above the Little Colorado River confluence.

Time Scales of Variability in the Colorado River Basin: Implications for the Glen Canyon Adaptive Management Program

Roger S. Pulwarty[1], Theodore S. Melis[2],Terrance S. Fulp[3], Randall Peterson[4]
[1]CIRES/Climate Diagnostics Center, Boulder, Colorado
[2]US Department of the Interior
Grand Canyon Monitoring and Research Center, Flagstaff, AZ
[3]US Bureau Reclamation and CADSWES
University of Colorado, Boulder, Colorado
[4]US Bureau of Reclamation
Salt Lake City, Utah

The Glen Canyon Adaptive Management program is intended to preserve and restore resources of the Colorado River ecosystem downstream of Glen Canyon Dam, as mandated by the 1992 Grand Canyon Protection Act, and the preferred operating alternative adopted by the Secretary of Interior in the December 1996, Record of Decision. Adaptive management is a process of learning through experimentation. At present, the experiments consist of managed high releases from Glen Canyon Dam, agreed upon by stakeholders, for the purpose of habitat restoration. The presently adopted hydrologic triggers for these flows are contingent on year-to-year and season-to season climate variability, but are limited to high-flow periods within the upper basin runoff season (January through July). The 1997–1998 ENSO event, because of its similarity in magnitude to 1982–1983, has resulted in changes in dam operations at Glen Canyon for this spring with impacts on flood control, power operations, and the establishment of triggering criteria. These triggers are also related to antecedent conditions of storage in Lake Powell, and resource criteria related to long-term management objectives (ecosystem and water resources).

Many management objectives also have to be met over periods of a decade or longer, such as Colorado River Compact releases of 75 million acre-feet per ten-year period, and recruitment of long-lived (30 years) endangered fishes, such as humpback chub. Variability of downstream sediment supply on longer time scales will be discussed by Topping, Melis, and Pulwarty at this meeting.

This study is a preliminary analysis of (1) natural-streamflow variability within the Colorado River Basin during this century at 29 nodes used for operational decision support and (2) the relationship of this information to the adaptive management process at Glen Canyon and Grand Canyon. Emphasis will be placed on the four following runoff-related issues: (1) intrabasin spatial variations; (2) decadal-to-interannual scale variations; (3) shifts in seasonal runoff patterns during the January through July period, and (4) an assessment of historical basin hydrology with respect to the likelihood of meeting triggering criteria for past years.

ENSO Phase, Streamflow, and Precipitation Frequency and Persistence

Kelly Redmond[1], Dan Cayan[2], and Larry Riddle[3]

[1]Western Regional Climate Center
Desert Research Institute
Reno, Nevada

[2]Scripps Institution of Oceanography and US Geological Survey
La Jolla, California

[3]Scripps Institution of Oceanography

Previous studies have shown that frequency distributions of daily precipitation and streamflow vary according to ENSO phase, especially in the upper percentiles. Further, the streamflow signal pattern in the west is an accentuated version of the precipitation signal pattern. The sense of the relation is wet winters in the Southwest with El Niño, opposite in the Northwest, and the opposite pattern for La Niña. High streamflow is favored by heavier, more frequent, and more persistent precipitation. Point data show that where ENSO phase produces higher runoff, (1) there are more days with precipitation, (2) there is more precipitation per precipitation day ("rainy" day), and (3) the conditional probability of a wet day given a previous wet day (which is always higher than the unconditional probability of a wet day) increases even more. A moving window technique shows these effects are present from about October until late March or early April. Composites of daily pattern progressions show more zonal structures in the Southwest for El Niño cases and more highly amplified shorter wavelength patterns for La Niña.

Winter Freshening of the Northeastern Pacific Coastal Plume by Interseasonal Reservoir Division of the Columbia River

C.C. Ebbesmeyer[1] and W. Tangborn[2]

[1]Evans-Hamilton, Incorporated
731 N. Northlake Way
Seattle, Washington 98103

[2]HyMet, Incorporated
366 Eastlake Avenue
Seattle, Washington 98102

Numerous reservoirs in the Columbia River watershed divert large volumes of river discharge from summer to winter, thereby contributing a net freshwater addition to the coastal plume of brackish water flowing northward along the northeastern Pacific Ocean. This addition (~44 km^3 annually) accounts for a large portion of the long-term (1935–1993) decreasing trends of winter coastal sea surface salinities along a significant length of the North American coast.

Development of an Exceedance Probability Streamflow Forecast Using ENSO and Pacific SST Predictors

Thomas Piechota[1], John Dracup[1], Francis Chiew[2] and Thomas McMahon[2]

[1]University of California, Los Angeles
Civil and Environmental Engineering Department
5732 Boelter Hall
P.O. Box 951593
Los Angeles, California 90095-1593

[2]University of Melbourne
Cooperative Research Centre for Catchment Hydrology
Parkville, Victoria 3052, Australia

Recent research at the Australian Bureau of Meteorology Research Centre (BMRC) has focused on predicting seasonal rainfall from Pacific Ocean sea surface temperatures (SSTs). The work here is a seasonal streamflow forecast methodology that uses the SST series in conjunction with a El Niño Southern Oscillation (ENSO) indicator and the serial correlation of streamflow. These forecast take the form of a continuous probability of exceedance of streamflow at varying levels. The use of a continuous probability of exceedance forecast gives water authorities a wider range of options for using the forecast based on their assumed risk level. An objective measure of the skill of the forecast is the Linear Error in Probability Space (LEPS) score, which was originally developed for assessing the position of forecast and observed values in the cumulative probability distribution and can be used for continuous and categorical variables. An optimal linear combination of the four predictors is developed by minimizing the LEPS score of the overall forecast. This seasonal streamflow forecast model is tested on five stations in Eastern Australia for the time period 1950–1996. Preliminary results suggest that forecasting of austral winter and spring streamflow are best accomplished with the previous season streamflow (in other words, serial correlation of streamflow). However, summer and autumn streamflow are best predicted using a combination of the previous season streamflow with either the ENSO indicator or a SST series. The methodology presented here may have implications for seasonal and long-range streamflow forecasting in other Pacific Rim countries.

Medium-range Prediction of Snowmelt Streamflow Surges in the Merced River, Sierra Nevada, 1996–1998

Michael Dettinger[1], Daniel Cayan[1], David Peterson[2], and Henry Diaz[3]

[1]US Geological Survey, Scripps Institution of Oceanography, La Jolla, California 92093–0224

[2]US Geological Survey, MS 412, 345 Middlefield, Menlo Park, California 94025

[3]NOAA/ERL/Climate Diagnostics Center, 325 Broadway, Boulder, Colorado 80303

Streamflow in the upper Merced River, as in many rivers of western North America (West), is dominated by surges of runoff from melting snow. During most years, the largest surges in the Merced River are in springtime and are part of a regional-scale transition from low wintertime streamflow rates to high springtime rates in high-altitude rivers throughout the West. During some winter storms (for example, New Year's Day 1997), regional episodes of snowmelt also occur in response to storms that bring warm rains to the snowpacks. The snowmelt episodes measured by Merced River streamflow variations are reflected almost simultaneously by other rivers over a large part of the West and yield rapid increases in streamflow once they begin. Because current weather prediction models most reliably predict regional, rather than local, weather patterns in the near future, the springtime streamflow surges and at least some winter streamflow surges are well suited for prediction by using output from current weather prediction models as direct inputs to watershed-scale streamflow models.

Medium-range streamflow predictions for the Merced River above the Happy Isles Bridge in Yosemite National Park, with lead times from 3 to 14 days, have been developed by combining daily NOAA/National Center for Environmental Prediction accumulated precipitation and air temperature predictions (for a 60,000 km^2 grid point) with a spatially detailed Precipitation Runoff Modeling System watershed model of the 500 km^2 river basin. The combination yielded successful forecasts of the snowmelt surges during the springs of 1996 through 1998, with lead times of as much as nine days; hindcasts using simpler, linear regression streamflow models yielded a similar predictability during the 17 springs from 1979 to 1995. During the winter storms in 19997 and 1998, streamflow predictions faced different conditions (rain on snow in 1997 and consecutive snow storms in 1998). The winter streamflow forecasts were encouragingly accurate in 1997, but were less successful during the El Niño conditions in 1998. Overall, the success of these streamflow predictions is attributed to the large scale of weather conditions that dominate snowmelt in the West.

Landslides and This Year's Precipitation in the San Francisco Bay Area

Donald L. Gautier and Raymond C. Wilson
US Geological Survey
Menlo Park, California

In response to NOAA's predictions of an extraordinarily wet winter for the San Francisco Bay area in 1997–1998, the US Geological Survey (USGS) launched an effort to develop digital data and maps to characterize areas susceptible to landslides—both slow moving landslides involving bedrock and the more dangerous, fast-moving debris flows. A protocol was established among the National Weather Service, the USGS, and the California Office of Emergency Services to share information concerning possible earth movement disasters. A list of private consultants qualified to work on earth movement problems was developed in cooperation with the Association of Engineering Geologists and a request for research and monitoring assistance was sent to nearby colleges and universities.

The early NOAA forecasts have proven to be remarkably accurate in the San Francisco Bay area, with seasonal precipitation near record levels (>200% of normal). The high rainfall accumulation has triggered a number of large, deep, bedrock landslides, causing considerable property damage. The season also produced an usually severe storm during 2 and 3 February 1998 that triggered life-threatening debris flows in several widely spaced areas with very high rainfall intensities. One fatality occurred. The distribution of debris flows, compared with recorded rainfall levels, appears to conform to the predictions of a rainfall and debris-flow threshold map released early in the season.

The near absence of earth-movement insurance, and resulting commonplace litigation, indicates the need for further interaction between climate modelers and earth scientists to affect public policy concerning liability, zoning, or mitigation for earth-movement hazards in the bay area and elsewhere.

Poster Presentations

North Pacific Climatic Connections with the Upper Mississippi River Streamflow

Connely K. Baldwin and Upmanu Lall
Utah State University
Utah Water Research Laboratory and
Department of Civil and Environmental Engineering
UMC 8200
Logan, Utah 84322-8200

The role of the North Pacific atmospheric and oceanic system in modulating the impact of El Niño is studied. Spectral analysis techniques based on Fourier analysis are used to identify coherent variability between the time series of climatic indices and other hydroclimatic variables such as streamflow or precipitation. The climate indices used are the NINO3 sea surface temperature anomaly, the central North Pacific (CNP) sea level pressure index and the North Atlantic Oscillation (NAO). It is found that all three indices have similar coherence with the upper Mississippi River streamflow. A number of changes in the phase and amplitude of streamflow coincide with changes in the spectral signature of streamflow and its coherence with the climate indices. It is also found that the interaction between the CNP and NAO indices play an important role in determining the low frequency variability of streamflow.

Evidence for a Substantial Increase in Jellyfish in the Bering Sea with Possible Links to Climate Change

Richard D. Brodeur[1] and James E. Overland[2]
[1]Alaska Fisheries Science Center
Seattle, Washington 98115
[2]Pacific Marine Environmental Laboratory
7600 Sand Point Way NE
Seattle, Washington 98115

We examined quantitative catches of large medusae from summer bottom trawl surveys which sampled virtually the same grid station on the eastern Bering Sea shelf and used the same methodology every year from 1979 to 1997. This series shows a gradual increase in biomass of medusae from 1979 to 1989, followed by a dramatic increase in the 1990s. The median biomass increased ten times between the 1982–1989 and the 1990–1997 periods. The majority of this biomass was found within the Middle Shelf Domain, with a higher rate of increase in the Northwest shelf region. Several large-scale winter and spring atmospheric and oceanographic variables in the Bering Sea exhibited concomitant changes beginning around 1990, indicating that a possible regime change occurred at this time. The apparent increased production of medusa may be related to increased sea surface temperatures caused by changes in the atmospheric general circulation. The April-through-July mean value of first rotated EOF of the 700 mb geopotential height over the Bering Sea shows a shift to positive values occurring around 1989. Increased geopotential heights over the Bering Sea implies reduced cloud cover with increased solar radiation at the sea surface, thus corresponding to years with positive summer SST anomalies.

Northern Benguela Sea Surface Temperatures, 1981–1991

James Cole
NOAA/NMFS, Pacific Fisheries Environmental Group
1352 Lighthouse Avenue, Pacific Grove, California 93950–2097

Sea surface temperature (SST) is an emergent property of a system's oceanography. In eastern boundary upwelling systems, SSTs are largely determined by the play between the following: wind-driven upwelling of cold water; solar warming of the surface layers; wind-driven turbulence; coastally trapped waves; the inward advection of warmer water masses from the edges of the system (remotely forced or otherwise); and the way these factors interact with local bathymetry. The recent compilation of time series of pre-processed SST satellite image composites by organizations such as NASA and the JRC (European Commission Joint Research Centre) offers a way whereby the dynamics of these and other marine systems characterized by strong thermal gradients may be monitored across a wide range of different spatio-temporal scales. Possible applications range from assessing the impact of climate change on the physical dynamics of these systems to detailed investigations into how oceanic variability can influence the size and distribution of commercial fish stocks. In this instance, mean monthly SST images of the northern benguela upwelling system from 1981 to 1991 were extracted from the Cloud and Ocean Remote Sensing around Africa (CORSA) data set held at the JRC and presented as a mosaic. Clearly identifiable are seasonal fluctuations in upwelling activity; the 1984 and 1988 'Benguela Niños,' as characterized by the strong southward advection of warm tropical Angolan water and reduced cold water upwelling during the austral summers of 1984 and 1988; and an impressive amount of detail on the mesoscale structure of the system, indicating that structures associated with upwelling activity, such as eddies and filaments, can be spatially coherent over time spans as long as a month.

Sierra Nevada Tree Rings and Storms

Gregg M. Garfin
University of Arizona
Laboratory of Tree Ring Research
Tucson, Arizona 85721

Southcentral Sierra Nevada extreme tree growth anomalies and their relationships to preferred storm tracks and storm characteristics are examined using positive vorticity advection (PVA) count, temperature, and precipitation data for the period 1947–1987. Twenty tree ring chronologies are reduced to two weighted average chronologies: one based on giant sequoia (*Sequoiadendron giganteum*) from ~2,000 m and one based on pine (*Pinus balfouriana*, *Pinus albicaulis*) from ~3,500 m. Composites of storm characteristics for November through March and storm tracks (based on PVA counts) for December through February are created for the highest and lowest deciles and quintiles of tree growth. Results show that both chronologies display extremely high growth when winter storms are of long duration, interstorm periods are warmer than average, and storm tracks are south of the mean north Pacific track. Low growth years for both chronologies are associated with more frequent short duration storms, few or no long duration storms, and a paucity of storm activity in the eastern Pacific between 20–40°N. Interestingly, during sequoia low-growth years, both storms and interstorms are warmer than average and storms tend to be deflected from the western North American coast toward the Alaskan Peninsula, whereas during pine low-growth winters, storms and interstorms are cooler than average and storm activity is enhanced along the mean storm track. These results show great promise for reconstruction of precipitation-relevant physical features, for example, preferred storm track, using the contrast in response between chronologies. They also indicate the value of using climate parameters collected on daily time scales, but tabulated monthly or seasonally, for future dendroclimatological reconstructions.

Cold-season Severe Sustained Droughts in the Western United States: The Role of Atmospheric Circulation

Henry H. Gu And John A. Dracup
University of California, Los Angeles
Department of Civil and Environmental Engineering
Los Angeles, California 90095–1593

The cold-season severe sustained drought (CSSD) events in a defined drought region in the western US have been identified by an objective procedure. The roles of the underlying dominant atmospheric dynamic factors have been investigated via anomaly and similarity pattern analyses. Potential for CSSD forecast is explored by assessing the lag similarity structures between precipitation and atmospheric pressure and temperature several months in advance. A CSSD mechanism is suggested in the framework of quasi-geostrophic dynamics. The analyses show that a CSSD is dominated by the local atmospheric anticyclonic thermodynamics and by (the abnormal changes in) the large-scale atmospheric circulation. The influence of pressure tends to be simultaneous, while that of surface temperature could spread into a longer period of time. In contrast to a multiyear flood, which is often associated with a solitary cyclone, a CSSD is always associated with a well-developed westward-tilted trough-ridge-trough train, with the ridge over the drought region, one trough in the upstream, northern Pacific-Aleutian area and one trough in the downstream, eastern Canada–Northern Atlantic region. Through differential advection, the upper tropospheric troughs (ridge) are intensified by the underneath cold (warm) advection. In the drought area, the warm advection also helps warm the upper atmosphere and suppress the growth of cumulus clouds due to the atmospheric static stability. This leads to more incoming short wave solar radiation and a warmer atmosphere. Through such a positive feedback mechanism, the drought situation can sustain for several years.

Application of Climatic Analyses for Historical and Future Simulations of Groundwater and Surface Water Flow in the Santa Clara–Calleguas Basin, Ventura County, California

R.T. Hanson
US Geological Survey, San Diego, California

Increased development of the surface water and groundwater resources in the coastal Santa Clara–Calleguas basin since the late 1800s has resulted in streamflow depletion and groundwater overdraft that, in turn, has resulted in sea water intrusion, changes in interaquifer flow, land subsidence, and groundwater contamination. A method was developed to incorporate climatic variation and to improve the historical calibration and future projection of ground water and surface water and provide a seamless transition between historical and future conditions simulated by the model. The resulting regional simulation model provides a better management tool to analyze the major problems affecting water resources management of a typical coastal watershed.

Climatically-based analyses and estimates with geostatistics, spectral analyses, and nonlinear regression were used to develop the driving-force inputs for a regional groundwater and surface water flow model of the Santa Clara–Calleguas basin. Since the 1890s there have been twelve, alternating, multiple-year wet and dry periods associated with precipitation variations characterized by periods of 2.2 to 2.9 years and 5.3 to about 22 years. These twelve periods form the basis for estimation of supply and demand components. Growing demands on the conjunctive use of groundwater and surface water must be considered within the context of these variations in supply. That interplay has (1) controlled the quantity and distribution of streamflow and recharge over the past several hundred years, (2) driven agricultural water demand, and (3) required the development of large-scale water supply projects. The shared climatic forcings of water use and recharge supply have resulted in a majority of the recharge and streamflow diversion occurring during wet periods. During dry periods

increased pumpage and reduced recharge cause water-level declines, sea water intrusion, and land subsidence.

In addition to the climatic segregations used for historical simulations, spectral estimates of precipitation were used as a basis for estimation of streamflow and recharge for future projection simulations. Since the future estimates were based upon an autoregressive model of spectral estimates, they provide a smooth transition in rates and magnitude from historical to future precipitation. For the first seven years of future projection, this method provides strong correlation with the historical data that results in a seamless transition from historical to future simulation conditions.

No El Niño, But Variable Precessional Insolation, Antiphase Inter-hemispheric Climate Trends, and Globally Synchronous Secondary Cycles

Thor Karlstrom
US Geological Survey
4811 SW Brace Point Drive
Seattle, Washington 98136

Additional time series, analyzed since the publication of my last paper (Karlstrom 1997), continue to support the Solar Insolation/Tidal Resonance Climate Model by recording latitudinal variability for longer-term climate trends, but globally-synchronous, shorter-term trends.

The Timing of Peak Spring Runoff from Yosemite National Park

John Keyantash and John A. Dracup
University of California, Los Angeles
Department of Civil and Environmental Engineering
Los Angeles, California 90095–1593

Streamflow records for the Merced River were analyzed to determine whether the peak spring runoff from Sierra Nevada snowpack is occurring earlier in the year due to global warming or other factors. The portion of the Merced River within Yosemite National Park was chosen because it is an unimpaired stream there, free from upstream diversions or regulations. Streamflow data, including daily mean and annual instantaneous peak flows, were analyzed to determine the timing of peak spring runoff for water.

The daily mean data set was segregated into twenty-year intervals, which were tested for trends using two nonparametric techniques, the Wilcoxon rank-sum test and the Kruskal-Wallis test. Both approaches returned identical results (at the 95 percent confidence level): the timing of the peak vernal daily mean runoff on the Merced River has not exhibited a discernible trend over the last eighty years.

Modeling the Influence of 1998 Winter Inflows on San Francisco Bay Salinities

Noah Knowles
Scripps Institution of Oceanography, Climate Research Division
La Jolla, California 92093–0224

The effect of variability of managed inflows on water quality in San Francisco Bay has long been a central issue of California water resources. Here, preliminary estimates of Sacramento–San Joaquin Delta outflow for water year 1998 are used to drive an intertidal model of bay-wide water quality. Delta outflow for water year 1998 was characterized by a broad peak, beginning in late January with sustained flows of 6,000-9,000 cubic meters per second

throughout February. Modeled salinity quickly dropped to ~5 psu during this period throughout the northern reach to Angel Island. Outflow subsided considerably in May, though the strong February freshwater signal continued to propagate into south bay. A short-lived resurgence reaching nearly 5,000 cm in late May and early April has kept northern reach salinities near ~5 psu through at least mid-April. The extended duration of the freshening appears to be the most unique aspect of the bay's behavior in water year 1998 when compared to recent years.

Monitoring the Impact of ENSO Events on New Production in Monterey Bay, California

Raphael Kudela
Monterey Bay Aquarium Research Institute
Moss Landing, California

New primary production is estimated using a physiologically-driven model of phytoplankton utilization of nitrate (analogous to new production) for the Monterey Bay, California, region. Primary inputs for the model come from time-series measurements of temperature and biomass (chlorophyll) data available from three moorings, which allows us to model new production for the mixed layer on a daily basis. The model successfully reproduces the seasonal pattern of nitrate utilization determined from shipboard experiments using traditional stable-isotope techniques. It is used to explore the effects of the 1992 El Niño event for this region and to track the development of the 1997–1998 event. During the 1992 ENSO event, significant anomalies in the central California region for both temperature and salinity were observed, including elevated sea surface temperatures, a deepening of the thermocline, and a severe decrease in surface nutrient concentrations in the Monterey Bay region. Despite the significant physical changes caused by the 1992 ENSO event, rates of primary productivity demonstrated only a minor decrease at the beginning of the year, with no statistically significant difference between the annual rates for 1992 and the non-ENSO period from 1989–1991.

Our model demonstrates a substantial decrease (about four times less) in new production during 1992. During this same period, new production was greatly reduced (more than four times) further away from shore and presumably downstream from the moorings during the spring upwelling season. We expect that the 1997–1998 event will have an even greater impact on new and primary productivity in Monterey Bay. Using the time-series data and our physiological model, we will document the ongoing effects of the 1997–1998 ENSO event in Monterey Bay and contrast this event with the historical data for 1992.

Decadal Variability in the Strength of ENSO Teleconnections with Precipitation in the Western United States

Gregory J. McCabe[1] And Michael D. Dettinger[2]
[1]US Geological Survey
Denver Federal Center, MS 412
Denver, Colorado 80225
[2]US Geological Survey and
Scripps Institution of Oceanography, Climate Research Division
La Jolla, California 92093-0224

Changing patterns of correlations between historical average June-through-November Southern Oscillation Index (SOI) values and October-through-March precipitation totals for 84 climate divisions in the western United States (US) indicate a large amount of variability in SOI/precipitation relations on decadal time scales. Correlations of western US precipitation with SOI and other indices of tropical El Niño Southern Oscillation (ENSO) processes were much weaker from 1920 to 1950 than during recent decades. This variability in teleconnections is

associated with the character of tropical air-sea interactions as indexed by number of out-of-phase SOI/tropical sea-surface temperature episodes, and with decadal variability in the North Pacific Ocean as indexed by the Pacific Decadal Oscillation (PDO). ENSO teleconnections with precipitation in the western US are strong when SOI and NINO3 are out of phase and PDO is negative. ENSO teleconnections are weak when SOI and NINO3 are in phase and PDO is positive. Decadal modes of tropical and North Pacific Ocean climate variability are important indicators of periods when ENSO indices, like SOI, can be used as reliable predictors of winter precipitation in the US.

El Niño Forcing of Higher-than-Normal Sea Level in San Francisco Bay

Holly Ryan, Marlene Noble, and Dave Peterson
US Geological Survey, Menlo Park, California 94025

The effects of El Niño on the coastal ocean have resulted in the remote and local forcing of sea level in San Francisco Bay. The remote forcing can be related to the passage of Kelvin waves that were generated near the equator in response to El Niño conditions, and then propagated to the north along the west coast of North America as coastally-trapped waves. Spectral analyses of a 100–year record of subtidal sea level records from San Francisco Bay show a broad-band energy peak at a 40-70 day period, consistent with that expected for coastally-trapped waves. During time periods of strong El Niño conditions such as during the 1982–1983 El Niño, the 40– to 70–day peak can be the dominant subtidal period. This past year, multiple coastally-trapped waves with an associated positive temperature signal were observed along the coast of central California starting in May, 1997 or perhaps earlier. The passage of these waves can result in a rise of sea level of up to 20 cm and a several degree Celsius increase in sea surface temperature near the coast. In addition, local forcing of subtidal sea level fluctuations can be related, in part, to wind stresses that during the 1997–1998 El Niño were oriented more to the north-northwest than normal. The northwestward winds caused sea level at the coast to rise, hence also the water level in San Francisco Bay.

Teleconnections and California Precipitation Prediction by Artificial Neural Networks

David Silverman and John A. Dracup
University of California, Los Angeles
Department of Civil and Environmental Engineering

Teleconnections are recurring and persistent large-scale pressure patterns and circulation anomalies that span large geographical areas. Artificial neural networks (ANNs) are especially useful for classification and function approximation and mapping problems and are tolerant of some imprecision, but which hard and fast rules cannot easily be applied. This study uses ANNs to map a year's (January through December) time series of the Northern Hemisphere teleconnection indices onto the water year (October through September) total precipitation of California's seven climatic zones with different lag times between the inputs and outputs. It was found that with a year lag (in other words, using teleconnection indices January through December of year n to predict the precipitation water year October of year $n - 1$ through September year $n + 2$) good predictability is possible for most years and climate zones.

Appendix A
Agenda

Fifteenth Annual Pacific Climate (PACLIM) Workshop
Wrigley Institute for Environmental Studies (WIES)
Two Harbors, Santa Catalina Island, California
April 27–30, 1998

PACLIM is a multidisciplinary workshop that broadly focuses on climate phenomena occurring in the eastern Pacific and western Americas. Its purpose is to understand the climate effects in this region by bringing together specialists from diverse fields including both physical and biological sciences. Time scales range from weather to paleoclimate.

Our theme sessions, convened throughout the day on Tuesday April 28, 1998, deal with this year's El Niño. The large scale and magnitude of this climate event ensured that its influence would be widespread and potentially important to many natural and social systems. Thus, our theme session is intended to report on the initial assessments of its impacts and significance.

This year, we are meeting for the second time at the Wrigley Institute for Environmental Studies Conference Center on Santa Catalina Island. The atmosphere of the Workshop is intentionally informal and room and board are provided for the participants. The Workshop is organized by a committee of representatives from several organizations, but historically it has been spearheaded by US Geological Survey scientists. Held annually, the Workshop has benefited from funding and other forms of support from several agencies, public and private (see Sponsors, page 1).

Agenda

Fifteenth Annual Pacific Climate (PACLIM) Workshop
Wrigley Institute for Environmental Studies (WIES)
Two Harbors, Santa Catalina Island, California
April 27–30, 1998

WIES Meal Schedule

Breakfast	7:30–8:30 AM
Lunch	12:00–1:00 PM
Dinner	6:00–7:00 PM

Monday Evening — April 27, 1998

Introductory Session

Moderator:	Janice Tomson, Long Beach City College
7:00–7:10 PM	Welcome and Announcements
7:10–7:30 PM	*An Overview of Western Climate Since PACLIM 1997* Kelly T. Redmond WRCC, Desert Research Institute, Reno, Nevada
7:30–7:50 PM	*How Does 1998 Floods and Water Supply Compare with 1997 and 1983?* Maurice Roos California Department of Water Resources, Sacramento, California
7:50–8:10 PM	*ENSO 1997–1998: Forecasts, Impacts, and Lesson* Liqiang Sun International Research Institute Scripps Institution of Oceanography, La Jolla, California
8:10 PM	Social Gathering

Tuesday Morning | **April 28, 1998**

1997–1998: El Niño of the Century?

Moderator: Dan Cayan, Scripps Institution of Oceanography and US Geological Survey

8:30–9:00 AM *Large-scale Weather Regimes and Local Climate Over the Western US*
Tom Murphree, Frank Schwing, and Huug Van Den
Naval Postgraduate School, Department of Meteorology
Monterey, California

9:00–9:30 AM *Forecasting the Atmospheric Response to the 1997–1998 ENSO*
Kingste Mo, M. Kanamitsu, and X.L. Wang
NCEP/NWS/NOAA, Climate Prediction Center, Washington D.C.

9:30–10:00 AM *Measuring the Strength of ENSO Events—How Does 1997–1998 Rank?*
Klaus Wolter
OAA-CIRES-CDC, University of Colorado, Boulder, Colorado

10:00–10:15 AM Break

10:15–10:35 AM *Toward Regional Downscaling of 1997–1998 El Niño GCM Predictions*
Andrew W. Robertson
University of California, Los Angeles
Department of Atmospheric Sciences
Los Angeles, California

10:35–10:55 AM *Biological–Physical Coupling in the Central Equatorial Pacific During the Onset of the 1997–98 El Niño*
Peter G. Strutton, F.P. Chavez, and M.J. McPhaden
Monterey Bay Aquarium Research Institute
Moss Landing, California

10:55–11:15 AM *Regional Transport Covariability in the California and Alaska Currents During the Onset of the 1997–1998 El Niño*
P. Ted Strub and Corinne James
Oregon State University
College of Oceanic and Atmospheric Sciences
Corvallis, Oregon

11:15–11:35 AM *El Niño 1997: Simultaneous Extrema in Gulf of Alaska Oceanography and Salmon Biology*
Skip McKinnell
Ocean Sciences Division, Pacific Biological Station
Nanaimo, British Columbia

Tuesday Morning, continued	**April 28, 1998**
11:35–11:55 AM	*The Impact of the 1997-1998 El Niño on World Grain Yields* Ray Garnett Canadian Grain Commission, Manitoba, Canada
12:00–1:30 PM	Lunch

Tuesday Afternoon	**April 28, 1998**
	1997–1998: El Niño of the Century?
Moderator:	Mike Dettinger, US Geological Survey, San Diego, California
1:30–2:00 PM	*El Niño, La Niña, and Flood Frequency in Arizona and Adjacent Regions* Robert H. Webb US Geological Survey, Tucson, Arizona
2:30–3:00 PM	*Nonstationarity in ENSO and Its Teleconnections: An Exploratory Analysis and a Nonlinear Dynamics Perspective* Upmanu Lall, B. Rajagopalan, and Mark Cane Utah State University, Utah Water Research Laboratory Logan, Utah
3:00–3:30 PM	*1997-1998: El Niño of the Past Three Centuries?* Michael E. Mann, R.S. Bradley, and M.K. Hughes University of Massachusetts, Department of Geosciences Amherst, Massachusetts
3:30–4:00 PM	Poster Introductions
4:00–4:15 PM	Break
4:15–5:30 PM	Posters
5:30–7:00 PM	Dinner

Tuesday Evening	**April 28, 1998**
	1997–1998: El Niño of the Century?
7:30–8:15 PM	*What to Expect from an Extreme La Niña—The Opposite of the Effect from an Extreme El Niño?* Marty Hoerling NOAA-CIRES-CDC, University of Colorado, Boulder Boulder, Colorado

Wednesday Morning | **April 29, 1998**

General Sessions

Moderator #1: Curt Ebbesmeyer, Evans-Hamilton, Inc., Seattle, Washington

8:30–8:50 AM
Watching Warm Events on Their Global Walkabout
Gary D. Sharp
Center for Climate–Ocean Resources Study, Monterey, California

8:50–9:10 AM
Interaction Between ENSO and the North Pacific Oscillation: Implications for Long-Range Predictability of Intraseasonal Hydrologic Extremes in the Western US
Alexander Gershunov, T. Barnett, D. Cayan, and L. Riddle
Scripps Institution of Oceanography, Climate Research Division
La Jolla, California

9:10–9:30 AM
Interpreting the Observed Patterns of Pacific Ocean Decadal Variations
Art Miller
Scripps Institution of Oceanography, Climate Research Division
La Jolla, California

9:30–9:50 AM
Ocean-wide Winter Drift Trajectories in the North Pacific Ocean Computed with the OSCURS Model Show Decadal and El Niño Patterns 1901–1998
W. James Ingraham, Jr. and C.C. Ebbesmeyer
Alaska Fisheries Science Center-NMFS-NOAA
Seattle, Washington

9:50–10:10 AM
A Comparison of Ship Winds with NSCAT Scatterometer Measurements in the Western Equatorial Pacific Warm Pool During January–February 1997
Kyozo Ueyoshi
Japan Marine Science and Technical Center
Ocean Research Division
Yokosuka, Japan

10:10–10:30 AM Break

Moderator #2: Malcolm Hughes, University of Arizona, Laboratory of Tree Ring Research

10:30–10:50 AM
Decadal Patterns in a Sandy Subtidal Community: Effects of Decreased Oceanic Productivity
Stacy Kim, J.S. Oliver, and P.N. Slattery
Moss Landing Marine Laboratories, Moss Landing, California

Wednesday Morning, continued **April 29, 1998**

10:50–11:10 AM *Climatic Inferences from a 1200–year Tree–ring Reconstruction of Sacramento River Flow*
David M. Meko, C.H. Basin, and M.K. Hughes
University of Arizona, Laboratory of Tree Ring Research
Tucson, Arizona

11:10–11:30 AM *Evidence for ENSO in Tree-Ring $\delta^{13}C$ Along a 500-KM E-W Transect in Southern Arizona and New Mexico*
Steven Leavitt, W.E. Wright, and A. Long
University of Arizona, Laboratory of Tree Ring Research
Tucson, Arizona

11:30–11:50 AM *ENSO Teleconnections: Eastern Pacific Sea Surface Correlations with $\delta^{18}O$ in Southeastern Arizona Precipitation and Tree Cellulose*
William E. Wright, S.W. Leavitt, and A. Long
University of Arizona, Laboratory of Tree Ring Research
Tucson, Arizona

12:00–1:30 PM Lunch

Wednesday Afternoon **April 29, 1998**

General Sessions

Moderator: Caroline Isaacs, US Geological Survey, Menlo Park, California

1:30–1:50 PM *The Late 1500 Severe Sustained Drought in the Colorado River Basin: Is It Real?*
John Dracup, H. Hidalgo, G. MacDonald, and T. Piechota
University of California, Los Angeles
Department of Civil and Environmental Engineering
Los Angeles, California

1:50–2:10 PM *Glacial to Interglacial Contrasts in Organic Matter Production and Preservation on the California Continental Margin*
Walter H. Dean and J.V. Gardner
US Geological Survey, Federal Center, Denver, Colorado

2:10–2:30 PM *Simulation of Climate and Runoff for the Bonneville Basin at the Last Glacial Maximum*
Susanne M. Clement, M.M. Timofeyeva, and R.C. Craig
Kent State University, Department of Geology, Kent, Ohio

Wednesday Afternoon, continued	**April 29, 1998**
2:30–2:50 PM	*A Revised Hypothesis for Evolution and Biogeography of Monterey Pine (Pinus radiata) Inferred from Fluctuating Quaternary Climates* Constance I. Millar US Department of Agriculture, Forest Service PSW Research Station, Albany, California
2:50–3:10 PM	*Last 2000 Years of Lake-level Variability at Pyramid Lake, Nevada* Steve Lund, Larry Benson, and Joe Snoot University of Southern California, Los Angeles, California
3:10–5:30 PM	Free Time
5:30–7:00 PM	Dinner

Wednesday Evening	**April 29, 1998**
	General Sessions
7:30–8:15 PM	*River Management and Climate Variability (The Grand Canyon Flood Experiment)* R. Webb and T. Melis US Geological Survey, Tucson, Arizona

Thursday Morning	**April 30, 1998**
	General Sessions
Moderator:	Ray Wilson, US Geological Survey, Menlo Park, California
8:30–8:50 AM	*ENSO and the Glen Canyon Dam Adaptive Management Program: Eastern North Pacific Forcing of Paria River Floods in 1997* David J. Topping, T. Melis, and R.S. Pulwarty US Geological Survey, Lakewood, Colorado
8:50–9:10 AM	*Time Scales of Variability in the Colorado River Basin: Implications for the Glen Canyon Adaptive Management Program* Roger Pulwarty, T.S. Melis, T.S. Fulp, and R. Peterson US Department of the Interior Grand Canyon Monitoring and Research Center Flagstaff, Arizona
9:10–9:30 AM	*ENSO Phase, Streamflow, and Precipitation Frequency and Persistence* Kelly Redmond, D. Cayan, and L. Riddle WRCC, Desert Research Institute, Reno, Nevada

Thursday Morning, continued	**April 30, 1998**
9:30–9:50 AM	*Winter Freshening of the Northeastern Pacific Coastal Plume by Interseasonal Reservoir Division of the Columbia River* C.C. Ebbesmeyer and W. Tangborn Evans-Hamilton, Inc., Seattle, Washington
9:50–10:10 AM	*The Spring Runoff Pulse from the Sierra Nevada: A Regional Transition* Dan Cayan Scripps Institution of Oceanography, La Jolla, California
10:10–10:30 AM	Break
10:30–10:50 AM	*Development of an Exceedence Probability Streamflow Forecast Using ENSO and Pacific SST Predictors* Tom Piechota, J. Dracup, F. Chiew, and T. McMahon University of California, Los Angeles Department of Civil and Environmental Engineering Los Angeles, California
10:50–11:10 AM	*Medium-range Prediction of Snowmelt Streamflow Surges in the Merced River, Sierra Nevada, 1996–1998* Michael Dettinger, D. Cayan, D. Peterson, and H. Diaz US Geological Survey, San Diego, California
11:10–11:35 AM	*Landslides and This Year's Precipitation in the San Francisco Bay Area* Donald Gautier and R.C. Wilson US Geological Survey, Menlo Park, California
11:35–11:50 AM	Leave-taking and Plans
12:00–1:30 PM	Lunch

Appendix B
Poster Presentations

Fifteenth Annual Pacific Climate (PACLIM) Workshop
Wrigley Institute for Environmental Studies (WIES)
Two Harbors, Santa Catalina Island, California
April 27–30, 1998

North Pacific Climatic Connections with the Upper Mississippi River Streamflow

C.K. Baldwin and U. Lall
Utah State University
Utah Water Resources Laboratory and
Department of Civil and Environmental Engineering

Evidence for a Substantial Increase in Jellyfish in the Bering Sea with Possible Links to Climate Change

R.D. Brodeau and J.E. Overland
Alaska Fisheries Science Center
Seattle, Washington

Northern Benguela Sea Surface Temperatures 1981–1991

James Cole
NOAA–NMFS, Pacific Fisheries Environmental Group
Pacific Grove, California

Sierra Nevada Tree Rings and Storms

G.M. Garfin
University of Arizona
Laboratory of Tree Ring Research
Tucson, Arizona

Cold Season Severe Sustained Droughts in the Western United States: The Role of Atmospheric Circulation

H.H. Gu and J.A. Dracup
University of California, Los Angeles
Department of Civil and Environmental Engineering
Los Angeles, California

Application of Climatic Analyses for Historical and Future Simulations of Groundwater and Surface Water Flow in the Santa Clara–Calleguas Basin, Ventura County, California

R.T. Hanson
US Geological Survey
San Diego, California

Variable Latitudinal Precessional Controls and Out-of-Phase Hemispheric Climates

T. Karlstrom
US Geological Survey
Seattle, Washington

The Timing of Peak Spring Runoff from Yosemite National Park

J. Keyantash and J.A. Dracup
University of California, Los Angeles
Department of Civil and Environmental Engineering
Los Angeles, California

Modeling the Influence of 1998 Winter Inflows on San Francisco Bay Salinities

Noah Knowles
Scripps Institution of Oceanography, Climate Research Division

Monitoring the Impact of ENSO Events on New Production in Monterey Bay, California

Raphael Kudela
Monterey Bay Aquarium Research Institute
Moss Landing, California

Decadal Variability in the Strength of ENSO Teleconnections with Precipitation in the Western US

G.J. McCabe and M.D. Dettinger
US Geological Survey
Denver, Colorado

El Niño Forcing of Higher-than-Normal Sea Level in San Francisco Bay

H. Ryan, M. Noble, and D. Peterson
US Geological Survey
Menlo Park, California

Teleconnections and California Precipitation Prediction by Artificial Neural Networks

D. Silverman and J.A. Dracup
University of California, Los Angeles
Department of Civil and Environmental Engineering
Los Angeles, California

Appendix C
Attendees

Fifteenth Annual Pacific Climate (PACLIM) Workshop
Wrigley Institute for Environmental Studies (WIES)
Two Harbors, Santa Catalina Island, California
April 27–30, 1998

Roger Anderson
University of New Mexico
Earth and Planetary Sciences
Albuquerque, NM 87161
(P) 505 277 1639
(F) 505 277 8843
ryand@unm.edu

Wolf Berger
Scripps Institution of Oceanography
9500 Gilman Drive
La Jolla, CA 92093–0215
(P) 619 534 2826
(F) 619 453 0167
wberger@ucsd.edu

Greg Bohr
San Diego State University
Geography
5840 Lindo Paseo #20
San Diego, CA 92115
(P) 619 583 8544
bohr@orhan.sdsu.edu

J. Platt Bradbury
US Geological Survey
Federal Center
P.O. Box 25046, MS 980
Denver, CO 80225
(P) 303 236 5666
(F) 303 236 5349
jbradbur@usgs.gov

Annette Casey
Ocean Research Institute
650 Loring Street
San Diego, CA 92109
(P) 619 483 6507

Richard Casey
Ocean Research Institute
650 Loring Street
San Diego, CA 92109
(P) 619 483 6507

Dan Cayan
Scripps Institution of Oceanography
Climate Research Division 0224
9500 Gilman Drive
La Jolla, CA 92093–0224
(P) 619 534 4507
(F) 619 534 8561
dcayan@ucsd.edu

Kenneth Cole
US Geological Survey
University of Minnesota
Forest Resources
St. Paul, MN 55108
(P) 612 624 4296
(F) 612 625 5212
kcole@forestry.umn.edu

Arlene Collins
University of Alberta
Dept. of Earth and Atmospheric Science
Edmonton, Alberta, Canada T6G2E3
(P) 403 492 1120
(F) 403 492 2030
acollins@aofc.forestry.ca

Loren Davis
University of Alberta
Anthropology, 13–15 Tory
Edmonton, Alberta, Canada T6G2H4
(P) 403 492 1120
(F) 403 492 5273
lgdavis@gpu.srv.ualberta.ca

Diane DeRobertis
University of California, Berkeley
Geography
2100 Channing Way #414
Berkeley, CA 94704
(P) 510 664 0792
dianamd@violet.berkeley.edu

Kathleen Dorsey
Kinnetic Laboratories
307 Washington Street
Santa Cruz, CA 95060
(P) 408 457 3950
(F) 408 426 0405
kinnetic@cruzio.com

John Dracup
University of California, Los Angeles
Atmospheric Sciences
5732 Boelter Hall
Los Angeles, CA 90095-1595
(P) 310 825 2176
(F) 310 206 7245
dracup@seas.ucla.edu

Richard Forester
US Geological Survey MS980 DFC
Denver, CO 80225
(P) 303 236 5656
(F) 303 236 5349
forster@usgs.gov

Sheri Fritz
Leheigh University
31 Williams Drive
Bethlehem, PA 18015
(P) 610 758 6580
(F) 610 758 3677
scfa@lehigh.edu

Gregg Garfin
University of Arizona
Laboratory of Tree Ring Research
Building 58, Room 105 D2
Tucson, AZ 85721
(P) 520 626 3142
(F) 520 621 8229
g@ltrr.arizona.edu

David Greenland
University of Oregon
Geography
Eugene, OR 97403-5351
(P) 541 346 4561
(F) 541 346 2067
greenland@oregon.uoregon.edu

Laurie Grigg
University of Oregon
Geography
Eugene, OR 97403
(P) 541 346 2698
(F) 541 346 2067
lgrigg@darkwing.uoregon.edu

Henry Gu
University of California, Los Angeles
Civil and Environmental Engineering
3066 Engineer I
Los Angeles, CA 90095-1593
(P) 310 206 8612
(F) 310 206 7245
henryg@seas.ucla.edu

Felipe Gutierrez
University of California, Los Angeles
3181 Sepulveda Boulevard 107
Los Angeles, CA 90034
(P) 310 398 1672
(F) 310 398 1672
fgutierr@ucla.edu

Steven R. Hare
International Pacific Halibut Commission
P.O. Box 95009
Seattle, WA 98145
(P) 206 634 1838 ext. 230
(F) 206 632 2983
hare@iphc.washington.edu

Hugo Hidalgo
62248 Metz Street
Long Beach, CA 90808
(P) 310 425 1331
hhidalgo@ucla.edud

Wayne Higgins
Climate Prediction Center
NCEP/NWS/NOAA
5200 Auth Road, Room 605
Camp Springs, MD 20746
(P) 301 763 8227 ext. 7547
(F) 301 763 8395

Steven Hodge
US Geological Survey
University of Puget Sound
Tacoma, WA 98416
(P) 206 593 6516
(F) 206 383 7967
smhoge@usgs.gov

Martin Hoerling
University of Colorado, Boulder
CIRES
Campus Box 449
Boulder, CO 80309
(P) 303 492 1114
(F) 303 497 7013
mph@cdc.noaa.gov

Malcolm Hughes
University of Arizona
Laboratory of Tree Ring Research
Tucson, AZ 85721
(P) 520 621 6670
(F) 520 621 8229
mhughes@ltrr.arizona.edu

B. Lynn Ingram
University of California, Berkeley
Department of Geography
Berkeley, CA 94720
(P) 510 643 1473
(F) 510 642 3370
ingram@socrates.berkeley.edu

W. James Ingraham, Jr.
NOAA–NMFS–Alaska Fisheries Science Center
7600 Sand Point Way, NE
BIN C15700
Seattle, WA 98115–0070
(P) 206 526 4241
(F) 206 526 6723
jingram@afsc.noaa.gov

Brenda Johnson
University of California, Davis
DES
Center for Ecological Health Research
Davis, CA 95616
(P) 916 756 7069
(F) 916 752 3350
bjohnson@mother.com

Thor and Carol Karlstrom
4811 SW Brace Point Drive
Seattle, WA 98136
(P) 206 935 7087

Charles D. Keeling
Scripps Institution of Oceanography
0220
La Jolla, CA 92093–0220
(P) 619 534 4230
(F) 619 534 8814
cdkeeling@ucsd.edu

Eileen Kincaid
University of South Carolina
Department of Geological Sciences
Columbia, SC 29208
(P) 803 777 4526
(F) 803 777 6610
kincaid@geol.sc.edu

Teh-Liang Ku
University of Southern California
Department of Earth Sciences
Los Angeles, CA 90089–0740
(P) 213 740 5826
(F) 213 740 8801
rku@earth.usc.edu

Carina Lange
Scripps Institution of Oceanography
9500 Gilman Drive
La Jolla, CA 92093–0215
(P) 619 534 4605
(F) 619 534 0784
clange@ucsd.edu

Steven Leavitt
University of Arizona
Laboratory of Tree Ring Research
105 West Stadium
Tucson, AZ 85721
(P) 520 621 6468
(F) 520 621 8229
sleavitt@ltrr.arizona.edu

Peggy Lehman
California Department of Water Resources
3251 S Street
Sacramento, CA 95816
(P) 916 227 7551
(F) 916 227 7554
plehman@water.ca.gov

Hong-Chun Li
University of Southern California
Earth Sciences
Los Angeles, CA 90089–0740
(P) 213 740 6736
(F) 213 740 8801
hli@earth.usc.edu

Mark Losleben
University of Colorado
Mountain Research Station
838 County Road 116
Nederland, CO 80466
(P) 303 492 8841
(F) 303 492 8841
markl@culter.colorado.edu

Nathan Mantua
University of Washington
JISAO
P.O. Box 354235
Seattle, WA 98195–4235
(P) 206 616 5347
(F) 206 616 5775
mantua@atmos.washington.edu

Vera Markgraf
INSTAAR
University of Colorado
Boulder, CO 80309–0450
(P) 803 492 5157
(F) 303 492 6388
markgraf@spot.colorado.edu

Kirsten Menking
University of New Mexico
Earth and Planetary Sciences
Northrup Hall
Albuquerque, NM 87151
(P) 505 277 1639
(F) 505 277 8843
menking@unm.edu

Art Miller
Scripps Institution of Oceanography
0224
University of California, San Diego
La Jolla, CA 92093–0224
(P) 619 534 8033
(F) 619 534 8561
ajmiller@ucsd.edu

Monika Olsen
1216 Babel
Concord, CA 94518
(P) 510 676 2228

Grigory Monterey
JIMAR
University of Hawaii

Tom Piechota
University of California, Los Angeles
Civil and Environmental Engineering
3066 Engineering I
Los Angeles, CA 90095–1593
(P) 310 206 8612
(F) 310 206 7245
piechota@seas.ucla.edu

Anthony Rathburn
Scripps Institution of Oceanography
MLRG–0218
9500 Gilman Drive
La Jolla, CA 92093–0218
(P) 619 534 18864
(F) 619 534 6500
rathburn@coast.ucsd.edu

Andrew Robertson
University of California, Los Angeles
Atmospheric Sciences
405 Hilgard Avenue
Los Angeles, CA 90095–1565
(P) 310 825 1038
(F) 310 206 5219
andy@atmos.ucla.edu

Christine Roensch
Pacific Gas & Electric
77 Beale Street, Room 1654
San Francisco, CA 94179
(P) 415 973 3560
(F) 415 9931521
cmra@pge.com

Kelly T. Redmond
Western Regional Climate Center
Desert Research Institute
P.O. Box 60220
Reno, NV 895006–0220
(P) 702 677 3139
(F) 702 677 3243
krwrcc@sage.dri.edu

Brendan Roark
University of California, Berkeley
Department of Geography
Room 501 McCone
Berkeley, CA 94720
(P) 510 643 1816
(F) 510 642 3370
ebbroark@violet.berkeley.edu

Maurice Roos
California Department of Water Resources
3310 El Camino Avenue, Room 200
P.O. Box 219000
Sacramento, CA 95821–9000
(P) 916 574 2625
(F) 916 574 2767
mroos@water.ca.gov

Jürgen Rollkötter
University of Oldenburg
P.O. Box 2503
D–26111
Oldenburg, Germany
(P) 49 441 970 6359
(F) 49 441 798 3404
jrullkoetter@ogc.icbm.uni-oldenburg.de

Donald M. Schell
Institute of Marine Science
University of Alaska, Fairbanks
Fairbanks, Alaska 99775
(P) 907 474 7978
(F) 407 474 5863
schell@ims.alaska.edu

Gary Sharp
Center for Climate and Ocean Resources Study
780 Harrison Road
Salinas, CA 93907
(P) 408 449 9212
(F) 408 582 3656
gary_sharp@monterey.edu

David Silverman
University of California, Los Angeles
1128 West 30th Street
Los Angeles, CA 90007
(P) 213 748 3043
(F) 818 222 3700
dsilverm@ucla.edu

Tom Suchanek
University of California, Davis
DES
Davis, CA 95616
(P) 916 752 9035
(F) 916 752 3350
thsuchanek@ucdavis.edu

Robert N. Swanson
Climatological Consulting Corporation
1216 Babel Lane
Concord, CA 94518
(P) 510 676 2228
rnswanson@worldnet.attt.net

Yves Tourre
Lamont–Doherty Earth Observatory
Columbia University
tourre@ldeo.columbia.edu

Jim Vaccaro
US Geological Survey
1201 Pacific, Suite 600
Tacoma, WA 98402
(P) 206 593 6510
(F) 206 593 6514

Pete Van de Water
University of Arizona
Laboratory of Tree Ring Research
2415 East First Street, #1
Tucson, AZ 85719
(P) 520 881 7418
(F) 520 881 7418
petevaw@hrp.arizona.edu

Eugene R. Wahl
University of Minnesota
Ecology
100 Ecology, Evolution, and Behavior
1987 Upper Buford Circle
St. Paul, MN 55108
(P) 612 624 6713
(F) 612 624 6777
wahl0040@ggold.tc.unm.edu

G. James West
US Bureau of Reclamation
3429 Oyster Bay
Davis, CA 95616
(P) 916 979 2478
(F) 916 979 2139
gjwest@prodigy.com

Warren B. White
Scripps Institution of Oceanography
PORD
8605 La Jolla Shores Drive
La Jolla, CA 92093–0230
(P) 619 534 4826
(F) 619 534 7452
wbwhite@ucsd.edu

Cathy Whitlock
University of Oregon
Department of Geography
Eugene, OR 97403
(P) 541 737 2940
(F) 541 750 7329
whitlock@oregon.uoregon.edu

Ray Wilson
US Geological Survey
345 Middle Field Road, MS–977
Menlo Park, CA 94025
(P) 415 329 4892
rwilson@mojave.wr.usgs.gov

Michael Wittman
University Weather and Aviation
6201 West Imperial Highway
Los Angeles, CA 90045
(P) 213 776 8651
(F) 213 776 9654
mikewitt@msn.com

Wally Woolfenden
US Department of Agriculture, Forest Service
Mono Lake Ranger Station
Inyo National Forest
P.O. Box 429
Lee Vining, CA 93541
(P) 619 647 3035
(F) 619 647 3027